The Pathology of Hereditary Cystatin C Amyloid Angiopathy (HCCAA)

Ásbjörg Ósk Snorradóttir

Thesis for the degree of Philosophiae Doctor

Supervisor:
Ástríður Pálsdóttir

Advisor:
Birkir Þór Bragason

Doctoral committee:
Helgi Jóhannes Ísaksson, Elías Ólafsson,
Hans Tómas Björnsson

Apríl 2017

UNIVERSITY OF ICELAND
SCHOOL OF HEALTH SCIENCES
FACULTY OF MEDICINE

Meinafræði arfgengrar heilablæðingar

Ásbjörg Ósk Snorradóttir

Ritgerð til doktorsgráðu

Umsjónarkennari:
Ástríður Pálsdóttir

Leiðbeinandi:
Birkir Þór Bragason

Doktorsnefnd:
Helgi Jóhannes Ísaksson, Elías Ólafsson,
Hans Tómas Björnsson

Apríl 2017

UNIVERSITY OF ICELAND
SCHOOL OF HEALTH SCIENCES
FACULTY OF MEDICINE

ISBN 978-9935-9365-4-7

Printing by Háskólaprent ehf

Reykjavik, Iceland 2017

Ágrip

Arfgeng heilablæðing (Hereditary cystatin C amyloid angiopathy (HCCAA)) er sérístenskur mýlildissjúkdómur, sem erfist ókynbundið ríkjandi og stafar af stökkbreytingu í cystatin C geninu, *CST3*. HCCAA tilheyrir fjölbreyttum hópi sjúkdóma sem heita cerebral amyloid angiopathy (CAA). Þeir eiga það sameiginlegt að mýlidi safnast fyrir í heilaæðum miðtaugakerfisins. Í HCCAA myndar stökkbreytt cystatin C mýlildi í æðaveggjum heilaslagæða–/slagæðlinga sem leiðir til heilablæðinga og dauða hjá ungum arfberum. Þótt HCCAA sé réttilega flokkaður sem CAA sjúkdómur vegna sjúkdómsmyndar hans í heilanum, þá verða mýlildisútfellingar líka í öðrum líffærum. Markmið þessarar rannsóknar var að fá betri skilning á meinafræði sjúkdómsins, sérstaklega innan æðaveggjarins, og rannsaka millistig atburða í framvindu meingerðarinnar með því að skoða líffæri utan miðtaugakerfis þar sem lokastig meingerðarinnar í miðtaugakerfinu kom í veg fyrir að hægt væri að rannsaka þá þætti í slíkum sýnum.

Fyrsta markmiðið var að skoða meingerð heilaæða í sjúklingum með því að nota krufningasýni úr heila. Niðurstöðurnar sýndu mikil, og alvarleg, frávik í byggingu æðaveggja slagæða/slagæðlinga miðað við eðlilegar æðar. Breytingarnar voru meðal annars þykknun á æðaþeli, fjölgun mýófíbróblasta, trosnuð elastica, fækkun æðaþelsfrumna og sléttvöðvafrumna, smádrep (e. microinfarcts) og mikil uppsöfnun utanfrumuefna. Dreifing cystatin C útfellinga innan heilans var athuguð. Sú athugun sýndi að umfang CAA útfellingarinnar í heilum allra sjúklinganna var undantekningarlaust alvarleg (e. severe) óháð heilasvæðum. Auk útfellinga innan æðaveggja sáust útfellingar utan við æðar. Einnig greindust cystatin C skellur (e. focal deposits) í heilavef, sem ekki hefur verið lýst áður. Ónæmissvar var í kringum æðar, og innan þeirra, en einnig kringum skellurnar. Svarið samanstóð af taugatróðsöri (e. glial scar) utan um slagæðar/slagæðlinga. Ummerki heilablæðinga voru til staðar í öllum sjúklingum og sáust í öllum heilasvæðum, staðsetning þeirra var þó breytileg milli sjúklinga.

Í seinni hluta rannsóknarinnar færðist áherslan frá heila yfir á líffæri utan miðtaugakerfis. Húðsýni úr arfberum, bæði arfberum með einkenni og einkennalausum arfberum, voru rannsökuð og borin saman við húðsýni úr viðmiðum. Rannsóknin leiddi í ljós cystatin C útfellingar í grunnhimnu ýmissa svæða í húð arfbera. Magn útfellingarinnar var meira í arfberum með einkenni en í einkennalausum arfberum. Cystatin C útfellingin í arfberunum var í nánum tengslum við uppsöfnun á kollageni IV (COLIV). Ólíkt cystatin C uppsöfnuninni þá var ekki magnmunur á COLIV uppsöfnun í arfberunum eftir sjúkdómsstigi, heldur var sambærileg aukning á COLIV í húðsýnum allra arfberanna miðað við sýni úr viðmiðunum. Aukinn fjöldi fíbróblasta greindist í efri hluta leðurhúðarinnar í arfberunum og skoðun með lagsjá sýndi að cystatin C útfellingin, sem og aukin ónæmislitun COLIV, í arfberasýnunum var tengd þessum fíbróblöstum en ekki öðrum frumugerðum í húðinni. Uppsöfnun COLIV í heilanum og í húðinni, og sterk tengsl þess við fíbróblasta og cystatin C útfellingar, bendir til þess að þykknun á grunnhimnu gerist snemma í framvindu meingerðarinnar og sé mikilvægur hluti í framgangi hennar, sem stuðlað geti að útfellingu, og mýlildismyndun, stökkbreytts cystatin C.

Þó að HCCAA sé kerfisbundinn sjúkdómur þá eru klínísku einkennin næstum bara bundin við miðtaugakerfið. Það er vegna þess að meingerð sjúkdómsins er mest í heilaæðunum og leiðir til veikari æðaveggja og heilablæðinga. Aftur á móti var meingerðin í líffærum utan miðtaugakerfis mildari og var sjaldan tengd klínískum einkennum. Þessi meingerð gæti hins vegar þróast í alvarlega með tíma en það verður sjaldan vegna þess að banvænar heilablæðingar gerast á undan.

Lykilorð:

Arfgeng heilablæðing, mýlildi, cystatin C, COLIV, utanfrumuprótein, grunnhimna.

Abstract

Hereditary Cystatin C Amyloid Angiopathy (HCCAA) is an amyloid disorder in Icelandic families caused by an autosomal dominant mutation in the cystatin C gene, *CST3*. HCCAA is classified as a cerebral amyloid angiopathy (CAA), a group of diseases in which amyloid deposits in the walls of blood vessels in the central nervous system (CNS). Mutant cystatin C forms amyloid deposits within the walls of cerebral arteries/arterioles resulting in haemorrhagic strokes in young adults. Although HCCAA is rightly classified as a CAA disorder due to its strong cerebral presentation, amyloid deposition is systemic and also found in other internal organs. The objectives of this study were to increase understanding of HCCAA pathogenesis, especially within the vessel wall itself, and to gain information about intermediate events in the pathogenesis by studying peripheral tissues because the severity of pathology in the CNS hindered the use of CNS samples for that purpose.

The first aim was to examine the cerebral vascular pathology of HCCAA patients using post-mortem brain samples. The results revealed severe changes in the architecture of the walls of cerebral arteries/arterioles, e.g. intimal thickening, myofibroblast proliferation, a frayed elastic layer, degeneration of endothelial and smooth muscle cell cells, microinfarcts, and excessive accumulation of extracellular matrix constituents. The topographical distribution of cystatin C deposition within brain areas was assessed. The extent of the CAA deposition in the brains of HCCAA patients was uniformly severe throughout the brain. In addition to deposition within vessel walls, perivascular cystatin C deposits were observed and a novel finding was that of parenchymal cystatin C focal deposits. A neuroinflammatory response was seen around affected vessels, and the focal deposits, consisting of glial scar formation. Hemorrhages were observed in all patients and were found in all brain areas examined; however, their location was varied.

In the second part of the study the focus shifted from the brain to the periphery. Skin biopsies from L68Q-*CST3* mutation carriers, symptomatic and asymptomatic, were studied in comparison to control biopsies. This revealed deposition of cystatin C in the basement membranes (BMs) of various skin structures in the carrier biopsies. The quantity of deposition in symptomatic carriers was greater than in asymptomatic carriers. Cystatin C deposition was closely associated with collagen IV (COLIV) accumulation in the BMs of the same skin areas. In contrast to cystatin C deposition, COLIV immunoreactivity did not differ by disease status but was elevated in all carriers to the same extent compared to controls. An increased number of fibroblasts was observed in the upper dermis of carriers and confocal microscopy revealed that cystatin C deposition, and the enhanced COLIV immunoreactivity, was associated with dermal fibroblasts but not other cell types. Cumulatively, the excess deposition of COLIV in the brain, and in the skin, and its tight association with fibroblasts and cystatin C deposition suggests that basement membrane thickening is an early and important event in HCCAA pathogenesis that facilitates cystatin C deposition and aggregation.

Although HCCAA is a systemic disorder, its clinical symptoms are almost exclusively confined to the CNS. This is due to the comparatively advanced pathology in the brain resulting in weaker vasculature and brain hemorrhages. In contrast, the pathology in peripheral tissues was mild or intermediate, and rarely associated with clinical presentation. Those changes could, however, progress to severe with time, but rarely do because they are preceded by fatal brain hemorrhages.

Keywords:

Hereditary Cystatin C Amyloid Angiopathy, amyloid, cystatin C, COLIV, extracellular matrix protein, basement membrane.

Acknowledgements

This study was carried out at the Institute for Experimental Pathology, University of Iceland, Keldur, at the Department of Pathology, Landspitali University Hospital, the Faculty of Medicine, University of Iceland, and the Department of Cellular Neurology, Hertie Institute for Clinical Brain Research, University of Tübingen, Germany. I would like to thank all of the institutions, faculties and all the people who contributed to this study. I have met incredible colleagues and new friends throughout this study.

First of all, I would like to thank my supervisors, Ástríður Pálsdóttir and Birkir Þór Bragason, for the opportunity of working on this disease, their support, guidance, encouragement, friendship and scientific discussions through the years.

I am grateful to the members of my doctoral committee, Helgi Jóhannes Ísaksson, Elías Ólafsson and Hans Tómas Björnsson for their constructive support, guidance, friendship and discussions.

My sincere gratitude to Mathias Jucker, Stephan Kaeser, Angelos Skodras and the staff at the Department of Cellular Neurology, Hertie Institute for Clinical Brain Research, University of Tübingen, Sævar Ingþórsson at the Faculty of Medicine, University of Iceland, Steinunn Árnadóttir and Margrét Jónsdóttir who worked at Keldur and all of the staff at Keldur and the Department of Pathology, Landspitali, for technical assistance and guidance.

I would like to thank my husband and my daughters for their endless support, encouragement and for always believing in me.

My sincere gratitude to my parents for their support, understanding and encouragement.

I am grateful to my parents-in-law and my family-in-law for their support and help.

Finally, I would like to thank all of the people who underwent skin biopsies and donated samples for this study.

This work was funded by the Icelandic Centre for Research (RANNÍS), the University of Iceland Research Fund, the Memorial Fund of Hafdis Kjartansdottir, the Memorial Fund of Helga Jonsdottir and Sigurlidi Kristjansson, the Icelandic Association of Biomedical Scientists and the Heilavernd fund.

Contents

List of abbreviations

a.a.	Amino acid
AD	Alzheimer's disease
AGC1	Aggrecan
ANS	Autonomic nervous system
APOE	Apolipoprotein E
APOJ	Apolipoprotein J
APP	Amyloid precursor protein
Aβ	Amyloid β protein
$A\beta_{40}$	40 amino acid form of Aβ
$A\beta_{42}$	42 amino acid form of Aβ
Aβ-CAA	Aβ-type cerebral amyloid angiopathy
BBB	Blood-brain barrier
BM	Basement membrane
CAA	Cerebral amyloid angiopathy
CADASIL	Cerebral autosomal dominant arteriopathy with subcortical infarcts and leukoencephalopathy
CD68	Cluster of differentiation 68
CJD	Creutzfeldt-Jakob disease
CNS	Central nervous system
COLIV	Collagen IV
CSF	Cerebrospinal fluid
CSPG	Chondroitin sulfate proteoglycan
CST3	Cystatin C gene
ECM	Extracellular matrix
EMT	Epithelial–mesenchymal transition
EndMT	Endothelial–mesenchymal transition
ERK	Extracellular signal-regulated kinase
FAD	Familial Alzheimer's disease
FAP	Familial amyloid polyneuropathy
FBD	Familial British dementia
FDD	Familial Danish dementia

GFAP	Glial fibrillary acid protein
GSS	Gerstmann-Sträussler-Scheinker syndrome
H&E	Hematoxylin and eosin staining
HA	Hyaluronic acid
HCCAA	Hereditary cystatin c amyloid angiopathy
HCHWA	Hereditary cerebral hemorrhage with amyloidosis
HCHWA-D	Hereditary cerebral hemorrhage with amyloidosis – Dutch type
HCHWA-I	Hereditary cerebral hemorrhage with amyloidosis – Icelandic type
HLA-DR	Major histocompatibility complex class II-antigen
HSPG	Heparan sulfate proteoglycans
IBA1	Ionized calcium-binding adaptor molecule-1
IEL	Internal elastic lamina
IPF	Idiopathic pulmonary fibrosis
ISF	Interstitial fluid
JNK	c-jun-n-terminal kinase
MAPK	p38 mitogen-activated protein kinase
NFT	Neurofibrillary tangle
PEFA	Protein elimination failure angiopathy
PNS	Peripheral nervous system
ROI	Region of interest
SMC	Smooth muscle cell
TGF-β	Transforming growth factor beta
TβRI	The serine/threonine receptor kinases type I
TβRII	The serine/threonine receptor kinases type II

List of figures

List of tables

List of original papers

This thesis is based on the following original publications, which are referred to in the text by their Roman numerals:

I. **Deposition of collagen IV and aggrecan in leptomeningeal arteries of hereditary brain haemorrhage with amyloidosis.** Snorradottir, A.O., Isaksson H.J., Kaeser S.A., Skodras A.A., Olafsson E., Palsdottir A., Bragason B.T. *Brain Research* 2013;1535:106-114.

II. **Parenchymal cystatin C focal deposits and glial scar formation around brain arteries in Hereditary Cystatin C Amyloid Angiopathy.** Osk Snorradottir A., Isaksson H.J., Kaeser S.A., Skodras A.A., Olafsson E., Palsdottir A., Bragason B.T. *Brain Research* 2015;1622:149-162.

III. **Pathological changes in basement membranes and connective tissue of skin from patients with Hereditary Cystatin C Amyloid Angiopathy.** Snorradottir, A.O., Isaksson H.J., Ingthorsson S., Olafsson E., Palsdottir A., Bragason B.T. *Lab Invest*. 2017.

Declaration of contribution

I took part in the planning, set-up, and execution of the study. I also took part in writing grant applications and acquiring funds. I performed all of the experiments described in all three papers. They were performed at the Institute for Experimental Pathology at Keldur, University of Iceland (UI), at the Department of Pathology, Landspitali University Hospital, Faculty of Medicine (UI), and at the Department of Cellular Neurology, Hertie Institute for Clinical Brain Research, University of Tübingen, Germany. Throughout the study I had a major role in aquisitation of data, i.e. imaging, quantification of immunostainings, data analyses, and interpretation of data. I took part in building up collaborations throughout the study; for example, I went to the Department of Cellular Neurology in Tübingen to learn quantification methods for the analyses of immunostaining. I wrote, and revised, all three papers along with my supervisors, Ástríður Pálsdóttir and Birkir Þór Bragason.

1 Introduction

1.1 Amyloidosis

Amyloidosis are a heterogeneous group of diseases in which proteins that are normally soluble assemble to form insoluble and toxic fibers that deposit as amyloid in tissues and organs throughout the body, most commonly in extracellular space (Chiti & Dobson, 2006a; Merlini & Bellotti, 2003). Amyloidosis can be localized or progressive systemic diseases. They are clinically heterogeneous because one or more organs can be involved, such as the central nervous system (CNS), heart, kidneys, liver, pancreas, and others (Blancas-Mejia & Ramirez-Alvarado, 2013). In localized amyloidoses, both extracellular and intracellular amyloid deposits can occur and only in the organ, or tissue, of precursor protein synthesis. Examples include Parkinson's disease, Alzheimer's disease (AD) and Huntington's disease (Chiti & Dobson, 2006a; Merlini & Bellotti, 2003). In systemic amyloidosis deposits are predominantly extracellular and the amyloid precursor protein is expressed and secreted at locations that are often distinct from the main sites of deposition and can affect multiple organs/tissues (Blancas-Mejia & Ramirez-Alvarado, 2013). Examples of systemic amyloidosis are light chain amyloidosis and familial amyloid polyneuropathy (FAP) (Blancas-Mejia & Ramirez-Alvarado, 2013; Revesz et al., 2003).

Amyloidosis can be sporadic, familial, or transmissible and their anatomical distribution can vary greatly (Liberski, 1993b; Pinney & Hawkins, 2012). Amyloidosis can also be a secondary condition, for instance in patients that have undergone long term hemodialysis (Bardin et al., 1987). Each type of amyloidosis is characterized by one distinct fibril-forming protein and to date 31 known fibril proteins have been identified that form amyloid in humans (Table1) (Sipe et al., 2014). Seven of these proteins are known to form amyloid in the CNS (Revesz et al., 2003).

Sporadic amyloidosis occurs randomly in the aging population. The most prevalent, and well known, sporadic amyloid disease in the CNS is AD, which

can also be familial, although that is rare (Revesz et al., 2003). Another well-known sporadic amyloidosis is the human prion disease, Creutzfeldt - Jakob disease (CJD), which can also be familial or acquired. However, the sporadic form is most prevalent and accounts for about 85% of CJD cases (Puoti et al., 2012). Familial amyloidosis is a condition where a gene mutation results in the misfolding of a precursor protein. Examples of familial amyloidosis that affect the CNS are Familial AD (FAD) and Hereditary Cerebral Hemorrhage With Amyloidosis-Dutch (HCHWA-D) and Icelandic (HCHWA-I) type (Maat-Schieman et al., 2005; Palsdottir et al., 2006). The latter is also referred to as Hereditary Cystatin C Amyloid Angiopathy (HCCAA); this abbreviation will be used throughout this thesis (Palsdottir et al., 2006). Transmissible amyloidosis is caused by the infection of a pathogen, called prion. An example of transmissible prion diseases found in the CNS are CJD and Kuru (Liberski, 1993a).

Diagnosis of amyloidosis can be difficult and is often only made late in the course of the disease. The diagnosis is often made by organ/tissue biopsy if there are no underlying genetic factors responsible. Imaging techniques can also be helpful (Pinney & Hawkins, 2012).

Table 1. Amyloid fibrils proteins and their precursors in human.
Table from (Sipe et al., 2014), reprinted with permission from Taylor & Francis.

Fibril protein	Precursor protein	Systemic and/or localized	Acquired or hereditary	Target organs
AL	Immunoglobulin Light Chain	S, L	A, H	All organs except CNS
AH	Immunoglobulin Heavy Chain	S, L	A	All organs except CNS
AA	(Apo) Serum Amyloid A	S	A	All organs except CNS
ATTR	Transthyretin, wild type	S	A	Heart mainly in males, Ligaments, Tenosynovium
	Transthyretin, variants	S	H	PNS, ANS, heart, eye, leptomen.
Aβ2M	β2-Microglobulin, wild type	L	A	Musculoskeletal System
	β2-Microglobulin, variant	S	H	ANS
AApoAI	Apolipoprotein A I, variants	S	H	Heart, liver, kidney, PNS, testis, larynx (C terminal variants), skin (C terminal variants)
AApoAII	Apolipoprotein A II, variants	S	H	Kidney
AApoAIV	Apolipoprotein A IV, wild type	S	A	Kidney medulla and systemic
AGel	Gelsolin, variants	S	H	PNS, cornea
ALys	Lysozyme, variants	S	H	Kidney
ALECT2	Leukocyte Chemotactic Factor-2	S	A	Kidney, primarily
AFib	Fibrinogen α, variants	S	H	Kidney, primarily
ACys	Cystatin C, variants	S	H	PNS, skin
ABri	ABriPP, variants	S	H	CNS
ADan*	ADanPP, variants	L	H	CNS
Aβ	Aβ protein precursor, wild type	L	A	CNS
	Aβ protein precursor, variant	L	H	CNS
APrP	Prion protein, wild type	L	A	CJD, Fatal insomnia
	Prion protein variants	L	H	CJD, GSS syndrome, Fatal insomnia
ACal	(Pro)calcitonin	L	A	C-cell thyroid tumors
AIAPP	Islet Amyloid Polypeptide†	L	A	Islets of Langerhans, Insulinomas
AANF	Atrial Natriuretic Factor	L	A	Cardiac atria
APro	Prolactin	L	A	Pituitary prolactinomas, aging pituitary
AIns	Insulin	L	A	Latrogenic, local injection
ASPC‡	Lung Surfactant Protein	L	A	Lung
AGal7	Galectin 7	L	A	Skin
ACor	Corneodesmosin	L	A	Cornified epithelia, Hair follicles
AMed	Lactadherin	L	A	Senile aortic, Media
Aker	Kerato-epithelin	L	A	Cornea, hereditary
ALac	Lactoferrin	L	A	Cornea
AOAAP	Odontogenic Ameloblast-Associated Protein	L	A	Odontogenic tumors
ASem1	Semenogelin 1	L	A	Vesicula seminalis
AEnf	Enfurvitide	L	A	Latrogenic

* ADan is the product of the same gene as ABri. † Also called amylin. †† Not proven by amino acid sequence analysis. PNS: Peripheral nervous system. ANS: Autonomic nervous system.

1.2 Amyloid – definition and formation

The term amyloid was first coined in 1838 by Matthias Schleiden, and subsequently used by Rudolph Virchow in 1854, to describe deposits in the liver (Kyle, 2001; Virchow, 1854). Amyloid refers to abnormal fibril proteins which are formed by normally soluble proteins that have converted into insoluble fibrils which are structurally dominated by β-sheet structures. Amyloid is deposited, mainly extracellularly in tissues and organs (Merlini & Bellotti, 2003; Picken, 2010). As mentioned, over 31 proteins are known to form amyloid (Table 1). Despite the differences in function, size, and biochemical composition between these proteins in their normal form, the amyloid fibrils formed by them share common morphological, physical and histochemical properties (Figure 1) (Pinney & Hawkins, 2012). Once formed, amyloid fibrils are inherently stable, insoluble, and resistant to proteolytic degradation, which makes effective clearance of amyloid difficult (Rambaran & Serpell, 2008).

Studies by electron microscopy show that amyloid consists of aggregated, unbranched, twisted fibrils about 6-10 nm wide and of indeterminate length (Chiti & Dobson, 2006a; Makin & Serpell, 2005). X-ray diffraction and other techniques have revealed that amyloid fibrils contain highly ordered structures which are common to all amyloid. The initial phase of amyloid fibril formation includes the formation of dimers, trimers, and tetramers (also known as oligomers) of the amyloid-forming protein which later make up structures called protofilaments (Serpell et al., 2000). The number of protofilaments can differ from 2-6, each 2.5-3.5 nm in diameter, and twist around one another to form the mature amyloid fibril (Figure 1) (Chiti & Dobson, 2006b; Rambaran & Serpell, 2008). Studies indicate that oligomers may be toxic molecules (Lambert et al., 1998).

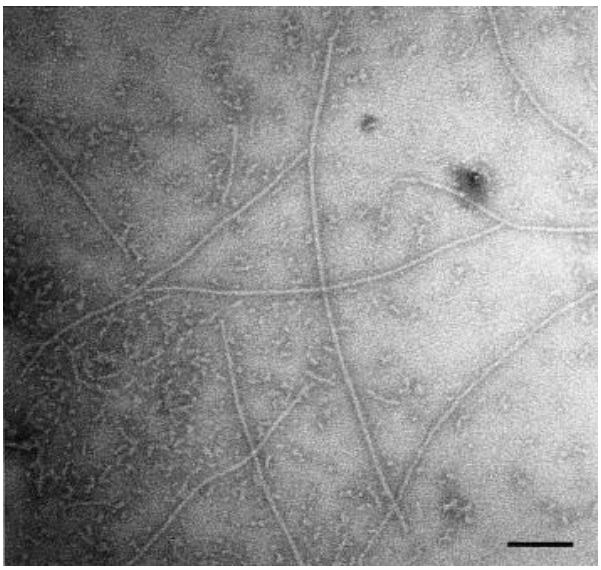

Figure 1. Amyloid fibrils.
An electron micrograph of unbranched amyloid fibrils and aggregates. Bar: 1000 Å. Reprinted from (Serpell, 2000) with permission from Elsevier.

In vitro studies have shown that almost all proteins can be driven towards amyloid formation by destabilizing their structure (Bucciantini et al., 2002). Several factors can induce the fibril formation process, such as post-translational modifications or genetic factors (Revesz et al., 2003). A well known example of a post-translational modification is the cleavage of the amyloid precursor protein (APP) into amyloid β protein (Aβ), which causes AD (Ghiso & Frangione, 2002). Mutations in a precursor protein, resulting in an amino acid (a.a.) substitution, can alter or influence the conversion of a native protein into a fibrillar conformation. Examples of such mutations are those associated with HCHWA-D and HCCAA (Revesz et al., 2003). Other factors that enhance amyloid formation can be an increased concentrations of proteins (molecular crowding), low pH, metal ions, and co-deposition of amyloid-associated proteins (Revesz et al., 2003). Such amyloid-associated proteins are, for example, apolipoprotein E (APOE), apolipoprotein J (APOJ), serum amyloid-P component, vitronectin, α1-antichymotrypsin, complement

proteins, glycosaminoglycans, and extracellular matrix (ECM) proteins (Figure 2) (Revesz et al., 2003).

Amyloid shows up as pink, homogenous, acellular deposits in hematoxylin and eosin (H&E) slices. All amyloid deposits show specific binding to the dye Congo red, resulting in apple green birefringence of amyloid when Congo red stained samples are examined under polarized light in a light microscope (Puchtler, 1965). Congo red staining has been the gold standard to determine the presence of amyloid in tissue, but Thioflavin S can also be used, which causes amyloid to display green fluorescence in a similar manner to Congo red. Further diagnosis of amyloid can be made by immunohistochemistry to determine the protein composition of the amyloid deposits (Kyle, 2001).

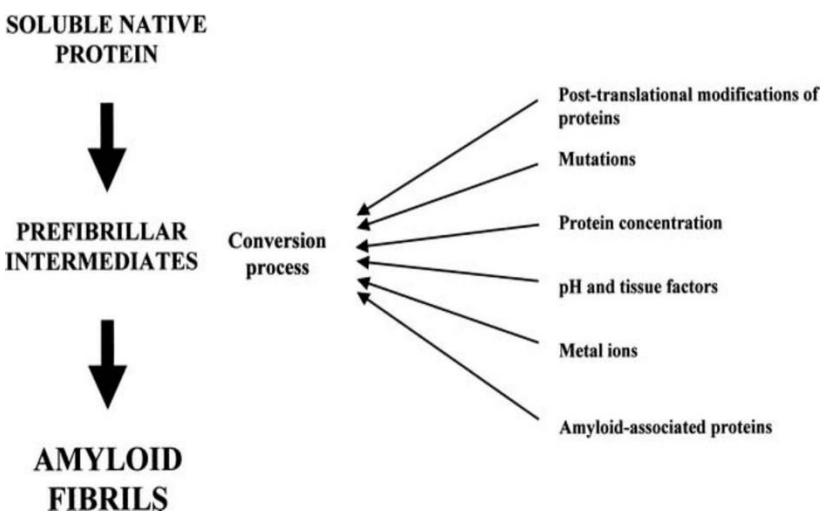

Figure 2. A schematic diagram of the process of amyloid formation.
Factors that influence the conversion of precursor proteins into amyloid fibrils are shown. Reprinted from (Revesz et al., 2003) with permission from Oxford University Press.

1.3 Alzheimer's disease

AD was first described by Alois Alzheimer, a Bavarian psychiatrist, in 1907. In his report he described features of AD that are still considered diagnostic today, both the clinical and pathological symptoms (Moller & Graeber, 1998).

AD is a progressive neurodegenerative disease that leads to dementia and cognitive decline in millions of people worldwide (Thal et al., 2013). AD can be either sporadic or familial (FAD). Sporadic AD is the most common form of the disease, while the familial form is rather rare (about 5% of all AD cases). The major risk factors for sporadic late-onset AD (onset ≥60 years of age) are age and the possession of the ε4 and ε2 allele of the *APOE* gene (Tanzi, 2012). FAD has an autosomal dominant inheritance and is associated with mutations in either the *APP* gene or the *PSEN1* or *PSEN2* genes. These mutations cause early-onset AD *(*onset <60 years of age) (Goate et al., 1991; Tanzi, 2012). Mutations in the *APP* gene are rarer than mutations in the *PSEN1* or *PSEN2* genes, which account for most FAD cases (Tanzi, 2012). *PSEN1* and *PSEN2* encode the precursor proteins presenilin-1 and 2, respectively, transmembrane proteins involved in normal APP processing through their effects on γ-secretase, the enzyme that cleaves APP. Mutations in the *PSEN1* or *PSEN2* genes result in an increased production of the Aβ protein which is more prone to oligomerization and fibril formation (Suzuki et al., 1994a). The pathological hallmarks of AD are: (1) accumulation of Aβ in parenchymal amyloid deposits and in the walls of brain vessels as CAA, (2) neurofibrillary tangles (NFTs), and (3) neurofibrillary changes that include neuritic amyloid plaques, NFTS, and neuropil threads (Braak & Braak, 1991; Glenner & Wong, 1984; Hyman et al., 2012; Jellinger, 2002). Other pathological features are a progressive loss of synapses and cortical neurons, progressive brain atrophy, activation of astrocytes and microglia, degenerative changes in the white matter, and granulovacuolar degeneration (Braak & Braak, 1991; Glenner & Wong, 1984; Hyman et al., 2012; Jellinger, 2002). NFTs are aggregates of hyperphosphorylated and misfolded tau and are primarily made of paired helical filaments (Figure 3). The progression of NFTs correlates with the severity of AD and can be divided into six stages (I-

VI) by criteria proposed by Braak and Braak, 1991 (Braak & Braak, 1991). In stages I and II the NFTs are mainly found in the transentorhinal region of the brain, in stages III and IV they are also observed in the limbic regions such as the hippocampus, and in stages V and VI there is extensive neocortical involvement (Braak & Braak, 1991).

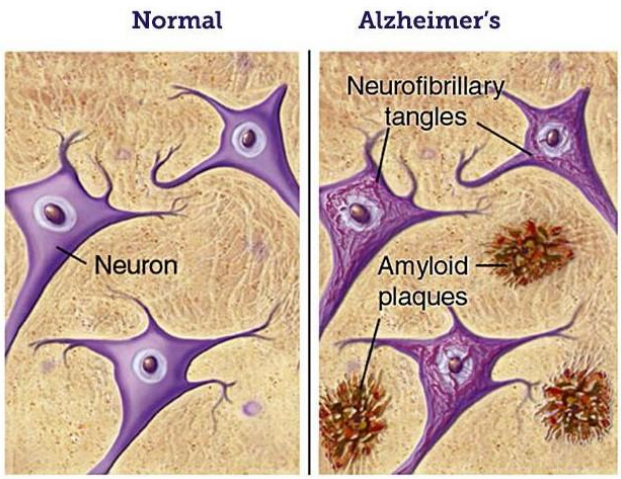

Figure 3. Amyloid plaques and neurofibrillary tangles in Alzheimer's disease. Reprinted from http://www.brightfocus.org/alzheimers/infographic/amyloid-plaques-and-neurofibrillary-tangles with permission from the BrightFocus Foundation.

Neuritic plaques contain Aβ amyloid and dystrophic neurites within and around the plaque. The plaques are often associated with immune cells such as activated microglia and reactive astrocytes. Diffuse plaques can also be observed in AD cases (Dickson, 1997; Itagaki et al., 1989; Rozemuller et al., 1989).

Over 80% of AD patients have Cerebral Amyloid Angiopathy (CAA) but it is usually mild. Capillary CAA (CAA type 1, see definition in section 1.5.2) is more common in AD than in other CAA diseases and can cause capillary inclusions and cerebral blood flow disturbance (Thal et al., 2009; Thal et al., 2002a). CAA in AD rarely leads to intracerebral hemorrhages, but extensive Aβ deposition and other vascular changes at later-stages can lead to CAA-related intracerebral hemorrhages (Mandybur, 1986).

1.4 Cerebral Vessels

Cerebral blood vessels are crucial for the normal function of the brain by delivering an adequate supply of oxygen and nutrients to the organ. The term “blood vessels” encompasses arteries, arterioles, veins, venules and capillaries (Lee, 1995). In CAA, and HCCAA, the most affected vessels are the cerebral arteries and arterioles (Gudmundsson et al., 1972; Vinters, 1987).

The wall of cerebral arteries and arterioles consists of three layers: the *tunica intima*, the *tunica media,* and the *tunica adventitia* (Lee, 1995). The *tunica intima* in cerebral arteries has a single layer of endothelial cells, a basement membrane (BM) and an internal elastic lamina (IEL). The lumen of all cerebral vessels is lined with endothelial cells which take part in controlling vessel tone, vascular permeability, and form the blood-brain barrier (BBB) along with astrocyte end-feet and pericytes (Ballabh et al., 2004). The BM is a thin structure consisting mainly of collagen IV (COLIV), laminin, and heparan sulfate proteoglycans (HSPGs) (see detailed description of BM in section 1.7.8 (Lee, 1995; Lindblom A, 1996). The IEL contributes to the mechanical integrity and elasticity of arteries. With age and disease, elastic fibers can degrade and fragment leading to increased stiffness of the arterial wall (Martinez-Lemus, 2012; Xu & Shi, 2014). The *tunica media* is composed mainly of vascular smooth muscle cells (SMCs) along with some elastin and collagen fibers. The number of SMC layers varies depending on the size of the arteries; parenchymal arterioles, for example, contain fewer SMCs than pial arteries (Xu & Shi, 2014). The primary function of SMCs in the media is to control vascular diameter through cell contraction and relaxation. Each individual SMC is surrounded by BM and the SMCs are important for maintaining BM integrity (Stegemann et al., 2005). The outermost layer of cerebral arteries and arterioles is the *tunica adventitia* which is mostly composed of collagen fibers, fibroblasts, and associated cells. Cerebral arteries do not contain external elastic lamina and cerebral arterioles do not have an IEL or a *tunica adventitia (Engelhardt et al., 2016)*.

Cerebral veins consist of the same three layers as arteries, but are thin-walled in comparison and have less SMC, collagen, and elastin than arteries (Kilic & Akakin, 2008). Cerebral capillaries are only composed of endothelium and a BM (Engelhardt et al., 2016).

1.5 Cerebral Amyloid Angiopathy

CAA is a general term used to describe a group of sporadic, and hereditary, diseases which present with vascular amyloid deposition in the CNS (Vinters, 1987). CAA is one of the major causes of recurrent intracerebral hemorrhages, which may contribute to cognitive decline (Vinters, 1987).

The classification of CAA disease type is based on the identity of the amyloid forming protein involved. As mentioned, there are several proteins that can form amyloid, however, only seven amyloid proteins have been reported to cause CAA. These proteins are: Aβ, cystatin C, prion protein, BRI2 protein (also known as integral membrane protein 2B; two different mutations result in two different amyloid proteins), transthyretin, and gelsolin (Biffi & Greenberg, 2011; Frangione et al., 2001; Revesz et al., 2003; Revesz et al., 2009). There are both sporadic and hereditary familial forms of CAA diseases. HCCAA was the first familial CAA to be described. That was in 1935 by Árni Árnason (Arnason, 1935). Sporadic CAA mostly affects the elderly while the rarer hereditary forms, which are determined by underlying mutations (Table 2), affect younger individuals and are generally more severe (Yamada & Naiki, 2012). Sporadic Aβ-type CAA (Aβ-CAA) is the most common form of CAA and is found in 10-40% of elderly individuals (> 65 years of age) and in over 80% of patients with AD (Jellinger, 2002). The hereditary forms of CAA are: **1) Hereditary Cerebral Hemorrhage With Amyloidosis (HCHWA)**: Six Aβ associated HCHWA types have been discovered to date; HCHWA – Dutch, - Arctic, -Piedmont, -Iowa, -Flemish, and -Italian; the most studied of these diseases is HCHWA-D. All these disorders are due to different point-mutations in the *APP* gene on chromosome 21 which encodes the APP. **2) FAD** which is caused by mutations in the *APP* gene and mutations in the *PSEN1* or *PSEN2* genes on chromosome 14; the *PSEN* genes encode the precursor proteins presenilin-1

and 2, respectively which are involved in APP precursor protein cleavage. **3) HCCAA** which is caused by a mutation in the *CST3* gene on chromosome 20 that encodes the precursor protein cystatin C. **4) Familial British dementia (FBD)** and **Familial Danish dementia (FND)** are caused by mutations in the *BRI2* gene on chromosome 13 that encodes the precursor protein BRI2. **5) Familial amyloidosis, Finnish type** caused by mutations in the *GSN* gene, which encodes the precursor protein gelsolin. **6) Gerstmann–Sträussler–Scheinker syndrome (GSS)** which is associated with mutations in the *PRNP* gene on chromosome 20, encoding the prion protein precursor, and **7) Familial amyloid polyneuropathy (FAP)** which is associated with a mutation in the *TTR* gene on chromosome 18, that encodes the precursor protein transthyretin (Table 2) (Biffi & Greenberg, 2011; Levy et al., 1990; Revesz et al., 2003; Yamada & Naiki, 2012).

Table 2. Sporadic and hereditary forms of Cerebral Amyloid Angiopathy.

Precursor protein	Amyloid peptide	Gene	Chr.	Disease
Amyloid precursor protein	Aβ	*APP*	21	Sporadic CAA
Amyloid precursor protein	Aβ	*APP*	21	CAA in AD
Amyloid precursor protein	Aβ	*APP*	21	FAD
Amyloid precursor protein	Aβ	*APP*	21	Down‘s syndrome
Amyloid precursor protein	Aβ	*APP*	21	HCHWA-Dutch
Amyloid precursor protein	Aβ	*APP*	21	HCHWA-Arctic
Amyloid precursor protein	Aβ	*APP*	21	HCHWA-Piedmont
Amyloid precursor protein	Aβ	*APP*	21	HCHWA-Iowa
Amyloid precursor protein	Aβ	*APP*	21	HCHWA-Flemish
Amyloid precursor protein	Aβ	*APP*	21	HCHWA-Italian
Presenilin 1	Aβ	*PSEN1*	14	FAD
Presenilin 2	Aβ	*PSEN2*	14	FAD
Cystatin C	ACys	*CST3*	20	HCCAA
Prion protein	PrP^{Sc}	*PRNP*	20	GSS
BRI2	ABri	*BRI2*	13	FBD
BRI2	ADan	*BRI2*	13	FDD
Gelsolin	AGel	*GSN*	9	FAF
Transthyretin	ATTR	*TTR*	18	FAP

Abbreviations: CAA: Cerebral Amyloid Angiopathy, AD: Alzheimer's disease, HCHWA: Hereditary Cerebral Hemorrhage with Amyloidosis, FAD: Familial AD, HCCAA: Hereditary Cystatin C Amyloid Angiopathy, GSS: Gerstmann-Sträussler-Scheinker syndrome, FBD: Familial British dementia, FBN: Familial Danish dementia, FAF: Familial Amyloidosis, Finnish type and, FAP: Familial amyloid polyneuropathy (FAP).

1.5.1 Pathological features of CAA

Pathological changes in CAA are most commonly found in vessels of the cerebral and cerebellar lobes and in rare instances in the basal ganglia, brain stem, thalamus, or white matter (Yamada, 2015). CAA is observed most often in leptomeningeal and cortical vessels, with small and medium-sized arteries and arterioles most frequently affected; capillaries may be affected but rarely veins (Mandybur, 1986; Vinters & Farag, 2003). The pathogenesis of CAA begins in leptomeningeal vessels and is then subsequently observed in cortical vessels of the neocortical areas and then in vessels of allocortical areas and the cerebellum. In some rare cases, vessels of other brain areas can be affected (Thal et al., 2003). Studies have shown that amyloid initially deposits in the BM and in BMs around SMCs in the media. From there the

deposition spreads to the adventitia of the vessel wall, before it gradually extends towards the IEL and then to the endothelium of arteries/arterioles (Carare et al., 2008; Vinters, 1987; Yamaguchi et al., 1992). In capillaries, amyloid deposits are found within the BM and with increasing CAA severity extending into the adjacent neuropil. As the severity of the CAA increases, amyloid deposits can be seen throughout the entire vessel wall of small arteries/arterioles (Biffi & Greenberg, 2011; Revesz et al., 2003; Yamada, 2015). This is followed by the degeneration of SMCs and the appearance of other vascular degenerative changes, such as changes of the architecture of affected blood vessels, fibrinoid necrosis, hyaline degeneration, "double-barreling", microaneurysm formation, and in some cases loss of endothelial cells (Mandybur, 1986; Vinters, 1987; Vinters & Farag, 2003; Vonsattel et al., 1991).

1.5.2 The topography of CAA

The severity, topography, and progression of CAA can be assessed by well-defined criteria. The **severity** can be graded by the criteria defined by Vonsattel *et al.* (Vonsattel et al., 1991) which defines three severity stages: mild, moderate, or severe. CAA is graded mild if amyloid deposits are mainly restricted to the outer BM with the SMC layer intact, moderate if amyloid deposits are seen in the outer BM and between the SMCs, and severe if amyloid deposition is extensive and observed throughout the vessel wall. The **topography and progression** of CAA throughout the brain can be defined by criteria defined by Thal *et al.* (Thal et al., 2003; Thal et al., 2008). These criteria divide CAA into three stages based on distribution. In stage 1, CAA is present in leptomeningeal, or parenchymal, vessels of neocortical areas, in stage 2 in allocortical, cerebellar, and midbrain vessels, and in stage 3, in subcortical nuclei such as the basal ganglia, the thalamus, the white matter, or the lower brainstem. The third criterion defined by Thal *et al.* (Thal et al., 2002a) divides CAA into two types, CAA type 1 and CAA type 2, based on the presence of capillary involvement; capillaries are affected in type 1 but not in type 2. The ε4 and ε2 alleles of the *APOE* gene are associated with an

increased risk of developing AD and the ε4 allele is also associated with an increased risk for CAA (Liu et al., 2013). The *APOE* ε4 allele is found to be more common in CAA type 1 than in CAA type 2 (Thal et al., 2002a). CAA type 2 does not evolve into CAA type 1 with time, as both type 1 and type 2, are seen in mild and severe CAA, and the mean age of occurrence of the two types does not differ (Thal et al., 2002a).

1.5.3 Clinical features of CAA

The clinical presentation of CAA may include lobar macro- and micro-hemorrhages, leukoencephalopathy, ischemic infarcts, microinfarcts, white-matter lesions, progressive cognitive decline and dementia, loss of consciousness, headaches, seizures, and death. CAA can also be completely asymptomatic (Biffi & Greenberg, 2011; Cadavid et al., 2000; Mandybur, 1986; Soontornniyomkij et al., 2010; Vonsattel et al., 1991).

1.5.4 Diagnosis of CAA

The diagnosis of CAA can be made by obtaining a brain sample, at autopsy, via brain biopsy for histological examination, or by a genetic test in the case of a known underlying mutation. CAA pathology can be observed by H&E staining due to the characteristic acellular, and homogenous, eosinophilic appearance of thickened vessel walls which are visible by standard light microscopy (Vinters, 1987). However, Congo red staining, or Thioflavin S staining, are necessary to demonstrate amyloid deposition (Vinters, 1987). These two staining methods, and immunohistochemistry using an antibody to the amyloid forming protein, are used to confirm CAA. Another diagnostic tool are the Boston criteria for CAA. A diagnosis by these criteria is based on clinical data, imaging data showing cerebral hemorrhage or hemorrhages with magnetic resonance imaging or computed tomography, and histopathologic examination. The Boston criteria divide CAA into the following categories: definitive CAA, probable CAA with supporting pathology, probable CAA, and possible CAA (Knudsen et al., 2001). A diagnosis of definite CAA requires a full post-mortem examination (Knudsen et al., 2001).

1.5.5 Aβ-CAA – production and clearance

The most common form of CAA in the brain is due to Aβ-CAA. The Aβ peptide is formed by cleavage from its precursor protein, APP (Lamb et al., 1993; Yoshikai et al., 1991). This proteolytic cleavage is performed by two enzymes, β- and γ-secretase, in a pathway referred to as “the amyloidogenic pathway” (Haass & Selkoe, 1993). After cleavage, Aβ can be found in extracellular fluids such as cerebrospinal fluid (CSF), where it is abundant, or in plasma in which its concentration is much lower (Seubert et al., 1992). An alternative processing pathway of APP is referred to as “the anti-amyloidogenic pathway” which prevents Aβ formation. In this pathway, APP is cleaved by α-secretase, generating a truncated APP form.

The most abundant forms of Aβ are the 40 a.a. form ($A\beta_{40}$) and the 42 a.a. form ($A\beta_{42}$). $A\beta_{40}$ is more soluble than the longer $A\beta_{42}$ form, and vascular Aβ deposits are mainly composed of $A\beta_{40}$. $A\beta_{42}$ is more fibrillogenic, and insoluble, and is predominantly found in amyloid plaques (Figure 4) (Dickson et al., 1988; Suzuki et al., 1994b).

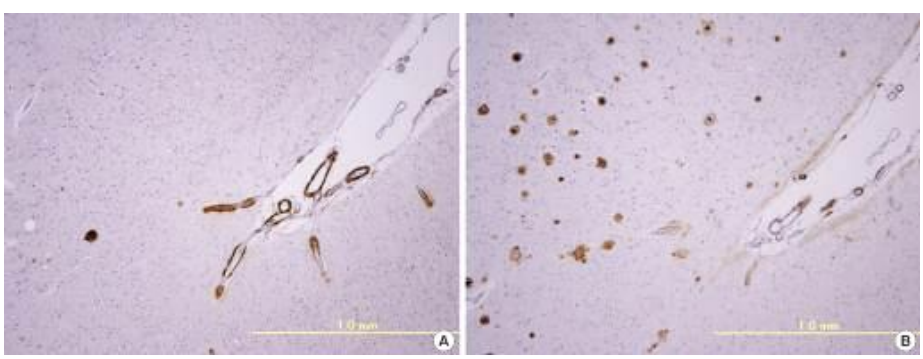

Figure 4. CAA deposits and amyloid plaques.
Adjacent brain sections from a patient with Aβ-CAA immunohistochemically stained using antibodies to $A\beta_{40}$ and $A\beta_{42}$. **(A)** $A\beta_{40}$ immunoreactivity is mainly observed in vessel walls, whereas **(B)** Aβ42 immunoreactivity is mainly observed in amyloid plaques. Reprinted from (Yamada, 2015) with permission from the *Journal of Stroke*.

The development of Aβ-CAA and AD is believed to result from an imbalance between Aβ production and clearance. In 1992, Hardy and Higgins published the “amyloid cascade“ hypothesis (Hardy & Higgins, 1992). According to this hypothesis, neurodegeneration in AD is caused by excessive deposition of Aβ and the accumulation of Aβ in the brain is the primary driving factor of AD pathogenesis (Hardy & Selkoe, 2002; Hardy & Higgins, 1992). Results from several studies suggest that overproduction of Aβ plays a major role in the pathogenesis of AD (Cacace et al., 2016). For example, the FAD associated mutations in *APP, PSEN1*, and *PSEN2*, result in overproduction of Aβ. Furthermore, Down‘s syndrome individuals, with trisomy of chromosome 21 (that contains the APP gene) develop almost identical pathological hallmarks as seen in AD (Cacace et al., 2016). In contrast, there is no firm evidence for overproduction of Aβ in sporadic cases of AD. Under normal conditions, Aβ is degraded by neprilysin or insulin-degrading enzyme and further clearance is mediated through the BBB and along perivascular drainage pathways (Preston et al., 2003; Weller et al., 2000). Weller and colleagues (Weller et al., 2008) suggested that, rather than being due to the overproduction of Aβ, the deposition of arterial Aβ is due to reduced Aβ removal from the brain via the perivascular drainage pathway of interstitial fluid (ISF) and solutes from the brain parenchyma along the vascular BM, a drainage pathway employed by the brain as it does not have a conventional lymphatic system (Morris et al., 2016). This drainage pathway was identified by studies that showed that fluorescent tracers that were injected into mouse brains became located in the BM of both arteries and capillaries within a few minutes from the time of injection (Carare et al., 2008).

1.5.6 Hereditary Cerebral Hemorrhage with Amyloidosis - D

HCHWA-D was first described in 1964 and is an autosomal dominant hereditary form of amyloidosis, like HCCAA, but is limited to the CNS (Luyendijk et al., 1988; Luyendijk & Schoen, 1964; Maat-Schieman et al., 2005; Wattendorff et al., 1982). HCHWA-D is clinically characterized by recurrent strokes and dementia (van Duinen et al., 1987; Wattendorff et al.,

1982). Genetic tests have shown that the cause of HCHWA-D is a point mutation in the *APP* gene on chromosome 21 which encodes for Aβ, that results in a single a.a. substitution, glutamine for glutamic acid, at residue 22 of Aβ (Bakker et al., 1991; Levy et al., 1990). HCHWA-D patients have reduced levels of APP in their CSF; the reason is unknown (Van Nostrand et al., 1992).

The pathological features of HCHWA-D include severe CAA, where the most affected arteries are cerebral and cerebellar meningeal arteries and cerebral cortical arteries (Luyendijk et al., 1988; Wattendorff et al., 1982; Wattendorff et al., 1995). The CAA in HCHWA-D is most severe in the occipital lobe but can affect vessels of other brain areas such as the cerebellar cortex, thalamus, and brain stem in severe cases. The spinal cord and its arachnoid mater have not been found to be affected by CAA in HCHWA-D (Maat-Schieman et al., 2005; Wattendorff et al., 1995). Initial Aβ deposits have been found to be located at the junction of the media and adventitia and can extend throughout the entire vessel wall (Maat-Schieman et al., 2005; Maat-Schieman et al., 1996). Notable pathological changes within affected vessels are a thickening of the vessel wall with lumenal narrowing, vessel-within-vessel configurations, CAA associated microvasculopathies, and amyloid deposition is accompanied with degeneration of SMCs (Luyendijk et al., 1988; Natte et al., 2001; Natte et al., 1998; Vinters et al., 1998). Studies have revealed that the main Aβ isoform in the vascular deposits is $A\beta_{40}$ (Ozawa et al., 2002). In addition to vascular Aβ deposition, perivascular deposits may be found that contain Aβ amyloid (Maat-Schieman et al., 2005).

Parenchymal deposits in the form of plaques are a part of the pathology in HCHWA-D. The plaques can be fine or dense diffuse, coarse, or homogenous; the ratio of the plaque types is age-related (Maat-Schieman et al., 2000). All of the plaques types are $A\beta_{42}$ immunoreactive, $A\beta_{40}$ immunoreactivity in plaques is variable and only some of the plaque type are congophilic (Maat-Schieman et al., 1994; Maat-Schieman et al., 2000). Some HCHWA-D patients have NFTs and dystrophic neurites with Braak stages

ranging from I-III (Maat-Schieman et al., 2004; Natte et al., 2001). Neuroinflammation consisting of reactive astrocytes and activated microglia can in some cases be observed around cerebrocortical CAA

New and old hemorrhages, along with infarcts, are found in the cerebral cortex and subcortical white matter with leukoencephalopathy, hemorrhages are rarely seen in the frontal lobes (Maat-Schieman et al., 2005). Dementia is the second most common clinical symptom of HCHWA-D and cognitive deterioration can develop in patients after the first stroke (Bornebroek et al., 1999). Unnoticed micro-hemorrhages, or microinfarcts, and diffuse white matter damage are a frequent finding in HCHWA-D and these increase with age (Maat-Schieman et al., 2005). The mean age of stroke occurrence is 50 years and the mean survival time after the first stroke is 10 years; the mean age at death is 60 years (Bornebroek et al., 1999).

Several proteins have been shown to co-deposit with Aβ in HCHWA-D, e.g. cystatin C, ApoE, several ECM proteins, amyloid-P, and ubiquitin (Haan et al., 1994a; Haan et al., 1994b; Maat-Schieman et al., 1996; van Duinen et al., 1995). The *APOE* ε4 allele in HCHWA-D patients does not influence the clinical presentation, nor does it correlate with the severity of CAA or dementia (Haan et al., 1994b; Natte et al., 2001). Demented patients show more advanced CAA load than non-demented; however no association is seen between dementia and plaques or NFTs (Natte et al., 2001).

1.5.7 Neuroinflammation in the CNS

The CNS has been described as an immune privileged site, as the BBB isolates the CNS from the peripheral immune system, however, this view is constantly under revision (Shrestha et al., 2013). Immune reactions, i.e. neuroinflammation, occur within the CNS where they are mainly driven by astrocytes, microglia, and macrophages (Figure 5) (Guillemin & Brew, 2004; McGeer & McGeer, 2013). Neuroinflammation within the CNS is a prominent pathological hallmark in AD and HCHWA-D (Maat-Schieman et al., 1997; Maat-Schieman et al., 2004; Mandybur, 1989; Shrestha et al., 2013). Neuroinflammation in AD is especially found in association with neuritic

plaques, as reactive astrocytes and activated microglia cluster around, and within, the neuritic plaque (Dickson, 1997; Itagaki et al., 1989; Rozemuller et al., 1989). Reactive astrocytes and microglia/macrophages have been observed around some arteries and capillaries in AD and HCHWA-D; however, the extent of the accumulation of these immune cells varies between vessel types and the severity of the Aβ accumulation (Maat-Schieman et al., 1997; Maat-Schieman et al., 2004; Mandybur, 1989; Rozemuller et al., 2005).

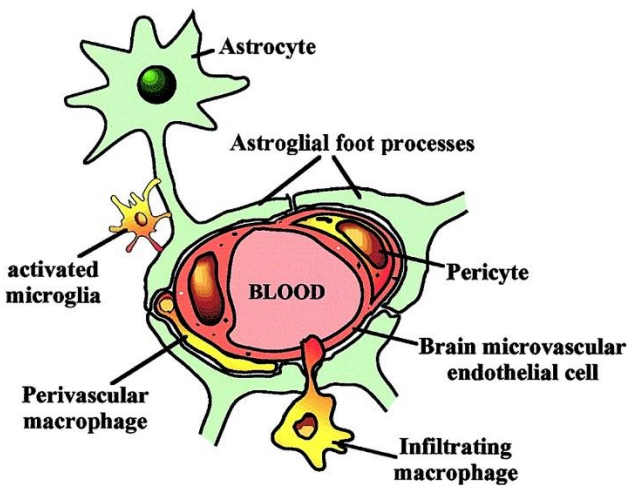

Figure 5. Immune cells in the CNS.
A simplified drawing of immune cells surrounding a normal blood vessel. Reprinted from (Guillemin & Brew, 2004) with permission from the Journal of Leukocyte Biology.

Astrocytes have a critical role in maintaining the BBB. They cover the endothelial cells of the BBB and are involved in the transport of proteins, glucose, and other products cross the BBB (Batarseh et al., 2016). Astrocytes are important for neurons and are neurosupportive as they envelope neuronal synapses (Haydon, 2001). In their natural form astrocytes are usually found in a resting state during which they have a star-like appearance and are the most abundant cell type in the CNS (Kacem et al., 1998). Astrocytes react to all forms of CNS injuries through a process referred to as “reactive astrogliosis” (Sofroniew & Vinters, 2010). During acute, or chronic, CNS injury, astrocytes react by proliferation and

morphological changes. These changes result in morphologic changes, i.e. a thicker cell body, thicker and extended processes, as well as an enhanced expression of glial fibrillary acid protein (GFAP). Reactive astrocytes can phagocytose and release proinflammatory cytokines and growth factors (Batarseh et al., 2016; Kettenmann & Verkhratsky, 2008).

Microglia are considered the first line of defense in the CNS. Resting microglia are ramified, motile, and are constantly surveilling their environment (Nimmerjahn et al., 2005). Microglia are considered the brain's macrophages. However, perivascular macrophages can cross through the BBB and into the brain (Cashman et al., 2008). When activated, microglia proliferate and their morphology changes from a small cell body with fine processes into a large cell body with thick processes. Microglia can phagocytose, act as antigen-presenting cells, and, once activated, they express the major histocompatibility complex class II-antigen (HLA-DR), secrete proinflammatory cytokines, and promote tissue repair (Kim & de Vellis, 2005; Liu et al., 2011; McGeer et al., 1988). Aggregated Aβ deposits are potent stimuli for the microglia response, as accumulation of microglia expressing HLA-DR is seen within, and around, Aβ deposits (McGeer et al., 1988). Studies on AD patients have shown that macrophages can cross the BBB but are ineffective in the clearance of Aβ in neuritic plaques (Cashman et al., 2008). *In vitro* studies show that microglia and astrocytes from AD patients can phagocytose amyloid, although their ability to degrade amyloid seems to be impaired, leading to ineffective clearance of Aβ (Fiala et al., 2005; Wyss-Coray & Rogers, 2012).

It has been suggested that the neuroinflammatory response plays an early and prominent role in AD (Cagnin et al., 2001). The literature is conflicting, as some studies suggest that the neuroinflammatory response in AD is an important reaction to tissue damage and tissue restoration, whereas others suggest that it is harmful by exacerbating Aβ deposition and contributing to neuronal dysfunction (reviewed in (Wyss-Coray & Rogers, 2012). As mentioned, the amyloid cascade hypothesis proposes that abnormal production and clearance of Aβ is the primary cause of AD and that

neurodegeneration is secondarily caused by excessive deposition of Aβ (Hardy & Selkoe, 2002; Hardy & Higgins, 1992). However, this has been questioned because studies have shown that an Aβ plaque burden does not correlate with the extent of the progression of dementia (Braak et al., 1998). Alternatively, it has been suggested that the inflammatory response in AD plays a bigger part in the pathology of the disease (McGeer & McGeer, 2013).

1.5.7.1 Glial scars

Activated astrocytes can form a so-called “glial scar”, also referred to as reactive gliosis, at the site of a CNS injury. Astrocytes are the major cellular component of this scar and the first cell type to be activated (Kawano et al., 2012; Raposo & Schwartz, 2014; Sofroniew, 2009; Sofroniew & Vinters, 2010). Reactive astrocytes upregulate their expression of GFAP, become hypertrophic, proliferate, and surround the injury site. Following CNS blood vessel injury, the BM in the blood vessel becomes the center of the injury as the astrocytes attach to the BM and the glial scar surrounds the blood vessels (Stichel & Muller, 1998). Microglia are also involved by expressing and releasing various bioactive substances along with astrocytes (Kawano et al., 2012; Raposo & Schwartz, 2014). Microglia stimulate, and recruit, endothelial cells and fibroblasts which contribute to the formation of the scar (Raposo & Schwartz, 2014). Both reactive astrocytes and fibroblasts secrete ECM proteins after CNS injury (Benarroch, 2015; Raposo & Schwartz, 2014). Fibroblasts proliferate and secrete ECM proteins, such as, laminin, COLIV, chondroitin sulfate proteoglycans (CSPGs), fibronectin, keratin sulfate proteoglycans, and tenascin C (Table 3) (Bartus et al., 2012; Kawano et al., 2012; Raposo & Schwartz, 2014; Sofroniew, 2009; Sofroniew & Vinters, 2010). Transforming growth factor-β (TGF-β) is found to be upregulated in astrocytes during glial scar formation, TGF-β being the driving factor behind the ECM production of fibroblasts (See description on TGF-β in section 1.7.8) (Logan et al., 1994; Raposo & Schwartz, 2014).

The function of the glial scar is to form a barrier between damaged and healthy tissue and it has been shown to have numerous positive functions

such as wound closure, neuronal protection, and repair of the BBB (Sofroniew, 2015). However, the glial scar can also have negative effects such as exacerbating inflammation, and it can hinder axonal regeneration after CNS injury (Raposo & Schwartz, 2014). In addition to glial scar formation around damaged arteries, reactive astrocytes with upregulated GFAP expression have been found to encircle Aβ deposits in the form of a glial scar in AD patients (Sofroniew, 2009)

Table 3. Glial scar.
Cells and extracellular components found in a glial scar.

Cell type	Extracellular components
Reactive astrocytes	BM
Microglia/macrophages	COLIV
Fibroblasts	Laminin
Endothelial cells	Fibronectin
Oligodendrocytes	CSPGs
	HSPG
	Keratan sulfate proteoglycan
	Tenascin C
	Thrombospondin

1.6 Parenchymal deposits in CNS amyloid diseases

The nomenclature for parenchymal amyloid deposits or plaques can be confusing and varies in the literature. Terms that are used include, for example: senile plaques, neuritic plaques, diffuse plaques and stellate plaques. Duyckaerts *et al.* (Duyckaerts et al., 2009) defined a classification of parenchymal deposits in AD which gives a good overview over the types of parenchymal deposits found in CNS amyloid diseases. According to Duyckaerts *et al.*, all extracellular accumulations of amyloid-forming proteins should be called deposits and the deposit types can be further defined based on immunohistochemistry, H&E, Congo red, or Thioflavin S staining. According to the outcome of these staining methods the type of deposit is defined as focal, diffuse, or stellate.

Focal deposits are visible with H&E staining, immunohistochemistry, and are smaller than diffuse plaques. Whether they consist of amyloid or have a neuritic corona varies. Focal deposits can be non-amyloid and with no

neuritic corona. Focal deposits that contain amyloid almost always have a neuritic corona. If the amyloid-containing focal deposit is surrounded by a clear halo, then they are said to be “cored” deposits and are also referred to as neuritic plaque. Neuritic plaques are associated with astrocytes and microglia.

Diffuse deposits are larger than focal deposits, i.e. ranging in diameter from 50 µm up to several hundred µm. They are not visible in H&E staining, are Congo red negative, poorly immunoreactive and are non-neuritic. Stellate deposits are small amyloid plaques that have not been studied extensively. They are small, i.e. < 5 µm in diameter, and composed of few immunoreactive granules and are likely related to astrocytes (Duyckaerts et al., 2009).

1.7 Hereditary Cystatin C Amyloid Angiopathy

HCCAA is a rare, autosomal dominant, familial amyloid disease with high penetrance, manifest by recurrent intracerebral hemorrhages in otherwise healthy, normotensive young adults. The disease is caused by mutation in the cystatin C gene (*CST3*) (Ghiso et al., 1986; Levy et al., 1989; Palsdottir et al., 1988) and is restricted to Iceland with one exception (Graffagnino et al., 1995). The disease is classified as a CAA (Palsdottir et al., 2006). Amyloid deposition in HCCAA is systemic with the most prominent pathology in the brain, but amyloid deposition is also found in organs outside of the CNS (Benedikz et al., 1990; Lofberg et al., 1987; Palsdottir et al., 2006; Thorsteinsson et al., 1988). Gene carriers have normal values of cystatin C (wild type and mutant) in their plasma, but have less than half the normal value of cystatin C in their CSF (Grubb et al., 1984a).

1.7.1 Historical background of HCCAA

The first description of the disease was in a doctoral thesis from 1935 by Árni Árnason (Arnason, 1935). He was a country physician and noticed that many young people in the northwest of Iceland were dying of brain hemorrhages. Árnason included 17 families in his study, of which he found 10 families to be

affected by the disease. There were 449 individuals in these 10 families, and by the end of his study, 79 of them had died from cerebral hemorrhage and 59% of these 79 individuals before the age of 40. Árnason concluded that the disease was genetic with dominant inheritance. Furthermore, he noted that there was a tendency for lifespan reduction through generations. A second paper about the disease was not published until 1972 by Guðmundsson *et al.* (Gudmundsson et al., 1972), they confirmed the genetic nature of the disease and that the disorder was characterized by anticipation, as indicated by Árnason in 1935 (Arnason, 1935). They also reported clinical and pathological features of the disease in post-mortem samples from five individuals. They noticed that cerebral arteries in these individuals had thickened walls and Congo red staining showed amyloid deposition. Furthermore, they suggested there was a connection between the cerebral amyloid deposition and hemorrhages in these five patients as none had a history of high blood pressure and concluded that the disease could be classified as a hereditary cerebral amyloidosis (Gudmundsson et al., 1972). In 1983, Cohen *et al.* (Cohen et al., 1983) purified amyloid fibrils from leptomeningeal vessels in post-mortem HCCAA samples and found that the amyloid contained the protein cystatin C, formerly known as gamma-trace. Later it was found that HCCAA is caused by a single base substitution mutation in the *CST3* gene (Ghiso et al., 1986; Levy et al., 1989; Palsdottir et al., 1988).

1.7.2 Genetic aspects of HCCAA

Genetic tests have shown that all HCCAA patients, and carriers, that have been investigated to date, have the same mutation in the *CST3* gene and are heterozygous for the mutated allele (Abrahamson et al., 1992; Levy et al., 1989). The mutation is a single base substitution of thymidine (T) for adenine (A) which is located in exon 2 of the gene. This part of the gene encodes the hydrophobic core of the protein and the mutation results in the exchange of leucine for glutamine at a.a. 68 of the mature form of the protein, hereafter

referred to in this thesis as L68Q-*CST3* (Ghiso et al., 1986; Levy et al., 1989; Palsdottir et al., 1988).

1.7.3 Epidemiology of HCCAA

In total, 15 HCCAA sub-families have been identified in Iceland. Most of them have been traced to ancestors who lived around the Breiðafjördur area in the West of Iceland (Palsdottir et al., 2008). The oldest known ancestor was born in that region in 1686 and moved to the South of Iceland where two subfamilies have been traced to him. At present, the mutation is still found in five families with living carriers and patients.

Microsatellite analysis suggests that the cystatin C mutation occurred about 18 generations ago. That corresponds to the 16th century. The analysis was done using DNA from 36 patients and 722 non-carrier controls using 20 microsatellites spanning 23.6 Mb on chromosome 20 (Palsdottir et al., 2008). Family trees have been constructed with the aid of pedigree data from the Blood bank, the Book of Icelanders (a database online, islendingabok.is) and from parish records in the State Archive. The parish records contain dates of birth and death and cause of death if known. Death certificates, first issued around 1911, have also been examined. By using the above data, a database with individuals suspected to have carried the mutation has been compiled and the number of individuals in this database now stands at 335 (Palsdottir, unpublished). Obligate carriers were identified due to their position in family trees relative to individuals in which the disease has been confirmed. Siblings of carriers with no offspring were only included in the database if their cause of death was registered as “brain hemorrhage” in parish records or death certificates.

At present, the average life span of carriers is approximately 30 years when calculated based on the lifespan of carriers born after 1900. In two families a marked tendency for longevity, compared to this average, has been observed. Carriers in these families live longer, and acquire symptoms later, than carriers in other families. By pooling all known families, and comparing the life span of carriers in these families in relation to year of birth

going back in time, it became evident that a marked reduction in lifespan occurred in carriers during the 19th century, starting in carriers born around 1820 (Figure 6). These data, when associated with the estimated age of the mutation, seem to suggest that the penetrance of the mutation was less during the three centuries between the mutational event (ca. 16th century) and the onset of lifespan reduction in the 19th century. Furthermore, this lifespan reduction occurred in all sub-families simultaneously regardless of the region they lived in, i.e. the West, the West Fjords, or the South of Iceland. By 1900, the lifespan had decreased from around 65 (in ca. 1820) to around 30 years, i.e. the present-day average. This negative selection on lifespan sometimes resulted in offspring of carriers dying at approximately the same time as their parents. Intriguingly, a maternal effect emerged during the same period such that carriers who inherit the mutation from their mother die on average 7.4 years earlier than those who inherit the mutation from their father (Palsdottir et al., 2008).

The driving factor behind this negative selection might be the drastic change in food habits that occurred in Iceland during the 19th century, during which the Icelandic diet became more “European” as reflected in increased imports of sugar, grain and salt. Furthermore, during this period the use of immersion in acid whey as the predominant way of preventing food from being spoiled was partially replaced by other methods. Despite this overall reduction in lifespan of carriers, a small subset of HCCAA carriers (estimated 2-4%) lives a “normal” lifespan; the reason is unknown (Palsdottir et al., 2008).

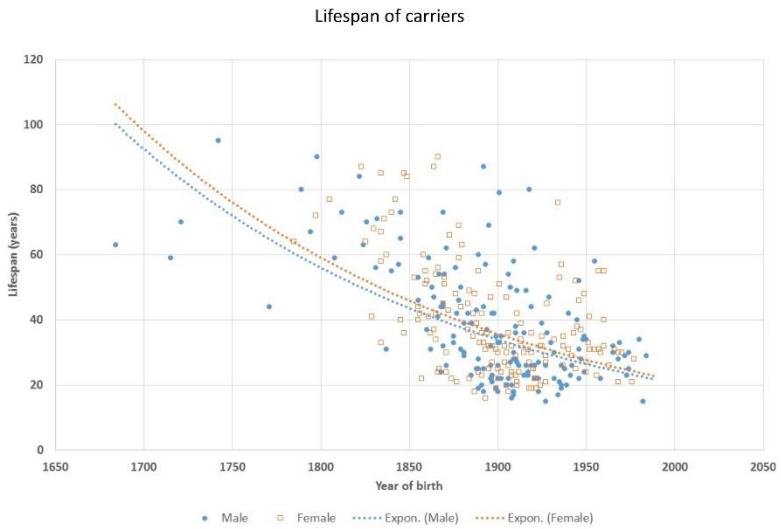

Figure 6. Lifespan of carriers by year of birth.
This figure shows the relationship between the life span of L68Q-*CST3* mutation carriers and their year of birth and the reduction in life span that occurred in L68Q-*CST3* carriers during the 19th century. The observed values for females are denoted with open squares (red), males with filled circles (blue). The x-axis shows the year of birth of each individual and the y-axis shows the lifespan in years. Updated figure 3 from (Palsdottir et al., 2008).

1.7.4 Pathological features of HCCAA

In 1972, Guðmundsson *et al.* (Gudmundsson et al., 1972), published the first paper describing post-mortem brain examination of HCCAA patients. Congo red staining confirmed amyloid deposition in the form of CAA (Gudmundsson et al., 1972). Other post-mortem studies followed and microscopic examination showed acellular, homogenous material and thickening of the walls of small and medium-sized cerebral arteries and arterioles, which narrowed their lumen, in some cases to complete occlusion. Observations showed that veins and capillaries were not, or only minimally, affected (Gudmundsson et al., 1972; Jensson et al., 1986; Jensson et al., 1987; Lofberg et al., 1987). Studies by electron microscopy showed a dense network of fibrillary material throughout the media of vessels, which were randomly arranged in non-branching fibrils (Jensson et al., 1987). Other vascular changes observed included fibrinoid necrosis, hyaline degeneration,

splitting of the media and “double-barreling”, and degeneration of SMCs in the media of the vessel wall. Finally, observations made in samples from two HCCAA patients described monocytes/macrophages in association with leptomeningeal and cortical vessels (Blondal et al., 1989; Gudmundsson et al., 1972; Jensson et al., 1986; Lofberg et al., 1987; Palsdottir et al., 2006; Wang et al., 1997; Yamada et al., 1996).

Immunohistochemical studies with cystatin C antibodies showed that arterial cystatin C amyloid deposition was strongest in the leptomeninges, but also present in the cerebrum, cerebellum, basal ganglia and spinal cord (Jensson et al., 1987; Lofberg et al., 1987). The arterial deposition was more prominent in grey matter but also found in the white matter and present throughout the vessel wall, though the intima was sometimes free of amyloid (Jensson et al., 1987; Lofberg et al., 1987; Thorsteinsson et al., 1988). Perivascular cystatin C deposits were also found in the hippocampus and basal ganglia (Thorsteinsson et al., 1988). Macroscopic and microscopic examination of the brain of HCCAA patients often showed multiple, new and old, micro- and macro-hemorrhagic lesions in both cerebral lobes, the basal ganglia and white matter in all lobes (Jensson et al., 1987; Olafsson & Grubb, 2000; Olafsson et al., 1996).

Studies have shown that organs outside the CNS do not show any macroscopic pathologic changes, though cystatin C immunohistochemistry has shown deposition in vessels, and interstitial connective tissue, of peripheral tissues such as lymph nodes, submandibular salivary glands, seminal vesicles, spleen, and skin. The cystatin C deposition in some of these tissues showed green birefringence after Congo red staining, i.e. amyloid, but not all (Benedikz et al., 1990; Lofberg et al., 1987; Palsdottir et al., 2006; Thorsteinsson et al., 1988).

1.7.5 Clinical features of HCCAA

Stroke in previously healthy young adults is the dominant clinical symptom of HCCAA. Usually patients have a sudden appearance of stroke symptoms with no precipitating event. The patient will often survive the first hemorrhage

but continue to have recurrent strokes of varying severity. The hemorrhages can lead to sensorimotor hemiparesis with or without aphasia, symptoms of neglect, and personality changes with gradual deterioration over years and progressive dementia (Blondal et al., 1990; Gudmundsson et al., 1972; Jensson et al., 1987; Sveinbjornsdottir et al., 1996). In some cases patients will suffer one or two small strokes followed by a relatively full recovery and symptom-free period which can sometimes last for several years (Blondal et al., 1990; Jensson et al., 1987). The overall symptoms depend on the location of the hemorrhage and are not different to general stroke symptoms except for their occurrence in young normotensive adults. (Blondal et al., 1990; Gudmundsson et al., 1972; Jensson et al., 1987; Sveinbjornsdottir et al., 1996).

1.7.6 Diagnosis of HCCAA

The diagnosis of HCCAA is based on a genetic test to see if the patients have the L68Q-*CST3* mutation and/or by post-mortem examination of the brain with respect to cystatin C amyloid deposition. A previously used diagnostic test was the measurement of cystatin C levels in the CSF, as L68Q-*CST3* gene carriers have abnormally low levels of CSF cystatin C (Grubb et al., 1984a).

1.7.7 Extracellular matrix

The ECM is a well-organized network composed of collagens, elastin, fibronectin, laminins, proteoglycans, hyaluronic acid, and several other glycoproteins (Theocharis et al., 2016). ECM is found in all tissues and organs where it provides structural and biochemical support to the surrounding cells along with the interstitial matrix and the BM. The ECM undergoes continuous remodeling during normal and pathological conditions which is mediated by several matrix-degrading enzymes and its composition and specific structures vary from tissue to tissue (Theocharis et al., 2016; Zimmermann & Dours-Zimmermann, 2008). Collagen is the most abundant ECM protein, as well as playing a major role in BMs. Its synthesis and secretion in the ECM is mainly by fibroblasts (Theocharis et al., 2016). The

ECM has a diverse role. It provides support, regulates tissue architecture, and influences cell behavior, e.g. cell proliferation, migration, and cellular phenotype. The formation of ECM is essential for various processes, e.g. the formation of BMs, growth, wound healing, and fibrosis (Theocharis et al., 2016; Zimmermann & Dours-Zimmermann, 2008). ECM proteins in vessels play an important role in regulating vascular function, both in normal and pathological circumstances. The ECM affects the stiffness and elasticity of the vascular wall, which is primarily dependent on collagen and elastin concentration (Xu & Shi, 2014).

The ECM in the CNS accounts for 10-20% of the total volume of the brain and is found in extracellular spaces, perineuronal nets, perisynaptic nets, and forms the cerebrovascular BM which plays an important role in the BBB (Benarroch, 2015). The composition of the ECM varies between these structures, and the ECM in the CNS has a different structure than in peripheral tissues (Benarroch, 2015). Both glial cells and neurons contribute to ECM formation in the CNS, and the expression of ECM proteins are upregulated in reactive astrocytes after CNS injury (Benarroch, 2015). The main components of the ECM in the CNS, excluding that of BM (the components of the BM are discussed in section 1.7.8), are hyaluronic acid, CSPGs (aggrecan, versican, neurocan, brevican, and phosphacan), tenascin-R, and link proteins (Benarroch, 2015; Zimmermann & Dours-Zimmermann, 2008).

An excessive deposition of ECM has been reported in various sporadic and hereditary cerebral amyloid, and non-amyloid, vascular diseases such as AD, CAA, HCHWA-D, cerebral autosomal dominant arteriopathy with subcortical infarcts and leukoencephalopathy (CADASIL), and atherosclerosis (Dong et al., 2012; Kalaria & Pax, 1995; Lan et al., 2013; Szpak et al., 2007; Tian et al., 2006; van Duinen et al., 1995; van Horssen et al., 2001). Studies have shown that various ECM proteins are associated with CAA and amyloid plaques in AD and HCHWA-D, where they interact directly with, and influence, Aβ deposition and aggregation and could thus be actively involved in the pathogenesis of these diseases (Castillo et al., 1997; Cotman et al., 2000; Kalaria & Pax, 1995; Perlmutter, 1994; van Duinen et al., 1995; van Horssen et al., 2001).

1.7.8 Basement membranes

BMs are thin sheets of specialized ECM proteins, 50 to 100 nm in thickness, which were initially identified by transmission electron microscopy (Kalluri, 2003). They are found basolateral to all cell monolayers, e.g. epithelium and endothelium, in the body and around fat and Schwann cells as well as individual SMCs in veins and arteries (Hallmann et al., 2005; Kalluri, 2003). BMs are always in contact with other cells and their function is to separate cell monolayers from connective tissue, to separate tissue compartments, and provide structural support to tissues. They are important in modulating cellular signaling pathways and provide information that influences cell proliferation, migration, and differentiation (Hallmann et al., 2005). The four major protein components of BMs are COLIV, laminin, nidogen, and HSPGs. Other minor protein components of the BM include: collagen XV, collagen XVII, agrin, fibulin, BM40, and BM90 (LeBleu et al., 2007; Sorokin, 2010).

The BM proteins are large oligomeric molecules that self-assemble to form three-dimensional networks. They are insoluble and show a tendency to aggregate (Hallmann et al., 2005). Studies have revealed that COLIV and laminin self-assemble into a network independently of each other. Nidogen has been shown to bridge the two networks and interact with HSPGs and thereby stabilize the BM network (Hallmann et al., 2005). Isoforms of each of the BM proteins exist, which combine to form structurally and functionally distinct BM (LeBleu et al., 2007; Sorokin, 2010). There are 6 isoforms of COLIV, 16 isoforms of laminin, 2 isoforms of nidogen and 2 isoforms of HSPGs (LeBleu et al., 2007; Sorokin, 2010). These different isoforms of the ECM proteins assemble in many ways which results in protein heterogeneity and in BMs that are not only structurally, but also functionally, distinct (LeBleu et al., 2007; Sorokin, 2010).

The cerebrovascular BM plays an important role in the BBB, in brain vessel development, and migration of peripheral cells into the brain (Figure 7). In addition to cerebral blood vessels, BMs in the brain surround endothelial cells in the choroid plexus and the pial surface (Benarroch, 2015). The predominant ECM constituents of the cerebrovascular BM are COLIV, laminin, HSPGs, perlecan, nidogen, and agrin. The assembly of the cerebrovascular BMs can vary, especially the assembly of laminin isoforms

between different cerebral vessel types [reviewed in (Morris et al., 2014; Yousif et al., 2013)]. Furthermore, SMCs, astrocytes, pericytes, and endothelial cells all contribute to the composition of the cerebrovascular BM [reviewed in (Morris et al., 2014)]. Cerebrovascular BMs have been reported to control the migration and differentiation of vascular cells, contributing to the mechanical properties of the vessel wall and possibly providing a pathway for the clearance of solutes out of the brain (Carare et al., 2008; Engelhardt et al., 2016; Weller et al., 1998; Weller et al., 2008).

Studies have suggested that change in cerebrovascular BM integrity and composition affect the development of CAA and have also revealed that Aβ deposits initially in the BM (Carare et al.; Perlmutter, 1994; Vinters & Pardridge, 1986; Weller et al., 2008; Yamaguchi et al., 1992).

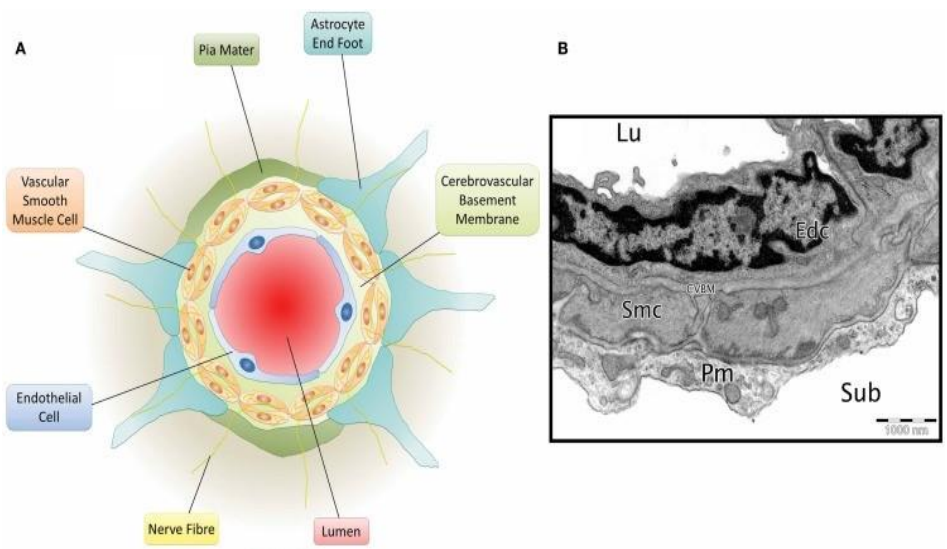

Figure 7. The cerebrovasular basement membrane.
(**A**) A diagram of a leptomeningeal artery that shows the cerebrovascular BM basolateral to the endothelium and around individual SMCs. **(B)** A micrograph of a mouse cortical artery showing cerebrovascular BM (CVBM) basolateral to endothelial cell (Edc) and around SMCs. Lu: lumen, Sub: subarachnoid space, Pm: pia mater. Reprinted from (Morris et al., 2014) with permission from Frontiers.

1.7.9 Fibrosis and TGF-β signaling

Fibrosis is characterized by excessive accumulation of ECM proteins that results in scarring and thickening of the affected tissue or organ, and is initially triggered by some kind of chronic injury to the normal architecture of the tissue (Rockey et al., 2015). Fibrosis affects the architecture and function of the underlying tissue such that connective tissues, mainly collagen, progressively replace and destroy the normal tissue architecture. It is, in fact, an exaggerated wound healing response that affects the normal function of the tissue (Wynn, 2008). Vascular fibrosis involves accumulation of ECM proteins that are normal constituents of the vessel wall. This contributes to scar formation, increased stiffness and thickness of the vessel wall, as vessels depend on the right quantities of ECM in their vessel wall to function normally (Lan et al., 2013).

TGF-β is considered to be the most important ECM regulator. The TGF-β superfamily of growth factors are the most pleiotropic and multifunctional peptides found and are expressed by many cell types (Massague, 1998). They have a wide range of cell functions, including ECM production, cell differentiation, cell proliferation, and the regulation of tissue homeostasis and repair (Massague, 1998; Piersma et al., 2015). Three different isoforms of TGF-β are found in mammals, TGF-β1, TGF-β2, and TGF-β3. TGF-β1 is the most prevalent and ubiquitously expressed isoform, while the other isoforms have a more tissue specific expression pattern (Biernacka et al., 2011; Massague, 1998). TGF-β1 is the predominantly expressed isoform in the vascular wall and is expressed by fibroblasts, vascular SMCs, endothelial cells, myofibroblasts, and macrophages (Ruiz-Ortega et al., 2007). TGF-β is synthesized as a latent complex with the latency-associated peptide (LAP). It is trapped in the ECM with latent TGF-β binding protein (LTB) in a larger complex called the large latent complex (LLC). This prevents TGF-β from making connections with TGF-β receptors. TGF-β is activated by proteolytic cleavage of the LLC and TGF-β has a high affinity for the TGF-β receptors. Signaling through the canonical TGF-β signaling pathway (Smad-dependent) is thought to be the predominant signaling pathway in fibrosis (Massague, 1998). TGF-β signals through the serine/threonine receptor kinases type I

(TβRI) and type II (TβRII). The signaling cascade begins with the binding of TGF-β to TβRII. This interaction catalyzes the phosphorylation of TβRI. The activated TβRI then binds, and phosphorylates, Smad proteins which translocate into the cell nucleus (Massague, 1998, 2012). TGF-β can also signal through alternative non-canonical (non-Smad) pathways, e.g. extracellular signal-regulated kinase (ERK), p38 mitogen-activated protein kinase (MAPK) and c-jun-n-terminal kinase (JNK) (Figure 8) (Massague, 1998, 2012).

TGF-β1 is a major regulator of fibroblast phenotype and proliferation and a potent inductor of tissue collagen deposition by fibroblasts (Massague, 1998, 2012). Locally activated tissue fibroblasts are believed to be the primary producers of ECM in response to injury. Upon activation by TGF-β1, fibroblasts migrate to the site of injury and transit to their active form, myofibroblasts, which are characterized by their elevated expression of α-SMA (Hinz, 2007).

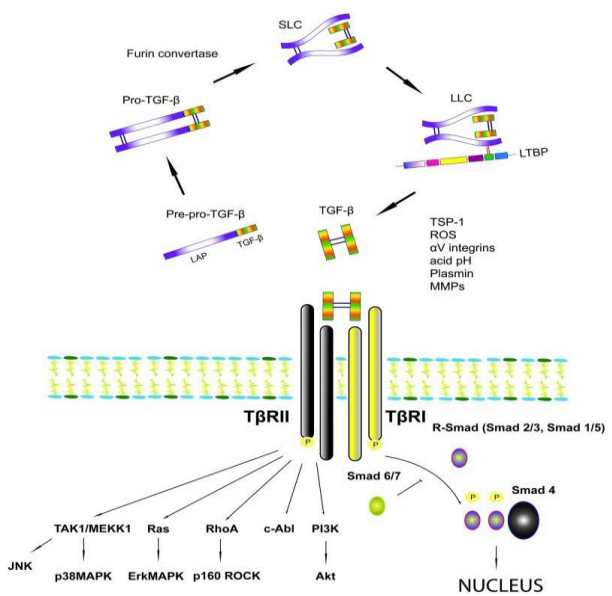

Figure 8. The TGF-β signaling pathway.
Activation of TGF-β requires proteolytic cleavage of the LLC from TGF-β. TGF-β binds to the receptors: TβRI and TβRII. TGF-β signals through the canonical pathway, which is predominant in fibrosis and is Smad-dependent, but TGF-β signals also through the non-canonical Smad-independent pathways (e.g. JNK, MAPK). Reprinted from (Biernacka et al., 2011) with permission from Taylor & Francis.

The activation and proliferation of local fibroblasts at an injury site is therefore an important step in the fibrotic cascade (Figure 9). In addition to resident fibroblasts, myofibroblasts can be derived from multiple sources. Myofibroblasts can be derived from epithelial cells in a process termed epithelial–mesenchymal transition (EMT) or from endothelial cells, in which case the process is termed endothelial–mesenchymal transition (EndMT) (Hinz, 2016; Kalluri & Weinberg, 2009). During EMT, epithelial cells, which interact with the BM, lose their epithelial characteristics and acquire a mesenchymal-like phenotype. This phenotype change is, for example, associated with E-cadherin downregulation and upregulation of vimentin and p63 in the same cells (Jonsdottir et al., 2015; Kalluri & Weinberg, 2009). These phenotype changes result in enhanced ECM production, migratory capacity, as well as resistance to apoptotic signals.(Kalluri & Weinberg, 2009).

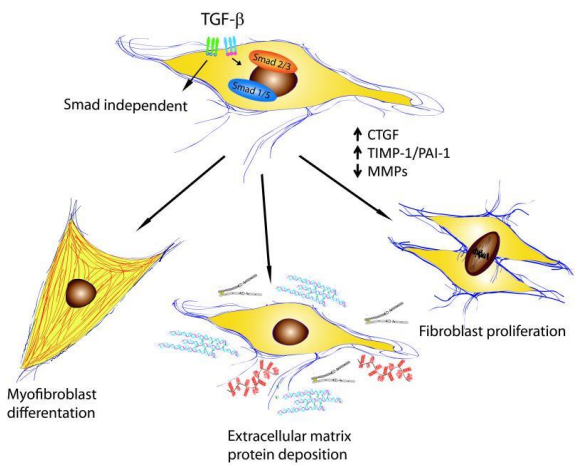

Figure 9. The effects of TGF-β on fibroblast phenotype.
TGF-β influences the phenotype and function of fibroblasts so that they transition into myofibroblasts and enhance ECM production. Reprinted from (Biernacka et al., 2011) with permission from Taylor & Francis.

1.8 Cystatins

The cystatins are a superfamily of reversible cysteine protease inhibitors which belong to the papain (C1) and legumain (C13) families (Abrahamson et al., 2003; Grubb, 2000; Turk et al., 2008). Among the first cystatins proteins identified was in the egg white from chicken. Subsequent, studies revealed that various proteins had similarities in an a.a. sequence to this chicken cystatin. These proteins are today referred to as the cystatin superfamily (Abrahamson et al., 2003; Barrett, 1986; Rawlings et al., 2016; Wallin et al., 2010). In the MEROPS database (http://merops.sanger.ac.uk), the cystatin superfamily is placed in the I25 family which is categorized into three major protein subfamilies based on size, location, and the complexity of their polypeptide chain (Abrahamson et al., 2003; Rawlings et al., 2016; Wallin et al., 2010). These families are: **1) I25A or the cystatin type 1 superfamily** (also referred to as the stefin family); cystatin A and cystatin B (stefin A and B) belong to this family. They are single polypeptide chains of about 100 a.a. residues in length, lack a signal sequence, are unglycosylated, and do not contain disulfide bonds. They are mainly found intracellularly in the cytosol of many cells, but are also found in body fluids (Abrahamson et al., 1986; Wallin et al., 2010). **2) I25B or the cystatin type 2 superfamily**; cystatin C, D, E, F, S, SA, and SN belong to this family. They consist of a single polypeptide chain of about 120 a.a. residues in length in their mature form, have a signal sequence for import into the secretory system, two disulfide bonds in the C-terminal region of the polypeptide chain, and some of them can be glycosylated. They are widely distributed throughout the body, are found primarily in the extracellular space and in most body fluids (Abrahamson et al., 2003; Barrett, 1986; Wallin et al., 2010). **3) I25C or cystatin type 3 superfamily** (also referred to as kininogens). Three different mammalian kininogens belong to this family: high and low molecular mass kininogens and T-kininogens which are only found in rats. They consist of three cystatin type 2-like domains, are glycosylated, and contain internal disulfide bonds. These cystatins are mainly found intravascular in blood plasma, and in amniotic and synovial fluid as a result of diffusion (Abrahamson et al., 2003; Barrett, 1986; Ochieng & Chaudhuri, 2010; Wallin et al., 2010).

1.8.1 Cystatin C

Human cystatin C, formerly known as gamma-trace because of its electrophoretic gamma-motility (Hochwald et al., 1967) belongs to the cystatin type 2 superfamily of cysteine protease inhibitors (Barrett, 1986). Cystatin C is the most abundant, best studied, and one of the most important extracellular cysteine protease inhibitors (Abrahamson et al., 1986; Abrahamson et al., 1988). Cystatin C is encoded by the *CST3* gene which is located in the cystatin multigene locus on chromosome 20 in humans (Schnittger et al., 1993). The gene is 4.3 kb in size and is composed of three exons and two introns and has high GC content (Abrahamson et al., 1990). The gene encodes a 146 a.a. protein. Like other cystatin type 2 proteins, cystatin C has a signal sequence for import into the secretory system which is 26 a.a. in cystatin C (Abrahamson et al., 1988). The mature form of human cystatin C thus consists of 120 a.a. residues in a single polypeptide chain (Grubb & Lofberg, 1982). Fully processed cystatin C has two internal disulfide bonds (Grubb et al., 1984b). The natural state of cystatin C is as a monomer (Abrahamson & Grubb, 1994). Monomeric cystatin C is a potent inhibitor of cysteine proteases of the papain and legumain families, especially the human papain (C1) enzymes, e.g. cathepsins B, H, K, L and S (Abrahamson et al., 1986; Grubb, 2000; Turk & Bode, 1991), a group of proteases that are predominantly found in lysosomes (Turk et al., 1997). Cystatin C forms a very tight, but reversible, complex with cathepsins (Wallin et al., 2010). Cystatin C itself is inhibited and proteolyzed by cathepsin D and elastase (Lenarcic et al., 1991). Cystatin C has been suspected to play a role in diseases besides HCCAA, e.g. AD, multiple sclerosis, and cardiovascular diseases (Table 4).

Cystatin C is produced at a constant rate and secreted by most nucleated cells (Abrahamson et al., 1986; Grubb, 1992) and is ubiquitously expressed in virtually all organs of the body and found in most body fluids (Abrahamson et al., 1986). Its concentration is particularly high in seminal plasma (~50 mg/l) and CSF (~5.8 mg/l) (Grubb et al., 1983; Lofberg & Grubb, 1979). The majority of cystatin C in the CSF is produced by the choroid plexus (Tu et al., 1992) and cystatin C is also highly abundant in brain tissue (Hakansson et al., 1996). Cystatin C levels in the CSF are five times higher than in plasma (Grubb, 1992).

Table 4. Association between cystatin C and diseases.
Table modfied and reprinted from (Jurczak et al., 2016) with permission from John Wiley and Sons.

Disease	Cystatin C
Hereditary cystatin C amyloid angiopathy (Icelandic form)	**Lower mutant cystatin C levels correspond to disease. Cystatin C is deposited as amyloid**
Rheumatoid arthritis	Higher cystatin C levels correspond to inflammation and disease
Cardiovascular disease	Higher cystatin C levels correspond to disease. Results uninfluenced by age, sex, or body-mass index of patients
Subclinical brain infarction	Higher cystatin C levels correspond to disease
Stroke	Higher cystatin C levels correspond to disease
Alzheimer's disease	*High cystatin C concentrations are toxic, optimal cystatin C concentrations protect neurons against amyloid deposition and degeneration. Low cystatin C levels in cerebrospinal fluid correlate with disease*
Multiple sclerosis	*Cleavage of carboxy terminus of cystatin C*
Diabetes	*Higher cystatin C levels correspond to disease*
Neurodegenerative diseases	*Optimal cystatin C concentrations protect neurons against amyloid deposition and degeneration*
Atherosclerosis, abdominal aortic aneurysm	*Lower cystatin C levels cause an increased activity in cysteine proteases*
Shrunken pore syndrome	*A specific pattern of the ratio of five glomerular filtration rate markers suggests that the pore diameter in the glomerular membrane is reduced*
Dementia	*Polymorphism of cystatin C gene is associated with higher or lower risk of disease*
Age-related macular degeneration	*Recessive inheritance of the cystatin C A25M mutant leads to a higher incidence of the disease, which is characterized by plaque formation. The A25T mutation is also related to this disease and the mutation occurs in an aggregation-prone region that also affects cystatin C signal cleavage*
Breast cancer	*Cystatin C is inducible by p53 leading to suppressed protein concentrations in breast cancer. Low cystatin C concentrations correlate with poor breast cancer prognosis*

[a]Bold text corresponds to diseases with definitive links to cystatin C; normal text corresponds to diseases where cystatin C protein levels can be useful for disease diagnosis; italicized text corresponds to diseases with changes in cystatin C protein levels that still require further investigation.

1.8.2 The cystatin C variant - L68Q-*CST3*

The cystatin C variant, L68Q-*CST3* differs from wild-type cystatin C in more than just the a.a. substitution. The L68Q mutation makes the mutated cystatin C protein less structurally stable and more prone to dimerization and aggregation compared to wild type cystatin C which is stable as a monomer (Abrahamson & Grubb, 1994). The mutated protein forms dimers and amyloid fibrils easily *in vitro* and *in vivo.* Wild-type cystatin C can be induced to dimerize

under special conditions, e.g. elevated temperature, low pH or with mild chemical denaturation (Abrahamson & Grubb, 1994; Bjarnadottir et al., 2001; Ekiel & Abrahamson, 1996; Nilsson et al., 2004; Wahlbom et al., 2007). Cystatin C dimers are present in the CSF and blood plasma of HCCAA patients, whereas only the monomer form is found in these fluids from healthy controls (Bjarnadottir et al., 2001).

Cystatin C amyloid isolated from HCCAA post-mortem samples showed that the protein in the amyloid deposits lacks the first ten a.a. from the N-terminus of the mature form (Cohen et al., 1983; Ghiso et al., 1986). The mutated protein retains its inhibitory function against proteases *in vitro* and the removal of the N-terminal amino acids is most likely due to post-translational modification as DNA studies have shown that the gene is intact in HCCAA patients (Abrahamson et al., 1987; Abrahamson et al., 1990). The truncation does not seem to affect the proteins stability nor does it lead to higher forms of aggregates and it has not been shown to have a relevance to the disease (Gerhartz & Abrahamson, 2002). Cystatin C isolated from monocytes and CSF from HCCAA patients, and from transfected kidney cells, consist of full length and intact protein (Asgeirsson et al., 1998; Lofberg et al., 1987; Olafsson et al., 1990; Wei et al., 1998). One study on wild-type cystatin C from CSF suggested that this truncation of cystatin C could be a storage related artefact rather than due to physiological or pathological processing of the protein (Carrette et al., 2005).

1.8.3 Cystatin C structure

The monomeric form of cystatin C consists of a five stranded antiparallel β-pleated sheet wrapped around a 5-turn α1-helix; the N-terminal subdomain of the protein in predominantly in α-helical form and the C-terminal predominantly β-sheet (Figure 10A) (Bode et al., 1988). The connectivity within the β-sheet is: (N)-β1-(α1)–β2-L1-β3-(AS)-β4-L2-(C). The inhibitory epitope in the cystatin C protein against proteases of the papain family includes the N-terminal peptide Ser1–Val10 and two β-hairpin loops, L1 and L2, aligned in a wedge-like fashion at one side of the molecule and the AS structure, which is a broad “appending structure” positioned at the opposite end of the β-sheet harbors the inhibitory epitope for proteases of the legumain family (Figure 10A) (Alvarez-Fernandez et al., 1999; Bode et al., 1988).

The dimerization of cystatin C occurs by three-dimensional domain swapping (Janowski et al., 2001) such that cystatin C refolds to produce a perfectly 2-fold symmetrical domain swapped dimer (Figure 10B). The swapped structural element consists of the α-helix and the two flanking strands, β1 and β2. Cystatin C domain swapping causes a loss of the β-hairpin loop L1 and, therefore, the loss of inhibitory activity against C1 type proteases (Ekiel & Abrahamson, 1996; Ekiel et al., 1997). An *in vitro* study on wild-type and L68Q cystatin C showed that the mutation not only leads to an enhanced tendency for dimerization but also increased amyloid fibril formation compared to the wild-type (Wahlbom et al., 2007). Electron microscopy analysis in this study showed that the mutated cystatin C fibrils showed a higher tendency for interconnection compared to the wild-type and that the cystatin C oligomers are “doughnut”-shaped. The oligomers showed a higher rate of fibrillization than the monomeric form, which indicates that the oligomers are intermediates in the transformation to amyloid fibrils (Wahlbom et al., 2007). Some studies suggest that oligomers are more physiologically toxic than the mature amyloid fibrils (Baskakov et al., 2002).

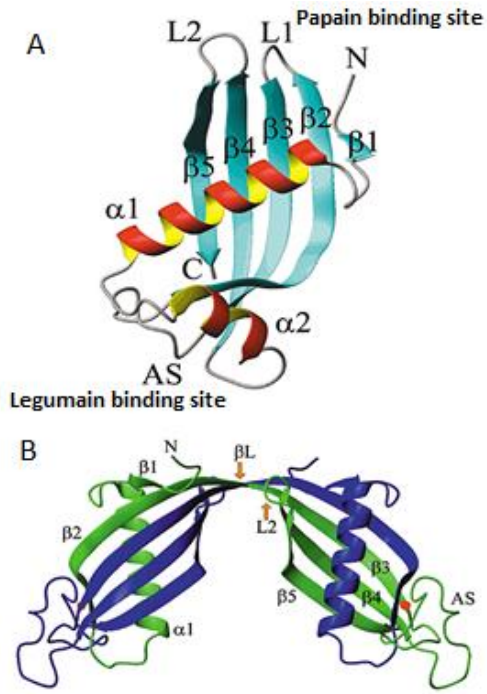

Figure 10. The structure of human cystatin C.
(**A**) The structure of monomeric cystatin C. (**B**) Domain-swapped dimer of cystatin C, red dot showing the L68Q mutation. Modified from (Janowski et al., 2001) with permisson from Nature Publishing Group.

1.8.4 Cystatin C and Aβ

Cystatin C has been found to co-localize with Aβ amyloid in amyloid-laden vascular walls and plaques in the brains of patients with AD, HCHWA-D, Down's syndrome, and cerebral infarction (Haan et al., 1994a; Itoh et al., 1993; Maruyama et al., 1990; Vinters et al., 1990) and *in vitro* studies have demonstrated high affinity binding between cystatin C and Aβ (Sastre et al., 2004). Patients with brain vessel amyloid consisting of co-localized Aβ and cystatin C are more prone to subcortical hemorrhages and have more severe vessel amyloid deposition (Maruyama et al., 1990). In these deposits, cystatin C is soluble whereas Aβ is fibrillary (Maruyama et al., 1992). Co-localization of cystatin C and Aβ has also been observed in the brains of transgenic mice that overexpress human APP (Levy et al., 2001) and in APP

transgenic mice crossbred with transgenic mice overexpressing human cystatin C (Kaeser et al., 2007). In the brains and plasma of these crossbred mice, cystatin C binds to soluble Aβ and inhibits its fibril formation (Kaeser et al., 2007). In humans, cystatin C binds to Aβ in the brain and CSF of both control and AD patients; thus, cystatin C and Aβ can interact prior to Aβ aggregation, suggesting that cystatin C plays a role in inhibiting Aβ fibril formation (Sastre et al., 2004) and furthermore, that cystatin C inhibits formation of Aβ oligomeric assemblies (Mi et al., 2009). Several studies have shown that polymorphisms within the *CST3* gene lead to an increased risk of developing AD and accelerate disease progression in AD patients, e.g. the B/B polymorphism in *CST3* results in a less efficient cleavage of the signal peptide and reduced secretion of cystatin C (Benussi et al., 2003). This reduced level of cystatin C could result in less inhibition of Aβ fibril formation and thus increase the risk of AD (Benussi et al., 2003; Sastre et al., 2004).

2 Aims

There was a lack of basic research on the pathological changes in HCCAA and the aetiology of HCCAA pathology required clarification. The first aim of this study was to increase the understanding of the pathogenesis in HCCAA with post-mortem brain samples, with special emphasis on structural changes within the arterial wall, as well as to examine the surrounding brain tissue. The results from this part of the study created a foundation for further understanding of the disorder and for the subsequent evaluation of the skin biopsies and other peripheral tissues in the second part of the study.

The second aim was to gain information about intermediate events in the pathogenesis of the disease and cell types by studying peripheral tissues, with special emphasis on the BM protein COLIV and its close association with cystatin C.

Specific aims:

- Examine in detail the cerebral vascular pathology of HCCAA by routine staining methods and immunohistochemical staining for markers normally found within the arterial wall.
- Analyse the cystatin C distribution in the CNS, its severity and topography using well defined criteria, which have been applied to other CAA diseases, as well as the distribution of cystatin C deposition in regard to hemorrhages.
- Examine the neuroinflammatory response to cystatin C deposition within the CNS.
- Examine the BM and its association with cystatin C deposition, as studies in other CAA disease have suggested that BM play an important part in the pathogenesis of those disorders.
- Evaluate intermediate events in HCCAA pathogenesis in peripheral tissues and identify the cell type responsible for the production of deposited cystatin C.

3 Material and methods

Detailed descriptions of materials and methods are present in each paper (I-III). In this section I discuss the quantification method used on immunohistochemistry data in more detail. An overview of the antibodies used in the study can be found in Table 5.

3.1 Ethics statement

All necessary permits for the use of post-mortem samples from the brain and peripheral tissues of deceased HCCAA patients and controls, skin biopsies from L68Q-*CST3* carriers and controls, and records associated with samples as well as medical information, were obtained from the National Bioethics Committee, reference numbers 04-046-S2 and 15-060-S1.

3.2 Peripheral samples (Unpublished)

Peripheral samples from three deceased patients, aged 31-57, were used and control samples from the same organs from three patients, aged 32-62. Samples were taken from the heart, tonsil, kidney, liver, lungs and stomach.

Table 5. Antibodies used in the study for immunohistochemistry.
The table shows details of the primary antibodies antibodies used for immunohistochemistry and immunofluorscence experiments in the study, as well as the staining kits and experimental conditions for each antibody.

Target protein	Company, catalog nr.	Species	Pre-treatment	Dilution and incubation
Aggrecan	Millipore, AB1031	Rabbit polyclonal	Citrat buffer, pH 2.5	1:100 for 60 min at RT*
CD31	DAKO, M0823	Mouse monoclonal	EnVision™Flex	1:10 for 60 min at RT*
CD68	DAKO, M0876	Mouse monoclonal	Citrate buffer, pH 6.0	1:200 overnight at 4°C
CTGF	SantaCruz, sc14939	Goat polyclonal	Citrate buffer, pH 6.0	1:100 for 60 min at RT*
Collagen IV	SIGMA, C1926	Mouse monoclonal	Citrate buffer, pH 6.0	1:500 for 60 min at RT*
Cystatin C	DAKO, A0451	Rabbit polyclonal	None	1:500 for 60 min at RT*
Cystatin C	Sigma, HPA013143	Rabbit polyclonal	None	1:100 for 60 min at RT*
E-cadherin	BD, BD610921	Mouse monoclonal	TE buffer, pH 9.0	1.100 overnight at 4°C
Elastin	SIGMA, E4013	Mouse monoclonal	Proteinase K[2]	1:10 for 60 min at RT*
GFAP	DAKO, Z0334	Rabbit polyclonal	None	1:250 for 60 min at RT*
HLA-DR	DAKO, M0746	Mouse monoclonal	Citrate buffer, pH 6.0	1:25 overnight at 4°C
IBA-1	Wako, 19741	Rabbit polyclonal	Citrate buffer, pH 6.0	1:1000 for 60 min at RT*
Laminin	SIGMA, L8271	Mouse monoclonal	Citrate buffer, pH 6.0	1.200 for 60 min at RT*
p63	DAKO, M7317	Mouse monoclonal	TE buffer, pH 9.0	1:50 for 60 min at RT*
Smooth muscle actin	ABCAM, ab7817	Mouse monoclonal	TE buffer, pH 9.0	1:100 for 60 min at RT*
Smooth muscle actin	DAKO, M0851	Mouse monoclonal	Citrate buffer, pH 6.0	1.50 for 60 min at RT*
Vimentin	DAKO, M7020	Mouse monoclonal	TE buffer, pH 9.0	1:500 for 60 min at RT*
pSMAD2/3	Santa Cruz, sc11769	Rabbit polyclonal	TE buffer, pH 9.0	1:200 for 60 min at RT

[1]EnvisionTM FLEX, High pH, DAKO, K8000, [2]Protease XVII, SIGMA P8038, *RT: room temperature.

3.3 Quantification of histological immunostaining

Bright field images of histological brain sections immunostained with a COLIV, laminin, or AGC1 (a aggrecan marker) antibodies (Paper I) were captured with a Zeiss Axioplan 2 microscope, coupled to an AxioCam (Carl Zeiss, Jena), at a resolution of 1300 x 1030 pixels using a Zeiss Plan Neofluar x10/0.3NA objective (Carl Zeiss, Jena). Bright field images of histological brain sections immunostained with a GFAP (an astrocyte marker), CD68 (cluster of differentiation 68, a macrophage marker), or IBA1 (ionized calcium-binding adaptor molecule 1, a microglial marker) antibodies (Paper II) and skin biopsy sections immunostained with a cystatin C or COLIV antibodies (Paper III) were captured with a Nikon Eclipse 50i microscope, equipped with a Nikon DS-Fil digital camera and a Nikon Digital Sight DS-U2 camera controller, at a resolution of 2560 x 1920 pixels using a Nikon x10/0.3NA objective for brain sections and using a Nikon x4/0.3NA objective for skin biopsy sections. Before image capture, the Köhler illumination was carefully adjusted on the microscope and the camera was calibrated for uniform field shading and white balance to ensure consistent color fidelity of the acquired images. Accurate color representation is of pivotal importance for the subsequent image analysis.

To quantify immunostaining, RGB color images were imported in ImageJ (http://rsbweb.nih.gov/, v1.47) for image analyses. For the quantification of COLIV, laminin and AGC1 deposition load within leptomeningeal arteries (Paper I), a region of interest (ROI) was drawn to outline the boundary of ten randomly chosen arteries in the stained sample (Figure 11A). For quantification of GFAP, CD68 and IBA1 immunostaining within and around arteries, an ROI was drawn by measuring randomly chosen arteries from cerebral grey and white matter in each cortical section (five arteries were measured in each sample), both vertically and horizontally and making an oval ROI surrounding the artery by adding 150 µm in every direction to the vertical/horizontal measurements (Figure 11B). For quantification of cystatin C and COLIV immunostaining in carrier and control skin biopsies, a

rectangular ROI was drawn from the peripheral edge of the epidermis and well down into the dermis (Figure 11C).

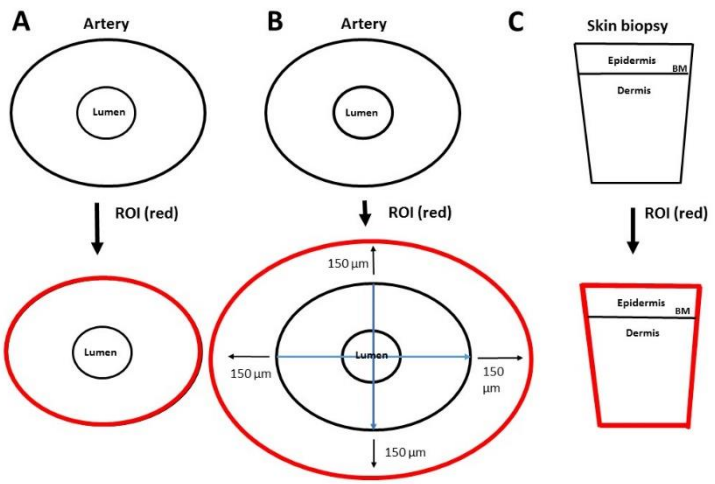

Figure 11. Region of interest (ROI).
(**A**) ROI was drawn to outline the boundary of the artery, to measure the COLIV; laminin and AGC1 deposition load within the vessel wall. (**B**) ROI was drawn by measuring each artery both vertically and horizontally and making an oval ROI surrounding the artery by adding 150 µm in every direction to the vertical/horizontal measurements. (**C**) A retangular ROI was drawn from the peripheral edge of the epidermis and well down into the dermis.

After import into ImageJ, the RGB images were transformed to the CIELAB color space which was used to replicate on the computer the colors created by the brown dye (Diaminobenzidine [DAB]) in all of the immunostainings. Channel a* or channel b* (different between immunostainings, see Papers I-III) was selected, which yielded a much higher contrast between the signal staining and differential staining or section background (an example of brain arterial cystatin C staining is illustrated in Figure 12). This was experimentally confirmed to be much superior to using any of the RGB channels (Figure 12). The selected channel a* or b* was thresholded, using the automated threshold function of ImageJ and fine-adjusted to correspond to all stained areas in the section, ensuring a minimal bleed through of differentially stained structures. Thresholded areas were marked in red by ImageJ. Using the thresholded image, the pre-selected ROIs were re-introduced, and the

percentage area fraction covered by the threshold was calculated. The resulting number reasonably describes the staining load.

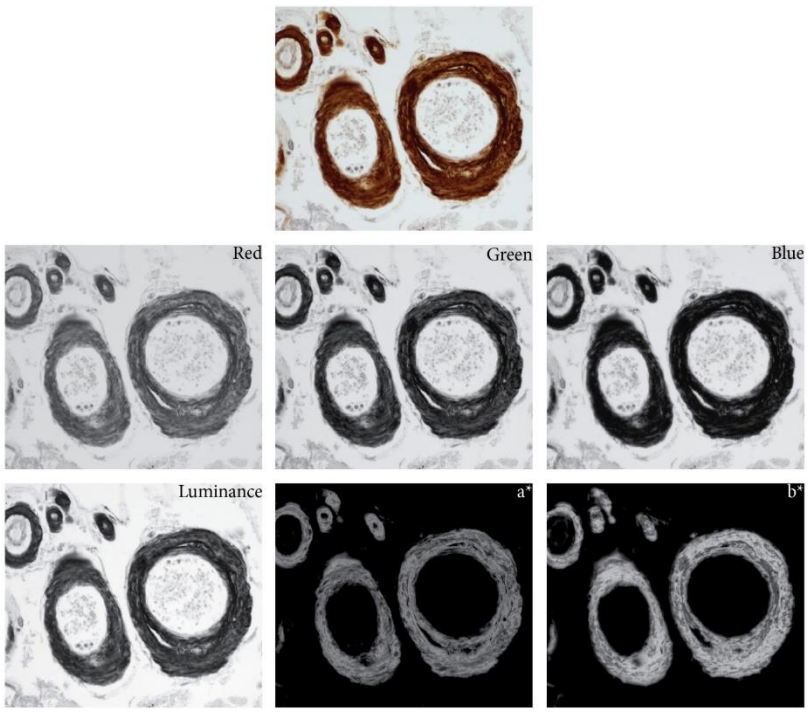

Figure 12. **An example of image analysis.**
Color image acquired on the microscope (top picture), split to its RGB channels (red, green, blue) and to its LAB components following the CIELAB colour transformation. The greatest contrast is yielded by a* and b* component of the CIELAB. Structures that are not of interest are excluded on the a* and b* channels as they contain different chromatic components, which are transformed to lower intensities in the CIELAB color space but would otherwise be present in the RGB.

4 Results

In this chapter the data presented in the published papers, appended to the thesis, will be summarized and unpublished data that are relevant to the results in the papers will be presented. The order in which the results are presented is not necessarily the same as in the papers. The Results chapter is divided into four main sections, 4.1 HCCAA brain pathology, 4.2 HCCAA skin pathology, 4.3 HCCAA pathology in peripheral organs (unpublished data), and 4.4 Proliferation and differentiation of fibroblasts in brain arteries (unpublished data).

4.1 HCCAA brain pathology

All brain samples were immunostained with a cystatin C antibody to confirm HCCAA. Leptomeningeal arteries have been shown to be the first arteries affected in Aβ-CAA (Thal et al., 2003). In order to compare the pathological profile of vessels in HCCAA patients and controls (Paper I), leptomeningeal arteries were chosen because samples from this tissue were available in autopsy material from all patients included in that study. However, examination of samples from other brain regions showed that the pathological changes seen in the leptomeningeal vascular walls of HCCAA patients were also observed in vessels in other brain areas as well. Because of this, hereafter in this section (4.1), the vascular changes described and discussed refer to vessels in all brain areas of post-mortem HCCAA samples. The characteristic pathological vascular changes, described below, were thus observed in all HCCAA brain samples, from all areas examined, i.e. sections from the cerebrum, cerebellum, midbrain, and thalamus (samples studied in Paper I and II).

4.1.1 General tissue structure

H&E staining revealed pink, acellular, homogenous deposits and thickening of the walls of most arteries and arterioles in the brain of patients. This was especially evident in the walls of small and medium-sized arteries and arterioles (Figures 13A-D). Veins and capillaries were not, or minimally, affected (Figure 1 in Paper II). In the most affected arteries/arterioles the lumen was sometimes completely occluded due to amyloid. Vessels with a "double-barrel" lumen and vessels that had undergone fibrinoid degeneration, or necrosis, were also observed. Another pathological hallmark observed in the HCCAA brain samples were infarcts (Figure 13E) and a novel finding was the that of microinfarcts which were observed in 34.6% of HCCAA patients examined in the study, as described in Paper II (Figure 13F below and Table 1 in Paper II). Of the brain areas, the most advanced pathological changes were observed in leptomeningeal arteries, however, arteries/arterioles in other brain areas, such as the cerebrum, thalamus, midbrain and cerebellum, were also highly affected (Figure 13).

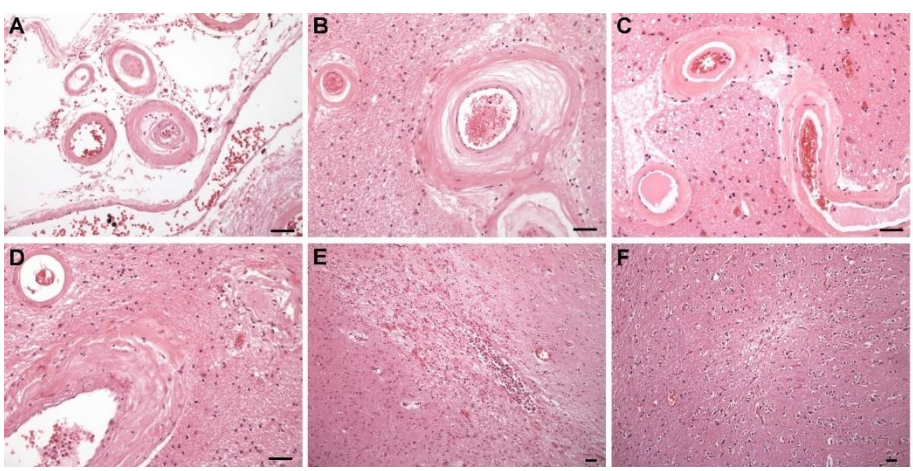

Figure 13. H&E staining of HCCAA vessels.
(**A-D**) Characteristics of pathological vascular changes of HCCAA, e.g. acellular, hyalinized amyloid deposits with thickening of the vascular wall, and arteries/arterioles with "double-barrel" lumen. (**A**) In the leptomeningeal space, (**B**) In the molecular layer of the cerebellum. (**C**) In the midbrain and, (**D**) In the thalamus. (**E**) An infarct in the thalamus. (**F**) A microinfarct in the cerebrum. Scale bars: 50 µm on all figures.

Verhoeff´s elastica staining revealed that the elastic layer in arteries of HCCAA patients was frayed. This was especially evident in smaller arteries (Figures 14A-B below and Figure 1 in Paper I). This observation also drew attention to the intima, which in some arteries was abnormal and thickened (Figure 14B below and Figure 1 in Paper I). Examination of the endothelial layer of arteries/arterioles (CD31 immunoreactivity) showed that it was sparser, and less distinct (Figures 14C-D below and Figure 1 in Paper I), than in the control samples, in which the endothelia formed a continuous layer lining the lumen. Endothelial attenuation was more evident in HCCAA arteries/arterioles that had a substantially thickened arterial wall (Figures 14C-D below and Figure 1 in Paper I). The arterial SMC layer in HCCAA has been reported to be affected (Wang et al., 1997), which concurs with the findings presented in this thesis, i.e. a degeneration of the media of the arterial wall with a significant loss of SMCs, especially in small arteries and arterioles (Figures 14E-F below and Figure 1 in Paper I).

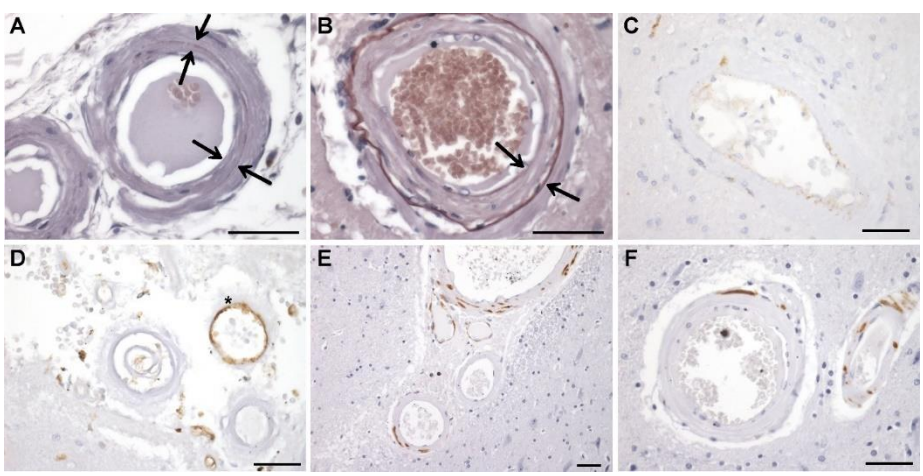

Figure 14. Pathological vascular changes in HCCAA arteries/arterioles.
(**A**) A frayed elastic layer (arrows) in leptomeningeal arterioles. (**B**) Intima thickening seen with Verhoeff´s elastica staining (arrows depict the intima) in an arteriole of the thalamus. (**C**) A sparser and less distinct endothelial layer in a cortical artery (CD31 immunoreactivity). (**D**) Degeneration of the endothelial layer (CD31 immunoreactivity) in affected leptomeningeal arterioles compared to a less affected arteriole (denoted with an asterisk) in the same image with a relatively intact endothelial layer. (**E**) Degeneration of the vascular SMC layer in cortical arteries (αSMA immunoreactivity). (**F**) A cortical artery and arteriole with few vascular SMCs (αSMA immunoreactivity). Scale bars: 50 µm on all figures.

4.1.2 Hemorrhages

Hemorrhages were observed in all brain areas, variable between patients. As described below, the availability of samples from particular brain areas (cerebrum, cerebellum, midbrain, and thalamus, Table 6) was variable between patients. Hemorrhages were not observed in tissues outside the brain.

Table 6. Hemorrhages.
An overview of the location of hemorrhages observed in the HCCAA post-mortem brain samples studied.

Cerebrum	Cerebellum	Midbrain	Thalamus
In 24 of 26 patients	In 8 of 10 patients	In 6 of 6 patients	In 5 of 5 patients

In the cerebrum, hemorrhages were observed in both grey and white matter (cerebral samples from 24 of 26 patients), although more frequently in the grey matter. In the cerebellum, evidence of hemorrhages were found in the molecular layer, and in the leptomeningeal space, in cerebellar samples from 8 of 10 patients. In the midbrain (samples from 6 patients) and the thalamus (samples from 5 patients), remnants of hemorrhages were found in all patients. Arteries/arterioles in the leptomeningeal space in all brain areas showed evidence of hemorrhages (Figure 15A). Hemorrhages in the cerebellum and thalamus of HCCAA patients had not been documented in the literature (Figures 15B-C) prior to this study.

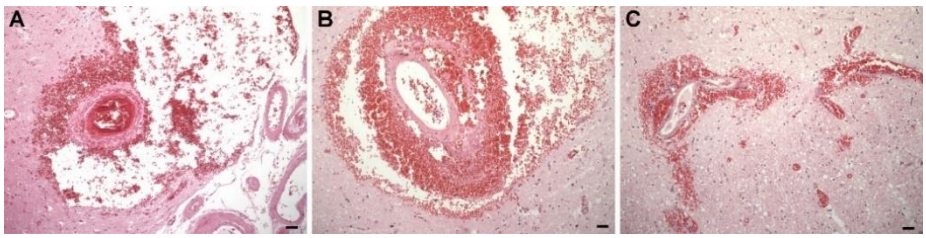

Figure 15. Hemorrhages in HCCAA.
(**A**) Evidence of hemorrhage in the leptomeningeal space. (**B**) Hemorrhage in the midbrain, near the tectum. (**C**) Evidence of hemorrhages in the thalamus. Scale bars: 50 µm on all figures.

4.1.3 Vascular cystatin C deposition in the brain

In all brain areas examined (cerebrum, cerebellum, midbrain, and thalamus) in the HCCAA patients, cystatin C deposition was observed in almost all arteries and arterioles (Figures 16 and 17). Cystatin C deposition was not observed in the controls (Figure 1 in Paper I). The distribution of cystatin C deposition, and the CAA severity, was assessed topographically in all of the brain samples. It should be noted that compared to the cerebrum, a lower number of samples were available from other brain areas, i.e. from the cerebellum, midbrain, and thalamus (Table 1 in Paper II). Cystatin C immunostaining revealed that cystatin C deposits were present in all layers of the vessel wall of affected arteries/arterioles (Figures 16A-B and Figure 17). However, in a few arteries the intima, or part of it, was devoid of cystatin C deposition (Figure 16C). As previously mentioned, the intima in many affected vessels was of abnormal thickness (Figure 16C).

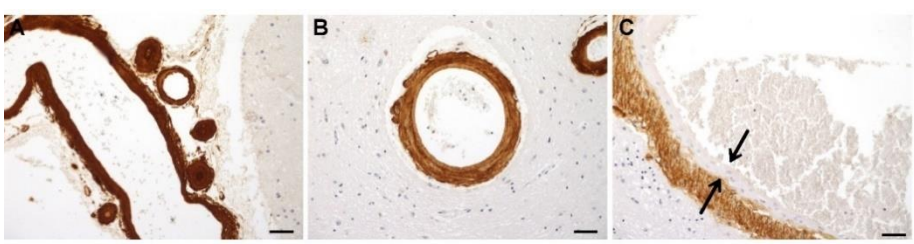

Figure 16. Cystatin C deposition.
(**A**) Cystatin C deposition in the entire vessel wall of leptomeningeal arteries/arterioles. (**B**) Cystatin C deposition in the entire wall of an artery in the midbrain. (**C**) An artery in the thalamus with cystatin C immunoreactivity in the media and adventitia but not in the intima (intima denoted by arrows). Scale bars: 50 µm on all figures.

Perivascular cystatin C deposition around affected arteries was seen in some of the patients and, in some cases, it was observed in all brain areas examined (Table 1 in Paper II). While cystatin C deposits in the vascular wall showed apple-green birefringence when viewed under polarized light following Congo red staining, perivascular deposits around affected arteries did not (Figure 2 in Paper II), suggesting that, in contrast to the deposits within vascular walls, they did not contain fully formed amyloid.

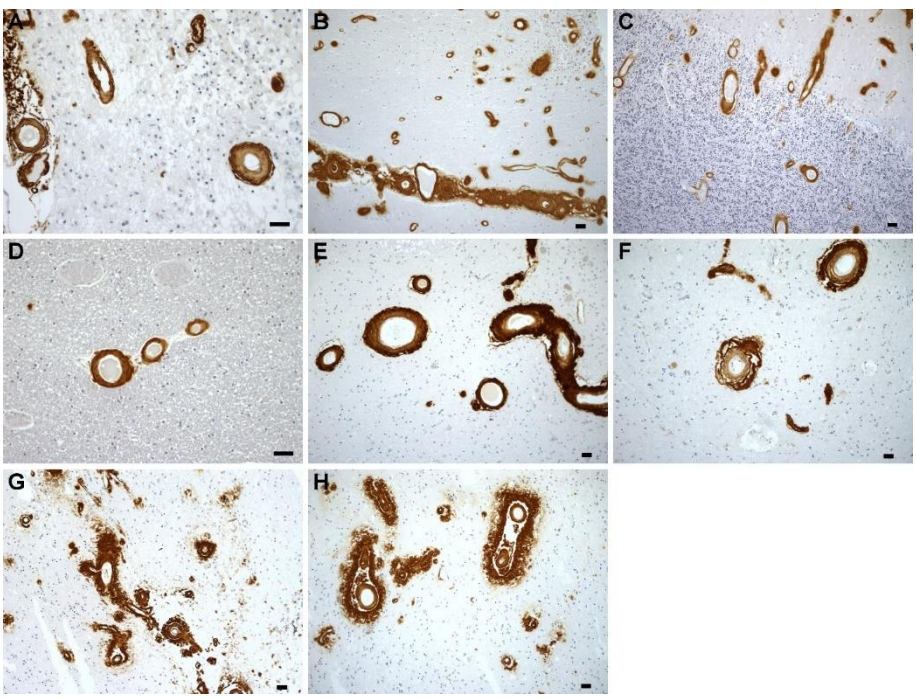

Figure 17. The distribution of cystatin C deposition in HCCAA brain samples. (**A**) Cystatin C immunoreactivity in leptomeningeal arteries and in arteries at the surface of the cerebral cortex. (**B**) Cystatin C immunoreactivity in leptomeningeal arteries in the sulcus and in the molecular layer of the cerebellum. (**C**) Cystatin C immunoreactivity in arteries in the granular layer and (**D**) in the white matter of the cerebellum. (**E**) Cystatin C deposition in arteries and perivascular deposition in the tectum of the midbrain. (**F**) Cystatin C deposition in arteries in the superior colliculus of the midbrain. (**G**) Cystatin C immunoreactivity in arteries with prominent perivascular deposition and focal deposits in the thalamus, close to the ventricle. (**H**) Cystatin C immunoreactivity showing perivascular cystatin C deposition in the thalamus, adjacent to the lateral ventricle. Figure reprinted and modified from *(Snorradottir et al., 2015)* with permission from Elsevier. Scale bars: 50 µm on all figures.

4.1.4 CAA severity

According to criteria defined by Thal *et al*. (Thal et al., 2002a), CAA severity in the brain can be classified into CAA type 1 and type 2 dependent on capillary involvement, i.e. capillaries are affected in type 1 but not in type 2. The CAA pathology can further be defined into three stages; mild, moderate, and severe, according to criteria defined by Vonsattel *et al.* (Vonsattel et al., 1991). A detailed description of these criteria is provided in section 1.5.2 of the Introduction. By applying these criteria to the HCCAA brain samples, the CAA pathology was classified as CAA type 2, i.e. capillaries were not affected in HCCAA. Furthermore, the CAA pathology was graded as “severe” in the cerebrum, cerebellum, midbrain, and thalamus of all patients examined (Figure 17).

4.1.5 Extracellular matrix accumulation in association with cystatin C deposition

The distribution of the extracellular matrix proteins COLIV, laminin, and the chondroitin sulfate proteoglycan aggrecan (AGC1), was examined in leptomeningeal vessels of HCCAA samples and compared to that of controls in the comparative study described in Paper I (Figure 2 and Table 1 in Paper I). The leptomeninges were chosen for this comparison because samples from this tissue were available in autopsy material from all the patients and controls included in that study, whereas this was not always the case for samples from other brain areas. However, similar changes in ECM distribution were also observed in vessels in all other brain areas studied from HCCAA patients and will also be addressed in this thesis.

Masson’s trichrome staining revealed extensive collagen staining in vessel walls of HCCAA patients. This staining also showed a sparse, or absent, SMC layer and an acellular appearance of the wall of the most affected arteries/arterioles, especially in arterioles (Figure 18A). Immunostaining with a COLIV antibody showed extensive, and intense, COLIV immunoreactivity in vessel walls of patients (Figures 18B-D) compared to controls, where such immunoreactivity was restricted to the BM

(Figure 2D in Paper I). The COLIV immunoreactivity in the vessels of HCCAA patients was present in all layers of the wall, i.e. the intima, media, and adventitia. In contrast to cystatin C immunoreactivity, which was sometimes absent from the intima (as described above), COLIV immunoreactivity was invariably present in the intima (Figures 18B-D). Quantitative analyses of COLIV immunoreactivity in leptomeningeal arteries of HCCAA patients and controls showed a significant increase of the immunoreactivity in the patients (Figure 6 in Paper I).

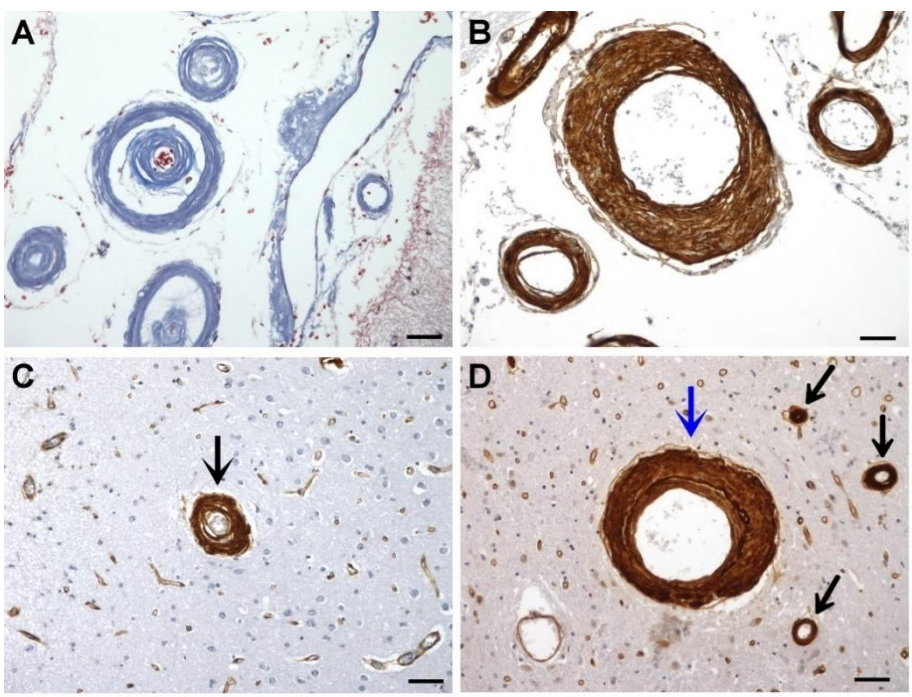

Figure 18. Collagen accumulation in HCCAA vessels.
(**A**) Masson's trichrome staining showing collagen accumulation in leptomeningeal vessels. (**B**) COLIV Immunoreactivity in leptomeningeal vessels, showing COLIV accumulation throughout the entire vessel wall. (**C**) COLIV accumulation in an arteriole (arrow) in the cortical grey matter. (**D**) COLIV accumulation in an artery (blue arrow) and arterioles (black arrows) in the midbrain in contrast to normal COLIV immunoreactivity in the capillaries that are evenly distributed in the sample. Scale bars: 50 µm on all figures.

The distribution of cystatin C and COLIV immunoreactivity in HCCAA arteries/arterioles was similar such that cystatin C deposition was always accompanied with COLIV accumulation (Figure 19). COLIV immunoreactivity in the capillaries of HCCAA patients was normal (Figures 18C-D) and, similarly, cystatin C deposition was not observed in the capillaries. This indicated a close association between COLIV accumulation and cystatin C deposition in arteries/arterioles of HCCAA patients.

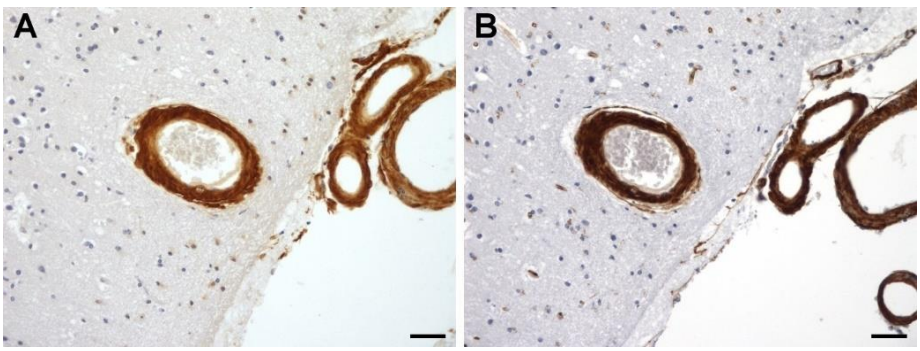

Figure 19. Cystatin C and COLIV association in HCCAA patients.
(**A-B**) Serial sections of the same vessels. (**A**) Cystatin C immunoreactivity in a cortical artery and in leptomeningeal arteries. (**B**) COLIV immunoreactivity in the same arteries shown in panel (A). Scale bars: 50 µm on both figures.

Immunohistochemical staining for laminin showed thicker laminin structures in the BMs of arteries/arterioles in patients than in controls (Figure 20A below and Figure 2 in Paper I). Quantitative analyses of laminin immunoreactivity confirmed that difference (Figure 6 in Paper I). Finally, AGC1 was distributed throughout the arterial wall of patients (Figure 20B), whereas no staining was visible in arteries of controls (Figure 2 in Paper I). Quantitative analyses of the AGC1 immunoreactivity was performed (Figure 6 in Paper I).

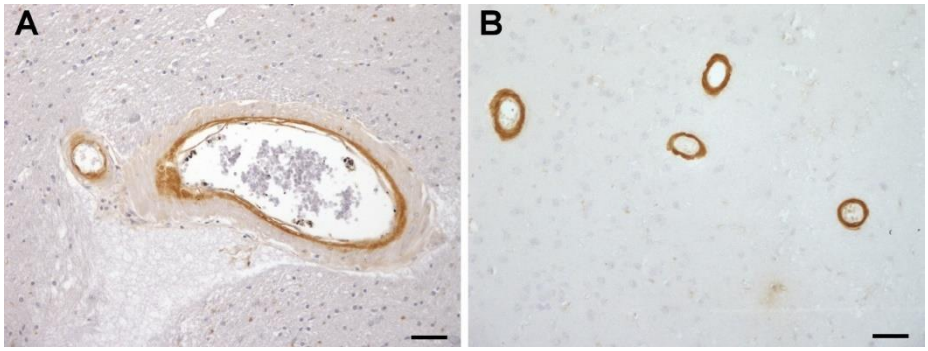

Figure 20. Laminin and AGC1 in HCCAA brain.
(**A**) A cortical artery and arteriole in the cerebrum with thick laminin structures.
(**B**) Cortical arterioles in the cerebrum with AGC1 accumulation in their vessel walls. Scale bars: 50 µm on both figures.

4.1.6 Parenchymal cystatin C immunoreactive focal deposits

Parenchymal cystatin C deposits were observed in some of the patients (Table 1 in Paper II). These deposits were found in all brain areas (Figure 21), but their location varied between patients in which they occurred. All of the deposits detected were in close regional association with areas containing severely affected arteries. The deposits showed strong cystatin C immunoreactivity, were visible by H&E staining, and were associated with neuroinflammation (Figure 4 in Paper II). However, they did not show birefringence under polarized light following Congo red staining (Figure 2 in Paper II). The size of the focal deposits was in the range of 30-50 µm in diameter. According to criteria defined by Duyckaerts *et al*. (Duyckaerts et al., 2009) (described in section 1.6 of the Introduction), these features of the deposits showed that they could be defined as focal deposits.

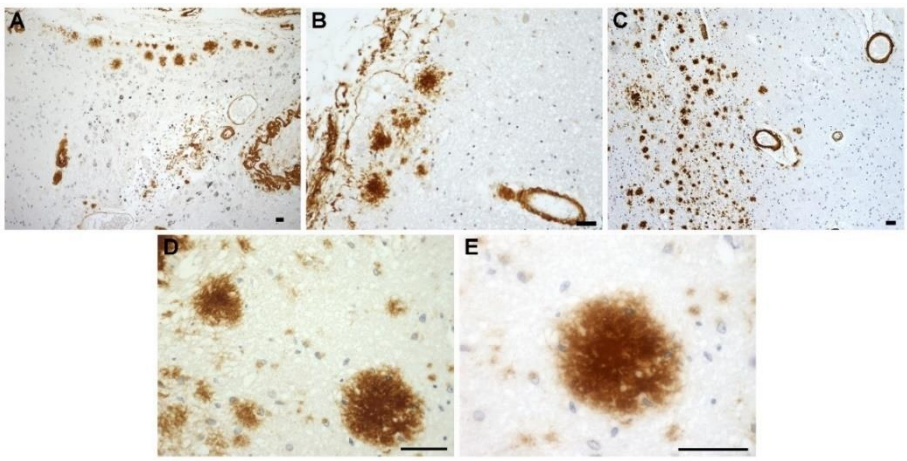

Figure 21. Focal deposits.
Cystatin C immunoreactive focal deposits in the: (**A**) cerebrum, (**B**) cerebellum and, (**C**) thalamus. (**D**) Higher magnification image of cystatin C immunoreactive focal deposits in the thalamus. (**E**) Higher magnification image of a focal deposit in the midbrain. Scale bars: 50 µm on all figures.

4.1.7 Neuroinflammation in association with cystatin C deposition

The distribution of immune cells (Paper II) was examined in all brain areas, i.e. cerebrum, thalamus, midbrain and cerebellum, of HCCAA patients by immunostaining with antibodies against GFAP (an astrocyte marker), IBA1 (a microglia marker), CD68 (a macrophage marker), and HLA-DR (an immune signalling molecule). For comparison, the immunoreactivity of GFAP, CD68, and IBA1 was quantified in cortical sections from HCCAA patients and controls.

Reactive astrocytes were observed in all brain samples from HCCAA patients. These astrocytes were immunoreactive for GFAP and had characteristics of hypertrophic/gemistocytic astrocytes, i.e. a thicker cell body and thicker, extended, processes (Figure 22).

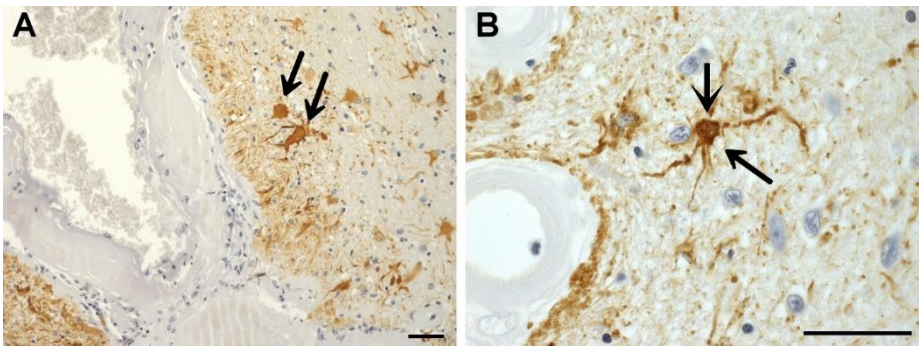

Figure 22. GFAP immunoreactivity in HCCAA.
(**A**) GFAP immunoreactivity showing reactive astrocytes with thick cell bodies and extended processes (arrows) around an amyloid-laden artery in the thalamus. (**B**) A reactive astrocyte in higher magnification, showing characteristics of a hypertrophic astrocyte (arrows). Scale bars: 50 µm on all figures.

Reactive astrocytes were in close association with cystatin C deposition in arteries (Figure 23). The number of activated astrocytes was increased around affected arteries/arterioles and the astrocytes encircled them with a compact “glial scar” (Figure 23B). Activated microglia/macrophages were also found within the glial scar (Figure 23C). In some cases, astrocyte processes were seen within perivascular cystatin C deposits surrounding arteries (Figure 5C in Paper II). In contrast, GFAP immunoreactivity in control brain samples was weak and astrocytes were found in small numbers scattered throughout grey and white matter (Figure 5 in Paper II). Quantitative analysis of GFAP immunoreactivity in cortical sections showed that the increase in immunoreactivity around arteries in patients was significant compared to controls (Figure 6 in Paper II).

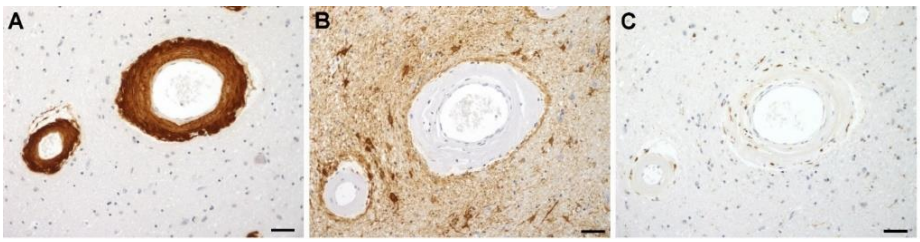

Figure 23. **A glial scar.**
(**A-C**) Serial sections of the same artery (center) and arteriole (left) in the midbrain: (**A**) Cystatin C immunoreactivity. (**B**) GFAP immunoreactivity showing a glial scar around the vessels. (**C**) CD68 immunoreactivity (macrophages) around the vessels and within the glial scar. Scale bars: 50 µm on all figures.

In addition to astrocytes and microglia cells, ECM proteins are also a part of glial scars in the CNS (Raposo & Schwartz, 2014). As described above in section 4.1.5, the accumulation of ECM proteins in HCCAA arteries/arterioles was observed. A glial scar was always found around affected vessels and these vessels also showed accumulation of ECM proteins within the vessel wall, an example of this is shown in Figure 24

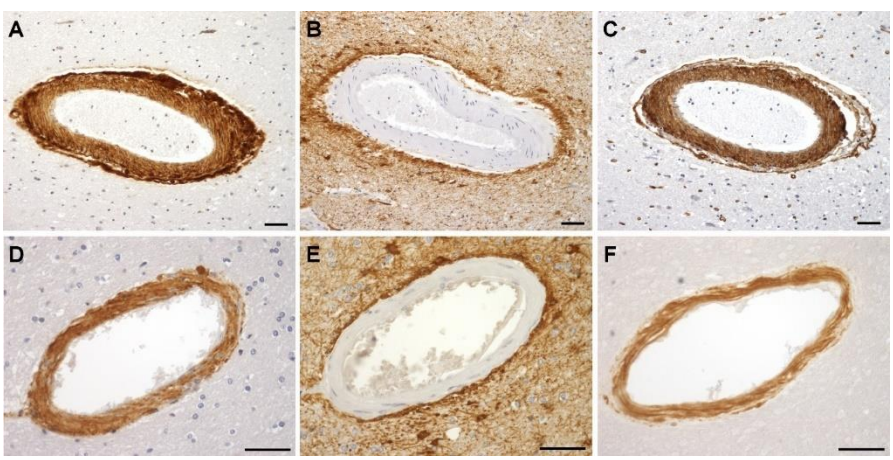

Figure 24. Glial scar and ECM proteins.
(**A-C**) Serial sections of the same midbrain artery: (**A**) Cystatin C deposition. (**B**) GFAP immunoreactivity showing a glial scar. (**C**) COLIV accumulation. (**D-F**) Serial sections of the same cerebral artery: (**D**) Cystatin C deposition. (**E**) GFAP immunoreactivity showing a glial scar. (**F**) AGC1 deposition. Scale bars: 50 µm on all figures.

Microglia close to affected arteries and around focal deposits in patients displayed morphologic features of activated microglia, i.e. enlarged cell bodies with thick, and short, processes (Figure 25). In contrast, IBA1 immunoreactive microglia in controls displayed a ramified morphology and were evenly distributed in both the grey and white matter. Quantitative analyses on the cortical sections showed that the increase in IBA1 immunoreactivity around arteries in patients was significant compared to controls (Figure 6 in Paper II). Immune cells in the affected amyloid-laden arterial wall (in the media and adventitia) of HCCAA patients which had morphologic characteristics of both activated microglia and macrophages were immunoreactive for IBA1 as well as HLA-DR; this was determined by double staining for the both markers. (Figure 7 in Paper II).

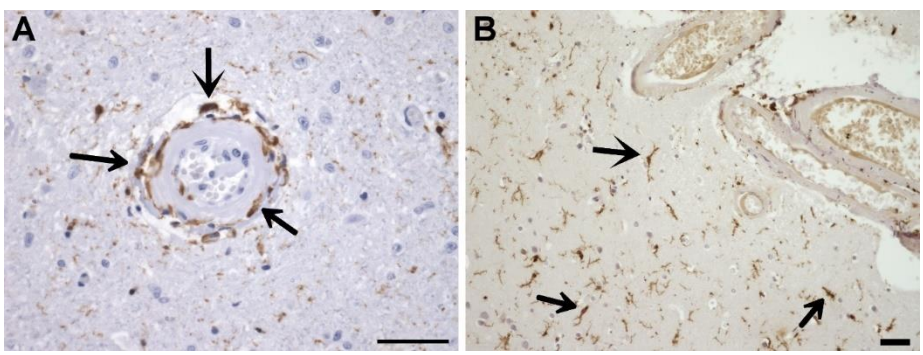

Figure 25. **Microglia response in HCCAA.**
(**A**) IBA1 immunoreactivity showing a microglial response (examples shown with arrows) around, and within, an affected arteriole in the midbrain. (**B**) IBA1 positive microglia (examples shown with arrows) adjacent to affected leptomeningeal vessels. Scale bars: 50 µm on both figures.

CD68 immunoreactive cells, i.e. macrophages, were present around, and within, affected amyloid-laden arteries (Figures 26A-B). As observed for the other immune cell markers discussed above, CD68 immunoreactivity was stronger around/within arteries with perivascular deposits. “Gaps” could be seen in the cystatin C immunoreactive areas where CD68 positive macrophages were located, suggesting that the macrophages were attempting to clear cystatin C deposits (Figures 26C-E). CD68 immunoreactive cells were also detected in infarcts after hemorrhages. In contrast, the distribution of macrophages in control brain samples was not

clustered, as seen in patient samples (Figure 5 in Paper II). Quantitative analyses of cortical sections showed that the increase in CD68 immunoreactivity around arteries in patients was significant compared to controls (Figure 6 in Paper II).

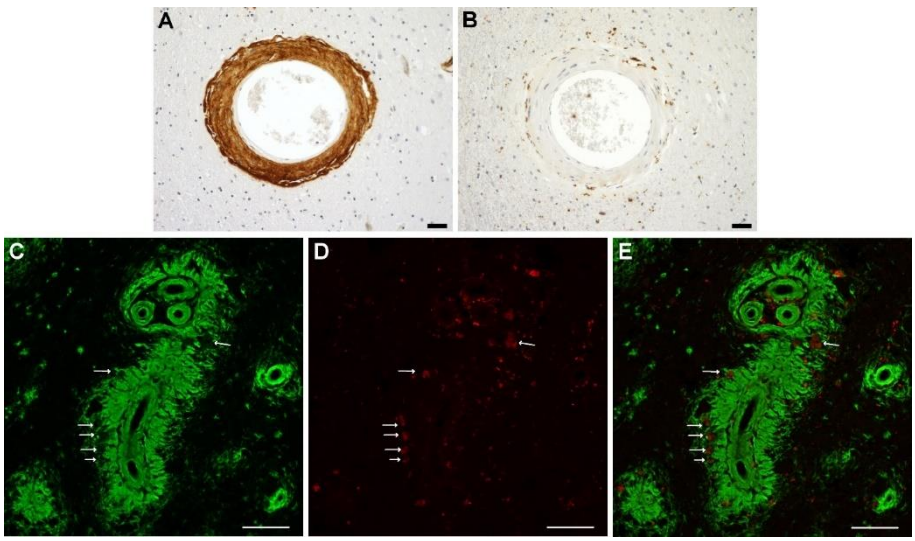

Figure 26. Macrophages in HCCAA.
(**A**) Cystatin C immunoreactivity in an artery in the midbrain. (**B**) Same artery as in panel (A) showing CD68 immunoreactivity around, and within, the vascular wall. (**C**) Cystatin C immunofluorescence staining (green fluorescence) in vessels with perivascular deposits in the thalamus. The arrows in the picture point to “gaps” In the cystatin C staining. (**D**) CD68 immunoreactivity (red fluorescence) showing macrophages (examples indicated by the arrows). (**E**) A merged picture showing both cystatin C and CD68 immunoreactivity which shows that some of the macrophages were situated within the “gaps” of the cystatin C immunoreactivity. Scale bars: 50 µm on all figures.

In addition to vessels, immunoreactivity for GFAP, IBA1, and CD68 was seen around, and within, focal deposits, and the immune cells around the deposits displayed similar characteristics of activation as the cells around vessels (Figure 27).

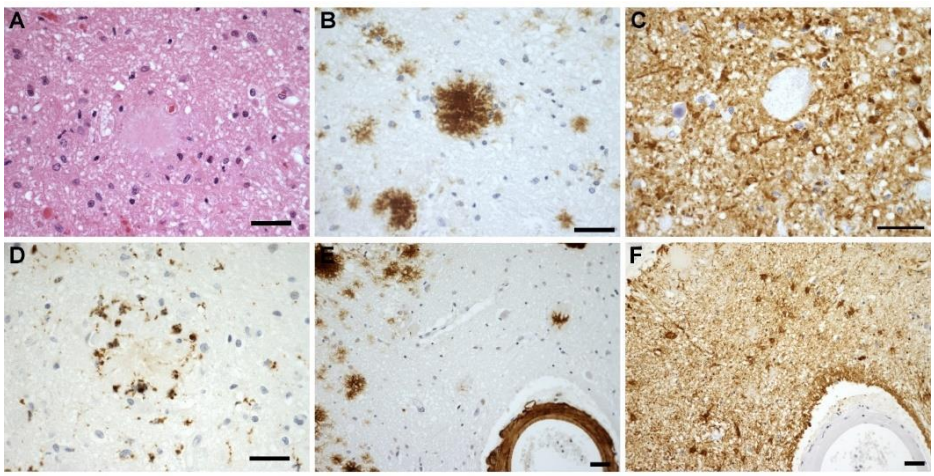

Figure 27. Focal deposits and neuroinflammation.
(**A**) A focal deposit visible by H&E staining (centre). (**B-D**) Serial sections of the same focal deposit showing: (**B**) Cystatin C immunoreactivity, (**C**) GFAP immunoreactivity, and (**D**) CD68 immunoreactivity. (**E**) Cystatin C immunoreactivity of focal deposits (upper left) and an affected artery (lower right) in the midbrain. (**F**) Same area as in (E) showing GFAP immunoreactivity and activated astrocytes. Figure modified and reprinted from (Snorradottir et al., 2015) with permission from Elsevier. Scale bars: 50 µm on all figures.

4.2 HCCAA skin pathology

Skin deposition of cystatin C in HCCAA was initially described by Benedikz *et al*. (Benedikz et al., 1990). In this study, skin biopsies were chosen because of the mild or intermediate stage of the disease in peripheral tissues and, therefore, the possibility of gaining information about early pathological changes during HCCAA pathogenesis compared to the end-stage pathology found in the brain samples. Skin biopsies from L68Q-*CST3* carriers and controls were used to perform a detailed comparison of general tissue structure, cell type distribution in the skin, as well as cystatin C and COLIV immunoreactivity. The L68Q-*CST3* carriers were divided into two categories: symptomatic or asymptomatic. Carriers were termed symptomatic if they had

been hospitalized due to cerebral hemorrhage/hemorrhages and asymptomatic if they had no record of cerebral hemorrhage before the time of biopsy.

4.2.1 General tissue structure of HCCAA skin

The examination of H&E stained skin biopsies from the central back of L68Q-*CST3* carriers did not show the characteristic vascular pathology observed in CNS arteries/arterioles, i.e. acellular, homogenous, arterial walls in dermal arteries and arterioles. However, H&E staining did reveal increased cell numbers in the upper dermis, right below the epidermis, in carrier skin biopsies (Figure 1 in Paper III). Mild inflammation was detected in biopsies from two of fourteen carriers included in the study (data not shown). Apart from this, no major deviations from the structure of normal skin (controls) were seen in the L68Q-*CST3* carrier skin biopsies (Figure 28) and the carriers did not show any clinical symptoms from the skin.

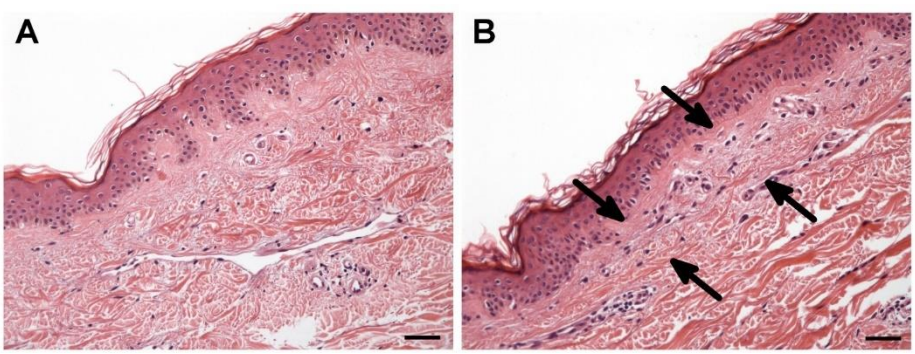

Figure 28. H&E stained skin sections.
(**A**) H&E stained control skin biopsy showing the epidermis and dermis. (**B**) H&E stained skin biopsy from a carrier showing proliferation of cells in the dermis right below epidermis (arrows). Scale bars: 50 µm on all figures.

4.2.2 Cystatin C deposition in skin biopsies

Cystatin C deposition was observed in skin biopsies from all the L68Q-*CST3* carriers, but the degree of the deposition, i.e. its quantity as well as the extent of its distribution, varied between carriers. In contrast, no cystatin C

immunoreactivity was observed in the skin biopsies from controls with the staining protocol used.

In symptomatic carriers, the cystatin C deposition was most evident in the BM between the epidermis and dermis, but was also present in BMs around dermal arteries, arterioles, veins, hair follicles, sebaceous glands, fat/sweat glands, and arrector pili muscles (Figure 29 below and Figure 1 in Paper III). In asymptomatic carriers, the deposition was not as extensive as in the symptomatic carriers, i.e. cystatin C immunoreactivity was seen in the same structures but to a lesser extent (Figure 1 in Paper III), and in three of the six asymptomatic carriers it was only observed in the BM between the epidermis and dermis (Figure 29C). Cystatin C deposition in dermal vessels was seen in both arteries/arterioles and in veins, whereas the brain veins were not, or only minimally, affected. The cystatin C deposits in Congo red stained carrier biopsies did not show apple-green birefringence under polarized light, which showed that the deposits were not in an amyloid form.

A quantitative comparison of cystatin C immunoreactivity between asymptomatic and symptomatic carriers revealed that there was an association between disease status within the central nervous system and the quantity of cystatin C immunoreactivity in skin biopsies, i.e. the cystatin C deposition in skin biopsies from symptomatic carriers was significantly elevated compared to that of asymptomatic carriers (Figure 2 in Paper III).

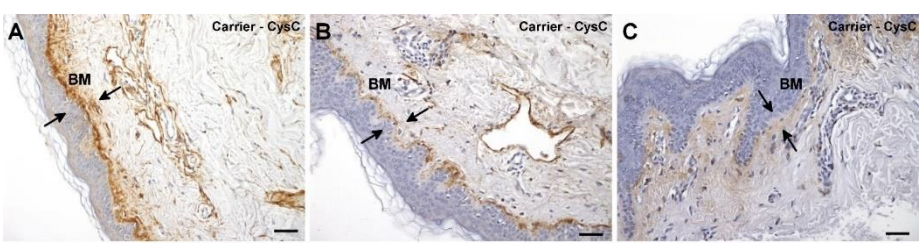

Figure 29. Cystatin C deposition in skin biopsies from L68Q-*CST3* carriers.
(**A**) Cystatin C immunoreactivity in a symptomatic carrier in the BM between the epidermis and dermis (arrows, BM) and in the BMs around dermal vessels. (**B**) Cystatin C immunoreactivity in an asymptomatic carrier showing less extensive cystatin C deposition in the BM (arrows) between the dermis and epidermis and in the BMs of other structures. (**C**) Cystatin C immunoreactivity restricted to the BM between the epidermis and dermis in an asymptomatic carrier. Figure modified and reprinted from *(Snorradottir et al., 2017)* with permission from Nature Publishing Group. Scale bars: 50 µm on all figures.

4.2.3 COLIV immunoreactivity in skin biopsies

The extensive COLIV accumulation in HCCAA brain arteries/arterioles, and its close association with cystatin C deposition, raised the question whether a similar effect could be seen in the skin of carriers and HCCAA patients. As expected, due to its expression in skin, the skin biopsies from both L68Q-*CST3* carriers and controls were immunoreactive for COLIV, which was present in the BM between the epidermis and dermis, as well as in BMs of dermal arteries, arterioles, veins, fat/sweat glands, hair follicles, sebaceous glands, and arrector pili muscles. As described in section 4.2.2, these were the same areas in the skin where cystatin C deposition was observed in the L68Q-*CST3* biopsies, manifesting the close association between COLIV and cystatin C deposition in HCCAA previously observed in the CNS (Figure 30 below and Figure 3 in Paper III).

There was a difference in the extent of COLIV deposition in the carrier biopsies compared to the controls. This difference was especially evident in the BM between the epidermis and dermis (Figure 30). In carriers the COLIV immunoreactivity in this region was more extensive, i.e. it was spread to some degree up into the epidermis and further down into the dermis (Figure 30B). In the controls COLIV immunoreactivity in this area consisted of a thin, and relatively well defined, line marking the border between the dermis and epidermis (Figures 30C-D). Quantitative analysis of COLIV immunoreactivity showed that there was a significantly elevated COLIV immunoreactivity in the carrier biopsies versus controls (Figure 2 in Paper III). However, there was no significant difference between COLIV immunoreactivity between symptomatic and asymptomatic carriers (Figure 2 in Paper III).

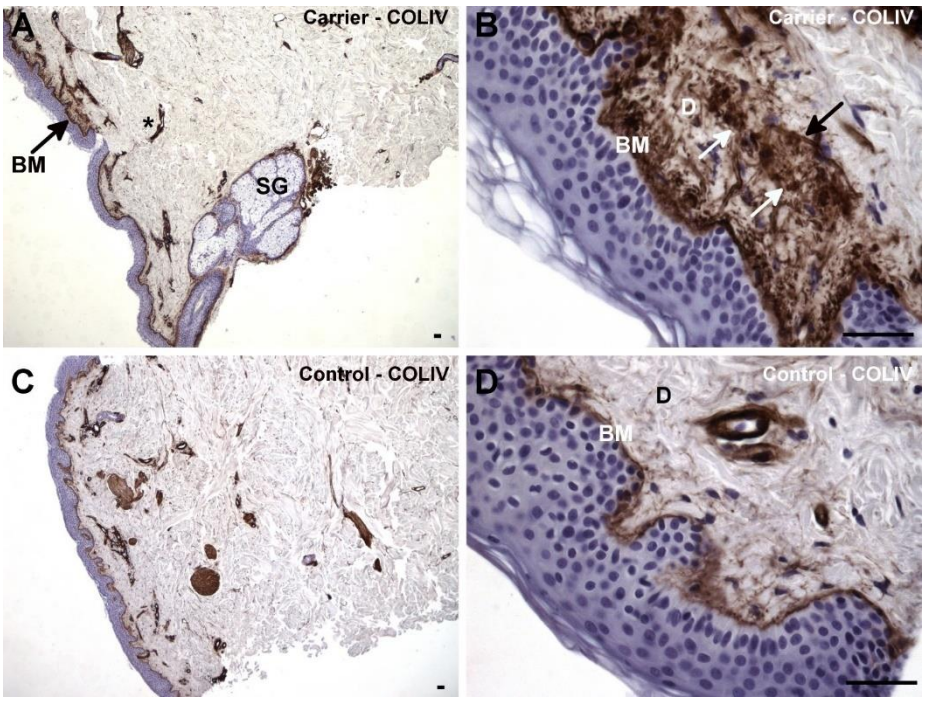

Figure 30. **COLIV immunoreactivity in skin biopsies.**
(**A**) COLIV immunoreactivity in a skin biopsy from a carrier, showing COLIV in the BM between the epidermis and dermis and in the BMs in vessels (asterisk), sebaceous glands (SG), and sweat glands. (**B**) A higher magnification image of a region from panel (A) showing COLIV immunoreactivity in the BM between the dermis (D) and epidermis and the extended, and more diffuse COLIV distribution and how it extends down into the dermis. White arrows point to density of COLIV immunoreactive cells (fibroblasts) and black arrows to thread-like collagen structures. (**C**) COLIV immunoreactivity in a control biopsy, showing a normal distribution and magnitude of COLIV immunoreactivity in the same structures as in panel (A). (**D**) A higher magnification image of panel (C) showing the BM region between the dermis and epidermis. Figure modified and reprinted from *(Snorradottir et al., 2017)* with permission from Nature Publishing Group. Scale bars: 50 µm on all figures.

4.2.4 The association between cystatin C deposition and COLIV

As mentioned, the COLIV immunoreactivity, and Masson's trichrome staining, in the carrier skin biopsy samples showed that the distribution of COLIV was very similar to that of the cystatin C deposition (Figure 31).

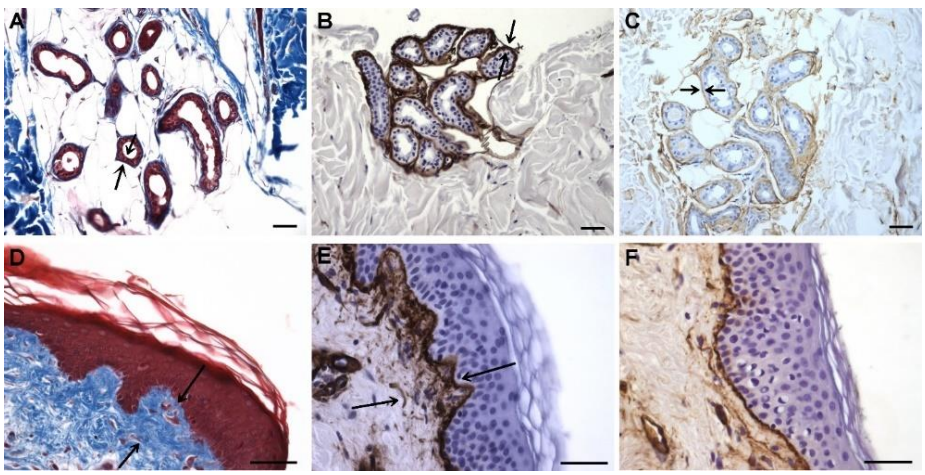

Figure 31. The close association between cystatin C and COLIV in L68Q-*CST3* skin biopsies.
(**A**) Masson's trichrome stain of sweat glands showing collagen staining (blue) in the BM (arrows). (**B**) COLIV immunoreactivity in the BM of sweat glands (arrows). (**C**) Cystatin C immunoreactivity (deposition) in the BM of sweat glands (arrows). (**D**) Masson's Trichrome staining of the BM between the epidermis and dermis, showing accumulation of collagen (darker blue) in this area (arrows). (**E**) COLIV immunoreactivity in the BM between epidermis and dermis, confirming that the collagen deposition in (D) contains COLIV. (**F**) COLIV immunoreactivity in the BM between epidermis and dermis of a control, showing a thin, relatively well defined line. Scale bars: 50 µm on all figures.

Analysis by confocal immunofluorescence microscopy confirmed that there was a close association between cystatin C deposition and COLIV in the carrier skin biopsies. In many cases, the association between the two proteins was to the degree of co-localization, i.e. an overlap of fluorescent markers (Figure 32 below and Figure 3 in Paper III), and in those instances where the proteins were not co-localized they were in close proximity.

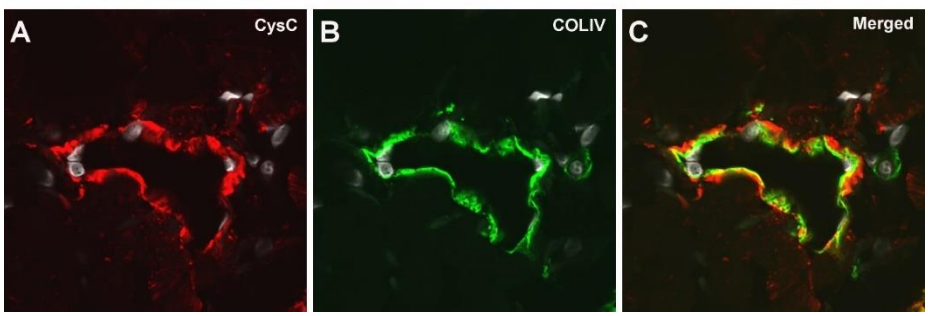

Figure 32. The association between cystatin C deposition and COLIV in L68Q-*CST3* skin biopsies.
(**A**) Cystatin C deposition in the wall of a vein. (**B**) COLIV immunoreactivity in the BM of the same vein. (**C**) The merged image shows spatial overlap (co-localization, i.e. a yellow color) of the red fluorescent label of cystatin C and of the green fluorescent label of COLIV.

In the study, the spatial overlap of fluorescent markers (co-localization) was assessed such that, in the software for the confocal microscope, a region of interest (ROI) was selected to generate an intensity profile graph for the fluorescence channels. The example shown in Figure 33 shows the intensity profile of the red fluorescence (cystatin C) and the green fluorescence (COLIV) in the ROI defined by the white line in Figure 33A. The close association of the generated profiles (Figure 33B) indicates that the location of cystatin C and COLIV immunoreactivity in the BM of the vessel was in close proximity.

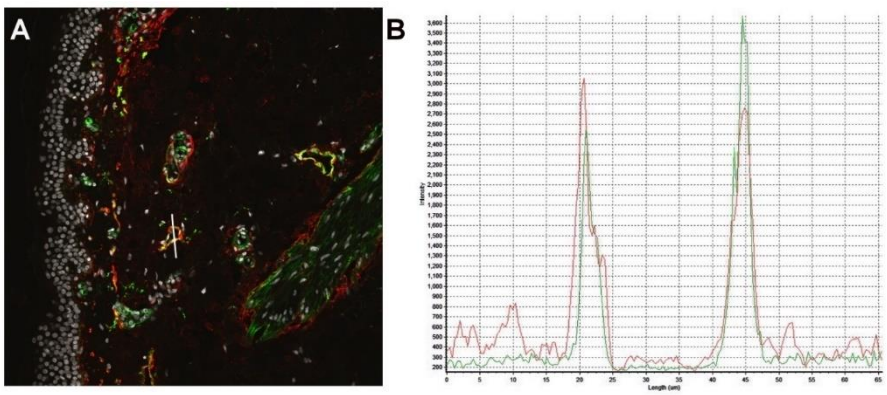

Figure 33. An example of an intensity profile analysis with regards to the spatial overlap of cystatin C and COLIV immunoreactivity in the skin of a carrier.
(**A**). A region of interest (ROI) was defined (indicated by the white line) that extended through a vessel (fluorescent markers: white: DAPI, green: COLIV, and red: cystatin C). (**B**) The intensity profile for the fluorescent markers in the ROI shows that there was a spatial association of the green (COLIV) and red (cystatin C) fluorescent markers.

4.2.5 Cystatin C and COLIV deposition were associated with fibroblasts in the skin

Certain cell types that are present in the walls of cerebral arteries are also present in the skin. Therefore, analyses of cell types that associate with cystatin C and COLIV in the skin might give important information regarding pathogenesis within arteries in the brain. Analyses with confocal immunofluorescence microscopy and immunohistochemistry were used to study the association of cystatin C and COLIV with cell types found in skin (Paper III). As mentioned, H&E staining showed a proliferation of cells in the upper dermis, right beneath the BM between the epidermis and dermis in carrier skin biopsies. These proliferating cells were positive for vimentin (a fibroblast marker) and had the morphological characteristics of stimulated fibroblasts, i.e. an enlarged cell body (Figure 34). Furthermore, these cells were negative for p63, whose expression is restricted to epithelial cells of stratified epithelia in normal skin, as well as negative for both the epithelial cell adhesion molecule E-cadherin and αSMA, which is a smooth muscle cell marker (Figure 4 in Paper III).

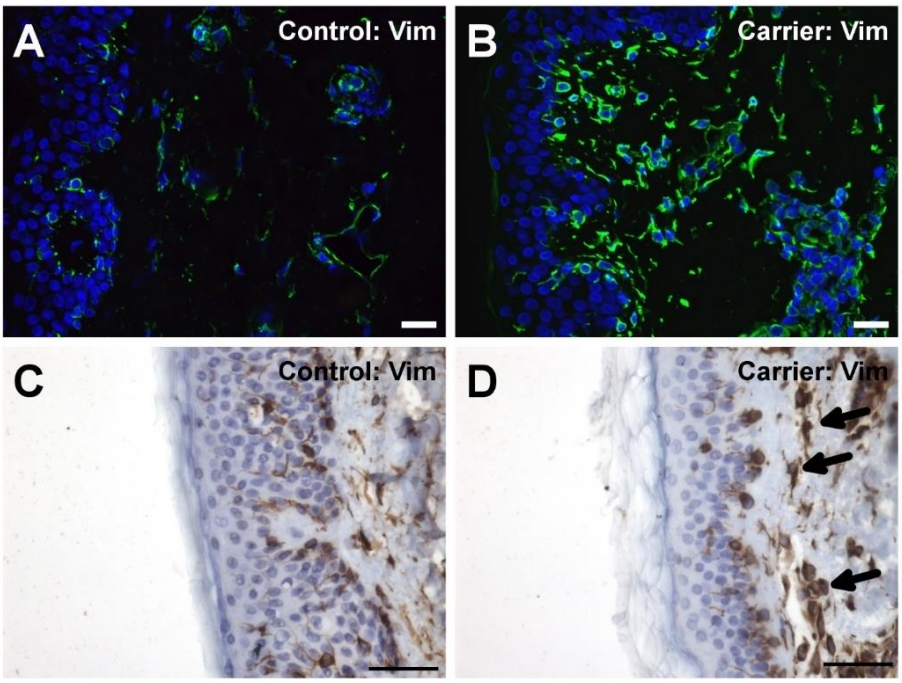

Figure 34. The proliferation of fibroblasts in L68Q-*CST3* skin biopsies.
(**A**) An image of a control biopsy showing vimentin immunoreactivity (green fluorescence) of fibroblasts in the upper dermis (blue fluorescence: DAPI). **(B)** An image of a similar area in a carrier biopsy showing an increased number of vimentin immunoreactive fibroblasts with enlarged cell bodies. **(C)** An image of a control biopsy showing the normal distribution of fibroblasts (vimentin immunoreactivity) in the epidermis and upper dermis. **(D)** A carrier biopsy showing an increased number of fibroblasts (vimentin immunoreactivity) with expanded cell bodies (arrows) in the epidermis and upper dermis. Figure reprinted and modified from *(Snorradottir et al., 2017)* with permission from Nature Publishing Group. Scale bars: 50 µm on all figures.

The analyses performed by confocal immunofluorescence microscopy highlighted the close association between fibroblasts, cystatin C deposition and COLIV (Figure 35), and in some cases cystatin C and COLIV seemed to be intracellular in fibroblasts (Figure 5 in Paper III).

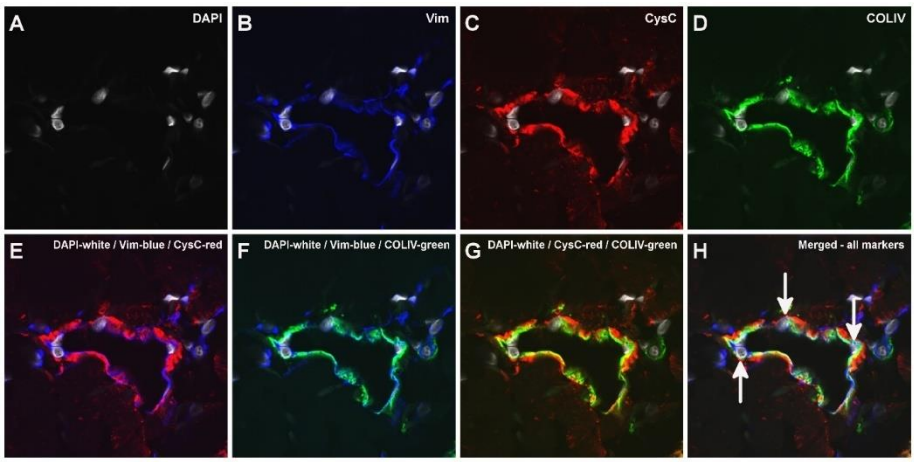

Figure 35. Close association of fibroblasts, COLIV and cystatin C.
(**A-H**) High magnification images showing immunofluorescence staining (white: DAPI, blue: vimentin, green: COLIV, and red: cystatin C) of a vein demonstrating the close association of vimentin, COLIV, and cystatin C deposition in the BM and showing cells that were immunoreactive for all three markers (arrows in H).

An ROI was defined in the vein shown in Figure 35 to assess the co-localization of the fluorescence channels with fluorescence associated with fibroblasts (vimentin immunoreactivity, blue), cystatin C (red) and COLIV (green). This profile shows the close association between these three markers (Figure 36).

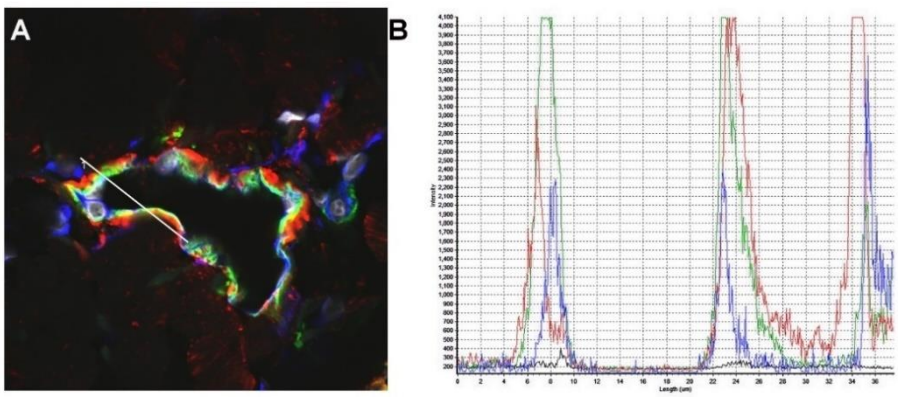

Figure 36. Intensity profile analysis of the spatial overlap of cystatin C, COLIV and vimentin in the wall of a dermal vein of a L68Q-*CST3* carrier.
(**A**). An ROI was defined (indicated by the white line) that extended through the wall of a vein (fluorescent markers: white: DAPI, blue: vimentin, green: COLIV, and red: cystatin C). (**B**) The intensity profile generated for the ROI shows that there was a close association of the blue (vimentin), green (COLIV) and red (cystatin C) fluorescent labels.

TGF-β can stimulate collagen production in fibroblasts through a SMAD-dependent signalling cascade. One step in this cascade is the phosphorylation of SMAD2/3 (Massague, 1998, 2012). The increased COLIV immunoreactivity in the carrier skin biopsies could be due to elevated TGF-β stimulation in fibroblasts. The immunoreactivity of pSMAD2/3 was examined in the skin biopsies with confocal immunofluorescence microscopy (Paper III). The nuclei of fibroblasts in biopsies from carriers and controls were immunoreactive for pSMAD2/3 (Figure 37). The difference between the pSMAD2/3 immunoreactivity between carriers and controls was therefore mainly because of the denser population of fibroblasts in the carrier biopsies compared to the controls (Figure 6 in Paper III).

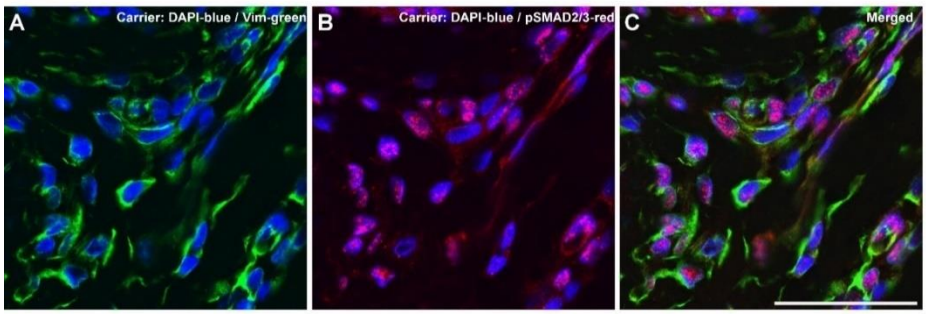

Figure 37. pSMAD2/3 immunoreactivity fibroblasts in a skin biopsy from a L68Q-*CST3* carrier.
Immunofluorescence staining (blue: DAPI, green: vimentin, and red: pSMAD2/3) of a carrier showing vimentin positive fibroblasts with pSMAD2/3 immunoreactivity in the nucleus. Figure reprinted and modified from *(Snorradottir et al., 2017)* with permission from Nature Publishing Group. Scale bar: 50 µm on all figures.

4.3 HCCAA pathology in peripheral organs (unpublished)

4.3.1 General tissue structure

When it came to peripheral tissues, relatively few post-mortem samples were available compared to the CNS and the skin. Furthermore, appropriate controls were difficult to obtain. Thus, at present, the association between cystatin C, collagen, and COLIV in peripheral HCCAA tissues has yet to be pursued further then described here in this section.

Post-mortem samples from peripheral tissues of three patients were examined. These tissues were: heart, liver, kidney, lung, tonsil, and stomach. H&E staining of sections from these samples showed normal tissue architecture, except in the case of one patient in which fibrotic changes were detected in the heart.

4.3.2 Cystatin C deposition in organs outside the CNS

Cystatin C deposition in organs outside the CNS in HCCAA patients, such as lymph nodes, submandibular salivary glands, seminal vesicles, spleen, and skin, has been described before in the literature (Benedikz et al., 1990; Lofberg et al., 1987; Palsdottir et al., 2006; Thorsteinsson et al., 1988) but it has not been previously addressed in the heart, liver, lung, or stomach. Cystatin C deposition in the three patients examined was most profound in the heart and of the peripheral tissues examined, Congo red staining of cystatin C deposits only displayed green birefringence under polarized light in samples from the heart and stomach (Figure 38). Cystatin C immunoreactivity in the heart was observed in vessels (arteries and veins) in connective tissue of focal interstitial fibrosis. In lungs and liver, the deposition was only present in vessels. In kidney, cystatin C immunoreactivity was found in vessels and tubular-interstitial tissue. In stomach and tonsil, deposition was found in vessels, interstitial tissue, and perivascular connective tissue. Examples of cystatin C immunoreactivity in these peripheral tissues are shown in Figure 39.

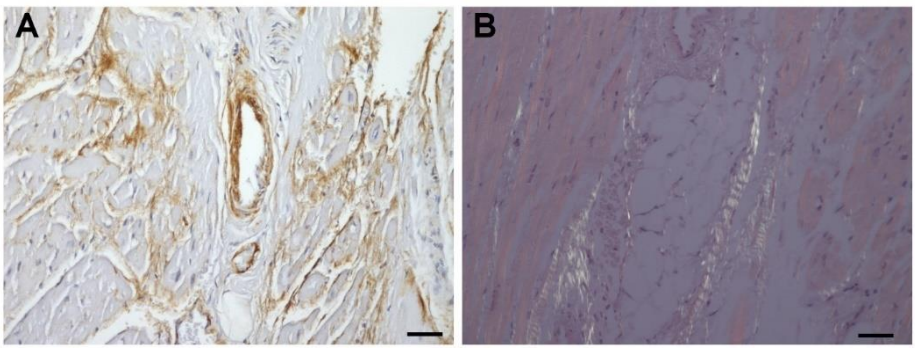

Figure 38. Cystatin C amyloid in the heart.
(**A**) Cystatin C deposition in vessels and in connective tissue. (**B**) Birefringence in polarized light in a Congo red stained heart section shows that the cystatin C deposits contain amyloid. Scale bar: 50 µm on both figures.

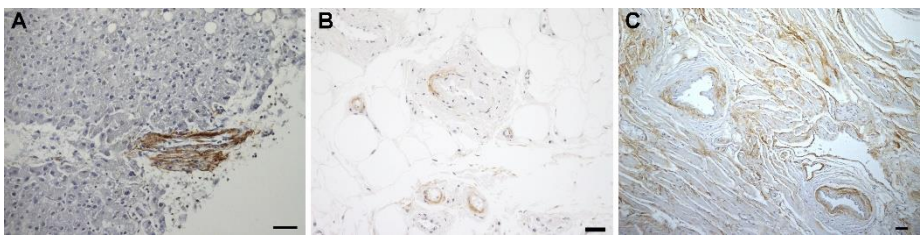

Figure 39. Cystatin C deposition in peripheral tissues from HCCAA patients.
(**A**) Cystatin C deposition in vessels in the liver. (**B**) Cystatin C deposition in vessels in the stomach. (**C**). Cystatin C deposition in vessels and in connective tissue of focal interstitial fibrosis of the heart. Scale bars: 50 µm on all figures.

4.3.3 Collagen accumulation in peripheral tissues

As in the CNS and skin, there was an association between cystatin C deposition and collagen in the peripheral tissues examined, i.e. the distribution of cystatin C deposition and that of collagen was very similar. Masson's trichrome staining showed that the collagen distribution within the tissues was the same as that of the cystatin C deposition. This was especially evident in the heart. Furthermore, Masson's trichrome staining of the heart showed focal interstitial fibrosis in one patient (Figure 40).

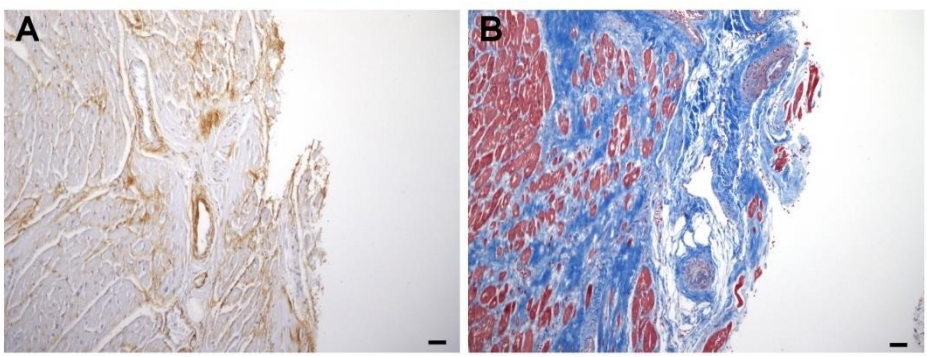

Figure 40. Cystatin C deposition and collagen accumulation in the heart of an HCCAA patient.
(**A**) Cystatin C deposition in vessels and connective tissue. (**B**) Masson's trichrome staining showing fibrosis (blue). Scale bars: 50 µm on both figures.

4.4 Proliferation and differentiation of fibroblasts in brain arteries (Unpublished)

The results from the skin described in Paper III, i.e. the close association between cystatin C, COLIV and fibroblasts, coupled with the close association of cystatin C and COLIV immunoreactivity in brain arteries/arterioles (Paper I) and in peripheral tissues (section 4.3 of this thesis), raised the question whether similar changes as those observed in the skin might also be found in some brain arteries despite the advanced pathology in the brain. Therefore, all of the brain sections from Papers I and II, were examined again to look for arteries/arterioles which displayed a slightly less advanced pathology, i.e. with the intima free of cystatin C deposition. Samples from 30 HCCAA patients were examined. The number of sections from each patient was variable as was the availability of samples

from different areas. Throughout all the samples examined (55 sample sections), only 30 arteries were found and of these there was one large artery where cystatin C deposition was only present in the BM (Figure 41). As described above, the CAA pathology in HCCAA was invariably severe and, overall, arteries in which cystatin C deposition were not found throughout the entire vessel wall were a very rare finding. When observed, however, this was almost always such that the intima was free, or partially free, of deposition.

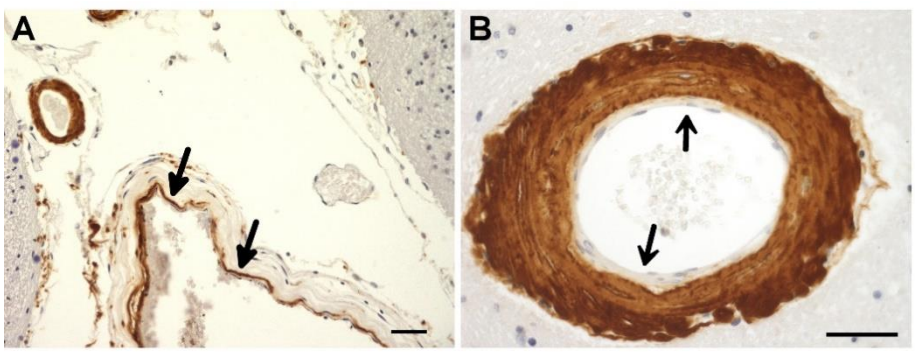

Figure 41. Cystatin C deposition in less affected HCCAA arteries.
(**A**) In 30 HCCAA patients, one large leptomeningeal artery in the cerebrum was found in which cystatin C deposition was only present in the BM (arrows). (**B**) Cystatin C immunoreactivity in a midbrain artery with part of the intima free of cystatin C deposition. Scale bars: 50 µm on both figures.

Vessels in which the intima, or part of the intima, was free of cystatin C deposition had an abnormally thick intima which appeared to contain a proliferation of cells with fibroblast morphology; fibroblasts are not normally found in the intima (Figure 41B and Figure 42). As described in the Introduction (section 1.4) the intima of normal cerebral arteries/arterioles consists of one layer of endothelial cells which is supported by the IEL and the BM (Ballabh et al., 2004). As previously mentioned, many affected arteries in HCCAA have abnormally thick intima as seen before with Verhoeff´s elastin staining and cystatin C immunostaining (Figure 14B in section 4.1.1 and Figure 41B above). By examining sections of arteries in which the intima was devoid of cystatin C deposition, the cystatin C deposition in these arteries was close to the BM/IEL and extended from the BM/IEL through the media and adventitia, whereas the intima was free of

deposition (Figure 42). Figure 42 shows an artery with cystatin C deposition reaching from the BM/IEL (blue arrows) and into the media/adventitia, with the intima free of cystatin C and containing proliferating cells. The cells found in thickened intima devoid of cystatin C deposition had an elliptical nucleus and were immunoreactive for α-SMA, which is also a marker for myofibroblasts (Figure 42C). In Figure 42C (α-SMA immunoreactivity), a few α-SMA negative endothelial cells can be seen (red arrow pointing to one) lining the lumen.

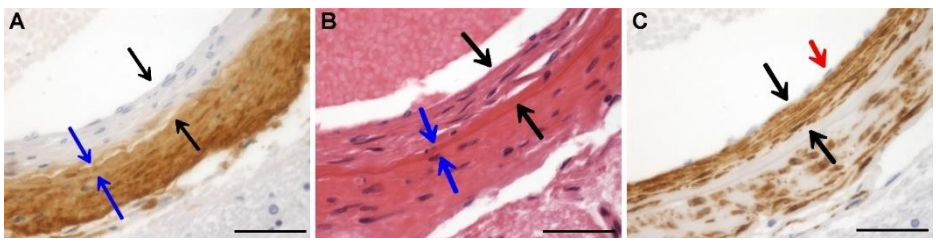

Figure 42. Cystatin C deposition and fibroblasts in an HCCAA artery.
(**A-C**) Serial sections of the same HCCAA artery in the thalamus: (**A**) Cystatin C immunoreactivity in the media and adventitia and a thickened intima free of cystatin C (black arrows) with a proliferation of cells (black arrows) and the deposition stops at the BM/IEL (blue arrows). (**B**) H&E stain showing the proliferation of cells in the thickened intima (black arrows) and the BM/IEL (blue arrows). (**C**) The proliferating cells were immunoreactive for α-SMA (black arrows). The red arrow points to an endothelial cell that does not show α-SMA immunoreactivity. Scale bars: 50 µm on all figures.

In the advanced stages of cystatin C deposition, it extended towards the intima and the endothelial cells, as seen in Figure 43 which shows more advanced deposition which has reached past the BM/IEL (blue arrows) and further into the intima compared to the larger leptomeningeal artery, with less advanced pathology in Figure 42. Furthermore, fewer cells were present in the intima in the artery shown in Figure 43 (black arrows) than in the larger artery in Figure 42. Arteries in which the intima were free of cystatin C deposition were COLIV immunoreactive throughout their entire wall (Figure 43), as were other affected vessels. This suggests that the COLIV expansion happened before the cystatin C deposition. Furthermore, COLIV immunoreactivity was found within the same area as the proliferating α-SMA

immunoreactive cells which were most likely the source of the COLIV accumulation (Figure 43).

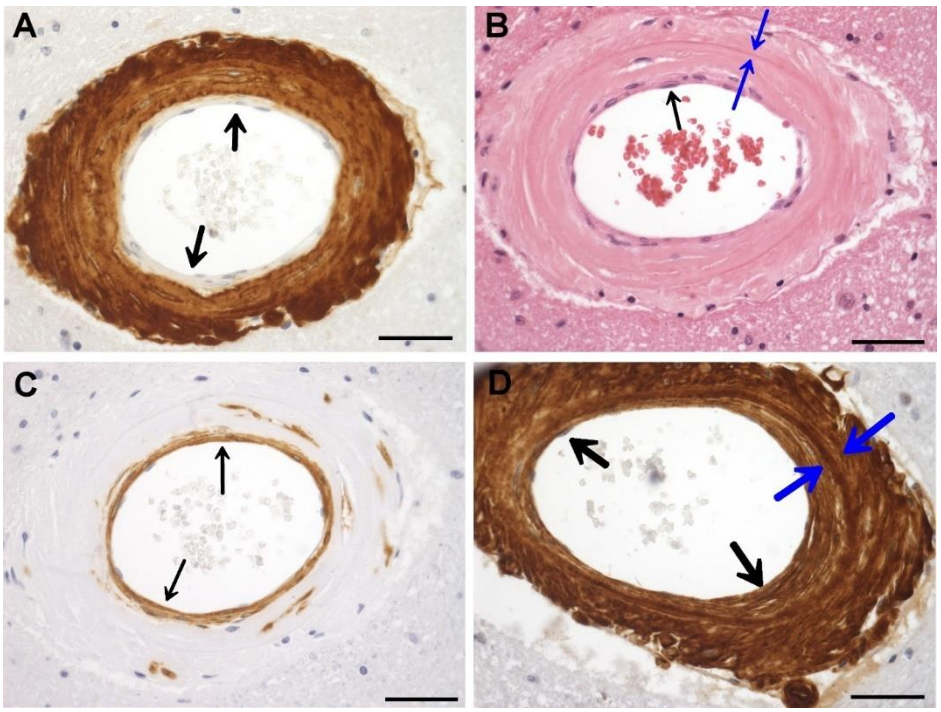

Figure 43. Cystatin C deposition and COLIV accumulation.
(**A-D**) Serial sections of the same HCCAA artery in the midbrain: (**A**) Cystatin C immunoreactivity showing that part of the intima was free of cystatin C deposition, but contained proliferating cells (arrows). (**B**). H&E stain showing the IEL (elastica, blue arrows), a very thickened intima, cells in the innermost part of the artery (black arrow) where there was no cystatin C deposition (as shown in (A)) and an acellular appearance of other parts of the arterial wall. (**C**) α-SMA immunoreactivity in the proliferating cells of the intima (arrows). (**D**) COLIV immunoreactivity throughout the entire vessel wall, black arrows point to COLIV immunoreactivity in the intima and blue arrows point to the IEL. Scale bars: 50 µm on all figures.

Arteries/arterioles with cystatin C immunoreactivity in the entire vessel wall had a relatively acellular appearance compared to arteries/arterioles in which the intima, or part of it, was free of cystatin C deposition (Figure 44).

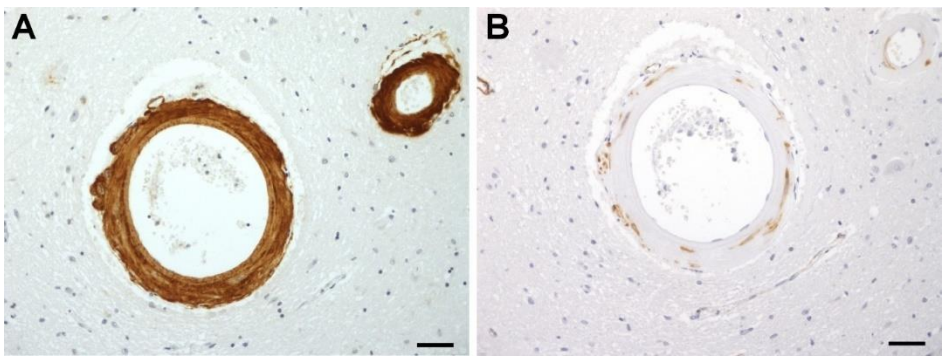

Figure 44. Cystatin C and smooth muscle cells in HCCAA.
(**A**) Cystatin C immunoreactivity in two vessels in the midbrain with cystatin C deposition through the entre vessel wall. (**B**) αSMA immunoreactivity in the same vessels as in (A) showing that there are few smooth muscle cells left in the vessel walls. Scale bars: 50 µm on both figures.

5 Discussion

HCCAA is classified as a CAA disorder because of its strong cerebral presentation. Mutant cystatin C forms amyloid deposits in the walls of cerebral arteries resulting in cerebral hemorrhages and premature death in young adults. The average life expectancy of carriers is 30 years although a small subset of carriers (estimated 2-4%) lives longer; the reasons are unknown (Palsdottir et al., 2008; Palsdottir et al., 2006). This study was performed to advance understanding of details of the pathogenesis of HCCAA, both in the CNS as well as in peripheral tissues, as well as to evaluate the intermediate events during the progress of HCCAA pathogenesis and, in addition, to identify cell types involved in the disease.

The study showed that pathological changes were most severe within the CNS and consequently the clinical symptoms appear to be associated with alterations to the blood vessels and parenchyma of the brain. Although the most advanced pathological changes are found within the CNS, the pathology in HCCAA is systemic and characterized by the presence of cystatin C deposits, and Congo red birefringent amyloid, in peripheral tissues of patients as well as in the brain, as shown in this study and those of others (Benedikz et al., 1990; Lofberg et al., 1987; Palsdottir et al., 2006; Thorsteinsson et al., 1988).

The material used for this study were brain samples available from autopsies, post-mortem peripheral tissue samples, and skin biopsy samples from L68Q-*CST3* carriers. Detailed analyses were performed on the pathology of the arterial wall and associated changes in the post-mortem brain samples showing the end-stage pathology of the disease. Although these samples gave important results regarding the pathology, the lack of intermediate pathological changes in the samples made interpretation of the sequence of pathological events difficult.

There is no functional animal model of HCCAA. Transgenic mice have been produced that express the L68Q-*CST3* variant under the control of the

neuron specific Thy-1 promoter (Kaeser et al., 2007) as well as the human *CST3* promoter (Pawlik et al., 2004), but neither model showed cystatin C amyloid deposition or cerebral hemorrhages. In this study, skin biopsy samples were chosen to try to evaluate intermediate events in the pathogenesis of HCCAA. This tissue type was chosen because it had been previously shown that carriers have cystatin C deposits in various structures of the skin (Benedikz et al., 1990). Another reason was the relative ease of access and non-invasive nature of sampling, thus facilitating a comparative study of carriers and controls using samples of the same size and from the same location (upper back).

It was hypothesized that cell types that could be responsible for cystatin C production, and therefore its deposition, in the brain were probably found within the arterial wall, or its vicinity. Furthermore, because cystatin C deposition is systemic, it was likely that such cell types were to be found systemically throughout the body and not limited to the CNS. Due to the end stage pathology of the brain samples it was difficult to use them to address this question. In the brain samples, almost all arteries/arterioles were severely affected by amyloid deposition and consequently cell death. However, a few arteries (n=30) were identified with a slightly less advanced pathology which had an increased number of fibroblasts in the intima. In contrast to the brain, the skin biopsies had very mild, or intermediate, HCCAA pathogenesis. Therefore, they gave important information about HCCAA pathogenesis and its association with at least one cell type that could be linked to cystatin C deposition and COLIV accumulation in the skin and in the vasculature in the brain, notably fibroblasts.

5.1 General tissue structure in HCCAA

The prominent pathological CAA changes described in this study were found within, as well as peripheral to, the vascular wall of brain vessels and were similar to pathological features that have been described in other CAA diseases (Attems et al., 2010; Biffi & Greenberg, 2011; Maat-Schieman et al., 2005; Tian et al., 2004; Yamada & Naiki, 2012) and features previously described for HCCAA, i.e. the cystatin C deposition and SMC degeneration (Blondal et al., 1989; Cohen et al.; Gudmundsson et al., 1972; Lofberg et al., 1987; Wang et al., 1997).

The pathological changes were: amyloid deposition in the form of CAA, intimal thickening, degeneration of SMCs and other cells in the vessel wall as most of the walls displayed an acellular appearance. In the few arteries where the intima was free of amyloid there appeared to be cell proliferation within the intima. Other pathological features observed were degeneration of the endothelia, fragmentation of the elastic layer, parenchymal cystatin C focal deposits, infarcts, hemorrhages, microinfarcts, vessels with a “double barrel” lumen, fibrinoid necrosis, accumulation of ECM proteins and a neuroinflammatory response around affected arteries as well as cystatin C deposition in the parenchyma.

These changes were most pronounced in arteries/arterioles in the leptomeningeal space, although arteries in other brain areas were also severely affected and displayed all of the pathological features mentioned above. Furthermore, these pathological hallmarks were invariably observed in samples from all the HCCAA patients, thus highlighting the severity of the disease. The severity of the pathology in the post-mortem brain samples, i.e. an end-stage pathology, made it difficult to determine a sequence of events during pathogenesis.

Overall, the peripheral tissues from HCCAA patients and L68Q-*CST3* carriers did not show pathological changes in normal tissue architecture and there was no apparent tissue damage or functional disturbance of the tissue as seen in the brain. However, a proliferation of fibroblasts in the upper dermis of carrier skin biopsies was seen and fibrosis was evident in the heart

of one patient with relatively late-onset HCAA, which affected normal heart function.

In the skin biopsies, the vessel walls were normal with an intact SMC layer despite cystatin C deposition and COLIV accumulation. The pathological vascular changes we observed in cerebral arteries/arterioles, in contrast to the observation of normal vessel wall structure in the peripheral tissues, indicated an association between cerebral vascular amyloid deposition, and perhaps ECM accumulation, with the pathological changes in the cerebral arteries/arterioles such as the loss of SMCs and other cerebral vascular cells, degeneration of the endothelia and fragmentation of the elastic layer. The peripheral tissues of HCCAA patients had a less advanced pathology than seen in the CNS, but it is likely that this pathology could progress to a more severe stage with time, and higher age, as cystatin C and COLIV deposition accelerated.

Hemorrhages and infarcts were widely distributed in the brain samples from the HCCAA patients and were found in all brain areas examined. Macro-hemorrhages were found in the midbrain and thalamus, which are areas of the brain in which such hemorrhages are rarely found in Aβ-CAA diseases and only in severe cases of HCHWA-D and sporadic Aβ-CAA (Wattendorff et al., 1995; Yamada & Naiki, 2012). The study revealed that HCCAA brain vessels affected by CAA, even in relatively young individuals, were severely damaged to an extent that undoubtedly weakened the overall structure of the vessel and consequently led to predisposition towards cerebral infarction and cerebral hemorrhaging, which explains the young age at death of HCCAA patients. In contrast to the brain, hemorrhages or infarcts were not found in the peripheral tissues. The more widespread nature and higher occurrence of hemorrhages in the young HCCAA patients compared to other CAA diseases could to some extent be due to the nature of cystatin C itself. For example, patients with Aβ-CAA, in which there is a co-localization of wild-type cystatin C and Aβ in affected vessels, have an increased likelihood of fatal subcortical hemorrhages (Maruyama et al., 1990).

5.2 Cystatin C deposition

Cystatin C deposition and distribution were examined in post-mortem brain samples from HCCAA patients and in peripheral tissues from HCCAA patients and L68Q-*CST3* carriers.

5.2.1 Cystatin C deposition in the brain

Cystatin C deposition and its distribution in the brain were assessed in the leptomeningeal space, cerebrum, cerebellum, thalamus, and midbrain. The deposition was most severe in small arteries and arterioles and was seen in both grey and white matter in all brain areas examined. Veins and capillaries, on the other hand, were not, or only minimally, affected. Arteries/arterioles in the leptomeningeal space showed the highest level of cystatin C deposition; however, arteries/arterioles in other brain areas also showed severe cystatin C deposition. Cystatin C immunoreactivity was found in all layers of the walls of almost all medium- and small-sized arteries and arterioles, some of which were completely occluded due to cystatin C amyloid. Perivascular cystatin C deposition was also seen around many affected arteries/arterioles.

The severity of cystatin C deposition within the vessel wall was assessed using criteria defined by Vonsattel *et al*. (Vonsattel et al., 1991) (see description of these criteria in section 1.5.2 in the Introduction). The application of this severity scale showed that the CAA in HCCAA was severe, i.e. deposition was observed almost or completely throughout the vessel wall. The distribution of the cystatin C deposition was assessed using criteria defined by Thal *et al.* (see definition in section 1.5.2 in the Introduction) (Thal et al., 2003; Thal et al., 2008) by which the progression of CAA (Aβ) throughout the brain is divided into three stages based on distribution where stage 3 refers to the most widespread distribution. As the cystatin C distribution in the HCCAA patients was such that it was seen in all of the brain areas mentioned above, the progression of CAA in HCCAA was determined to be stage 3 according to these criteria.

Severe CAA amyloid deposition in the midbrain, thalamus, and in white matter arteries/arterioles, along with hemorrhages in these brain areas, as

described for HCCAA in this study, is rarely seen in other CAA diseases except in severe cases (Maat-Schieman et al., 1996; Yamada & Naiki, 2012). The young age at death of the HCCAA patients from which samples were examined in this study (mean age at death 36 years based on all brain samples used in the study), with some patients younger than 30 years at death, underlines the rapid disease progression of HCCAA and its severity compared to the other CAA types, even the other familial types such as HCHWA-D.

A very minor fraction of arteries (30 arteries in total of all arteries in all the patient sample sections) were observed in which the intima was devoid, either completely or to a degree, of cystatin C deposition; this was never observed in arterioles. In these arteries, the deposition adhered to the BM as well as being present in the media and adventitia. In some of them the cystatin C deposition had extended past the BM and partially into the intima. A close examination of the sample material from all the patients revealed one large leptomeningeal artery in which cystatin C deposition was only present by the BM with no deposition in other parts of the vascular wall. Apart from this deposition the artery appeared structurally normal.

Taken together, these observations suggest that cystatin C deposition starts in the BM, and perhaps in the BM surrounding SMCs, from which it then extends into the media and adventitia, and then in the final stages of deposition it progresses into the intima and endothelia. These findings are similar to those described for Aβ-CAA (Carare et al.; Perlmutter, 1994; Vinters & Pardridge, 1986; Yamaguchi et al., 1992; Zarow et al., 1997). The progression of arterial cystatin C deposition in HCCAA could therefore be as shown in Figure 45.

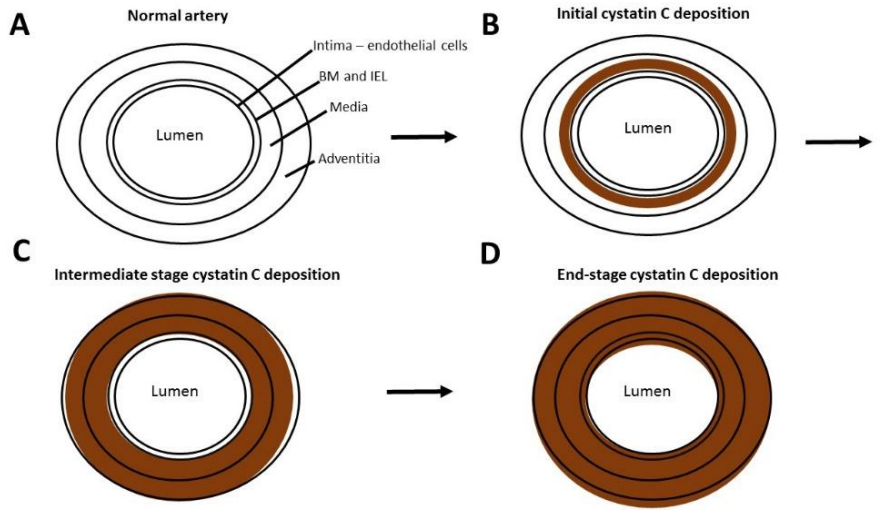

Figure 45. A schematic picture showing the hypothetical progression of cystatin C deposition in HCCAA.
(**A**) A normal cerebral artery showing the layers of the arterial wall. (**B**) Initial cystatin C deposition in the BM and in the BM around SMCs. (**C**) Intermediate stage of cystatin C deposition with deposition adhering to the BM, as well as in the media and adventitia, with the intima free of deposition. (**D**) End-stage cystatin C deposition with deposition throughout the entire vessel wall and in some cases perivascular.

5.2.2 Cystatin C deposition in the peripheral tissues

Cystatin C deposition was also observed in all the peripheral tissues examined from HCCAA patients, i.e. heart, lung, kidney, tonsil, liver, and stomach. In these organs, the deposition was mostly found in vessels, both arteries and arterioles, as well as in veins and venules. In some of the peripheral tissues cystatin C deposition was found within the interstitial tissue and connective tissue. This was especially evident in fibrotic tissue in a heart sample from one patient.

In the skin biopsies cystatin C immunoreactivity was most prominent in the BM between epidermis and dermis and was also found in the BM of vessels, as well is BMs around various structures in the skin, i.e. sebaceous glands, sweat glands, and arrector pili muscles. The location of cystatin C deposits in the skin concurred with that described previously by Benedikz *et al*. (Benedikz et al., 1990).

Benedikz *et al*. commented in their paper that individuals that had a longer history of the disease showed more cystatin C deposition. The results of the

study described here provided quantitative confirmation of this suggestion, i.e. symptomatic carriers had significantly higher levels of cystatin C immunoreactivity in their skin than asymptomatic carriers. The fact that the quantity of cystatin C deposition in skin was associated with the progression of the disease in the CNS shows that skin biopsies could be used to assess disease progression and could, therefore, be of use in the evaluation of therapeutic interventions.

In contrast to cerebral arteries/arterioles, in which cystatin C deposition was severe, the deposition in dermal vessels was mainly observed in their BMs, although in some cases it was observed throughout the entire wall of veins. Occluded vessels were never observed. Based on this observation, and that the SMC layer in the dermal vessels was intact and no other major abnormalities in the vessel wall structure were noticed apart from cystatin C deposition and COLIV accumulation, the deposition in the skin could be described as mild, or moderate, if one were to transfer the CAA criteria defined by Vonsattel *et al*. (Vonsattel et al., 1991) to the vessels in the skin.

5.2.3 Cystatin C deposition in the form of focal deposits

Parenchymal focal deposits were observed in all HCCAA brain areas examined. This was a novel observation in HCCAA. The focal deposits were always found close to regions with affected arteries and were most prominent in the thalamus, a brain area that was found to be highly affected in the HCCAA patients and in which many arteries/arterioles had perivascular cystatin C deposits. This indicated that focal deposit distribution correlated with the severity of the CAA pathology.

The distribution of Aβ deposits in the brains of AD patients has been categorized into five phases by Thal *et al*. (Thal et al., 2002b) dependent on the extent of distribution within the brain. In phase 1, Aβ deposits are found exclusively in the neocortex. As the disease progresses, additional brain areas are affected and phase 5 represents the most severe stage of pathology. In phases 4 and 5 deposits are present in the brain stem and cerebellum. Thal *et al.* also showed that phases 4 and 5 represent fully

developed Aβ amyloidosis in AD, i.e. the final stage of a process that starts with phase 1 and ends with phases 4 and 5.

In HCCAA, focal deposits were observed in both the brain stem and cerebellum, i.e. similar to phases 4 and 5 of Aβ deposition, underlining the severity of the cystatin C deposition and advanced CAA disease status in the young patients. The focal deposits did not show birefringence under polarized light after Congo red staining, i.e. they did not contain fully formed amyloid.

According to criteria defined by Duyckaerts *et. al* (Duyckaerts et al., 2009), focal deposits can be non-amyloid or amyloid. Amyloid focal deposits usually have a neuritic corona and are surrounded by a clear halo and are referred to as cored deposits or neuritic plaques. The cystatin C deposits in HCCAA are referred to as non-amyloid focal deposits and cannot be referred to as cored deposits. Neurons have not been shown to be affected in HCCAA and, therefore, it is unlikely that the focal deposits in HCCAA evolve to cored deposits.

5.2.4 Cystatin C amyloid

Amyloid formation in amyloid diseases involves the transformation of a soluble monomeric protein into insoluble amyloid fibrils, the intermediate step in this process is the formation of oligomers of different sizes, as has been shown with experiments on the cystatin C protein (Abrahamson & Grubb, 1994; Bjarnadottir et al., 2001; Wahlbom et al., 2007). These studies have shown that L68Q cystatin C has an increased tendency to form dimers and can also produce higher oligomeric forms (Abrahamson & Grubb, 1994; Bjarnadottir et al., 2001; Wahlbom et al., 2007).

In the HCCAA brain samples, cystatin C deposits in cerebral arteries/arterioles showed green birefringence after Congo red staining, i.e. they contained amyloid. In contrast, the perivascular deposits and the focal deposits did not. Of the peripheral organs examined in this study, only the cystatin C deposits in the heart and stomach of one patient had reached amyloid form (as determined by Congo red staining). This patient was older at death than the average lifespan of carriers. Furthermore, other studies

have shown that cystatin C deposition in post-mortem samples from peripheral tissues can reach amyloid form, as demonstrated with Congo red staining (Lofberg et al., 1987; Palsdottir et al., 2006; Thorsteinsson et al., 1988).

Taken together, this indicates that the deposits of cystatin C, which did not show birefringence under polarized light after Congo red staining, could consist of different oligomeric forms. This concurs with the study of Benedikz *et al*. (Benedikz et al., 1990) which observed amyloid-like threads using electron microscopy in 13 of 21 skin biopsy sections from carriers/patients which all showed cystatin C deposition. Therefore, the non-birefringent cystatin C deposits found could be described as a midway step towards forming amyloid, compared to the complete cystatin C amyloid form present in the cerebral arteries/arterioles.

5.3 Extracellular matrix changes in HCCAA

This results of this study showed that accumulation of the ECM proteins laminin, COLIV, and AGC1 were present in the cerebral vascular walls of HCCAA patients and that this was a part of the HCCAA pathogenesis. The distribution of cystatin C deposition was very similar to, and tightly associated with, COLIV accumulation in the BMs of cerebral arteries/arterioles as well as in the BMs of various structures in carrier skin biopsies. This was especially evident in the BM between the epidermis and dermis.

There are multiple reports about changes in ECM composition in AD, Aβ-CAA, and HCHWA-D (Kalaria & Pax, 1995; Tian et al., 2006; van Duinen et al., 1995; van Horssen et al., 2001). The results presented in research reports are conflicting regarding the type of ECM proteins involved, the magnitude of their accumulation, and what role they play in these diseases. Studies have shown that COLIV, nidogen, and HSPG are associated with CAA and amyloid plaques in AD and HCHWA-D where they interact directly with, and influence, Aβ deposition and aggregation and could thus be actively involved in the pathogenesis of these diseases (Cotman et al., 2000; Kalaria & Pax, 1995; Perlmutter, 1994; van Duinen et al., 1987; van Horssen et al., 2001). AGC1 has been documented to facilitate aggregation of Aβ (Ariga et

al., 2010) and a protective role of AGC1 has been reported such that neurons with AGC1 in their perineuronal net are protected against the pathological processes of AD and show enhanced recovery after neural injury (Morawski et al., 2012). Other studies have shown that the BM proteins COLIV, laminin, HSPG, and nidogen interact with Aβ and can inhibit its fibrillization (Bronfman et al., 1998; Castillo et al., 1997; Cotman et al., 2000; Kiuchi et al., 2002; Merlini et al., 2011). It has also been suggested that increased laminin in the BMs of vessels affected by CAA is a response to the vascular damage, resulting in BM thickening, thereby giving it increased strength (Merlini et al., 2011). There are differences in the type, and magnitude, of ECM proteins that are deposited in these diseases. For example, there are different types of HSPG subtypes involved with Aβ in AD compared to HCHWA-D (van Horssen et al., 2001).

A dysfunction of proteolytic systems within the cell has been implicated as a causative factor in ECM remodelling in several diseases including AD, ischemic stroke, atherosclerosis, and amyotrophic lateral sclerosis (Bengtsson et al., 2005; Kurzepa et al., 2014; Lukaszewicz-Zajac et al., 2014; Mroczko et al., 2014; Rivera et al., 2010; Sukhova et al.). Cysteine cathepsins are important in ECM remodelling and regulation of BM function. They are also able to degrade, for example, AGC1, COLIV, and laminin (Fonovic & Turk, 2014). Matrix metalloproteinases (MMPs) are a group of proteinases that take part in the degradation of ECM proteins, e.g. collagens, proteoglycans, elastin or fibronectin, in normal physiological processes such as wound healing, and are inhibited by tissue endogenous inhibitors (TIMPs) (Rivera et al., 2010). The concentration of MMP-9, also known as type IV collagenase, has been shown to be significantly lower in the CSF of AD patients compared to controls (Mroczko et al., 2014). Lower concentrations of MMP-9, which degrades COLIV, could therefore result in COLIV accumulation. Cystatins have been found to stabilize and protect MMPs (Ochieng & Chaudhuri, 2010). Another study has shown that cystatins, e.g. cystatin C, can protect MMP-9 from autolytic degradation (Ray et al., 2003). Moreover, studies have shown that the balance between cystatins, MMPs,

TIMPs, and cathepsins is important for the regulation of ECM remodelling (Bengtsson et al., 2005; Ochieng & Chaudhuri, 2010; Sukhova et al.). A dysregulation of other MMPs has also been found in AD, which could affect other ECM proteins (Horstmann et al., 2010). Therefore, the balance between MMPs, cystatin C, and cathepsins could be important for the ECM remodelling in HCCAA. The L68Q-*CST3* mutation could affect that balance.

In conclusion, the association of COLIV, laminin, and AGC1, with HCCAA pathogenesis could possibly influence cystatin C deposition and aggregation, play a protective role, or each ECM protein could play a different role in the pathogenesis of HCCAA. The close association between COLIV and cystatin C in all of the samples examined, from different tissue types, indicates that COLIV influences the cystatin C deposition. However, the role of each ECM protein in HCCAA needs further investigation. One possible reason for the accumulation of these ECM proteins could lie in a dysfunction of proteolytic systems. These factors require further clarification and would make an interesting basis for further investigation into HCCAA pathogenesis.

5.3.1 Basement membrane abnormalities in HCCAA

BM alterations and increased thickness of BMs are evident in HCCAA with accumulation of COLIV and a thicker laminin layer in cerebral arteries/arterioles and accumulation of COLIV in BMs in the carrier skin biopsies. This suggests that BM abnormalities are systemic in HCCAA.

There are many studies that suggest that cerebrovascular BMs, along with ECM proteins, play a role in the deposition of amyloid proteins in CAA due to biochemical, anatomical, and morphological alterations of BMs (Carare et al., 2008; Kalaria & Pax, 1995; Perlmutter, 1994; Weller et al., 2008; Zarow et al., 1997). Reports are not in complete agreement regarding changes in the ECM proteins in cerebrovascular BMs in CAA diseases. COLIV was found to be increased by 55% in the cerebrovascular BMs of AD subjects (Kalaria & Pax, 1995) and an increased BM thickness, with 20% higher COLIV levels, has been reported in a transgenic AD mouse model (Bourasset et al., 2009). Other studies have, however, reported moderate, or

normal levels of COLIV in AD, HCHWA-D, and in a transgenic mouse model of the London APP mutation (Van Dorpe et al., 2000; van Duinen et al., 1987; Zhang et al., 1998) a decrease in COLIV in AD has even been reported (Christov et al., 2008). van Horssen *et al.* investigated HSPG in the BMs of AD and HCHWA-D patients and found that it had increased (van Horssen et al., 2001). Increased laminin staining in the leptomeningeal BM of arteries with CAA changes has been demonstrated at an early stage of Aβ deposition in transgenic arcAβ mice (Merlini et al., 2011) and lower levels of laminin in cerebral capillaries of an aged wild-type mouse have been reported (Hawkes et al., 2011).

The inconsistencies between these reports and the results presented here, and between diseases, might be partly explained by underlying factors, e.g. different disease-causing mutations, age of study subjects, or the identity of the depositing protein.

A recent study showed that an increase in the levels of the ECM components COLIV, perlecan, and fibronectin, occurs in early stages of AD in subclinical AD patients, with no significant difference in the levels of these ECM proteins between subclinical AD and AD patients (Lepelletier et al., 2015). The study showed that COLIV expression did not increase further as the disease progressed following the subclinical stage and that the increase in vascular COLIV was in agreement with a previous study on AD patients made by Kalaria *et al.*, cited above; both studies reported similar increases in COLIV (~ 55%) (Kalaria & Pax, 1995; Lepelletier et al., 2015).

A study performed on a mouse model of HCHWA-D, created by overexpression of human E693Q APP, showed thickening of the cerebrovascular BM with amyloid fibrils found within the BM (Herzig et al., 2004) and overexpression of TGF-β1 in transgenic mice results in thicker BMs which precedes the development of murine CAA (Wyss-Coray et al., 2000).

Arteries/arterioles in all brain areas examined in HCCAA patients were severely affected, i.e. in the cerebrum, cerebellum, thalamus, and midbrain. In sporadic Aβ-CAA and AD, cortical and leptomeningeal vessels are

primarily affected and only in rare severe cases are vessels in the basal ganglia, brain stem, thalamus, or white matter, affected (Yamada, 2015). It has been suggested that the association of Aβ distribution with these particular brain areas in Aβ-CAA and AD is due to differences in the ECM composition of the cerebrovascular BMs between brain areas as well as the influence of age on the cerebrovascular BMs, resulting in increased thickness (Hawkes et al., 2013). A study by Hawkes *et al.* (Hawkes et al., 2013) showed that the thickness of cerebrovascular BMs increased with age in wild-type mice in the same brain areas in which CAA pathology is observed in AD mouse models. In support of this, a study in AD patients showed significant correlation between COLIV and Aβ immunoreactivity, i.e. Aβ immunoreactivity was seen in vessels with increased levels of COLIV, perlecan, and fibronectin (Lepelletier et al., 2015).

Taken together, the results from these studies were in line with the results presented here in this thesis, i.e. the increased content of the BM proteins COLIV and laminin. In HCCAA, COLIV accumulation in cerebral arteries/arterioles was present throughout the entire vessel wall. This was also the case in in the relatively rare arteries that had a slightly less advanced cystatin C deposition, i.e. in which the intima was free, or partially free, of cystatin C deposition. The intima in these arteries was COLIV immunoreactive.

The results of this study suggest that COLIV accumulation in cerebral arteries/arterioles in HCCAA precedes cystatin C deposition. The results from the skin biopsies support this hypothesis. In the carrier skin biopsies, the quantity of cystatin C deposition was dependent on whether they were from symptomatic or asymptomatic carriers, i.e. the results suggested that the skin deposition was increasing as the disease progressed. In contrast, the COLIV immunoreactivity was elevated in biopsies from symptomatic and asymptomatic carriers to the same extent, i.e. regardless of disease status, suggesting that the increase might have reached a “fixed level”, before that of cystatin C, or that it had been elevated to a similar degree in the carriers from

the outset. This result was interpreted such that the cystatin C deposition was occurring into this fixed environment created by the elevated COLIV.

The results presented in this thesis show that abnormalities in cerebrovascular BMs were not restricted to certain brain areas in the patients, nor were the cystatin C deposition and BM changes found in the skin biopsies of carriers limited to vessels. Cystatin C deposition, and COLIV immunoreactivity, in the L68Q-*CST3* skin biopsies was observed in BMs, and the initial deposition in asymptomatic carriers occurred in the BM between epidermis and dermis. COLIV and cystatin C immunoreactivity in affected HCCAA arteries/arterioles, and in the carrier skin biopsies, showed a very similar staining pattern and distribution, indicating a close association between cystatin C deposition and BM proteins. Veins were found to be minimally or not affected in HCCAA brain samples, whereas cystatin C deposition in the skin biopsies was systematically observed in the walls of veins/venules; this was also seen in veins in some of the peripheral tissues examined. In addition, cystatin C deposition in venous sinuses of the spleen of HCCAA patients has been described (Palsdottir et al., 2006). The reason for this difference between veins in the CNS and peripheral tissues could lie in the fact that CNS veins have very little BM relative to veins in the periphery (Hawkes et al., 2014), which could be why veins were minimally affected in the brain.

5.3.2 Protein elimination failure angiopathy in HCCAA

The results reported in this thesis indicate that initial cystatin C deposition in HCCAA occurs in the altered BM and/or in the BM around SMCs in affected cerebral arteries/arterioles as well as in BMs in various structures throughout the body. Furthermore, this study also suggests that BM abnormalities are an early event, and key step, in HCCAA pathogenesis which precedes the cystatin C deposition.

Multiple lines of evidence support the proposition that Aβ accumulation in AD-CAA occurs along the altered and thickened BM of vessels during drainage of ISF and that the affinity of BM proteins for Aβ influences the

development of CAA (Carare et al., 2008; Hawkes et al., 2011; Kalaria & Pax, 1995; Weller et al., 2000; Weller et al., 2008; Zarow et al., 1997). Dextran that was injected intracerebrally into both wild-type mice and a transgenic AD mouse model was found to co-localize with laminin in the BM, strongly supporting the association of solutes in the perivascular drainage with the BM (Carare et al., 2008; Hawkes et al., 2011). Studies performed on aging mouse brains suggest that one of the causes of Aβ-CAA is failure of Aβ elimination from the CNS by impaired perivascular drainage of ISF along structurally altered cerebrovascular BMs termed protein elimination failure angiopathy (PEFA) (Bell & Zlokovic, 2009; Carare et al., 2008; Hawkes et al., 2011; Weller et al., 2008). PEFA has also been shown to occur in other amyloid and non-amyloid diseases that show protein accumulation in cerebral vascular walls, for example in CADASIL and prion diseases (Carare et al., 2013). Finally, Herzig *et al.* (Herzig et al., 2004) found that neuronal overexpression of human E693Q APP in mouse models of HCHWA-D caused extensive CAA and associated CAA vascular degenerations, with amyloid fibrils found within the cerebrovascular BM. Therefore, cell types found outside the cerebrovascular wall could also contribute to the amyloid deposition.

Cystatin C is found in high concentrations in the CSF of healthy individuals, whereas L68Q-*CST3* carriers, and HCCAA patients, have significantly lower levels of cystatin C in their CSF (Grubb et al., 1983; Lofberg & Grubb, 1979). Impaired perivascular drainage of ISF could be a factor in HCCAA pathogenesis due to altered BM structure. As already discussed, the BM could provide a scaffold facilitating the deposition and aggregation of cystatin C in the cerebrovasculature. The levels of cystatin C in the CSF of HCCAA patients could be affected by this and it could have an impact on why fewer dimers were detected in the CSF of HCCAA patients compared to the plasma (Bjarnadottir et al., 2001), i.e. the dimers could be more prone to deposition in the BMs. The combination of this scenario in the CNS and cells found within and/or even outside the vascular wall contributing

to the cystatin C deposition, could be the reason for the severe pathology observed in the brain compared to peripheral tissues.

5.4 Cystatin C in relation to cell types and distribution

This systemic distribution of cystatin C deposition, shown in this study, in conjunction with data presented by others (Benedikz et al., 1990; Lofberg et al., 1987; Palsdottir et al., 2006; Thorsteinsson et al., 1988), suggested that the cell type, or cell types, responsible for cystatin C deposition in HCCAA was not limited to the CNS. The systemic nature of HCCAA could be due to the fact that cystatin C is ubiquitously expressed in all tissues and body fluids (Abrahamson et al., 1986; Grubb, 1992). The reason why the deposition and pathological changes are most pronounced in the CNS, and the clinical appearance seems to be confined to the CNS, could be, as mentioned above, due to the particularly high concentration of cystatin C in normal CSF (Grubb et al., 1983; Lofberg & Grubb, 1979). CSF cystatin C is produced by the choroid plexus (Tu et al., 1992) and has been shown to be expressed in other cells within the brain tissue, e.g. neurons, astrocytes, endothelial cells, and microglial cells (Hakansson et al., 1996; Kaur & Levy, 2012). In this context, it may be mentioned that a neuronal involvement, or cystatin C deposition within neurons, has not been observed in HCCAA, neither in this, nor other, studies on the disease.

In Aβ-CAA, primary cultures of SMCs isolated from the vasculature of AD patients have been found to produce extracellular deposits of Aβ (Frackowiak et al., 2005). Wang *et. al* (Wang et al., 1997) suggested that SMCs could be the cell type responsible for the cystatin C amyloid in cerebral arteries/arterioles in HCCAA (Wang et al., 1997). The results from the carrier skin biopsies in this thesis indicate that SMCs are not associated with cystatin C deposition and analysis by confocal immunofluorescence microscopy did not indicate a causal relationship between SMCs and cystatin C deposition in the skin. Furthermore, αSMA immunoreactivity did not differ between carrier and control skin biopsies. In contrast, extensive SMC death was observed in the cerebral vascular wall of small and medium sized arteries and arterioles in HCCAA patients. Solubilized cystatin C amyloid has

been shown to be toxic to cerebrovascular SMCs (Vilhjalmsson et al., 2007). Taken together, the results of this study suggest that SMCs are not the major cell type responsible for cystatin C deposition in HCCAA and that the degeneration of cerebral vascular SMCs might be due to cystatin C amyloid toxicity. SMCs in the vascular wall are surrounded by BM, and the affinity of cystatin C for BM and its initial deposition in the BM, could play a part in the degeneration of SMCs.

Cystatin C is a secreted protein (Abrahamson et al., 1986; Grubb, 1992). The endoplasmic reticulum (ER) is responsible for folding and initial post-translational modifications of secreted and transmembrane proteins mediated by ER resident proteins, for example, and chaperones protein disulphide isomerases and peptidyl prolyl isomerases (Tanjore et al., 2012). Aberrations in protein folding, e.g. due to mutations, can lead to the accumulation of misfolded proteins in the ER. This activates the “unfolded protein response” (UPR) to conserve ER function (Tanjore et al., 2012). ER stress has emerged as a direct causal factor of fibrosis in disorders such as idiopathic pulmonary fibrosis (IPF), liver fibrosis, and renal fibrosis (Chiang et al., 2011; Lenna & Trojanowska, 2012; Tanjore et al., 2012; Tanjore et al., 2013). The precise molecular mechanisms linking ER stress and fibrosis have not been defined, but severe, or chronic, ER stress can have several outcomes, e.g. activation of cell death pathways, inflammatory signalling, or phenotype shift (e.g. EMT) of the stressed cells, possibly to a cell type better able to cope with the stress, e.g. fibroblasts (Tanjore et al., 2013).

The results presented in this thesis, show that there was a convincing association between cystatin C deposition, COLIV accumulation and fibroblasts, both in the skin and in the brain (see also section 5.5). The expression of mutant cystatin C protein might cause ER stress in cells of carriers. Relevant to this, reports from cell based studies have shown intracellular retention, and accumulation, of mutant cystatin C compared to the wild-type (Benedikz et al., 1999; Bjarnadottir et al., 1998; Thorsteinsson et al., 1992). With respect to EMT due to ER stress, several cell types could go through a phenotype shift into fibroblasts due to ER stress, e.g. vascular

SMCs, and endothelial cells and then fibroblasts could differentiate into myofibroblasts.

5.5 HCCAA and fibroblasts

The skin biopsies revealed a close association between cystatin C, COLIV, and fibroblasts. This association between the proteins was so close that confocal microscopy sometimes showed them to be completely co-localized. Furthermore, in the few brain arteries that showed a less advanced HCCAA pathology, activated fibroblasts (myofibroblasts) were found in the intima which was devoid of cystatin C deposition but displayed COLIV accumulation. Finally, analyses of peripheral tissues, i.e. heart, liver, kidney, lung, tonsil, and stomach, also revealed that cystatin C deposition was affiliated with collagen accumulation. This indicated a close relationship between fibroblasts, cystatin C deposition, and COLIV accumulation in HCCAA pathogenesis in all organs.

Fibroblasts are present in every tissue of the body and in vessels (Baum & Duffy, 2011; Lee, 1995). In the heart, for example, fibroblasts can be over 60% of the total cell population (Baum & Duffy, 2011). Fibroblasts are the primary producers of ECM proteins and are important for the maintenance and production of the ECM; during wound healing collagen becomes the main product of activated fibroblasts (Baum & Duffy, 2011; Hinz, 2007). Collagen has been found to be the major component of the ECM in which it provides a scaffold that binds other proteins and proteoglycans (Kanta, 2015). The stimulation of fibroblasts by, for example, TGF-β results in their differentiation into myofibroblasts. Myofibroblasts produce excess collagen which leads to collagen accumulation and fibrosis (Baum & Duffy, 2011; Hinz, 2007). Studies have shown that during the process of differentiation from fibroblasts into myofibroblasts there is an intermediate stage in the process during which the fibroblasts take on a proto-myofibroblast phenotype. Myofibroblasts are characterized by their elevated expression of α-SMA, while fibroblasts and proto-fibroblasts do not show expression of α-SMA (Hinz, 2007).

TGF-β has been found to be the main factor that stimulates the fibroblast differentiation process and is an important ECM regulator in fibroblasts

(Blobe et al., 2000). TGF-β signals through the cell surface receptors TβRI and TβRII, with signalling beginning with the binding of TGF-β to TβRII which then binds to the TβRI receptor (Massague, 1998, 2012). TGF-β is produced in many cell types of the body, including fibroblasts, myofibroblasts, macrophages, endothelial cells, and epithelial cells (Hinz, 2010). In the vascular wall it is expressed by fibroblasts, vascular SMCs, endothelial cells, myofibroblasts, and macrophages (Ruiz-Ortega et al., 2007).

Several origins of tissue/vascular fibroblasts and myofibroblasts have been proposed (Figure 46): 1) By proliferation and differentiation of local fibroblasts and SMCs into fibroblasts and myofibroblasts. 2) Endothelial and epithelial cells can transition into myofibroblasts through EnMT and EMT processes, respectively. 3) The recruitment and transition of bone-marrow derived cells into fibroblasts (Hinz, 2016; Kalluri & Weinberg, 2009).

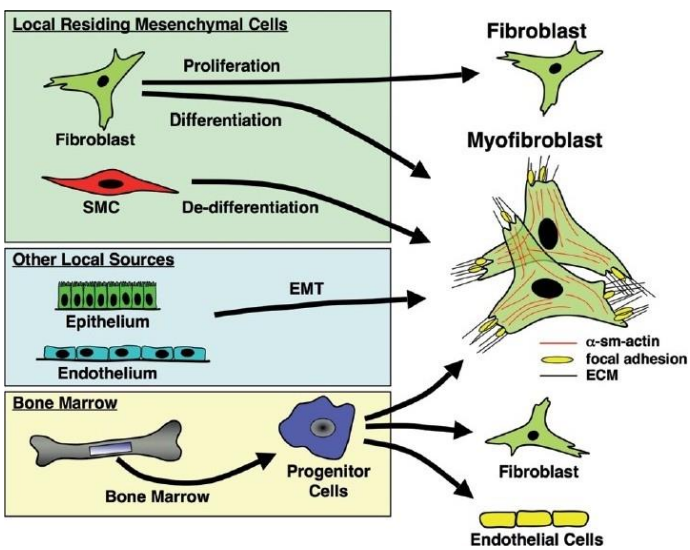

Figure 46. Probable sources of fibroblasts and myofibroblasts.
Fibroblasts and myofibroblasts can originate by differentiation of both local and bone-marrow derived cells. Figure reprinted from (Yeager et al., 2011) with permission from Pulmonary Circulation.

The denser population of fibroblasts in the L68Q-*CST3* skin biopsies showed nuclear pSMAD2/3 immunoreactivity but were not immunoreactive for α-SMA, suggesting that they were not myofibroblasts. However, their increased number relative to the control biopsies, their morphology, and the pSMAD2/3 immunoreactivity, suggests that they were activated fibroblasts, possibly proto-myofibroblasts. In contrast, the fibroblasts detected within the intima of cerebral arteries/arteriole were α-SMA immunoreactive, suggesting that they were myofibroblasts. As discussed above, the pathological changes in the brain are of a much more advanced nature than in the skin and other peripheral tissues, which could explain why myofibroblasts were observed in the brain but not in the skin.

Recent studies on the fibrotic lung disease IPF have shown that ER stress, along with activation of the UPR, is present in alveolar epithelial cells in the disease. This was first observed in the familial form of the disease (Tanjore et al., 2012; Wolters et al., 2014). The ER stress, and subsequent UPR, results in EMT and activation of TGF-β through the SMAD-dependent signalling cascade. This results in differentiation of epithelial cells into fibroblasts and then into myofibroblasts, i.e. EMT, which is associated with E-cadherin downregulation and upregulation of, for example, α-SMA, p63, and vimentin (Figure 47) (Jonsdottir et al., 2015; Wolters et al., 2014).

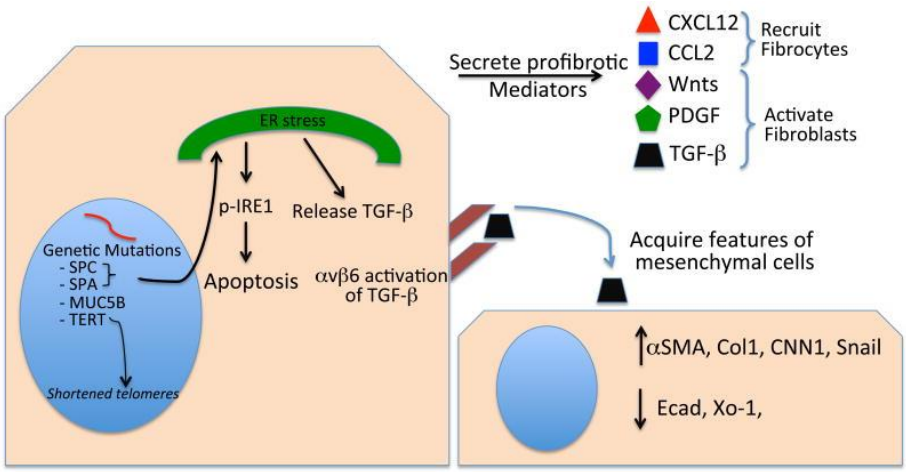

Figure 47. ER stress and EMT in Idiopathic pulmonary fibrosis.
Pro-fibrotic characteristics of epithelial cells in idiopathic pulmonary fibrosis (IPF) due to ER stress. Genetic mutations leads to ER stress. The ER stress leads to TGF-β activation and EMT. Figure reprinted from (Wolters et al., 2014) with permission from *Annual Reviews*.

Keloid, a skin disease with hypertrophic areas of fibrosis following trauma, is another example of a fibrotic disease characterized by EMT changes (Yan et al., 2015). Studies have shown that in Keloid, these phenotype changes occur with enhanced TGF-β1 expression and SMAD3 phosphorylation (Yan et al., 2015). The results presented here showed that the expression of E-cadherin and p63 immunoreactivity in L68Q-*CST3* carrier biopsies and control biopsies did not differ; however, upregulation of vimentin was seen in fibroblasts in the carrier skin biopsies and αSMA immunoreactivity was seen in fibroblasts in the thickened intima of affected HCCAA arteries. Therefore, unequivocal evidence of EMT was not detected in the carrier skin biopsies; however, the detection of putative myofibroblasts in the pathologically more advanced brain samples indicated the activity of EMT processes in the pathogenesis. Finally, studies on IPF have revealed different fibroblast phenotypes in the disorder, as the myofibroblast phenotype is not durable and requires constant TGF-β stimulation (Wolters et al., 2014).

Studies on fibroblasts from IPF patients have shown that if cathepsin B is inhibited by cystatin C then the differentiation of fibroblasts to myofibroblasts,

and the expression of α-SMA, was diminished. This inhibition of cathepsin B had an effect on the TGF-β signalling in fibroblasts through decreased SMAD2/3 phosphorylation (canonical pathway) with no effect on the non-canonical (non-SMAD) pathways, i.e. MAPK and JNK (Kasabova et al., 2014). Studies on heart fibroblasts have shown the same, i.e. cystatin C inhibits cathepsin B and therefore the accumulation of collagen and fibronectin (Xie et al., 2010).

Studies in fibroblasts have shown that cystatin C directly affects the binding of TGF-β to TβRII by interacting physically with TβRII and preventing its binding to TGF-β and, therefore, affecting the TGF-β signalling cascade (Sokol & Schiemann, 2004). Cystatin C has also been found to inhibit EMT/EnMT, the migratory and invasive properties of the epithelial/endothelial cells, and differentiation of fibroblasts by antagonizing SMAD-dependent TGF-β signaling (Sokol et al., 2005).

L68Q-*CST3* carriers are heterozygous, i.e. produce both the wild-type and the mutant cystatin C (Olafsson & Grubb, 2000). Indications of abnormal processing, intracellular accumulation, and reduced secretion of mutant cystatin C in primary cells and cell lines have been described (Benedikz et al., 1999; Bjarnadottir et al., 1998; Thorsteinsson et al., 1992). This might lead to a lowering of the amount of extracellular cystatin C in L68Q-*CST3* compared to healthy subjects that are homozygous for the wild-type allele. As previously mentioned, cystatin C levels in the CSF of HCCAA carriers and patients is lower than that of healthy individuals, whereas their plasma cystatin C levels do not differ (Bjarnadottir et al., 2001; Grubb et al., 1984a).

To summarize, the quantification and distribution of COLIV immunoreactivity in the skin biopsies and the cerebral arteries/arterioles showed that COLIV accumulation is probably an early event in HCCAA pathogenesis, suggesting that activation of fibroblasts is also an early event. The origin of the fibroblasts found in the skin and the cerebral arteries could be from multiple sources within the tissue and the vascular wall, e.g. from local or remote fibroblasts, SMC or EMT/EnMT processes. If the L68Q-*CST3* carriers or HCCAA patients have lower extracellular levels of cystatin C, as

several lines of evidence suggest might be the case, it could result in up-regulation of cathepsins and TGF-β. The up-regulation of cathepsins and TGF-β through SMAD-dependent signalling might therefore promote the proliferation and differentiation of fibroblasts, EMT/EnMT processes, excessive collagen accumulation, and a lower rate of collagen degradation could, thereby, result in changes in the ECM components of BMs and their thickening. The abnormalities in the BMs could provide a scaffold for the cystatin C deposition. This could also be the case in other cell types, e.g. SMC and endothelial cell.

In conclusion, the pathology of HCCAA does not seem to consist of "full-blown" fibrosis, but rather of some intermediate degree of fibrosis consisting of proto-myofibroblasts and therefore a lack of clear EMT signs in relation to keloids and IPF. It might be possible to detect such markers in CNS arteries that still retain some cells in their walls and this could be one avenue of further research into the pathology of HCCAA.

5.6 Neuroinflammation

The study revealed severe astrocytosis with compact glial scar formation around affected cerebral arteries/arterioles with activated microglia and macrophages. A reactive inflammatory response was also found in the tissue surrounding focal deposits. An inflammatory response towards cystatin C deposition in peripheral tissues, i.e. the skin and the other peripheral tissues examined, was not obvious except for mild inflammation in the skin biopsies from two carriers.

The results of some AD studies suggest that the neuroinflammatory response in AD is an important reaction to tissue damage, whereas others suggest that it is harmful by exacerbating Aβ deposition and contributing to neuronal dysfunction [reviewed in (Wyss-Coray & Rogers, 2012)]. Aβ itself can trigger a neuroinflammatory response by binding to microglial receptors and microglial cells have been shown to internalize Aβ; the same has been shown for astrocytes (Paresce et al., 1996; Rogers et al., 1992; Yan et al., 1998). However, studies have also shown that microglia and astrocytes are ineffective in Aβ clearance (Cashman et al., 2008; Fiala et al., 2005; Wyss-

Coray & Rogers, 2012). When the results of this thesis are viewed in light of these Aβ associated results, it appears likely that microglia and astrocytes in HCCAA respond to cystatin C amyloid in the same manner.

Most of the focus on neuroinflammation in AD has been on the neuroinflammatory response to plaques and the correlation between the progression of AD and the inflammatory response (Itagaki et al., 1989; Rozemuller et al., 2005; Rozemuller et al., 1989). Many studies have indicated that neuroinflammation occurs in the early stages of AD and that it contributes to disease progression and severity, and in fact might drive the pathological process in AD (Heneka et al., 2015; McGeer & McGeer, 2013). Neuritic plaques contain fibrillar Aβ, are associated with microglial cells and astrocytes, and are congophilic (Dickson, 1997; Itagaki et al., 1989; Rozemuller et al., 1989). Diffuse plaques, on the other hand, are low-fibrillar, non-congophilic, and are not associated with microglial cells or astrocytes. This, along with *in vitro* studies on Aβ and inflammation, indicates that a certain degree of fibrilization is needed to activate the neuroinflammatory response (Eikelenboom & Veerhuis, 1996). This could be the case in HCCAA where there is a prominent inflammatory response in the brain towards affected vessels and focal deposits even though the deposits were non-congophilic, i.e. not with a full amyloid form. However, the state of amyloid progression in cystatin C focal deposits and perivascular deposits in the brain could be of a higher degree of fibrillization compared to the non-congophilic deposits in the skin biopsies to which no evidence of an inflammatory response was found.

As mentioned, glial scar formation was found around affected cerebral arteries/arterioles in the HCCAA patients. The attenuation of endothelial cells in severely affected arteries/arterioles suggests a disturbance in the function of the BBB. As detailed in the Introduction, the formation of a glial scar is how the CNS responds to an injury. The first cells to react are astrocytes, which proliferate, become hypertrophic with thick extended processes, and surround the damaged area with a thick, compact, scar. The scar formation protects the surrounding, healthy, tissue from the damaged area,

reconstitutes the BBB, restricts inflammation, and preserves neural tissue (Burda et al., 2016; Kawano et al., 2012; Sofroniew, 2009, 2015). In addition to astrocytes, other cells and components play an important part in the scar formation, i.e. microglia and fibroblasts, and the BM and ECM proteins. The activated astrocytes and the fibroblasts interact to form a compact scar and both cell types show upregulated expression of ECM proteins. The glial scar, therefore, also contains a fibrotic scar which is formed by ECM proteins such as COLIV, laminin, and CSPGs (Burda et al., 2016; Kawano et al., 2012; Raposo & Schwartz, 2014; Sofroniew, 2009, 2015). The results of the research for this thesis show that in HCCAA there were pathological changes in BMs in the brain and skin vessels and in BMs around other structures of the skin, and, furthermore, that these changes occur early in the pathogenesis of the disease. In the brain, excessive accumulation of COLIV, laminin, and the CSPG protein AGC1 was observed in the walls of affected vessels. The extreme nature of this deposition could therefore be because of glial scar formation and the early accumulation of the BM proteins.

The neuroinflammatory response in the HCCAA is probably due to both the BBB disruption and the severe cystatin C amyloid deposition. As noted, inflammation was not found in the less advanced peripheral tissues of HCCAA patients and L68Q-*CST3* gene carriers, which could indicate that inflammation is perhaps not an early event or the driving factor in HCCAA pathogenesis, but rather a severe brain inflammatory response to a severe arterial pathology and cystatin C deposition consisting of aggregates in a higher degree of fibrilization than found in the peripheral tissues.

5.7 Similarities with other CNS diseases

In addition to similarities with other CAA disease, similar changes to the brain vascular pathological features of HCCAA, described here, are also found in non-amyloid diseases such as Hutchinson–Gilford Progeria Syndrome (HGPS), Marfan's syndrome, and CADASIL. Although the vascular pathology is similar between these diseases their overall clinical symptoms are different. HGPS is an extremely rare premature aging disease caused by mutations in the *LMNA* gene (reviewed in (Capell et al., 2007)) and CADASIL

is the most common form of hereditary stroke disorder which is caused by mutations in the *Notch 3* gene (Joutel et al., 2000). The cause of death in both diseases is often due to stroke. The overlap of the pathological features of HCCAA described in this study and HSPG and CADASIL include degeneration of vascular SMCs, ECM accumulation (including COLIV), intimal thickening, fragmentation of the elastic layer, degeneration of the endothelia and thickening of the BM (Dong et al., 2012; Stehbens et al., 2001; Stehbens et al., 1999; Szpak et al., 2007). Furthermore, CADASIL shows accumulation of granular osmophilic material, produced by SMCs and pericytes in the vascular wall, which infiltrate towards the BM and accumulate there due to PEFA (Lewandowska et al., 2011). Marfan's syndrome is a systemic disorder of connective tissue which affects the cardiovascular system the most with aortic aneurysms. It is caused by mutations in the *FBN1* gene which encodes fibrillin-1, a glycoprotein component of the ECM. Mouse models of the disease show that the aorta has abnormal thickening in the media with increased collagen deposition, fragmentation of elastic fibres, and elevated pSMAD2/3 immunoreactivity due to increased TGF-β signalling (Habashi et al., 2006).

The similarities in vascular pathology between HCCAA and unrelated non-amyloid disorders support the results presented in this thesis that the COLIV accumulation is probably a primary event in HCCAA pathogenesis, as indicated by the results obtained from the carrier biopsies and, furthermore, that the excessive ECM accumulation could be the cause of some of the vascular pathological changes in HCCAA in addition to the amyloid accumulation. The effect of the L68Q-*CST3* mutation could be such that it causes an overproduction of ECM proteins, and their accumulation, thereby instigating amyloid deposition and aggregation in the arterial wall rather than *vice versa*. Some studies have shown that excessive ECM material in vessel walls are associated with an increased degeneration of SMCs and that this is unrelated to amyloid deposition, indicating a relationship between the ECM accumulation and SMC degeneration (Lan et al., 2013; Szpak et al., 2007) On the other hand, as mentioned before, toxic effects of cystatin C amyloid

on SMC *in vitro* have been described (Vilhjalmsson et al., 2007), and similarly toxic effects of Aβ amyloid on SMCs and endothelia (Fossati et al., 2012). In the peripheral tissues of HCCAA patients, the vessel pathology was still mild, with only mild or moderate cystatin C deposition and COLIV accumulation but no other vascular abnormalities. Taken together, this indicates that the vascular degeneration in cerebral vessels of HCCAA patients could be due to a combination of cystatin C deposition, ECM accumulation, and the toxicity of the amyloid. The vascular pathology in the peripheral tissues could progress with time and a longer “disease period” in HCCAA patients.

6 Conclusions

Despite past publications about HCCAA pathology prior to this study, there was a lack of detailed basic research on the vascular pathological changes in HCCAA and the aetiology of HCCAA pathology required clarification. The main objectives of this study were to increase the understanding of HCCAA pathogenesis, especially the cerebrovascular pathology as the clinical symptoms appear to be mostly associated with alterations to cerebral arteries/arterioles, i.e. cerebral hemorrhage/hemorrhages. Another aim of the study was to gain information about intermediate events in the pathogenesis of HCCAA and cell types involved by studying peripheral tissues.

This study showed that cerebrovascular alterations are a prominent feature in the pathogenesis of HCCAA and include severe CAA, loss of important vascular elements with or without BBB disturbance, i.e. degeneration of endothelial cells in some affected arteries/arterioles, changes in vessel wall ECM content with subsequent alterations to the cerebrovascular BM, fragmentation of the elastic layer and degeneration of SMCs. The loss of fundamental elements in the anatomy of the cerebrovascular wall affects the stiffness and elasticity of the vascular wall, and can therefore affect arterial flexibility.The normal function of vessel walls is dependent on the right quantities of ECM and SMCs. Therefore, it is likely that the combined effects of amyloid deposition, ECM accumulation and other vascular structural changes in cerebral arteries/arterioles cause a general weakening of the vessel wall that results in the severe early-onset hemorrhages seen in HCCAA.

The results from the second part of the study indicated that BM alterations consisting of COLIV accumulation are probably an early event in HCCAA pathogenesis in association with activation of fibroblasts and, furthermore, that fibroblasts are one of the cell types responsible for both cystatin C deposition and COLIV accumulation. Moreover, the results showed that the ECM accumulation was more extensive in the cerebral vasculature compared

to the vessels in peripheral tissues, which could be due to both the changes in the composition of the cerebrovascular BM and the contribution of ECM proteins which are secreted by cells involved in cerebrovascular glial scar formation in the brain. These significant alterations to the BM of HCCAA arteries/arterioles could lead to impaired perivascular drainage and thereby influence cystatin C build-up by trapping it in the arterial wall, as well as reducing arterial elasticity which is necessary for efficient perivascular drainage.

Overall, the aims of the study were met and the results represent a significant advancement in the understanding of HCCAA pathology and pathogenesis. These results provide a platform for future studies of the disorder, and will hopefully aid in the development of therapeutic interventions for the patients.

References

Abrahamson, M., Alvarez-Fernandez, M., & Nathanson, C. M. (2003). Cystatins. *Biochem Soc Symp*(70), 179-199.

Abrahamson, M., Barrett, A. J., Salvesen, G., & Grubb, A. (1986). Isolation of six cysteine proteinase inhibitors from human urine. Their physicochemical and enzyme kinetic properties and concentrations in biological fluids. *J Biol Chem, 261*(24), 11282-11289.

Abrahamson, M., Dalboge, H., Olafsson, I., Carlsen, S., & Grubb, A. (1988). Efficient production of native, biologically active human cystatin C by Escherichia coli. *FEBS Lett, 236*(1), 14-18.

Abrahamson, M., & Grubb, A. (1994). Increased body temperature accelerates aggregation of the Leu-68-->Gln mutant cystatin C, the amyloid-forming protein in hereditary cystatin C amyloid angiopathy. *Proc Natl Acad Sci U S A, 91*(4), 1416-1420.

Abrahamson, M., Grubb, A., Olafsson, I., & Lundwall, A. (1987). Molecular cloning and sequence analysis of cDNA coding for the precursor of the human cysteine proteinase inhibitor cystatin C. *FEBS Lett, 216*(2), 229-233.

Abrahamson, M., Jonsdottir, S., Olafsson, I., Jensson, O., & Grubb, A. (1992). Hereditary cystatin C amyloid angiopathy: identification of the disease- causing mutation and specific diagnosis by polymerase chain reaction based analysis. *Hum Genet, 89*(4), 377-380.

Abrahamson, M., Olafsson, I., Palsdottir, A., Ulvsback, M., Lundwall, A., Jensson, O., & Grubb, A. (1990). Structure and expression of the human cystatin C gene. *Biochem J, 268*(2), 287-294.

Alvarez-Fernandez, M., Barrett, A. J., Gerhartz, B., Dando, P. M., Ni, J., & Abrahamson, M. (1999). Inhibition of mammalian legumain by some cystatins is due to a novel second reactive site. *J Biol Chem, 274*(27), 19195-19203.

Ariga, T., Miyatake, T., & Yu, R. K. (2010). Role of proteoglycans and glycosaminoglycans in the pathogenesis of Alzheimer's disease and related disorders: amyloidogenesis and therapeutic strategies--a review. *J Neurosci Res, 88*(11), 2303-2315.

Arnason, A. (1935). Apoplexie und ihre vererbung. *Acta Pcyshiat Neurol, suppl VII*.

Asgeirsson, B., Haebel, S., Thorsteinsson, L., Helgason, E., Gudmundsson, K. O., Gudmundsson, G., & Roepstorff, P. (1998). Hereditary cystatin C amyloid angiopathy: monitoring the presence of the Leu-68-->Gln cystatin C variant in cerebrospinal fluids and monocyte cultures by MS. *Biochem J, 329 (Pt 3)*, 497-503.

Attems, J., Yamaguchi, H., Saido, T. C., & Thal, D. R. (2010). Capillary CAA and perivascular Abeta-deposition: two distinct features of Alzheimer's disease pathology. *J Neurol Sci, 299*(1-2), 155-162.

Bakker, E., van Broeckhoven, C., Haan, J., Voorhoeve, E., van Hul, W., Levy, E., Lieberburg, I., Carman, M. D., van Ommen, G. J., & Frangione, B. (1991). DNA diagnosis for hereditary cerebral hemorrhage with amyloidosis (Dutch type)[comment]. *American Journal of Human Genetics, 49*(3), 518-521.

Ballabh, P., Braun, A., & Nedergaard, M. (2004). The blood-brain barrier: an overview: structure, regulation, and clinical implications. *Neurobiol Dis, 16*(1), 1-13.

Bardin, T., Zingraff, J., Shirahama, T., Noel, L. H., Droz, D., Voisin, M. C., Drueke, T., Dryll, A., Skinner, M., Cohen, A. S., & et al. (1987). Hemodialysis-associated amyloidosis and beta-2 microglobulin. Clinical and immunohistochemical study. *Am J Med, 83*(3), 419-424.

Barrett, A. J. (1986). The cystatins: a diverse superfamily of cysteine peptidase inhibitors. *Biomed Biochim Acta, 45*(11-12), 1363-1374.

Bartus, K., James, N. D., Bosch, K. D., & Bradbury, E. J. (2012). Chondroitin sulphate proteoglycans: key modulators of spinal cord and brain plasticity. *Exp Neurol, 235*(1), 5-17.

Baskakov, I. V., Legname, G., Baldwin, M. A., Prusiner, S. B., & Cohen, F. E. (2002). Pathway complexity of prion protein assembly into amyloid. *J Biol Chem, 277*(24), 21140-21148.

Batarseh, Y. S., Duong, Q. V., Mousa, Y. M., Al Rihani, S. B., Elfakhri, K., & Kaddoumi, A. (2016). Amyloid-beta and Astrocytes Interplay in Amyloid-beta Related Disorders. *Int J Mol Sci, 17*(3), 338.

Baum, J., & Duffy, H. S. (2011). Fibroblasts and myofibroblasts: what are we talking about? *J Cardiovasc Pharmacol, 57*(4), 376-379.

Bell, R. D., & Zlokovic, B. V. (2009). Neurovascular mechanisms and blood-brain barrier disorder in Alzheimer's disease. *Acta Neuropathol, 118*(1), 103-113.

Benarroch, E. E. (2015). Extracellular matrix in the CNS: Dynamic structure and clinical correlations. *Neurology, 85*(16), 1417-1427.

Benedikz, E., Blondal, H., & Gudmundsson, G. (1990). Skin deposits in hereditary cystatin C amyloidosis. *Virchows Arch A Pathol Anat Histopathol, 417*(4), 325-331.

Benedikz, E., Merz, G. S., Schwenk, V., Johansen, T. E., Wisniewski, H. M., & Rushbrook, J. I. (1999). Cellular processing of the amyloidogenic cystatin C variant of hereditary cerebral hemorrhage with amyloidosis, Icelandic type. *Amyloid, 6*(3), 172-182.

Bengtsson, E., To, F., Hakansson, K., Grubb, A., Branen, L., Nilsson, J., & Jovinge, S. (2005). Lack of the cysteine protease inhibitor cystatin C promotes atherosclerosis in apolipoprotein E-deficient mice. *Arterioscler Thromb Vasc Biol, 25*(10), 2151-2156.

Benussi, L., Ghidoni, R., Steinhoff, T., Alberici, A., Villa, A., Mazzoli, F., Nicosia, F., Barbiero, L., Broglio, L., Feudatari, E., Signorini, S., Finckh, U., Nitsch, R. M., & Binetti, G. (2003). Alzheimer disease-associated cystatin C variant undergoes impaired secretion. *Neurobiol Dis, 13*(1), 15-21.

Biernacka, A., Dobaczewski, M., & Frangogiannis, N. G. (2011). TGF-beta signaling in fibrosis. *Growth Factors, 29*(5), 196-202.

Biffi, A., & Greenberg, S. M. (2011). Cerebral amyloid angiopathy: a systematic review. *J Clin Neurol, 7*(1), 1-9.

Bjarnadottir, M., Nilsson, C., Lindstrom, V., Westman, A., Davidsson, P., Thormodsson, F., Blondal, H., Gudmundsson, G., & Grubb, A. (2001). The cerebral hemorrhage-producing cystatin C variant (L68Q) in extracellular fluids. *Amyloid, 8*(1), 1-10.

Bjarnadottir, M., Wulff, B. S., Sameni, M., Sloane, B. F., Keppler, D., Grubb, A., & Abrahamson, M. (1998). Intracellular accumulation of the amyloidogenic L68Q variant of human cystatin C in NIH/3T3 cells. *Mol Pathol, 51*(6), 317-326.

Blancas-Mejia, L. M., & Ramirez-Alvarado, M. (2013). Systemic amyloidoses. *Annu Rev Biochem, 82*, 745-774.

Blobe, G. C., Schiemann, W. P., & Lodish, H. F. (2000). Role of transforming growth factor beta in human disease. *N Engl J Med, 342*(18), 1350-1358.

Blondal, H., Guomundsson, G., Benedikz, E., & Johannesson, G. (1989). Dementia in hereditary cystatin C amyloidosis. *Prog Clin Biol Res, 317*, 157-164.

Blondal, H., Guomundsson, G., Benedikz, E., & Johannesson, G. (1990). [Hereditary cerebral hemorrhage. Dementia with cystatin C amyloidosis]. *Nord Med, 105*(3), 76-77, 81.

Bode, W., Engh, R., Musil, D., Thiele, U., Huber, R., Karshikov, A., Brzin, J., Kos, J., & Turk, V. (1988). The 2.0 A X-ray crystal structure of chicken egg white cystatin and its possible mode of interaction with cysteine proteinases. *Embo J, 7*(8), 2593-2599.

Bornebroek, M., Haan, J., & Roos, R. A. (1999). Hereditary cerebral hemorrhage with amyloidosis--Dutch type (HCHWA-D): a review of the variety in phenotypic expression. *Amyloid, 6*(3), 215-224.

Bourasset, F., Ouellet, M., Tremblay, C., Julien, C., Do, T. M., Oddo, S., LaFerla, F., & Calon, F. (2009). Reduction of the cerebrovascular volume in a transgenic mouse model of Alzheimer's disease. *Neuropharmacology, 56*(4), 808-813.

Braak, H., & Braak, E. (1991). Demonstration of amyloid deposits and neurofibrillary changes in whole brain sections. *Brain Pathol, 1*(3), 213-216.

Braak, H., de Vos, R. A., Jansen, E. N., Bratzke, H., & Braak, E. (1998). Neuropathological hallmarks of Alzheimer's and Parkinson's diseases. *Prog Brain Res, 117*, 267-285.

Bronfman, F. C., Alvarez, A., Morgan, C., & Inestrosa, N. C. (1998). Laminin blocks the assembly of wild-type A beta and the Dutch variant peptide into Alzheimer's fibrils. *Amyloid, 5*(1), 16-23.

Bucciantini, M., Giannoni, E., Chiti, F., Baroni, F., Formigli, L., Zurdo, J., Taddei, N., Ramponi, G., Dobson, C. M., & Stefani, M. (2002). Inherent toxicity of aggregates implies a common mechanism for protein misfolding diseases. *Nature, 416*(6880), 507-511.

Burda, J. E., Bernstein, A. M., & Sofroniew, M. V. (2016). Astrocyte roles in traumatic brain injury. *Exp Neurol, 275 Pt 3*, 305-315.

Cacace, R., Sleegers, K., & Van Broeckhoven, C. (2016). Molecular genetics of early-onset Alzheimer's disease revisited. *Alzheimers & Dementia, 12*(6), 733-748.

Cadavid, D., Mena, H., Koeller, K., & Frommelt, R. A. (2000). Cerebral beta amyloid angiopathy is a risk factor for cerebral ischemic infarction. A case control study in human brain biopsies. *J Neuropathol Exp Neurol, 59*(9), 768-773.

Cagnin, A., Brooks, D. J., Kennedy, A. M., Gunn, R. N., Myers, R., Turkheimer, F. E., Jones, T., & Banati, R. B. (2001). In-vivo measurement of activated microglia in dementia. *Lancet, 358*(9280), 461-467.

Capell, B. C., Collins, F. S., & Nabel, E. G. (2007). Mechanisms of cardiovascular disease in accelerated aging syndromes. *Circ Res, 101*(1), 13-26.

Carare, R. O., Bernardes-Silva, M., Newman, T. A., Page, A. M., Nicoll, J. A., Perry, V. H., & Weller, R. O. (2008). Solutes, but not cells, drain from the brain parenchyma along basement membranes of capillaries and arteries: significance for cerebral amyloid angiopathy and neuroimmunology. *Neuropathol Appl Neurobiol, 34*(2), 131-144.

Carare, R. O., Hawkes, C. A., Jeffrey, M., Kalaria, R. N., & Weller, R. O. (2013). Review: cerebral amyloid angiopathy, prion angiopathy, CADASIL and the spectrum of protein elimination failure angiopathies (PEFA) in neurodegenerative disease with a focus on therapy. *Neuropathol Appl Neurobiol, 39*(6), 593-611.

Carrette, O., Burkhard, P. R., Hughes, S., Hochstrasser, D. F., & Sanchez, J. C. (2005). Truncated cystatin C in cerebrospiral fluid: Technical [corrected] artefact or biological process? *Proteomics, 5*(12), 3060-3065.

Cashman, J. R., Ghirmai, S., Abel, K. J., & Fiala, M. (2008). Immune defects in Alzheimer's disease: new medications development. *BMC Neurosci, 9 Suppl 2*, S13.

Castillo, G. M., Ngo, C., Cummings, J., Wight, T. N., & Snow, A. D. (1997). Perlecan binds to the beta-amyloid proteins (A beta) of Alzheimer's disease, accelerates A beta fibril formation, and maintains A beta fibril stability. *J Neurochem, 69*(6), 2452-2465.

Chiang, C. K., Hsu, S. P., Wu, C. T., Huang, J. W., Cheng, H. T., Chang, Y. W., Hung, K. Y., Wu, K. D., & Liu, S. H. (2011). Endoplasmic reticulum stress implicated in the development of renal fibrosis. *Mol Med, 17*(11-12), 1295-1305.

Chiti, F., & Dobson, C. M. (2006a). Protein misfolding, functional amyloid, and human disease. *Annual Review of Biochemistry, 75*, 333-366.

Chiti, F., & Dobson, C. M. (2006b). Protein misfolding, functional amyloid, and human disease. *Annu Rev Biochem, 75*, 333-366.

Christov, A., Ottman, J., Hamdheydari, L., & Grammas, P. (2008). Structural changes in Alzheimer's disease brain microvessels. *Curr Alzheimer Res, 5*(4), 392-395.

Cohen, D. H., Feiner, H., Jensson, O., & Frangione, B. (1983). Amyloid fibril in hereditary cerebral hemorrhage with amyloidosis (HCHWA) is related to the gastroentero-pancreatic neuroendocrine protein, gamma trace. *J Exp Med, 158*(2), 623-628.

Cotman, S. L., Halfter, W., & Cole, G. J. (2000). Agrin binds to beta-amyloid (Abeta), accelerates abeta fibril formation, and is localized to Abeta deposits in Alzheimer's disease brain. *Mol Cell Neurosci, 15*(2), 183-198.

Dickson, D. W. (1997). The pathogenesis of senile plaques. *J Neuropathol Exp Neurol, 56*(4), 321-339.

Dickson, D. W., Farlo, J., Davies, P., Crystal, H., Fuld, P., & Yen, S. H. (1988). Alzheimer's disease. A double-labeling immunohistochemical study of senile plaques. *Am J Pathol, 132*(1), 86-101.

Dong, H., Blaivas, M., & Wang, M. M. (2012). Bidirectional encroachment of collagen into the tunica media in cerebral autosomal dominant arteriopathy with subcortical infarcts and leukoencephalopathy. *Brain Res, 1456*, 64-71.

Duyckaerts, C., Delatour, B., & Potier, M. C. (2009). Classification and basic pathology of Alzheimer disease. *Acta Neuropathol, 118*(1), 5-36.

Eikelenboom, P., & Veerhuis, R. (1996). The role of complement and activated microglia in the pathogenesis of Alzheimer's disease. *Neurobiol Aging, 17*(5), 673-680.

Ekiel, I., & Abrahamson, M. (1996). Folding-related dimerization of human cystatin C. *J Biol Chem, 271*(3), 1314-1321.

Ekiel, I., Abrahamson, M., Fulton, D. B., Lindahl, P., Storer, A. C., Levadoux, W., Lafrance, M., Labelle, S., Pomerleau, Y., Groleau, D., LeSauteur, L., & Gehring, K. (1997). NMR structural studies of human cystatin C dimers and monomers. *J Mol Biol, 271*(2), 266-277.

Engelhardt, B., Carare, R. O., Bechmann, I., Flugel, A., Laman, J. D., & Weller, R. O. (2016). Vascular, glial, and lymphatic immune gateways of the central nervous system. *Acta Neuropathol, 132*(3), 317-338.

Fiala, M., Lin, J., Ringman, J., Kermani-Arab, V., Tsao, G., Patel, A., Lossinsky, A. S., Graves, M. C., Gustavson, A., Sayre, J., Sofroni, E., Suarez, T., Chiappelli, F., & Bernard, G. (2005). Ineffective phagocytosis of amyloid-beta by macrophages of Alzheimer's disease patients. *J Alzheimers Dis, 7*(3), 221-232; discussion 255-262.

Fonovic, M., & Turk, B. (2014). Cysteine cathepsins and extracellular matrix degradation. *Biochim Biophys Acta, 1840*(8), 2560-2570.

Fossati, S., Ghiso, J., & Rostagno, A. (2012). Insights into caspase-mediated apoptotic pathways induced by amyloid-beta in cerebral microvascular endothelial cells. *Neurodegener Dis, 10*(1-4), 324-328.

Frackowiak, J., Potempska, A., LeVine, H., Haske, T., Dickson, D., & Mazur-Kolecka, B. (2005). Extracellular deposits of A beta produced in cultures of Alzheimer disease brain vascular smooth muscle cells. *J Neuropathol Exp Neurol, 64*(1), 82-90.

Frangione, B., Revesz, T., Vidal, R., Holton, J., Lashley, T., Houlden, H., Wood, N., Rostagno, A., Plant, G., & Ghiso, J. (2001). Familial cerebral amyloid angiopathy related to stroke and dementia. *Amyloid, 8 Suppl 1*, 36-42.

Gerhartz, B., & Abrahamson, M. (2002). Physico-chemical properties of the N-terminally truncated L68Q cystatin C found in amyloid deposits of brain haemorrhage patients. *Biol Chem, 383*(2), 301-305.

Ghiso, J., & Frangione, B. (2002). Amyloidosis and Alzheimer's disease. *Adv Drug Deliv Rev, 54*(12), 1539-1551.

Ghiso, J., Jensson, O., & Frangione, B. (1986). Amyloid fibrils in hereditary cerebral hemorrhage with amyloidosis of Icelandic type is a variant of gamma-trace basic protein (cystatin C). *Proc Natl Acad Sci U S A, 83*(9), 2974-2978.

Glenner, G. G., & Wong, C. W. (1984). Alzheimer's disease: initial report of the purification and characterization of a novel cerebrovascular amyloid protein. *Biochem Biophys Res Commun, 120*(3), 885-890.

Goate, A., Chartier-Harlin, M. C., Mullan, M., Brown, J., Crawford, F., Fidani, L., Giuffra, L., Haynes, A., Irving, N., James, L., & et al. (1991). Segregation of a missense mutation in the amyloid precursor protein gene with familial Alzheimer's disease. *Nature, 349*(6311), 704-706.

Graffagnino, C., Herbstreith, M. H., Schmechel, D. E., Levy, E., Roses, A. D., & Alberts, M. J. (1995). Cystatin C mutation in an elderly man with sporadic amyloid angiopathy and intracerebral hemorrhage. *Stroke, 26*(11), 2190-2193.

Grubb, A. (1992). Diagnostic value of analysis of cystatin C and protein HC in biological fluids. *Clin Nephrol, 38*(Suppl 1), S20-27.

Grubb, A., Jensson, O., Gudmundsson, G., Arnason, A., Lofberg, H., & Malm, J. (1984a). Abnormal metabolism of gamma-trace alkaline microprotein. The basic defect in hereditary cerebral hemorrhage with amyloidosis. *N Engl J Med, 311*(24), 1547-1549.

Grubb, A., & Lofberg, H. (1982). Human gamma-trace, a basic microprotein: amino acid sequence and presence in the adenohypophysis. *Proc Natl Acad Sci U S A, 79*(9), 3024-3027.

Grubb, A., Löfberg, H., & Barrett, A. J. (1984b). The disulphide bridges of human cystatin C (g-trace) and chicken cystatin. *FEBS Letters, 170*(2), 370-374.

Grubb, A. O. (2000). Cystatin C--properties and use as diagnostic marker. *Adv Clin Chem, 35*, 63-99.

Grubb, A. O., Weiber, H., & Lofberg, H. (1983). The gamma-trace concentration of normal human seminal plasma is thirty- six times that of normal human blood plasma. *Scand J Clin Lab Invest, 43*(5), 421-425.

Gudmundsson, G., Hallgrimsson, J., Jonasson, T. A., & Bjarnason, O. (1972). Hereditary cerebral haemorrhage with amyloidosis. *Brain, 95*(2), 387-404.

Guillemin, G. J., & Brew, B. J. (2004). Microglia, macrophages, perivascular macrophages, and pericytes: a review of function and identification. *J Leukoc Biol, 75*(3), 388-397.

Haan, J., Maat-Schieman, M. L., van Duinen, S. G., Jensson, O., Thorsteinsson, L., & Roos, R. A. (1994a). Co-localization of beta/A4 and cystatin C in cortical blood vessels in Dutch, but not in Icelandic hereditary cerebral hemorrhage with amyloidosis. *Acta Neurol Scand, 89*(5), 367-371.

Haan, J., Van Broeckhoven, C., van Duijn, C. M., Voorhoeve, E., van Harskamp, F., van Swieten, J. C., Maat-Schieman, M. L., Roos, R. A., & Bakker, E. (1994b). The apolipoprotein E epsilon 4 allele does not influence the clinical expression of the amyloid precursor protein gene codon 693 or 692 mutations. *Ann Neurol, 36*(3), 434-437.

Haass, C., & Selkoe, D. J. (1993). Cellular Processing of Beta-Amyloid Precursor Protein and the Genesis of Amyloid Beta-Peptide. *Cell, 75*(6), 1039-1042.

Habashi, J. P., Judge, D. P., Holm, T. M., Cohn, R. D., Loeys, B. L., Cooper, T. K., Myers, L., Klein, E. C., Liu, G., Calvi, C., Podowski, M., Neptune, E. R., Halushka, M. K., Bedja, D., Gabrielson, K., Rifkin, D. B., Carta, L., Ramirez, F., Huso, D. L., & Dietz, H. C. (2006). Losartan, an AT1 antagonist, prevents aortic aneurysm in a mouse model of Marfan syndrome. *Science, 312*(5770), 117-121.

Hakansson, K., Huh, C., Grubb, A., Karlsson, S., & Abrahamson, M. (1996). Mouse and rat cystatin C: Escherichia coli production, characterization and tissue distribution. *Comp Biochem Physiol B Biochem Mol Biol, 114*(3), 303-311.

Hallmann, R., Horn, N., Selg, M., Wendler, O., Pausch, F., & Sorokin, L. M. (2005). Expression and function of laminins in the embryonic and mature vasculature. *Physiol Rev, 85*(3), 979-1000.

Hardy, J., & Selkoe, D. J. (2002). The amyloid hypothesis of Alzheimer's disease: progress and problems on the road to therapeutics. *Science, 297*(5580), 353-356.

Hardy, J. A., & Higgins, G. A. (1992). Alzheimer's disease: the amyloid cascade hypothesis. *Science, 256*(5054), 184-185.

Hawkes, C. A., Gatherer, M., Sharp, M. M., Dorr, A., Yuen, H. M., Kalaria, R., Weller, R. O., & Carare, R. O. (2013). Regional differences in the morphological and functional effects of aging on cerebral basement membranes and perivascular drainage of amyloid-beta from the mouse brain. *Aging Cell, 12*(2), 224-236.

Hawkes, C. A., Hartig, W., Kacza, J., Schliebs, R., Weller, R. O., Nicoll, J. A., & Carare, R. O. (2011). Perivascular drainage of solutes is impaired in the ageing mouse brain and in the presence of cerebral amyloid angiopathy. *Acta Neuropathol, 121*(4), 431-443.

Hawkes, C. A., Jayakody, N., Johnston, D. A., Bechmann, I., & Carare, R. O. (2014). Failure of perivascular drainage of beta-amyloid in cerebral amyloid angiopathy. *Brain Pathol, 24*(4), 396-403.

Haydon, P. G. (2001). GLIA: listening and talking to the synapse. *Nat Rev Neurosci, 2*(3), 185-193.

Heneka, M. T., Carson, M. J., El Khoury, J., Landreth, G. E., Brosseron, F., Feinstein, D. L., Jacobs, A. H., Wyss-Coray, T., Vitorica, J., Ransohoff, R. M., Herrup, K., Frautschy, S. A., Finsen, B., Brown, G. C., Verkhratsky, A., Yamanaka, K., Koistinaho, J., Latz, E., Halle, A., Petzold, G. C., Town, T., Morgan, D., Shinohara, M. L., Perry, V. H., Holmes, C., Bazan, N. G., Brooks, D. J., Hunot, S., Joseph, B., Deigendesch, N., Garaschuk, O., Boddeke, E., Dinarello, C. A., Breitner, J. C., Cole, G. M., Golenbock, D. T., & Kummer, M. P. (2015). Neuroinflammation in Alzheimer's disease. *Lancet Neurol, 14*(4), 388-405.

Herzig, M. C., Winkler, D. T., Burgermeister, P., Pfeifer, M., Kohler, E., Schmidt, S. D., Danner, S., Abramowski, D., Sturchler-Pierrat, C., Burki, K., van Duinen, S. G., Maat-Schieman, M. L., Staufenbiel, M., Mathews, P. M., & Jucker, M. (2004). Abeta is targeted to the vasculature in a mouse model of hereditary cerebral hemorrhage with amyloidosis. *Nat Neurosci, 7*(9), 954-960.

Hinz, B. (2007). Formation and function of the myofibroblast during tissue repair. *J Invest Dermatol, 127*(3), 526-537.

Hinz, B. (2010). The myofibroblast: paradigm for a mechanically active cell. *J Biomech, 43*(1), 146-155.

Hinz, B. (2016). Myofibroblasts. *Exp Eye Res, 142*, 56-70.

Hochwald, G. M., Pepe, A. J., & Thorbecke, G. J. (1967). Trace proteins in biological fluids. IV. Physicochemical properties and sites of formation of gamma-trace and beta-trace proteins. *Proc Soc Exp Biol Med, 124*(3), 961-966.

Horstmann, S., Budig, L., Gardner, H., Koziol, J., Deuschle, M., Schilling, C., & Wagner, S. (2010). Matrix metalloproteinases in peripheral blood and cerebrospinal fluid in patients with Alzheimer's disease. *Int Psychogeriatr, 22*(6), 966-972.

Hyman, B. T., Phelps, C. H., Beach, T. G., Bigio, E. H., Cairns, N. J., Carrillo, M. C., Dickson, D. W., Duyckaerts, C., Frosch, M. P., Masliah, E., Mirra, S. S., Nelson, P. T., Schneider, J. A., Thal, D. R., Thies, B., Trojanowski, J. Q., Vinters, H. V., & Montine, T. J. (2012). National Institute on Aging-Alzheimer's Association guidelines for the neuropathologic assessment of Alzheimer's disease. *Alzheimers Dement, 8*(1), 1-13.

Itagaki, S., McGeer, P. L., Akiyama, H., Zhu, S., & Selkoe, D. (1989). Relationship of microglia and astrocytes to amyloid deposits of Alzheimer disease. *J Neuroimmunol, 24*(3), 173-182.

Itoh, Y., Yamada, M., Hayakawa, M., Otomo, E., & Miyatake, T. (1993). Cerebral amyloid angiopathy: a significant cause of cerebellar as well as lobar cerebral hemorrhage in the elderly. *J Neurol Sci, 116*(2), 135-141.

Janowski, R., Kozak, M., Jankowska, E., Grzonka, Z., Grubb, A., Abrahamson, M., & Jaskolski, M. (2001). Human cystatin C, an amyloidogenic protein, dimerizes through three-dimensional domain swapping. *Nat Struct Biol, 8*(4), 316-320.

Jellinger, K. A. (2002). Alzheimer disease and cerebrovascular pathology: an update. *J Neural Transm (Vienna), 109*(5-6), 813-836.

Jensson, O., Gudmundsson, G., Arnason, A., Blondal, H., Grubb, A., & Lofberg, H. (1986). Hereditary central nervous system gamma-trace amyloid angiopathy and stroke in icelandic families. In G. G. Glenner, E. F. Osserman, E. P. Benditt, E. Calkins, A. Cohen, & D. Zucker-Franklin (Eds.), *Amyloidosis* (pp. 585-590). New York: Plenum Publishing Corp.

Jensson, O., Gudmundsson, G., Arnason, A., Blondal, H., Petursdottir, I., Thorsteinsson, L., Grubb, A., Lofberg, H., Cohen, D., & Frangione, B. (1987). Hereditary cystatin C (gamma-trace) amyloid angiopathy of the CNS causing cerebral hemorrhage. *Acta Neurol Scand, 76*(2), 102-114.

Jonsdottir, H. R., Arason, A. J., Palsson, R., Franzdottir, S. R., Gudbjartsson, T., Isaksson, H. J., Gudmundsson, G., Gudjonsson, T., & Magnusson, M. K. (2015). Basal cells of the human airways acquire mesenchymal traits in idiopathic pulmonary fibrosis and in culture. *Lab Invest, 95*(12), 1418-1428.

Joutel, A., Dodick, D. D., Parisi, J. E., Cecillon, M., Tournier-Lasserve, E., & Bousser, M. G. (2000). De novo mutation in the Notch3 gene causing CADASIL. *Ann Neurol, 47*(3), 388-391.

Jurczak, P., Groves, P., Szymanska, A., & Rodziewicz-Motowidlo, S. (2016). Human cystatin C monomer, dimer, oligomer, and amyloid structures are related to health and disease. *FEBS Lett, 590*(23), 4192-4201.

Kacem, K., Lacombe, P., Seylaz, J., & Bonvento, G. (1998). Structural organization of the perivascular astrocyte endfeet and their relationship with the endothelial glucose transporter: a confocal microscopy study. *Glia, 23*(1), 1-10.

Kaeser, S. A., Herzig, M. C., Coomaraswamy, J., Kilger, E., Selenica, M. L., Winkler, D. T., Staufenbiel, M., Levy, E., Grubb, A., & Jucker, M. (2007). Cystatin C modulates cerebral beta-amyloidosis. *Nat Genet, 39*(12), 1437-1439.

Kalaria, R. N., & Pax, A. B. (1995). Increased collagen content of cerebral microvessels in Alzheimer's disease. *Brain Res, 705*(1-2), 349-352.

Kalluri, R. (2003). Basement membranes: structure, assembly and role in tumour angiogenesis. *Nat Rev Cancer, 3*(6), 422-433.

Kalluri, R., & Weinberg, R. A. (2009). The basics of epithelial-mesenchymal transition. *J Clin Invest, 119*(6), 1420-1428.

Kanta, J. (2015). Collagen matrix as a tool in studying fibroblastic cell behavior. *Cell Adh Migr, 9*(4), 308-316.

Kasabova, M., Joulin-Giet, A., Lecaille, F., Gilmore, B. F., Marchand-Adam, S., Saidi, A., & Lalmanach, G. (2014). Regulation of TGF-beta1-driven differentiation of human lung fibroblasts: emerging roles of cathepsin B and cystatin C. *J Biol Chem, 289*(23), 16239-16251.

Kaur, G., & Levy, E. (2012). Cystatin C in Alzheimer's disease. *Frontiers in Molecular Neuroscience, 5*.

Kawano, H., Kimura-Kuroda, J., Komuta, Y., Yoshioka, N., Li, H. P., Kawamura, K., Li, Y., & Raisman, G. (2012). Role of the lesion scar in the response to damage and repair of the central nervous system. *Cell Tissue Res, 349*(1), 169-180.

Kettenmann, H., & Verkhratsky, A. (2008). Neuroglia: the 150 years after. *Trends Neurosci, 31*(12), 653-659.

Kilic, T., & Akakin, A. (2008). Anatomy of cerebral veins and sinuses. *Front Neurol Neurosci, 23*, 4-15.

Kim, S. U., & de Vellis, J. (2005). Microglia in health and disease. *J Neurosci Res, 81*(3), 302-313.

Kiuchi, Y., Isobe, Y., Fukushima, K., & Kimura, M. (2002). Disassembly of amyloid beta-protein fibril by basement membrane components. *Life Sci, 70*(20), 2421-2431.

Knudsen, K. A., Rosand, J., Karluk, D., & Greenberg, S. M. (2001). Clinical diagnosis of cerebral amyloid angiopathy: validation of the Boston criteria. *Neurology, 56*(4), 537-539.

Kurzepa, J., Kurzepa, J., Golab, P., Czerska, S., & Bielewicz, J. (2014). The significance of matrix metalloproteinase (MMP)-2 and MMP-9 in the ischemic stroke. *Int J Neurosci, 124*(10), 707-716.

Kyle, R. A. (2001). Amyloidosis: a convoluted story. *Br J Haematol, 114*(3), 529-538.

Lamb, B. T., Sisodia, S. S., Lawler, A. M., Slunt, H. H., Kitt, C. A., Kearns, W. G., Pearson, P. L., Price, D. L., & Gearhart, J. D. (1993). Introduction and expression of the 400 kilobase amyloid precursor protein gene in transgenic mice [corrected]. *Nat Genet, 5*(1), 22-30.

Lambert, M. P., Barlow, A. K., Chromy, B. A., Edwards, C., Freed, R., Liosatos, M., Morgan, T. E., Rozovsky, I., Trommer, B., Viola, K. L., Wals, P., Zhang, C., Finch, C. E., Krafft, G. A., & Klein, W. L. (1998). Diffusible, nonfibrillar ligands derived from Abeta1-42 are potent central nervous system neurotoxins. *Proc Natl Acad Sci U S A, 95*(11), 6448-6453.

Lan, T. H., Huang, X. Q., & Tan, H. M. (2013). Vascular fibrosis in atherosclerosis. *Cardiovasc Pathol, 22*(5), 401-407.

LeBleu, V. S., Macdonald, B., & Kalluri, R. (2007). Structure and function of basement membranes. *Exp Biol Med (Maywood), 232*(9), 1121-1129.

Lee, R. M. (1995). Morphology of cerebral arteries. *Pharmacol Ther, 66*(1), 149-173.

Lenarcic, B., Krasovec, M., Ritonja, A., Olafsson, I., & Turk, V. (1991). Inactivation of human cystatin C and kininogen by human cathepsin D. *FEBS Lett, 280*(2), 211-215.

Lenna, S., & Trojanowska, M. (2012). The role of endoplasmic reticulum stress and the unfolded protein response in fibrosis. *Curr Opin Rheumatol, 24*(6), 663-668.

Lepelletier, F. X., Mann, D. M., Robinson, A. C., Pinteaux, E., & Boutin, H. (2015). Early changes in extracellular matrix in Alzheimer's disease. *Neuropathol Appl Neurobiol, 43*(2), 167-182.

Levy, E., Carman, M. D., Fernandez-Madrid, I. J., Power, M. D., Lieberburg, I., van Duinen, S. G., Bots, G. T., Luyendijk, W., & Frangione, B. (1990). Mutation of the Alzheimer's disease amyloid gene in hereditary cerebral hemorrhage, Dutch type. *Science, 248*(4959), 1124-1126.

Levy, E., Lopez-Otin, C., Ghiso, J., Geltner, D., & Frangione, B. (1989). Stroke in Icelandic patients with hereditary amyloid angiopathy is related to a mutation in the cystatin C gene, an inhibitor of cysteine proteases. *J Exp Med, 169*(5), 1771-1778.

Levy, E., Sastre, M., Kumar, A., Gallo, G., Piccardo, P., Ghetti, B., & Tagliavini, F. (2001). Codeposition of cystatin C with amyloid-beta protein in the brain of Alzheimer disease patients. *J Neuropathol Exp Neurol, 60*(1), 94-104.

Lewandowska, E., Dziewulska, D., Parys, M., & Pasennik, E. (2011). Ultrastructure of granular osmiophilic material deposits (GOM) in arterioles of CADASIL patients. *Folia Neuropathol, 49*(3), 174-180.

Liberski, P. P. (1993a). Subacute spongiform encephalopathies--the transmissible brain amyloidoses: a comparison with the non-transmissible brain amyloidoses of Alzheimer type. *J Comp Pathol, 109*(2), 103-127.

Liberski, P. P. (1993b). [Transmissible and non-transmissible brain amyloidoses: neurodegenerative disorders of different etiologies and the same pathogenesis]. *Patol Pol, 44*(1), 19-30.

Lindblom A, P. M. (1996). Basement Membranes. *In: Comper WD, editor. Extracellular Matrix. Amsterdam: Harwood Academic Publisher GmbH*, pp. 132–174.

Liu, C. C., Kanekiyo, T., Xu, H., & Bu, G. (2013). Apolipoprotein E and Alzheimer disease: risk, mechanisms and therapy. *Nat Rev Neurol, 9*(2), 106-118.

Liu, W., Tang, Y., & Feng, J. (2011). Cross talk between activation of microglia and astrocytes in pathological conditions in the central nervous system. *Life Sci, 89*(5-6), 141-146.

Lofberg, H., & Grubb, A. O. (1979). Quantitation of gamma-trace in human biological fluids: indications for production in the central nervous system. *Scand J Clin Lab Invest, 39*(7), 619-626.

Lofberg, H., Grubb, A. O., Nilsson, E. K., Jensson, O., Gudmundsson, G., Blondal, H., Arnason, A., & Thorsteinsson, L. (1987). Immunohistochemical characterization of the amyloid deposits and quantitation of pertinent cerebrospinal fluid proteins in hereditary cerebral hemorrhage with amyloidosis. *Stroke, 18*(2), 431-440.

Logan, A., Berry, M., Gonzalez, A. M., Frautschy, S. A., Sporn, M. B., & Baird, A. (1994). Effects of transforming growth factor beta 1 on scar production in the injured central nervous system of the rat. *Eur J Neurosci, 6*(3), 355-363.

Lukaszewicz-Zajac, M., Mroczko, B., & Slowik, A. (2014). Matrix metalloproteinases (MMPs) and their tissue inhibitors (TIMPs) in amyotrophic lateral sclerosis (ALS). *J Neural Transm (Vienna), 121*(11), 1387-1397.

Luyendijk, W., Bots, G. T., Vegter-van der Vlis, M., Went, L. N., & Frangione, B. (1988). Hereditary cerebral haemorrhage caused by cortical amyloid angiopathy. *J Neurol Sci, 85*(3), 267-280.

Luyendijk, W., & Schoen, J. H. (1964). Intracerebral Hematomas. A Clinical Study of 40 Surgical Cases. *Psychiatr Neurol Neurochir, 67*, 445-468.

Maat-Schieman, M. L., Radder, C. M., van Duinen, S. G., Haan, J., & Roos, R. A. (1994). Hereditary cerebral hemorrhage with amyloidosis (Dutch): a model for congophilic plaque formation without neurofibrillary pathology. *Acta Neuropathol, 88*(4), 371-378.

Maat-Schieman, M. L., Roos, R., & van Duinen, S. (2005). Hereditary cerebral hemorrhage with amyloidosis-Dutch type. *Neuropathology, 25*(4), 288-297.

Maat-Schieman, M. L., van Duinen, S. G., Bornebroek, M., Haan, J., & Roos, R. A. (1996). Hereditary cerebral hemorrhage with amyloidosis-Dutch type (HCHWA-D): II--A review of histopathological aspects. *Brain Pathol, 6*(2), 115-120.

Maat-Schieman, M. L., van Duinen, S. G., Rozemuller, A. J., Haan, J., & Roos, R. A. (1997). Association of vascular amyloid beta and cells of the mononuclear phagocyte system in hereditary cerebral hemorrhage with amyloidosis (Dutch) and Alzheimer disease. *J Neuropathol Exp Neurol, 56*(3), 273-284.

Maat-Schieman, M. L., Yamaguchi, H., Hegeman-Kleinn, I. M., Welling-Graafland, C., Natte, R., Roos, R. A., & Van Duinen, S. G. (2004). Glial reactions and the clearance of amyloid beta protein in the brains of patients with hereditary cerebral hemorrhage with amyloidosis-Dutch type. *Acta Neuropathol (Berl)*.

Maat-Schieman, M. L., Yamaguchi, H., van Duinen, S. G., Natte, R., & Roos, R. A. (2000). Age-related plaque morphology and C-terminal heterogeneity of amyloid beta in Dutch-type hereditary cerebral hemorrhage with amyloidosis. *Acta Neuropathol (Berl), 99*(4), 409-419.

Makin, O. S., & Serpell, L. C. (2005). Structures for amyloid fibrils. *Febs J, 272*(23), 5950-5961.

Mandybur, T. I. (1986). Cerebral amyloid angiopathy: the vascular pathology and complications. *J Neuropathol Exp Neurol, 45*(1), 79-90.

Mandybur, T. I. (1989). Cerebral amyloid angiopathy and astrocytic gliosis in Alzheimer's disease. *Acta Neuropathol, 78*(3), 329-331.

Martinez-Lemus, L. A. (2012). The dynamic structure of arterioles. *Basic Clin Pharmacol Toxicol, 110*(1), 5-11.

Maruyama, K., Ikeda, S., Ishihara, T., Allsop, D., & Yanagisawa, N. (1990). Immunohistochemical characterization of cerebrovascular amyloid in 46 autopsied cases using antibodies to beta protein and cystatin C. *Stroke, 21*(3), 397-403.

Maruyama, K., Kametani, F., Ikeda, S., Ishihara, T., & Yanagisawa, N. (1992). Characterization of amyloid fibril protein from a case of cerebral amyloid angiopathy showing immunohistochemical reactivity for both beta protein and cystatin C. *Neurosci Lett, 144*(1-2), 38-42.

Massague, J. (1998). TGF-beta signal transduction. *Annu Rev Biochem, 67*, 753-791.

Massague, J. (2012). TGFbeta signalling in context. *Nat Rev Mol Cell Biol, 13*(10), 616-630.

McGeer, P. L., Itagaki, S., & McGeer, E. G. (1988). Expression of the histocompatibility glycoprotein HLA-DR in neurological disease. *Acta Neuropathol, 76*(6), 550-557.

McGeer, P. L., & McGeer, E. G. (2013). The amyloid cascade-inflammatory hypothesis of Alzheimer disease: implications for therapy. *Acta Neuropathol, 126*(4), 479-497.

Merlini, G., & Bellotti, V. (2003). Molecular mechanisms of amyloidosis. *New England Journal of Medicine, 349*(6), 583-596.

Merlini, M., Meyer, E. P., Ulmann-Schuler, A., & Nitsch, R. M. (2011). Vascular beta-amyloid and early astrocyte alterations impair cerebrovascular function and cerebral metabolism in transgenic arcAbeta mice. *Acta Neuropathol, 122*(3), 293-311.

Mi, W., Jung, S. S., Yu, H., Schmidt, S. D., Nixon, R. A., Mathews, P. M., Tagliavini, F., & Levy, E. (2009). Complexes of amyloid-beta and cystatin C in the human central nervous system. *J Alzheimers Dis, 18*(2), 273-280.

Moller, H. J., & Graeber, M. B. (1998). The case described by Alois Alzheimer in 1911. Historical and conceptual perspectives based on the clinical record and neurohistological sections. *Eur Arch Psychiatry Clin Neurosci, 248*(3), 111-122.

Morawski, M., Bruckner, G., Arendt, T., & Matthews, R. T. (2012). Aggrecan: Beyond cartilage and into the brain. *Int J Biochem Cell Biol, 44*(5), 690-693.

Morris, A. W., Carare, R. O., Schreiber, S., & Hawkes, C. A. (2014). The Cerebrovascular Basement Membrane: Role in the Clearance of beta-amyloid and Cerebral Amyloid Angiopathy. *Front Aging Neurosci, 6*, 251.

Morris, A. W., Sharp, M. M., Albargothy, N. J., Fernandes, R., Hawkes, C. A., Verma, A., Weller, R. O., & Carare, R. O. (2016). Vascular basement membranes as pathways for the passage of fluid into and out of the brain. *Acta Neuropathol, 131*(5), 725-736.

Mroczko, B., Groblewska, M., Zboch, M., Kulczynska, A., Koper, O. M., Szmitkowski, M., Kornhuber, J., & Lewczuk, P. (2014). Concentrations of matrix metalloproteinases and their tissue inhibitors in the cerebrospinal fluid of patients with Alzheimer's disease. *J Alzheimers Dis, 40*(2), 351-357.

Natte, R., Maat-Schieman, M. L., Haan, J., Bornebroek, M., Roos, R. A., & van Duinen, S. G. (2001). Dementia in hereditary cerebral hemorrhage with amyloidosis-Dutch type is associated with cerebral amyloid angiopathy but is independent of plaques and neurofibrillary tangles. *Ann Neurol, 50*(6), 765-772.

Natte, R., Vinters, H. V., Maat-Schieman, M. L., Bornebroek, M., Haan, J., Roos, R. A., & van Duinen, S. G. (1998). Microvasculopathy is associated with the number of cerebrovascular lesions in hereditary cerebral hemorrhage with amyloidosis, Dutch type. *Stroke, 29*(8), 1588-1594.

Nilsson, M., Wang, X., Rodziewicz-Motowidlo, S., Janowski, R., Lindstrom, V., Onnerfjord, P., Westermark, G., Grzonka, Z., Jaskolski, M., & Grubb, A. (2004). Prevention of domain swapping inhibits dimerization and amyloid fibril formation of cystatin C. Use of engineered disulfide bridges, antibodies and carboxymethylpapain to stabilize the monomeric form of cystatin C. *J Biol Chem*.

Nimmerjahn, A., Kirchhoff, F., & Helmchen, F. (2005). Resting microglial cells are highly dynamic surveillants of brain parenchyma in vivo. *Science, 308*(5726), 1314-1318.

Ochieng, J., & Chaudhuri, G. (2010). Cystatin superfamily. *J Health Care Poor Underserved, 21*(1 Suppl), 51-70.

Olafsson, I., & Grubb, A. (2000). Hereditary cystatin C amyloid angiopathy. *Amyloid, 7*(1), 70-79.

Olafsson, I., Gudmundsson, G., Abrahamson, M., Jensson, O., & Grubb, A. (1990). The amino terminal portion of cerebrospinal fluid cystatin C in hereditary cystatin C amyloid angiopathy is not truncated: direct sequence analysis from agarose gel electropherograms. *Scand J Clin Lab Invest, 50*(1), 85-93.

Olafsson, I., Thorsteinsson, L., & Jensson, O. (1996). The molecular pathology of hereditary cystatin C amyloid angiopathy causing brain hemorrhage. *Brain Pathol, 6*(2), 121-126.

Ozawa, K., Tomiyama, T., Maat-Schieman, M. L., Roos, R. A., & Mori, H. (2002). Enhanced Abeta40 deposition was associated with increased Abeta42-43 in cerebral vasculature with Dutch-type hereditary cerebral hemorrhage with amyloidosis (HCHWA-D). *Annals of the New York Academy of Sciences, 977*, 149-154.

Palsdottir, A., Abrahamson, M., Thorsteinsson, L., Arnason, A., Olafsson, I., Grubb, A., & Jensson, O. (1988). Mutation in cystatin C gene causes hereditary brain haemorrhage. *Lancet, 2*(8611), 603-604.

Palsdottir, A., Helgason, A., Palsson, S., Bjornsson, H. T., Bragason, B. T., Gretarsdottir, S., Thorsteinsdottir, U., Olafsson, E., & Stefansson, K. (2008). A drastic reduction in the life span of cystatin C L68Q carriers due to life-style changes during the last two centuries. *PLoS Genet, 4*(6), e1000099.

Palsdottir, A., Snorradottir, A. O., & Thorsteinsson, L. (2006). Hereditary cystatin C amyloid angiopathy: genetic, clinical, and pathological aspects. *Brain Pathol, 16*(1), 55-59.

Paresce, D. M., Ghosh, R. N., & Maxfield, F. R. (1996). Microglial cells internalize aggregates of the Alzheimer's disease amyloid beta-protein via a scavenger receptor. *Neuron, 17*(3), 553-565.

Pawlik, M., Sastre, M., Calero, M., Mathews, P. M., Schmidt, S. D., Nixon, R. A., & Levy, E. (2004). Overexpression of human cystatin C in transgenic mice does not affect levels of endogenous brain amyloid Beta Peptide. *J Mol Neurosci, 22*(1-2), 13-18.

Perlmutter, L. S. (1994). Microvascular pathology and vascular basement membrane components in Alzheimer's disease. *Mol Neurobiol, 9*(1-3), 33-40.

Picken, M. M. (2010). Amyloidosis-where are we now and where are we heading? *Arch Pathol Lab Med, 134*(4), 545-551.

Piersma, B., Bank, R. A., & Boersema, M. (2015). Signaling in Fibrosis: TGF-beta, WNT, and YAP/TAZ Converge. *Front Med (Lausanne), 2*, 59.

Pinney, J. H., & Hawkins, P. N. (2012). Amyloidosis. *Ann Clin Biochem, 49*(Pt 3), 229-241.

Preston, S. D., Steart, P. V., Wilkinson, A., Nicoll, J. A., & Weller, R. O. (2003). Capillary and arterial cerebral amyloid angiopathy in Alzheimer's disease: defining the perivascular route for the elimination of amyloid beta from the human brain. *Neuropathol Appl Neurobiol, 29*(2), 106-117.

Puchtler, H. a. F. S. (1965). Congo red as a stain for fluorescence microscopy of amyloid. *J Histochem Cytochem, 13(8)*, 693-694.

Puoti, G., Bizzi, A., Forloni, G., Safar, J. G., Tagliavini, F., & Gambetti, P. (2012). Sporadic human prion diseases: molecular insights and diagnosis. *Lancet Neurol, 11*(7), 618-628.

Rambaran, R. N., & Serpell, L. C. (2008). Amyloid fibrils: abnormal protein assembly. *Prion, 2*(3), 112-117.

Raposo, C., & Schwartz, M. (2014). Glial scar and immune cell involvement in tissue remodeling and repair following acute CNS injuries. *Glia, 62*(11), 1895-1904.

Rawlings, N. D., Barrett, A. J., & Finn, R. (2016). Twenty years of the MEROPS database of proteolytic enzymes, their substrates and inhibitors. *Nucleic Acids Res, 44*(D1), D343-350.

Ray, S., Lukyanov, P., & Ochieng, J. (2003). Members of the cystatin superfamily interact with MMP-9 and protect it from autolytic degradation without affecting its gelatinolytic activities. *Biochim Biophys Acta, 1652*(2), 91-102.

Revesz, T., Ghiso, J., Lashley, T., Plant, G., Rostagno, A., Frangione, B., & Holton, J. L. (2003). Cerebral amyloid angiopathies: a pathologic, biochemical, and genetic view. *Journal Of Neuropathology And Experimental Neurology, 62*(9), 885-898.

Revesz, T., Holton, J. L., Lashley, T., Plant, G., Frangione, B., Rostagno, A., & Ghiso, J. (2009). Genetics and molecular pathogenesis of sporadic and hereditary cerebral amyloid angiopathies. *Acta Neuropathol*.

Rivera, S., Khrestchatisky, M., Kaczmarek, L., Rosenberg, G. A., & Jaworski, D. M. (2010). Metzincin proteases and their inhibitors: foes or friends in nervous system physiology? *J Neurosci, 30*(46), 15337-15357.

Rockey, D. C., Bell, P. D., & Hill, J. A. (2015). Fibrosis--a common pathway to organ injury and failure. *N Engl J Med, 372*(12), 1138-1149.

Rogers, J., Cooper, N. R., Webster, S., Schultz, J., McGeer, P. L., Styren, S. D., Civin, W. H., Brachova, L., Bradt, B., Ward, P., & et al. (1992). Complement activation by beta-amyloid in Alzheimer disease. *Proc Natl Acad Sci U S A, 89*(21), 10016-10020.

Rozemuller, A. J., van Gool, W. A., & Eikelenboom, P. (2005). The neuroinflammatory response in plaques and amyloid angiopathy in Alzheimer's disease: therapeutic implications. *Curr Drug Targets CNS Neurol Disord, 4*(3), 223-233.

Rozemuller, J. M., Eikelenboom, P., Pals, S. T., & Stam, F. C. (1989). Microglial cells around amyloid plaques in Alzheimer's disease express leucocyte adhesion molecules of the LFA-1 family. *Neurosci Lett, 101*(3), 288-292.

Ruiz-Ortega, M., Rodriguez-Vita, J., Sanchez-Lopez, E., Carvajal, G., & Egido, J. (2007). TGF-beta signaling in vascular fibrosis. *Cardiovasc Res, 74*(2), 196-206.

Sastre, M., Calero, M., Pawlik, M., Mathews, P. M., Kumar, A., Danilov, V., Schmidt, S. D., Nixon, R. A., Frangione, B., & Levy, E. (2004). Binding of cystatin C to Alzheimer's amyloid beta inhibits in vitro amyloid fibril formation. *Neurobiol Aging, 25*(8), 1033-1043.

Schnittger, S., Rao, V. V., Abrahamson, M., & Hansmann, I. (1993). Cystatin C (CST3), the candidate gene for hereditary cystatin C amyloid angiopathy (HCCAA), and other members of the cystatin gene family are clustered on chromosome 20p11.2. *Genomics, 16*(1), 50-55.

Serpell, L. C. (2000). Alzheimer's amyloid fibrils: structure and assembly. *Biochim Biophys Acta, 1502*(1), 16-30.

Serpell, L. C., Sunde, M., Benson, M. D., Tennent, G. A., Pepys, M. B., & Fraser, P. E. (2000). The protofilament substructure of amyloid fibrils. *J Mol Biol, 300*(5), 1033-1039.

Seubert, P., Vigo-Pelfrey, C., Esch, F., Lee, M., Dovey, H., Davis, D., Sinha, S., Schlossmacher, M., Whaley, J., Swindlehurst, C., & et al. (1992). Isolation and quantification of soluble Alzheimer's beta-peptide from biological fluids. *Nature, 359*(6393), 325-327.

Shrestha, R., Millington, O., Brewer, J., & Bushell, T. (2013). Is central nervous system an immune-privileged site? *Kathmandu Univ Med J (KUMJ), 11*(41), 102-107.

Sipe, J. D., Benson, M. D., Buxbaum, J. N., Ikeda, S., Merlini, G., Saraiva, M. J., & Westermark, P. (2014). Nomenclature 2014: Amyloid fibril proteins and clinical classification of the amyloidosis. *Amyloid, 21*(4), 221-224.

Snorradottir, A. O., Isaksson, H. J., Ingthorsson, S., Olafsson, E., Palsdottir, A., & Bragason, B. T. (2017). Pathological changes in basement membranes and dermal connective tissue of skin from patients with hereditary cystatin C amyloid angiopathy. *Lab Invest*.

Snorradottir, A. O., Isaksson, H. J., Kaeser, S. A., Skodras, A. A., Olafsson, E., Palsdottir, A., & Bragason, B. T. (2015). Parenchymal cystatin C focal deposits and glial scar formation around brain arteries in Hereditary Cystatin C Amyloid Angiopathy. *Brain Research, 1622*, 149-162.

Sofroniew, M. V. (2009). Molecular dissection of reactive astrogliosis and glial scar formation. *Trends Neurosci, 32*(12), 638-647.

Sofroniew, M. V. (2015). Astrocyte barriers to neurotoxic inflammation. *Nat Rev Neurosci, 16*(5), 249-263.

Sofroniew, M. V., & Vinters, H. V. (2010). Astrocytes: biology and pathology. *Acta Neuropathol, 119*(1), 7-35.

Sokol, J. P., Neil, J. R., Schiemann, B. J., & Schiemann, W. P. (2005). The use of cystatin C to inhibit epithelial-mesenchymal transition and morphological transformation stimulated by transforming growth factor-beta. *Breast Cancer Res, 7*(5), R844-853.

Sokol, J. P., & Schiemann, W. P. (2004). Cystatin C antagonizes transforming growth factor beta signaling in normal and cancer cells. *Mol Cancer Res, 2*(3), 183-195.

Soontornniyomkij, V., Lynch, M. D., Mermash, S., Pomakian, J., Badkoobehi, H., Clare, R., & Vinters, H. V. (2010). Cerebral microinfarcts associated with severe cerebral beta-amyloid angiopathy. *Brain Pathol, 20*(2), 459-467.

Sorokin, L. (2010). The impact of the extracellular matrix on inflammation. *Nat Rev Immunol, 10*(10), 712-723.

Stegemann, J. P., Hong, H., & Nerem, R. M. (2005). Mechanical, biochemical, and extracellular matrix effects on vascular smooth muscle cell phenotype. *J Appl Physiol (1985), 98*(6), 2321-2327.

Stehbens, W. E., Delahunt, B., Shozawa, T., & Gilbert-Barness, E. (2001). Smooth muscle cell depletion and collagen types in progeric arteries. *Cardiovasc Pathol, 10*(3), 133-136.

Stehbens, W. E., Wakefield, S. J., Gilbert-Barness, E., Olson, R. E., & Ackerman, J. (1999). Histological and ultrastructural features of atherosclerosis in progeria. *Cardiovasc Pathol, 8*(1), 29-39.

Stichel, C. C., & Muller, H. W. (1998). The CNS lesion scar: new vistas on an old regeneration barrier. *Cell Tissue Res, 294*(1), 1-9.

Sukhova, G. K., Wang, B., Libby, P., Pan, J. H., Zhang, Y., Grubb, A., Fang, K., Chapman, H. A., & Shi, G. P. (2005). Cystatin C deficiency increases elastic lamina degradation and aortic dilatation in apolipoprotein E-null mice. *Circ Res, 96*(3), 368-375.

Suzuki, N., Cheung, T. T., Cai, X. D., Odaka, A., Otvos, L., Jr., Eckman, C., Golde, T. E., & Younkin, S. G. (1994a). An increased percentage of long amyloid beta protein secreted by familial amyloid beta protein precursor (beta APP717) mutants. *Science, 264*(5163), 1336-1340.

Suzuki, N., Iwatsubo, T., Odaka, A., Ishibashi, Y., Kitada, C., & Ihara, Y. (1994b). High Tissue Content of Soluble Beta-1-40 Is Linked to Cerebral Amyloid Angiopathy. *American Journal of Pathology, 145*(2), 452-460.

Sveinbjornsdottir, S., Blondal, H., Gudmundsson, G., Kjartansson, O., & Jonsdottir, S. (1996). Progressive dementia and leucoencephalopathy as the initial presentation of late onset hereditary cystatin-C amyloidosis. Clinicopathological presentation of two cases. *J Neurol Sci, 140*(1-2), 101-108.

Szpak, G. M., Lewandowska, E., Wierzba-Bobrowicz, T., Bertrand, E., Pasennik, E., Mendel, T., Stepien, T., Leszczynska, A., & Rafalowska, J. (2007). Small cerebral vessel disease in familial amyloid and non-amyloid angiopathies: FAD-PS-1 (P117L) mutation and CADASIL. Immunohistochemical and ultrastructural studies. *Folia Neuropathol, 45*(4), 192-204.

Tanjore, H., Blackwell, T. S., & Lawson, W. E. (2012). Emerging evidence for endoplasmic reticulum stress in the pathogenesis of idiopathic pulmonary fibrosis. *Am J Physiol Lung Cell Mol Physiol, 302*(8), L721-729.

Tanjore, H., Lawson, W. E., & Blackwell, T. S. (2013). Endoplasmic reticulum stress as a pro-fibrotic stimulus. *Biochim Biophys Acta, 1832*(7), 940-947.

Tanzi, R. E. (2012). The genetics of Alzheimer disease. *Cold Spring Harb Perspect Med, 2*(10).

Thal, D. R., Capetillo-Zarate, E., Larionov, S., Staufenbiel, M., Zurbruegg, S., & Beckmann, N. (2009). Capillary cerebral amyloid angiopathy is associated with vessel occlusion and cerebral blood flow disturbances. *Neurobiol Aging, 30*(12), 1936-1948.

Thal, D. R., Ghebremedhin, E., Orantes, M., & Wiestler, O. D. (2003). Vascular pathology in Alzheimer disease: Correlation of cerebral amyloid angiopathy and arteriosclerosis/lipohyalinosis with cognitive decline. *Journal Of Neuropathology And Experimental Neurology, 62*(12), 1287-1301.

Thal, D. R., Ghebremedhin, E., Rub, U., Yamaguchi, H., Del Tredici, K., & Braak, H. (2002a). Two types of sporadic cerebral amyloid angiopathy. *J Neuropathol Exp Neurol, 61*(3), 282-293.

Thal, D. R., Griffin, W. S. T., de Vos, R. A. I., & Ghebremedhin, E. (2008). Cerebral amyloid angiopathy and its relationship to Alzheimer's disease. *Acta Neuropathologica, 115*(6), 599-609.

Thal, D. R., Rub, U., Orantes, M., & Braak, H. (2002b). Phases of A beta-deposition in the human brain and its relevance for the development of AD. *Neurology, 58*(12), 1791-1800.

Thal, D. R., von Arnim, C., Griffin, W. S., Yamaguchi, H., Mrak, R. E., Attems, J., & Upadhaya, A. R. (2013). Pathology of clinical and preclinical Alzheimer's disease. *Eur Arch Psychiatry Clin Neurosci, 263 Suppl 2*, S137-145.

Theocharis, A. D., Skandalis, S. S., Gialeli, C., & Karamanos, N. K. (2016). Extracellular matrix structure. *Adv Drug Deliv Rev, 97*, 4-27.

Thorsteinsson, L., Blondal, H., Jensson, O., & Gudmundsson, G. (1988). Distribution of cystatin C amyloid deposits in icelandic patients with hereditary cystatin C amyloid angiopathy. In T. Isobe, A. Shukuro, U. Fumiya, S. Kito, & E. Tsubura (Eds.), *Amyloid and Amyloidosis* (pp. 585-590): Plenum Publishing Corporation.

Thorsteinsson, L., Georgsson, G., Asgeirsson, B., Bjarnadottir, M., Olafsson, I., Jensson, O., & Gudmundsson, G. (1992). On the role of monocytes/macrophages in the pathogenesis of central nervous system lesions in hereditary cystatin C amyloid angiopathy. *J Neurol Sci, 108*(2), 121-128.

Tian, J., Shi, J., & Mann, D. M. (2004). Cerebral amyloid angiopathy and dementia. *Panminerva Med, 46*(4), 253-264.

Tian, J., Shi, J., Smallman, R., Iwatsubo, T., & Mann, D. M. (2006). Relationships in Alzheimer's disease between the extent of Abeta deposition in cerebral blood vessel walls, as cerebral amyloid angiopathy, and the amount of cerebrovascular smooth muscle cells and collagen. *Neuropathol Appl Neurobiol, 32*(3), 332-340.

Tu, G. F., Aldred, A. R., Southwell, B. R., & Schreiber, G. (1992). Strong conservation of the expression of cystatin C gene in choroid plexus. *Am J Physiol, 263*(1 Pt 2), R195-200.

Turk, B., Turk, V., & Turk, D. (1997). Structural and functional aspects of papain-like cysteine proteinases and their protein inhibitors. *Biol Chem, 378*(3-4), 141-150.

Turk, V., & Bode, W. (1991). The cystatins: protein inhibitors of cysteine proteinases. *FEBS Lett, 285*(2), 213-219.

Turk, V., Stoka, V., & Turk, D. (2008). Cystatins: biochemical and structural properties, and medical relevance. *Front Biosci, 13*, 5406-5420.

Van Dorpe, J., Smeijers, L., Dewachter, I., Nuyens, D., Spittaels, K., Van Den Haute, C., Mercken, M., Moechars, D., Laenen, I., Kuiperi, C., Bruynseels, K., Tesseur, I., Loos, R., Vanderstichele, H., Checler, F., Sciot, R., & Van Leuven, F. (2000). Prominent cerebral amyloid angiopathy in transgenic mice overexpressing the london mutant of human APP in neurons. *Am J Pathol, 157*(4), 1283-1298.

van Duinen, S. G., Castano, E. M., Prelli, F., Bots, G. T., Luyendijk, W., & Frangione, B. (1987). Hereditary cerebral hemorrhage with amyloidosis in patients of Dutch origin is related to Alzheimer disease. *Proc Natl Acad Sci U S A, 84*(16), 5991-5994.

van Duinen, S. G., Maat-Schieman, M. L., Bruijn, J. A., Haan, J., & Roos, R. A. (1995). Cortical tissue of patients with hereditary cerebral hemorrhage with amyloidosis (Dutch) contains various extracellular matrix deposits. *Lab Invest, 73*(2), 183-189.

van Horssen, J., Otte-Holler, I., David, G., Maat-Schieman, M. L., van den Heuvel, L. P., Wesseling, P., de Waal, R. M., & Verbeek, M. M. (2001). Heparan sulfate proteoglycan expression in cerebrovascular amyloid beta deposits in Alzheimer's disease and hereditary cerebral hemorrhage with amyloidosis (Dutch) brains. *Acta Neuropathol (Berl), 102*(6), 604-614.

Van Nostrand, W. E., Wagner, S. L., Haan, J., Bakker, E., & Roos, R. A. (1992). Alzheimer's disease and hereditary cerebral hemorrhage with amyloidosis- Dutch type share a decrease in cerebrospinal fluid levels of amyloid beta-protein precursor. *Ann Neurol, 32*(2), 215-218.

Vilhjalmsson, D. T., Blondal, H., & Thormodsson, F. R. (2007). Solubilized cystatin C amyloid is cytotoxic to cultured human cerebrovascular smooth muscle cells. *Exp Mol Pathol, 83*(3), 357-360.

Vinters, H. V. (1987). Cerebral amyloid angiopathy. A critical review. *Stroke, 18*(2), 311-324.

Vinters, H. V., & Farag, E. S. (2003). Amyloidosis of cerebral arteries. *Advances in Neurology, 92*, 105-112.

Vinters, H. V., Natte, R., Maat-Schieman, M. L., van Duinen, S. G., Hegeman-Kleinn, I., Welling-Graafland, C., Haan, J., & Roos, R. A. (1998). Secondary microvascular degeneration in amyloid angiopathy of patients with hereditary cerebral hemorrhage with amyloidosis, Dutch type (HCHWA- D). *Acta Neuropathol (Berl), 95*(3), 235-244.

Vinters, H. V., & Pardridge, W. M. (1986). The blood-brain barrier in Alzheimer's disease. *Can J Neurol Sci, 13*(4 Suppl), 446-448.

Vinters, H. V., Secor, D. L., Pardridge, W. M., & Gray, F. (1990). Immunohistochemical study of cerebral amyloid angiopathy. III. Widespread Alzheimer A4 peptide in cerebral microvessel walls colocalizes with gamma trace in patients with leukoencephalopathy.[comment]. *Annals of Neurology, 28*(1), 34-42.

Virchow, R. (1854). Zur Cellulose-Frage. *Virchows Arch Path Anat, 6*, 416-426.

Vonsattel, J. P., Myers, R. H., Hedley-Whyte, E. T., Ropper, A. H., Bird, E. D., & Richardson, E. P., Jr. (1991). Cerebral amyloid angiopathy without and with cerebral hemorrhages: a comparative histological study. *Ann Neurol, 30*(5), 637-649.

Wahlbom, M., Wang, X., Lindstrom, V., Carlemalm, E., Jaskolski, M., & Grubb, A. (2007). Fibrillogenic oligomers of human cystatin C are formed by propagated domain swapping. *J Biol Chem, 282*(25), 18318-18326.

Wallin, H., Bjarnadottir, M., Vogel, L. K., Wasselius, J., Ekstrom, U., & Abrahamson, M. (2010). Cystatins--Extra- and intracellular cysteine protease inhibitors: High-level secretion and uptake of cystatin C in human neuroblastoma cells. *Biochimie, 92*(11), 1625-1634.

Wang, Z. Z., Jensson, O., Thorsteinsson, L., & Vinters, H. V. (1997). Microvascular degeneration in hereditary cystatin C amyloid angiopathy of the brain. *Apmis, 105*(1), 41-47.

Wattendorff, A. R., Bots, G. T., Went, L. N., & Endtz, L. J. (1982). Familial cerebral amyloid angiopathy presenting as recurrent cerebral haemorrhage. *J Neurol Sci, 55*(2), 121-135.

Wattendorff, A. R., Frangione, B., Luyendijk, W., & Bots, G. T. (1995). Hereditary cerebral haemorrhage with amyloidosis, Dutch type (HCHWA-D): clinicopathological studies. *J Neurol Neurosurg Psychiatry, 58*(6), 699-705.

Wei, L., Berman, Y., Castano, E. M., Cadene, M., Beavis, R. C., Devi, L., & Levy, E. (1998). Instability of the amyloidogenic cystatin C variant of hereditary cerebral hemorrhage with amyloidosis, Icelandic type. *J Biol Chem, 273*(19), 11806-11814.

Weller, R. O., Massey, A., Kuo, Y. M., & Roher, A. E. (2000). Cerebral amyloid angiopathy: accumulation of A beta in interstitial fluid drainage pathways in Alzheimer's disease. *Ann N Y Acad Sci, 903*, 110-117.

Weller, R. O., Massey, A., Newman, T. A., Hutchings, M., Kuo, Y. M., & Roher, A. E. (1998). Cerebral amyloid angiopathy: amyloid beta accumulates in putative interstitial fluid drainage pathways in Alzheimer's disease. *Am J Pathol, 153*(3), 725-733.

Weller, R. O., Subash, M., Preston, S. D., Mazanti, I., & Carare, R. O. (2008). Perivascular drainage of amyloid-beta peptides from the brain and its failure in cerebral amyloid angiopathy and Alzheimer's disease. *Brain Pathol, 18*(2), 253-266.

Wolters, P. J., Collard, H. R., & Jones, K. D. (2014). Pathogenesis of idiopathic pulmonary fibrosis. *Annu Rev Pathol, 9*, 157-179.

Wynn, T. A. (2008). Cellular and molecular mechanisms of fibrosis. *J Pathol, 214*(2), 199-210.

Wyss-Coray, T., Lin, C., Sanan, D. A., Mucke, L., & Masliah, E. (2000). Chronic overproduction of transforming growth factor-beta1 by astrocytes promotes Alzheimer's disease-like microvascular degeneration in transgenic mice. *Am J Pathol, 156*(1), 139-150.

Wyss-Coray, T., & Rogers, J. (2012). Inflammation in Alzheimer disease-a brief review of the basic science and clinical literature. *Cold Spring Harb Perspect Med, 2*(1), a006346.

Xie, L., Terrand, J., Xu, B., Tsaprailis, G., Boyer, J., & Chen, Q. M. (2010). Cystatin C increases in cardiac injury: a role in extracellular matrix protein modulation. *Cardiovasc Res, 87*(4), 628-635.

Xu, J., & Shi, G. P. (2014). Vascular wall extracellular matrix proteins and vascular diseases. *Biochim Biophys Acta, 1842*(11), 2106-2119.

Yamada, M. (2015). Cerebral amyloid angiopathy: emerging concepts. *J Stroke, 17*(1), 17-30.

Yamada, M., Itoh, Y., Shintaku, M., Kawamura, J., Jensson, O., Thorsteinsson, L., Suematsu, N., Matsushita, M., & Otomo, E. (1996). Immune reactions associated with cerebral amyloid angiopathy. *Stroke, 27*(7), 1155-1162.

Yamada, M., & Naiki, H. (2012). Cerebral amyloid angiopathy. *Prog Mol Biol Transl Sci, 107*, 41-78.

Yamaguchi, H., Yamazaki, T., Lemere, C. A., Frosch, M. P., & Selkoe, D. J. (1992). Beta amyloid is focally deposited within the outer basement membrane in the amyloid angiopathy of Alzheimer's disease. An immunoelectron microscopic study. *Am J Pathol, 141*(1), 249-259.

Yan, L., Cao, R., Wang, L., Liu, Y., Pan, B., Yin, Y., Lv, X., Zhuang, Q., Sun, X., & Xiao, R. (2015). Epithelial-mesenchymal transition in keloid tissues and TGF-beta1-induced hair follicle outer root sheath keratinocytes. *Wound Repair Regen, 23*(4), 601-610.

Yan, S. D., Stern, D., Kane, M. D., Kuo, Y. M., Lampert, H. C., & Roher, A. E. (1998). RAGE-Abeta interactions in the pathophysiology of Alzheimer's disease. *Restor Neurol Neurosci, 12*(2-3), 167-173.

Yeager, M. E., Frid, M. G., & Stenmark, K. R. (2011). Progenitor cells in pulmonary vascular remodeling. *Pulm Circ, 1*(1), 3-16.

Yoshikai, S., Sasaki, H., Doh-ura, K., Furuya, H., & Sakaki, Y. (1991). Genomic organization of the human-amyloid beta-protein precursor gene. *Gene, 102*(2), 291-292.

Yousif, L. F., Di Russo, J., & Sorokin, L. (2013). Laminin isoforms in endothelial and perivascular basement membranes. *Cell Adh Migr, 7*(1), 101-110.

Zarow, C., Barron, E., Chui, H. C., & Perlmutter, L. S. (1997). Vascular basement membrane pathology and Alzheimer's disease. *Ann N Y Acad Sci, 826*, 147-160.

Zhang, W. W., Lempessi, H., & Olsson, Y. (1998). Amyloid angiopathy of the human brain: immunohistochemical studies using markers for components of extracellular matrix, smooth muscle actin and endothelial cells. *Acta Neuropathol (Berl), 96*(6), 558-563.

Zimmermann, D. R., & Dours-Zimmermann, M. T. (2008). Extracellular matrix of the central nervous system: from neglect to challenge. *Histochem Cell Biol, 130*(4), 635-653.

Papers I-III

Paper I

BRAIN RESEARCH 1535 (2013) 106–114

Available online at www.sciencedirect.com

ScienceDirect

www.elsevier.com/locate/brainres

Brain Research

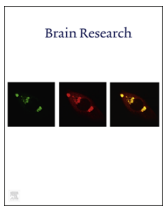

Research Report

Deposition of collagen IV and aggrecan in leptomeningeal arteries of hereditary brain haemorrhage with amyloidosis

Asbjorg Osk Snorradottir[a], *Helgi J. Isaksson*[b], *Stephan A. Kaeser*[c,d], *Angelos A. Skodras*[d,c], *Elias Olafsson*[e,f], *Astridur Palsdottir*[a], *Birkir Thor Bragason*[a,*]

[a]*Institute for Experimental Pathology at Keldur, University of Iceland, Reykjavik, Iceland*
[b]*Department of Pathology, Landspitali University Hospital, Reykjavik, Iceland*
[c]*Department of Cellular Neurology, Hertie Institute for Clinical Brain Research, University of Tübingen, Tübingen, Germany*
[d]*DZNE, German Centre for Neurodegenerative Diseases, Tübingen, Germany*
[e]*Faculty of Medicine, University of Iceland, Laeknagardur, Reykjavik, Iceland*
[f]*Department of Neurology, Landspitali University Hospital, Fossvogur, Reykjavik, Iceland*

ARTICLE INFO

Article history:
Accepted 15 August 2013
Available online 20 August 2013

Keywords:
Hereditary cystatin C amyloid angiopathy
Cystatin C
Immunohistochemistry
Vascular pathology
Extracellular matrix deposition

ABSTRACT

Hereditary Cystatin C Amyloid Angiopathy (HCCAA) is a rare genetic disease in Icelandic families caused by a mutation in the cystatin C gene, *CST3*. HCCAA is classified as a cerebral amyloid angiopathy and mutant cystatin C forms amyloid deposits in cerebral arteries resulting in fatal haemorrhagic strokes in young adults. The aetiology of HCCAA pathology is not clear and there is, at present, no animal model of the disease. The aim of this study was to increase understanding of the cerebral vascular pathology of HCCAA patients with an emphasis on structural changes within the arterial wall of affected leptomeningeal arteries. Examination of post-mortem samples revealed extensive changes in the walls of affected arteries characterised by deposition of extracellular matrix constituents, notably collagen IV and the proteoglycan aggrecan. Other structural abnormalities were thickening of the laminin distribution, intimal thickening concomitant with a frayed elastic layer, and variable reduction in the integrity of endothelia. Our results show that excess deposition of extracellular matrix proteins in cerebral arteries of HCCAA is a prominent feature of the disease and may play an important role in its pathogenesis.

1. Introduction

Hereditary Cystatin C Amyloid Angiopathy (HCCAA, MIM #105150) (also referred to as Hereditary Cerebral Haemorrhage with Amyloidosis-Icelandic type (HCHWA-I)) is a rare autosomal dominant disease in Icelandic families, which is manifested by amyloid deposition in cerebral arteries and fatal intracerebral haemorrhages in young adults. The disease belongs

*Correspondence to: Institute for Experimental Pathology, University of Iceland, Keldur, Keldnavegur 3, 112 Reykjavik, Iceland. Fax: +354 5673979.
E-mail address: birkirbr@hi.is (B.T. Bragason).

0006-8993/$ - see front matter © 2013 Elsevier B.V. All rights reserved.
http://dx.doi.org/10.1016/j.brainres.2013.08.029

to a group of disorders collectively called cerebral amyloid angiopathies (CAA), which are characterised by amyloid deposition, mainly in small and medium-sized arteries of the central nervous system (Biffi and Greenberg, 2011; Yamada and Naiki, 2012), most frequently in the leptomeningeal and cortical arteries. A number of different proteins (Yamada and Naiki, 2012) can be deposited as amyloid but the most common is the Alzheimer's disease (AD) associated protein, amyloid-β (Aβ). There are both sporadic and hereditary forms of CAA. The former are mostly diagnosed in the elderly while the rarer hereditary forms, caused by underlying mutations in the genes coding for the respective amyloid forming protein in each disease, affect younger individuals and are generally more severe in their presentation, e.g. HCCAA and Hereditary Cerebral Haemorrhage with Amyloidosis-Dutch type (HCHWA-D). Sporadic CAA is associated with AD-related pathology and more than 80% of AD patients have CAA (Jellinger, 2002; Jellinger and Attems, 2006). Both sporadic and hereditary forms of CAA result in varying degrees of cerebral haemorrhages (Gilbert and Vinters, 1983; Vinters and Gilbert, 1983), microhemorrhages and microinfarcts with associated cognitive decline and dementia (Biffi and Greenberg, 2011; Ghiso et al., 2010; Grinberg and Thal, 2010; Soontornniyomkij et al., 2010; Yamada and Naiki, 2012).

HCCAA is caused by a mutation in the cystatin C gene, *CST3* (Palsdottir et al., 1988) which has only been found in Iceland (population approximately 322,000 as of January 1st 2013 (Statistics Iceland)) with one exception (Graffagnino et al., 1995). Cystatin C is a secreted type 2 cysteine protease inhibitor that is present in all body fluids with highest amounts in seminal plasma and cerebrospinal fluid (Abrahamson et al., 1986). In mutant cystatin C, leucine is replaced by glutamine at position 68 of the mature protein resulting in decreased stability of the mutant protein and an increased tendency to dimerise and form aggregates compared to wild type cystatin C which is stable as a monomer (Abrahamson and Grubb, 1994). In HCCAA patients, amyloid consisting of mutant cystatin C (Ghiso et al., 1986) is detected in the walls of cerebral arteries and arterioles and also, to a lesser extent, in peripheral tissues such as in skin, glands, lymph nodes, and lymph vessels (Benedikz et al., 1990; Thorsteinsson et al., 1988). The L68Q mutation has high penetrance and mutation carriers suffer fatal intracerebral haemorrhages in their late twenties, on average, predominantly in the cerebral cortex, but also in the white matter of all lobes and in the basal ganglia region (Lofberg et al., 1987). A small subset of HCCAA carriers (estimated 1–2%) lives a "normal" lifespan (Palsdottir et al., 2008); the reason is unknown. In addition to the association of mutant cystatin C with HCCAA, co-localisation of wild-type cystatin C with Aβ has been described, e.g. in AD, and studies show that wild-type cystatin C can inhibit Aβ oligomerization and fibril formation; furthermore, it can protect neurons from Aβ toxicity (Kaur and Levy, 2012).

Although the disease causing mutation has been identified, the aetiology of HCCAA pathology is not clear. In contrast to several other CAA disorders there is no transgenic mouse model with the disease phenotype; transgenic mice expressing the mutant *CST3* gene do not accumulate amyloid or show other pathological characteristics (Kaeser et al., 2007; Mi et al., 2007). However, detailed knowledge of the end stage pathology could provide valuable clues regarding which research avenues to pursue in the study of HCCAA pathogenesis. Previous reports on the pathology of HCCAA have described hyalinization and thickening of the walls of cerebral arteries and arterioles and amyloid accumulation (Congo red staining) with extensive immunostaining for cystatin C (Blondal et al., 1989; Cohen et al., 1983; Gudmundsson et al., 1972; Lofberg et al., 1987). In addition, Wang et al. (1997) described smooth muscle cell (SMC) loss in cerebral arteries of HCCAA patients.

The primary aim of this study was to examine in detail how the integrity of the vessel wall of leptomeningeal arteries and arterioles is affected by L68Q cystatin C amyloid deposition. We also examined the relationship between cystatin C amyloid and arterial extracellular matrix (ECM) constituents because the latter have been found in amyloid deposits in AD and HCHWA-D, and studies have suggested that they are actively involved in the pathogenesis of these diseases (Perlmutter, 1994; van Duinen et al., 1995; van Horssen et al., 2001; Zarow et al., 1997).

2. Results

In all the patients included in the study, we confirmed previously reported pathological characteristics of HCCAA, i.e. hyalinization and thickening of the walls of cerebral arteries and arterioles and Congo red staining of amyloid in the walls of cerebral arteries with extensive immunostaining for cystatin C (Blondal et al., 1989; Cohen et al., 1983; Gudmundsson et al., 1972; Lofberg et al., 1987). In most arteries and arterioles cystatin C amyloid extended through the entire vessel wall (Fig. 1A). This was most evident in smaller vessels; however, in larger arteries amyloid deposits were sometimes restricted to the media and adventitia with the intima free of amyloid, as demonstrated in Fig. 1C, which shows a cortical artery in the cerebrum. In line with a previous report from a study of 6 HCCAA cases (Wang et al., 1997) we saw, in all cases, degeneration of the media with a significant loss of SMC (Fig. 1D) which were replaced with cystatin C amyloid and ECM constituents as demonstrated by immunohistochemical analyses, detailed below. The degree of SMC loss was greater in the smaller than in the larger muscular arteries. Elastin staining, both Verhoeff's elastin staining (Fig. 1K and L) and immunohistochemical staining with an elastin antibody (data not shown), revealed a frayed, and sometimes split, elastic layer in the leptomeningeal arteries, especially in the smaller arteries. An intact elastic layer was more often seen in larger arteries. Examination of the elastic layer drew attention to thickening of the intima in some arteries as demonstrated in Fig. 1C. The endothelial layer of the leptomeningeal arteries in the patients was affected, i.e. endothelial staining was less distinct and more sparse (Fig. 1G–J), compared to the immunostaining in controls (Fig. 1F) which showed a continuous layer. Because of the nature of the endothelial layer, i.e. a thin cell layer that can be affected by tissue processing, we examined the staining in serial sections, examples of which are shown in Fig. 1G–J. Throughout the patient samples the degree of

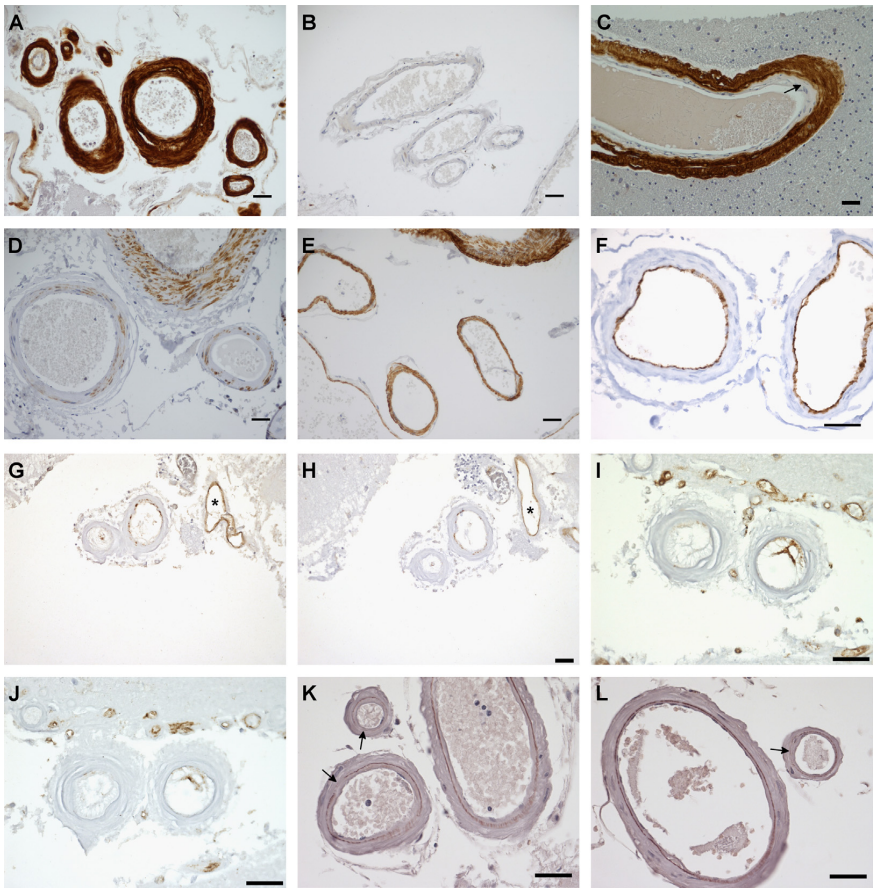

Fig. 1 – (A) Cystatin C amyloid was detected in HCCAA arteries by immunostaining with a cystatin C antibody, whereas arteries from a control individual (B) immunostained in the same manner revealed no cystatin C reactivity. (C) A cortical artery from the cerebrum that shows cystatin C reactive amyloid deposits in the media and adventitia while the intima (arrow) is free of amyloid. Immunostaining for smooth muscle actin in vascular SMC in HCCAA arteries (D) showed a significant loss of this cell type, especially in smaller arteries, whereas in controls immunostained in the same manner (E) the SMC layer was intact. The endothelium was affected in HCCAA arteries as demonstrated by CD31 immunostaining of serial sections from two patients (G,H and I,J) compared to intact endothelia in arteries from a control immunostained in the same manner (F). Figures G and H show two arteries (centre) with attenuated endothelia; in contrast, a vein (indicated by an asterisk, *) has an intact endothelial layer. Figures I and J show two arteries (centre) in which the endothelial layer is almost entirely absent as well as arteries at the surface of the cortex that are variably affected. Two examples of Verhoeff's elastin staining in HCCAA patients (K,L), which show examples of fragmentation of the elastic layer (arrows), that was especially seen in smaller arteries. Scale bar: 50 μm on all figures.

endothelial attenuation varied such that it was greater in arteries with a substantially thickened wall, such as shown in Fig. 1I and J.

Examination of ECM constituents in arteries of HCCAA patients with Masson's trichrome stain revealed extensive collagen (blue) staining (Fig. 2A) throughout the leptomeningeal wall. Consistent with the results presented in Fig. 1D, this staining method also showed that SMC (red) were sparse or absent (Fig. 2A). Further characterisation of the type of collagen in the arteries was performed revealing strong arterial reactivity for collagen IV (COLIV, Fig. 2C). COLIV is the major ECM component of the basement membrane (Zhang et al., 2003) consistent with the COLIV immunostaining in the controls (Fig. 2D). However, the distribution of COLIV reactivity in the arteries of patients was both more intense and extensive than in the controls, i.e. it was present in all layers (intima, media and adventitia) (Fig. 2C). This difference was statistically significant ($P<0.0001$, Fig. 3A) as determined by quantitative analyses of COLIV immunostaining in the patients and controls. Immunostaining for the basement membrane protein laminin, showed similar laminin distribution in HCCAA patients and controls (Fig. 2G and H), however,

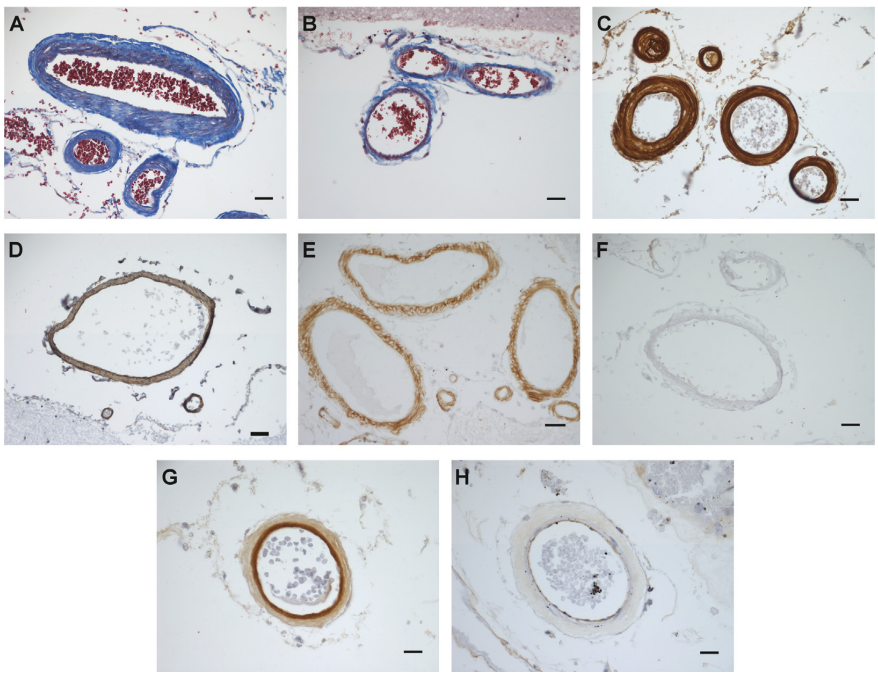

Fig. 2 – Masson's Trichrome staining of leptomeningeal arteries in HCCAA patients showed extensive collagen deposition (blue) (A) throughout the thickened arterial wall compared to arteries from controls stained in the same manner (B). Immunostaining for COLIV in HCCAA leptomeningeal arteries showed COLIV deposition throughout the arterial wall (C). In contrast, COLIV immunostaining in the controls was normal (D). Immunostaining for AGC1 in HCCAA showed AGC1 deposition throughout the arterial wall (E) compared to control arteries which were devoid of AGC1 (F). Immunostaining for laminin revealed a significantly thicker morphology of laminin in HCCAA arteries (G) compared to arteries from controls (H). (For interpretation of the references to color in this figure legend, the reader is referred to the web version of this article.)

the laminin structures were significantly thicker in the patients ($P<0.0001$, Fig. 3B). Taken together, the laminin and COLIV immunostaining results indicate significant abnormalities in the basement membrane structure of affected arteries in HCCAA patients. On the basis of unpublished observations from our studies on dermal fibroblast cultures from carriers of the *CST3*-L68Q mutation we examined the distribution of the chondroitin sulphate proteoglycan aggrecan, AGC1, in HCCAA. Immunohistochemical staining revealed that AGC1 was distributed throughout the arterial wall of HCCAA patients (Fig. 2E), whereas no staining was seen in arteries of controls (Fig. 2F). Quantitative analysis of AGC1 immunostaining showed that its extent within the arterial wall was similar to that of COLIV (Fig. 3C).

3. Discussion

This study revealed that, in addition to previously described deposition of cystatin C amyloid and SMC loss, there were extensive changes in the walls of affected leptomeningeal arteries in HCCAA patients characterised by degeneration of the endothelia, fragmentation of the elastic layer, an extended laminin distribution, and extracellular matrix deposition. These changes were consistently seen in all 28 patients.

Several of our observations concur with the vascular pathology reported in other cerebral amyloid angiopathies. SMC loss is observed in AD-CAA and HCHWA-D where it is most pronounced in small and medium sized leptomeningeal arteries, as was the case in HCCAA (Attems et al., 2010; Biffi and Greenberg, 2011; Kawai et al., 1993; Maat-Schieman et al., 2005; Szpak et al., 2007; Yamada and Naiki, 2012). Degeneration and changes of the endothelium have been described in AD-CAA (Fossati et al., 2011; Kalaria and Hedera, 1995; Soffer, 2006), CAA in idiopathic PD (Bertrand et al., 2008), and in a London APP mutant transgenic model (Van Dorpe et al., 2000). Fragmentation, or irregularities, of the elastic layer have been described in AD-CAA (Tian et al., 2004) and in the London APP mutant transgenic model (Van Dorpe et al., 2000), mentioned above. A thickening of the basement membrane of CAA arteries is evident in AD (Perlmutter, 1994; Zarow et al., 1997), and increased laminin staining, as detected in the HCCAA patients, has been demonstrated specifically in the vascular basement membrane of leptomeningeal arteries with CAA at an early stage in transgenic arcAβ mice (Merlini et al., 2011). At later stages this increase is also seen in other arteries, but in this as in other Aβ mouse

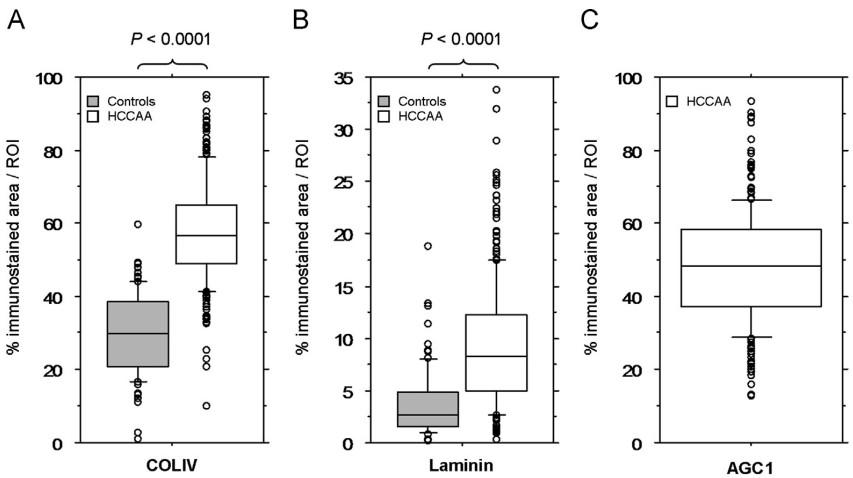

Fig. 3 – Box and whisker plots that show the results from quantitative analyses of COLIV, laminin and AGC1 immunostaining in leptomeningeal arteries. The whiskers show the 10th percentile and the 90th percentile. Values that fall above the 90th percentile and below the 10th percentile are presented as open circles. (A) The plot shows the % of COLIV immunostaining (per ROI, as defined in the experimental procedures) in leptomeningeal arteries of 10 controls (median (50th percentile)=30.0, n=100 (measurements)) and 28 HCCAA patients (median=56.5, n=280 (measurements)). The % COLIV staining in the patients was significantly higher than in the controls ($P<0.0001$, Mann Whitney U-test). (B) The plot shows the % laminin immunostaining per ROI in leptomeningeal arteries of 10 controls (median=2.7, n=100 (measurements)) and 28 HCCAA patients (median=8.3, n=280 (measurements)). The % laminin staining in the patients was significantly higher than in the controls ($P<0.0001$, Mann Whitney U-test). (C) The plot shows the % of AGC1 immunostaining per ROI in leptomeningeal arteries of 28 HCCAA patients (median=48.4, n=280 (measurements)). No AGC1 staining was detected in arteries of controls.

models (Hawkes et al., 2011), the leptomeningeal arteries are the first to be affected by CAA. In these transgenic mice the laminin staining co-localised with CAA in the vessels. Laminin expression was shown to be upregulated in AD (Bell and Zlokovic, 2009). In the light of this it has been suggested (Merlini et al., 2011) that increased laminin expression is in response to vascular damage and that the resulting thicker basement membrane strengthens the vessel wall; the same could apply to HCCAA. In addition, it has been demonstrated that laminin interacts with Aβ and can inhibit its fibrillization and neurotoxicity, thus adding another benefit to increased laminin expression in response to amyloid (Merlini et al., 2011; Morgan et al., 2002).

There was extensive AGC1 and COLIV reactivity in affected leptomeningeal arteries of the HCCAA patients. Within the central nervous system, AGC1 is found in the perineuronal net (PN), a component of the neural ECM formed around specific neurons which are reactive for parvalbumin. Studies have shown that neurons with aggrecan PN are protected against pathological processes of AD, suggesting a protective role for AGC1 (Morawski et al., 2012). Regarding COLIV deposition in CAA, the literature is conflicting. Zhang et al. (1998) reported moderately intense staining of COLIV and laminin in heavily amyloid-laden vessels in AD-CAA and CAA, and Kalaria and Pax (1995) described an increase in COLIV in the basement membrane of cerebral microvessels of AD patients, most of which were also immunoreactive for Aβ. van Duinen et al. (1995) investigated extracellular matrix deposits associated with amyloid in HCHWA-D and found weak staining of COLIV and laminin in amyloid laden arteries. In contrast, others do not see differences in COLIV reactivity in CAA, e.g. Van Dorpe et al. (2000) did not find increased COLIV deposition in their transgenic mouse model of the London APP mutant mentioned above, that apart from this exhibits general CAA pathological characteristics. Finally, a reduction in arterial COLIV has been documented, e.g. in AD (Christov et al., 2008) and CAA of idiopathic PD (Bertrand et al., 2008). Tian et al. (2006) studied COLIV reactivity and SMC loss in AD patients. Although they detected significant amounts of COLIV in some of the patients, their conclusion was, that the relationship between COLIV and CAA, or SMC loss, was not consistent and that the alterations in COLIV may be unrelated to amyloidosis. This may explain the discrepancies between CAA forms regarding COLIV, i.e. other underlying factors that differ between disorders affect COLIV deposition.

Studies indicate that ECM proteins have an affinity for Aβ, and vascular extracellular matrix components such as heparan sulphate proteoglycan, laminin, and COLIV have been identified in senile plaques and in vessels of AD and HCHWA-D patients suggesting that they could play a role in amyloid deposition (Kalaria and Pax, 1995; Narindrasorasak et al., 1992; Perlmutter, 1994; van Duinen et al., 1995; van Horssen et al., 2001; Vinters et al., 1998; Zarow et al., 1997). There is evidence that the accumulation of vascular amyloid in AD-CAA occurs along the basement membrane of arteries during drainage of interstitial fluid (ISF) due to trapping by extracellular matrix constituents (Weller et al., 2000;

Yamaguchi et al., 1992). In the light of this, it is possible that the expansion of COLIV, and laminin, in cerebral arteries in HCCAA, i.e. from the basement membrane to other layers of the vessel wall, along with the deposition of the proteoglycan AGC1, which is documented to facilitate aggregation of amyloid (Ariga et al., 2010), results in the sequestration and accumulation of cystatin C amyloid in HCCAA due to similar mechanisms as in AD-CAA.

Other than the similarities in pathology with other CAA disorders there are also interesting similarities between the HCCAA pathology described here and vascular pathology profiles that have been described in non-amyloid diseases, such as Hutchinson–Gilford Progeria Syndrome (HGPS, MIM #176670) and Cerebral Autosomal Dominant Arteriopathy with Subcortical Infarct and Leukoencephalopathy (CADASIL, MIM #125310). HGPS is an extremely rare premature aging disease caused by mutations in the *LMNA* gene (reviewed in Capell et al., 2007). HCCAA does not share the prominent physical features of HGPS; however, the cause of death in HGPS is often due to stroke and there are similarities in the cardiovascular pathology of HGPS (Capell et al., 2007) and the vascular pathology of HCCAA observed in our study. Both diseases share a severe loss of vascular SMC in the medial layer of arteries of all sizes, intimal thickening, replacement of vascular SMC with fibrous material, including COLIV, fragmentation of the elastic layer, and thickening of the basement membrane (Stehbens et al., 1999, 2001). Furthermore, dermal fibroblasts from HGPS patients have been shown to overexpress the AGC1 gene, *ACAN* (Csoka et al., 2004; Lemire et al., 2006), suggesting that AGC1 distribution may be altered in both HGPS and HCCAA. In CADASIL patients, deposition of COLIV has been described in leptomeningeal arteries and white matter arteries and capillaries, along with SMC loss and damage of the endothelia and the distribution of COLIV is similar to that demonstrated here in HCCAA (Dong et al., 2012; Szpak et al., 2007).

The overlap in vascular pathology between HCCAA and unrelated non-amyloid disorders raises the question of whether some of the pathological characteristics of HCCAA described here, e.g. the COLIV and AGC1 deposition, are primary events (in the aetiology of HCCAA) instigating amyloid deposition in the arterial wall rather than vice versa. Some reports suggest that amyloid toxicity is the reason for SMC death (Fossati et al., 2011; Mok et al., 2002, 2006) and endothelial cell death (Fossati et al., 2011), and indeed toxic effects of cystatin C amyloid on SMC in vitro have been described (Vilhjalmsson et al., 2007). However, because the vascular pathology of the non-amyloid diseases mentioned above are so similar to that in HCCAA, we believe the similarities warrant further examination. Specifically because studies have shown that degeneration of SMC and endothelia in familiar AD, and collagen accumulation, is observed in vessels with and without amyloid (Szpak et al., 2007), suggesting that excess ECM accumulation, specifically COLIV, could be a factor in the SMC loss observed in HCCAA.

Our observations show the end stage of HCCAA and the aetiology of the pathology remains to be determined, but our results suggest that excess deposition of COLIV, laminin and AGC1 could play a vital role in generating the pathology for example by facilitating amyloid deposition along the arterial basement membrane as has been shown for Aβ deposition in AD-CAA. Finally, it is likely that the combined effects of amyloid accumulation and ECM deposition along with the degeneration and loss of SMC, endothelial cells and the elastic layer cause a general weakening of the arterial wall and changes in vascular permeability that result in vessel rupture and the severe early-onset haemorrhages seen in HCCAA.

4. Experimental procedures

4.1. *Tissue samples*

All necessary permits for use of patient and control samples in this study, and the records associated with patient samples, were obtained from the National Bioethics Committee and the Data Protection Authorities in Iceland. Formalin fixed and paraffin-embedded sections (5 μm) from brain autopsy samples were obtained from the Department of Pathology, National University Hospital, Reykjavik, Iceland. HCCAA patient samples were from 28 individuals (Table 1) aged 21–79 years (median=31), 14 females and 14 males; HCCAA diagnosis was confirmed with Congo red staining and cystatin C immunoreactive amyloid. Control samples (Table 1) were obtained from 10 individuals aged 27–82 years (median=40), 7 females and 3 males, with no signs of amyloid angiopathy. Because of the rarity of the disease (69 deaths over the last 50 years) the HCCAA samples used in this study were from autopsies performed during a period spanning 43 years. We chose to compare the leptomeningeal artery between patients and controls due to the nature of the material studied, i.e. in the archives, post mortem samples from leptomeninges were consistently available from all the patients included in this study, whereas sample material from other brain areas varied. Therefore, it was possible to compare leptomeningeal arteries between all 28 patients and 10 controls, whereas this was not the case for arteries in other brain regions.

4.2. *Immunohistochemistry*

Paraffin was cleared from tissue sections by standard procedures. Endogenous peroxidase was blocked by incubation in 3% H_2O_2. Pre-treatment of samples for epitope retrieval was required for some of the antibodies used (Table 2). Sections were then immunostained with either the PAP method (DAKO) or with the Vectastain ABC Elite kit (Vector Laboratories) (Table 2). Haematoxylin and eosin staining, Verhoeff's elastic staining, and Masson's trichrome staining were performed according to standard procedures.

For the PAP method, unspecific protein binding was blocked for 20 min with 10% normal goat serum for mouse monoclonal antibodies or 10% swine serum for rabbit polyclonal antibodies. Incubations with primary antibodies were performed overnight at 4 °C. Appropriate antibody dilutions (Table 2) were determined in preliminary experiments. After incubation with a primary antibody, sections were incubated with one of the following secondary antibodies: goat anti-mouse or swine anti-rabbit (DAKO) for 30 min at room

temperature. Finally, the sections were incubated with mouse PAP complex or rabbit PAP complex (DAKO). Staining with the Vectastain ABC Elite kit, used for mouse monoclonal antibodies (Table 2), was performed according to the manufacturer's protocol. Sections were washed between steps with Tris buffer (0.5 M, pH 7.6).

All sections were incubated with 3,3′ diaminobenzidine (DAB) solution (DAKO) for 1–5 min. Sections were counterstained with haematoxylin for 5 min followed by washing with tap water for 10 min. Finally, sections were dehydrated with 100% ethanol and xylol followed by coverslipping with mounting medium (Pertex, Histolab). Images were acquired with a Nikon Eclipse 50i microscope equipped with a Nikon DS-Fil digital camera and a Nikon Digital Sight DS-U2 camera controller. Image panels were constructed using the GNU Image Manipulation Program (GIMP 2.8.2).

Table 1 – An overview of the HCCAA patient and control samples used in the study. The table shows the gender (female (F) or male (M)) of the patients and controls as well as their age at death.

Case	Gender	Age at death
HCCAA patient 1	M	31
HCCAA patient 2	F	36
HCCAA patient 3	M	22
HCCAA patient 4	M	23
HCCAA patient 5	M	38
HCCAA patient 6	F	29
HCCAA patient 7	M	36
HCCAA patient 8	M	49
HCCAA patient 9	M	33
HCCAA patient 10	F	52
HCCAA patient 11	M	79
HCCAA patient 12	M	33
HCCAA patient 13	F	24
HCCAA patient 14	M	61
HCCAA patient 15	M	29
HCCAA patient 16	M	30
HCCAA patient 17	F	30
HCCAA patient 18	F	31
HCCAA patient 19	F	25
HCCAA patient 20	F	42
HCCAA patient 21	F	32
HCCAA patient 22	F	30
HCCAA patient 23	M	28
HCCAA patient 24	F	27
HCCAA patient 25	F	34
HCCAA patient 26	F	41
HCCAA patient 27	M	26
HCCAA patient 28	F	21
Control 1	F	37
Control 2	F	45
Control 3	M	82
Control 4	M	57
Control 5	M	75
Control 6	F	43
Control 7	F	32
Control 8	F	27
Control 9	F	32
Control 10	F	27

4.3. *Quantification of immunostaining*

COLIV, laminin, and AGC1 immunostaining within leptomeningeal arteries of the patients and controls was quantified by semi-automated image analysis in the ImageJ program (http://rsbweb.nih.gov/, v1.47). Bright field images of sections were captured on a Zeiss Axioplan 2 microscope, coupled to an AxioCam camera (Carl Zeiss, Jena), at a resolution of 1300×1030 pixels using a Zeiss Plan Neofluar x10/0.3NA objective (Carl Zeiss, Jena). Before image capture, Köhler illumination was carefully adjusted on the microscope and the camera was calibrated for uniform field shading and white balance, to ensure consistent colour fidelity of the acquired images.

RGB colour images of the sections were imported to ImageJ. Ten arteries of various sizes were randomly chosen in each section, and a region of interest (ROI) was drawn to outline the boundary of each artery. The RGB image was transformed to the L*, a*, b* colour space (CIE 1976, CIELAB) (Chen et al., 2012) which was used to replicate the colours created by the orange-brown dye (DAB) of the immunostaining. The b* channel was selected for analyses because it yielded a higher contrast between the signal staining and differential staining, or section background, than the other two CIELAB channels. It was experimentally confirmed to be superior to any of the RGB channels or the other two CIELAB channels. The b* channel was thresholded using the automated threshold function of ImageJ and fine-adjusted to correspond to all stained areas on the section, ensuring a minimal bleed through of differentially stained structures. Using the thresholded image the preselected ROIs corresponding

Table 2 – Antibodies used for immunohistochemistry in the study. The table shows details of the primary antibodies used for immunohistochemistry experiments and the staining kits used for each antibody.

Target protein	Company	Species	Method	Pre-treatment	Antibody dil.
Aggrecan	Millipore, AB1031	Rabbit polycl.	Vectastain kit	Citrate buffer (pH 2.5)	1:100
CD31	DAKO, M0823	Mouse monocl.	PAP (DAKO)	EnVision™ FLEX[a]	1:10
Collagen IV	SIGMA, C1926	Mouse monocl.	Vectastain kit	Citrate buffer (pH 6)	1:500
Cystatin C	DAKO, A0451	Rabbit polycl.	PAP (DAKO)	None	1:500
Elastin	SIGMA, E4013	Mouse monocl.	Vectastain kit	Proteinase K[b]	1:10
Laminin	SIGMA, L8271	Mouse monocl.	Vectastain kit	Citrate buffer (pH 6)	1:200
Smooth muscle actin	DAKO, M0851	Mouse monocl.	PAP (DAKO)	Citrate buffer (pH 6)	1:50

[a] EnvisionTM FLEX, High pH, DAKO, K8000.
[b] Protease XVII, SIGMA P8038 1 μg mL^{-1}.

to specific arteries were re-introduced and the percentage area fraction covered by the threshold was calculated. The resulting number characterises the immunostaining load in the vessel and was subsequently used to quantitatively investigate differences in the degree of immunostaining between arteries in patient and control samples. The percentage of immunostained area per total ROI was calculated as described above for 10 arteries in all patient ($n=28$) and control ($n=10$) samples. Statistical analyses were performed on combined values from the patients and controls with the Mann–Whitney U test (Statview v5.0.1 software).

Acknowledgments

This work was supported by grants from the Icelandic Centre for Research (RANNIS), the University of Iceland Research Fund, the Icelandic Centre for Research - Student's Innovation Fund, the Heilavernd fund, the Memorial fund of Hafdis Kjartansdottir, and the Memorial fund of Helga Jonsdottir and Sigurlidi Kristjansson. We would like to thank Steinunn Arnadottir, Margret Jonsdottir and the staff at the department of Pathology, Landspitali University Hospital, Reykjavik, Iceland for technical assistance.

REFERENCES

Abrahamson, M., Barrett, A.J., Salvesen, G., Grubb, A., 1986. Isolation of six cysteine proteinase inhibitors from human urine. Their physicochemical and enzyme kinetic properties and concentrations in biological fluids. J. Biol. Chem. 261, 11282–11289.

Abrahamson, M., Grubb, A., 1994. Increased body temperature accelerates aggregation of the Leu-68–>Gln mutant cystatin C, the amyloid-forming protein in hereditary cystatin C amyloid angiopathy. Proc. Natl. Acad. Sci. U S A 91, 1416–1420.

Ariga, T., Miyatake, T., Yu, R.K., 2010. Role of proteoglycans and glycosaminoglycans in the pathogenesis of Alzheimer's disease and related disorders: amyloidogenesis and therapeutic strategies–a review. J. Neurosci. Res. 88, 2303–2315.

Attems, J., Jellinger, K., Thal, D.R., Van Nostrand, W., 2010. Review: sporadic cerebral amyloid angiopathy. Neuropathol. Appl. Neurobiol. 37, 75–93.

Bell, R.D., Zlokovic, B.V., 2009. Neurovascular mechanisms and blood-brain barrier disorder in Alzheimer's disease. Acta Neuropathol. 118, 103–113.

Benedikz, E., Blondal, H., Gudmundsson, G., 1990. Skin deposits in hereditary cystatin C amyloidosis. Virchows Arch. A Pathol. Anat. Histopathol. 417, 325–331.

Bertrand, E., Lewandowska, E., Stepien, T., Szpak, G.M., Pasennik, E., Modzelewska, J., 2008. Amyloid angiopathy in idiopathic Parkinson's disease. Immunohistochemical and ultrastructural study. Folia Neuropathol. 46, 255–270.

Biffi, A., Greenberg, S.M., 2011. Cerebral amyloid angiopathy: a systematic review. J. Clin. Neurol. 7, 1–9.

Blondal, H., Guomundsson, G., Benedikz, E., Johannesson, G., 1989. Dementia in hereditary cystatin C amyloidosis. Prog. Clin. Biol. Res. 317, 157–164.

Capell, B.C., Collins, F.S., Nabel, E.G., 2007. Mechanisms of cardiovascular disease in accelerated aging syndromes. Circ. Res. 101, 13–26.

Chen, J., Cranton, W., Fihn, M., 2012. Handbook of Visual Display Technology. Springer-Verlag, Berlin Heidelberg161–169.

Christov, A., Ottman, J., Hamdheydari, L., Grammas, P., 2008. Structural changes in Alzheimer's disease brain microvessels. Curr. Alzheimer Res. 5, 392–395.

Cohen, D.H., Feiner, H., Jensson, O., Frangione, B., 1983. Amyloid fibril in hereditary cerebral hemorrhage with amyloidosis (HCHWA) is related to the gastroentero-pancreatic neuroendocrine protein, gamma trace. J. Exp. Med. 158, 623–628.

Csoka, A.B., English, S.B., Simkevich, C.P., Ginzinger, D.G., Butte, A.J., Schatten, G.P., Rothman, F.G., Sedivy, J.M., 2004. Genome-scale expression profiling of Hutchinson-Gilford progeria syndrome reveals widespread transcriptional misregulation leading to mesodermal/mesenchymal defects and accelerated atherosclerosis. Aging Cell 3, 235–243.

Dong, H., Blaivas, M., Wang, M.M., 2012. Bidirectional encroachment of collagen into the tunica media in cerebral autosomal dominant arteriopathy with subcortical infarcts and leukoencephalopathy. Brain Res. 1456, 64–71.

Fossati, S., Ghiso, J., Rostagno, A., 2011. Insights into caspase-mediated apoptotic pathways induced by amyloid-beta in cerebral microvascular endothelial cells. Neurodegener. Dis. 10, 324–328.

Ghiso, J., Jensson, O., Frangione, B., 1986. Amyloid fibrils in hereditary cerebral hemorrhage with amyloidosis of Icelandic type is a variant of gamma-trace basic protein (cystatin C). Proc. Natl. Acad. Sci. U S A 83, 2974–2978.

Ghiso, J., Tomidokoro, Y., Revesz, T., Frangione, B., Rostagno, A., 2010. Cerebral amyloid angiopathy and Alzheimer's disease. Hirosaki Igaku 61, S111–S124.

Gilbert, J.J., Vinters, H.V., 1983. Cerebral amyloid angiopathy: incidence and complications in the aging brain. I. Cerebral hemorrhage. Stroke 14, 915–923.

Graffagnino, C., Herbstreith, M.H., Schmechel, D.E., Levy, E., Roses, A.D., Alberts, M.J., 1995. Cystatin C mutation in an elderly man with sporadic amyloid angiopathy and intracerebral hemorrhage. Stroke 26, 2190–2193.

Grinberg, L.T., Thal, D.R., 2010. Vascular pathology in the aged human brain. Acta Neuropathol. 119, 277–290.

Gudmundsson, G., Hallgrimsson, J., Jonasson, T.A., Bjarnason, O., 1972. Hereditary cerebral haemorrhage with amyloidosis. Brain 95, 387–404.

Hawkes, C.A., Hartig, W., Kacza, J., Schliebs, R., Weller, R.O., Nicoll, J.A., Carare, R.O., 2011. Perivascular drainage of solutes is impaired in the ageing mouse brain and in the presence of cerebral amyloid angiopathy. Acta Neuropathol. 121, 431–443.

Jellinger, K.A., 2002. Alzheimer disease and cerebrovascular pathology: an update. J. Neural. Transm. 109, 813–836.

Jellinger, K.A., Attems, J., 2006. Prevalence and impact of cerebrovascular pathology in Alzheimer's disease and parkinsonism. Acta Neurol. Scand. 114, 38–46.

Kaeser, S.A., Herzig, M.C., Coomaraswamy, J., Kilger, E., Selenica, M.L., Winkler, D.T., Staufenbiel, M., Levy, E., Grubb, A., Jucker, M., 2007. Cystatin C modulates cerebral beta-amyloidosis. Nat. Genet. 39, 1437–1439.

Kalaria, R.N., Hedera, P., 1995. Differential degeneration of the cerebral microvasculature in Alzheimer's disease. Neuroreport 6, 477–480.

Kalaria, R.N., Pax, A.B., 1995. Increased collagen content of cerebral microvessels in Alzheimer's disease. Brain Res. 705, 349–352.

Kaur, G., Levy, E., 2012. Cystatin C in Alzheimer's disease. Front. Mol. Neurosci. 5, 79.

Kawai, M., Kalaria, R.N., Cras, P., Siedlak, S.L., Velasco, M.E., Shelton, E.R., Chan, H.W., Greenberg, B.D., Perry, G., 1993. Degeneration of vascular muscle cells in cerebral amyloid angiopathy of Alzheimer disease. Brain Res. 623, 142–146.

Lemire, J.M., Patis, C., Gordon, L.B., Sandy, J.D., Toole, B.P., Weiss, A.S., 2006. Aggrecan expression is substantially and abnormally

upregulated in Hutchinson-Gilford Progeria Syndrome dermal fibroblasts. Mech. Ageing Dev. 127, 660–669.

Lofberg, H., Grubb, A.O., Nilsson, E.K., Jensson, O., Gudmundsson, G., Blondal, H., Arnason, A., Thorsteinsson, L., 1987. Immunohistochemical characterisation of the amyloid deposits and quantitation of pertinent cerebrospinal fluid proteins in hereditary cerebral hemorrhage with amyloidosis. Stroke 18, 431–440.

Maat-Schieman, M., Roos, R., van Duinen, S., 2005. Hereditary cerebral hemorrhage with amyloidosis-Dutch type. Neuropathology 25, 288–297.

Merlini, M., Meyer, E.P., Ulmann-Schuler, A., Nitsch, R.M., 2011. Vascular beta-amyloid and early astrocyte alterations impair cerebrovascular function and cerebral metabolism in transgenic arcAbeta mice. Acta Neuropathol. 122, 293–311.

Mi, W., Pawlik, M., Sastre, M., Jung, S.S., Radvinsky, D.S., Klein, A.M., Sommer, J., Schmidt, S.D., Nixon, R.A., Mathews, P.M., Levy, E., 2007. Cystatin C inhibits amyloid-beta deposition in Alzheimer's disease mouse models. Nat. Genet. 39, 1440–1442.

Mok, S.S., Turner, B.J., Beyreuther, K., Masters, C.L., Barrow, C.J., Small, D.H., 2002. Toxicity of substrate-bound amyloid peptides on vascular smooth muscle cells is enhanced by homocysteine. Eur. J. Biochem. 269, 3014–3022.

Mok, S.S., Losic, D., Barrow, C.J., Turner, B.J., Masters, C.L., Martin, L.L., Small, D.H., 2006. The beta-amyloid peptide of Alzheimer's disease decreases adhesion of vascular smooth muscle cells to the basement membrane. J. Neurochem. 96, 53–64.

Morawski, M., Bruckner, G., Arendt, T., Matthews, R.T., 2012. Aggrecan: Beyond cartilage and into the brain. Int. J. Biochem. Cell Biol. 44, 690–693.

Morgan, C., Bugueno, M.P., Garrido, J., Inestrosa, N.C., 2002. Laminin affects polymerization, depolymerization and neurotoxicity of Abeta peptide. Peptides 23, 1229–1240.

Narindrasorasak, S., Lowery, D.E., Altman, R.A., Gonzalez-DeWhitt, P.A., Greenberg, B.D., Kisilevsky, R., 1992. Characterisation of high affinity binding between laminin and Alzheimer's disease amyloid precursor proteins. Lab. Invest. 67, 643–652.

Palsdottir, A., Abrahamson, M., Thorsteinsson, L., Arnason, A., Olafsson, I., Grubb, A., Jensson, O., 1988. Mutation in cystatin C gene causes hereditary brain haemorrhage. Lancet 2, 603–604.

Palsdottir, A., Helgason, A., Palsson, S., Bjornsson, H.T., Bragason, B.T., Gretarsdottir, S., Thorsteinsdottir, U., Olafsson, E., Stefansson, K., 2008. A drastic reduction in the life span of cystatin C L68Q carriers due to life-style changes during the last two centuries. PLoS Genet. 4, e1000099.

Perlmutter, L.S., 1994. Microvascular pathology and vascular basement membrane components in Alzheimer's disease. Mol. Neurobiol. 9, 33–40.

Soffer, D., 2006. Cerebral amyloid angiopathy–a disease or age-related condition. Isr. Med. Assoc. J. 8, 803–806.

Soontornniyomkij, V., Lynch, M.D., Mermash, S., Pomakian, J., Badkoobehi, H., Clare, R., Vinters, H.V., 2010. Cerebral microinfarcts associated with severe cerebral beta-amyloid angiopathy. Brain Pathol. 20, 459–467.

Stehbens, W.E., Wakefield, S.J., Gilbert-Barness, E., Olson, R.E., Ackerman, J., 1999. Histological and ultrastructural features of atherosclerosis in progeria. Cardiovasc. Pathol. 8, 29–39.

Stehbens, W.E., Delahunt, B., Shozawa, T., Gilbert-Barness, E., 2001. Smooth muscle cell depletion and collagen types in progeric arteries. Cardiovasc. Pathol. 10, 133–136.

Szpak, G.M., Lewandowska, E., Wierzba-Bobrowicz, T., Bertrand, E., Pasennik, E., Mendel, T., Stepien, T., Leszczynska, A., Rafalowska, J., 2007. Small cerebral vessel disease in familial amyloid and non-amyloid angiopathies: FAD-PS-1 (P117L) mutation and CADASIL. Immunohistochemical and ultrastructural studies. Folia Neuropathol. 45, 192–204.

Thorsteinsson, L., Blondal, H., Jensson, O., Gudmundsson, G., 1988. Distribution of cystatin C amyloid deposits in the icelandic patients with hereditary cytstatin C amyloid angiopathy. In: Isobe, T, Araki, S, Uchino, F, Kito, S, Tsubura, E (Eds.), Amyloid and Amyloidosis. Plenum Publishing Corp, New York, pp. 585–590.

Tian, J., Shi, J., Mann, D.M., 2004. Cerebral amyloid angiopathy and dementia. Panminerva Med. 46, 253–264.

Tian, J., Shi, J., Smallman, R., Iwatsubo, T., Mann, D.M., 2006. Relationships in Alzheimer's disease between the extent of Abeta deposition in cerebral blood vessel walls, as cerebral amyloid angiopathy, and the amount of cerebrovascular smooth muscle cells and collagen. Neuropathol. Appl. Neurobiol. 32, 332–340.

Van Dorpe, J., Smeijers, L., Dewachter, I., Nuyens, D., Spittaels, K., Van Den Haute, C., Mercken, M., Moechars, D., Laenen, I., Kuiperi, C., Bruynseels, K., Tesseur, I., Loos, R., Vanderstichele, H., Checler, F., Sciot, R., Van Leuven, F., 2000. Prominent cerebral amyloid angiopathy in transgenic mice overexpressing the london mutant of human APP in neurons. Am. J. Pathol. 157, 1283–1298.

van Duinen, S.G., Maat-Schieman, M.L., Bruijn, J.A., Haan, J., Roos, R.A., 1995. Cortical tissue of patients with hereditary cerebral hemorrhage with amyloidosis (Dutch) contains various extracellular matrix deposits. Lab. Invest. 73, 183–189.

van Horssen, J., Otte-Holler, I., David, G., Maat-Schieman, M.L., van den Heuvel, L.P., Wesseling, P., de Waal, R.M., Verbeek, M.M., 2001. Heparan sulfate proteoglycan expression in cerebrovascular amyloid beta deposits in Alzheimer's disease and hereditary cerebral hemorrhage with amyloidosis (Dutch) brains. Acta Neuropathol. 102, 604–614.

Vilhjalmsson, D.T., Blondal, H., Thormodsson, F.R., 2007. Solubilized cystatin C amyloid is cytotoxic to cultured human cerebrovascular smooth muscle cells. Exp. Mol. Pathol. 83, 357–360.

Vinters, H.V., Gilbert, J.J., 1983. Cerebral amyloid angiopathy: incidence and complications in the aging brain. II. The distribution of amyloid vascular changes. Stroke 14, 924–928.

Vinters, H.V., Natte, R., Maat-Schieman, M.L., van Duinen, S.G., Hegeman-Kleinn, I., Welling-Graafland, C., Haan, J., Roos, R.A., 1998. Secondary microvascular degeneration in amyloid angiopathy of patients with hereditary cerebral hemorrhage with amyloidosis, Dutch type (HCHWA-D). Acta Neuropathol. 95, 235–244.

Wang, Z.Z., Jensson, O., Thorsteinsson, L., Vinters, H.V., 1997. Microvascular degeneration in hereditary cystatin C amyloid angiopathy of the brain. APMIS 105, 41–47.

Weller, R.O., Massey, A., Kuo, Y.M., Roher, A.E., 2000. Cerebral amyloid angiopathy: accumulation of A beta in interstitial fluid drainage pathways in Alzheimer's disease. Ann. N.Y. Acad. Sci. 903, 110–117.

Yamada, M., Naiki, H., 2012. Cerebral amyloid angiopathy. Prog. Mol. Biol. Transl. Sci. 107, 41–78.

Yamaguchi, H., Yamazaki, T., Lemere, C.A., Frosch, M.P., Selkoe, D.J., 1992. Beta amyloid is focally deposited within the outer basement membrane in the amyloid angiopathy of Alzheimer's disease. An immunoelectron microscopic study. Am. J. Pathol. 141, 249–259.

Zarow, C., Barron, E., Chui, H.C., Perlmutter, L.S., 1997. Vascular basement membrane pathology and Alzheimer's disease. Ann. N.Y. Acad. Sci. 826, 147–160.

Zhang, B., Fugleholm, K., Day, L.B., Ye, S., Weller, R.O., Day, I.N., 2003. Molecular pathogenesis of subarachnoid haemorrhage. Int. J. Biochem. Cell Biol. 35, 1341–1360.

Zhang, W.W., Lempessi, H., Olsson, Y., 1998. Amyloid angiopathy of the human brain: immunohistochemical studies using markers for components of extracellular matrix, smooth muscle actin and endothelial cells. Acta Neuropathol. 96, 558–563.

Paper II

BRAIN RESEARCH 1622 (2015) 149–162

Available online at www.sciencedirect.com

ScienceDirect

www.elsevier.com/locate/brainres

Brain Research

Research Report

Parenchymal cystatin C focal deposits and glial scar formation around brain arteries in Hereditary Cystatin C Amyloid Angiopathy

Asbjorg Osk Snorradottir[a], Helgi J. Isaksson[b], Stephan A. Kaeser[c,d], Angelos A. Skodras[d,c], Elias Olafsson[e,f], Astridur Palsdottir[a,g], Birkir Thor Bragason[a,g,*]

[a]Institute for Experimental Pathology at Keldur, University of Iceland, Reykjavik, Iceland
[b]Department of Pathology, Landspitali University Hospital, Reykjavik, Iceland
[c]Department of Cellular Neurology, Hertie Institute for Clinical Brain Research, University of Tübingen, Tübingen, Germany
[d]DZNE, German Centre for Neurodegenerative Diseases, Tübingen, Germany
[e]Faculty of Medicine, University of Iceland, Reykjavik, Iceland
[f]Department of Neurology, Landspitali University Hospital, Reykjavik, Iceland
[g]BioMedical Center, Faculty of Medicine, School of Health Sciences, University of Iceland, Iceland

ARTICLE INFO

Article history:
Accepted 16 June 2015
Available online 23 June 2015

Keywords:
Hereditary Cystatin C Amyloid Angiopathy
Cystatin C distribution
Focal deposits
Neuroinflammation
Glial scar

ABSTRACT

Hereditary Cystatin C Amyloid Angiopathy (HCCAA) is an amyloid disorder in Icelandic families caused by an autosomal dominant mutation in the cystatin C gene. Mutant cystatin C forms amyloid deposits in brain arteries and arterioles which are associated with changes in the arterial wall structure, notably deposition of extracellular matrix proteins. In this post-mortem study we examined the neuroinflammatory response relative to the topographical distribution of cystatin C deposition, and associated haemorrhages, in the leptomeninges, cerebrum, cerebellum, thalamus, and midbrain of HCCAA patients. Cystatin C was deposited in all brain areas, grey and white matter alike, most prominently in arteries and arterioles; capillaries and veins were not, or minimally, affected. We also observed perivascular deposits and parenchymal focal deposits proximal to affected arteries. This study shows for the first time, that cystatin C does not exclusively form CAA and perivascular amyloid but also focal deposits in the brain parenchyma. Haemorrhages were observed in all patients and occurred in all brain areas, variable between patients. Microinfarcts were observed in 34.6% of patients. The neuroinflammatory response was limited to the close vicinity of affected arteries and perivascular as well as parenchymal focal deposits. Taken together with previously reported arterial accumulation of extracellular matrix proteins in HCCAA, our results indicate that the central nervous system pathology of HCCAA is characterised by the formation of a glial scar within and around affected arteries.

*Corresponding author at: Institute for Experimental Pathology, University of Iceland, Keldur, Keldnavegur 3, 112 Reykjavik, Iceland. E-mail address: birkirbr@hi.is (B. Thor Bragason).

http://dx.doi.org/10.1016/j.brainres.2015.06.019
0006-8993/

1. Introduction

Hereditary Cystatin C Amyloid Angiopathy (HCCAA), also called hereditary cerebral haemorrhage with amyloidosis – Icelandic type (HCHWA-I), is a rare, fatal, autosomal dominant amyloid disease with high penetrance, caused by a mutation in the cystatin C gene (*CST3*) (Blondal et al., 1989; Ghiso et al., 1986; Palsdottir et al., 1988, 2008) which has almost exclusively been found in Iceland (Graffagnino et al., 1995). HCCAA is a cerebral amyloid angiopathy (CAA) (Palsdottir et al., 2006) and its pathology is characterised by deposition of cystatin C amyloid in the walls of cerebral arteries and arterioles along with associated changes in arterial wall structure and composition, notably loss of smooth muscle cells and accumulation of extracellular matrix (ECM) proteins (Snorradottir et al., 2013).

Mutant cystatin C is one of several proteins (Yamada and Naiki, 2012) known to form amyloid in the body. The most common is Alzheimer's disease associated protein amyloid-β (Aβ) which is also the most frequent amyloid forming protein associated with CAA (Biffi and Greenberg, 2011). Sporadic CAA caused by Aβ is fairly common with a 10–40% incidence in elderly individuals (Biffi and Greenberg, 2011). Examples of other diseases with Aβ-associated CAA are Alzheimer's disease (AD), in which over 80% of patients have CAA (AD-CAA) (Vinters and Gilbert, 1983), and Hereditary Cerebral Haemorrhage With Amyloidosis – Dutch type (HCHWA-D) which is caused by a point mutation within the Aβ region of the amyloid precursor protein APP (Maat-Schieman et al., 2005).

HCCAA typically has an early onset of severe recurrent cerebral haemorrhages in young adults. Most carriers suffer brain haemorrhages in their twenties leading to paralysis or dementia; the average age at death is 30 years (Gudmundsson et al., 1972; Palsdottir et al., 2008). However, a minority of carriers live longer due to unknown reasons (Palsdottir et al., 2008). Severe cerebral haemorrhages, comparable to those in HCCAA, are also seen in AD-related CAA (Aβ), sporadic CAA (Aβ), and HCHWA-D (Aβ), however, their onset in these disorders is typically later in life than in HCCAA, e.g. around 40–60 years of age in the hereditary disorder HCHWA-D (Wattendorff et al., 1982) and in individuals over 60 years of age in AD-related CAA and sporadic CAA (Gilbert and Vinters, 1983).

To this day, not much was known about cerebral inflammatory changes in HCCAA. Yamada et al. (1996) described the activation of macrophage cells around leptomeningeal and cortical vessels in two HCCAA patients that were included in a study which documented similar changes in cases of sporadic CAA (Aβ). The aim of our study was to get a more detailed understanding of the nature of cystatin C deposition in the brain of HCCAA patients, specifically regarding topographical distribution and severity grading in the parenchyma and to give a better insight into the reaction of the central nervous system to this cystatin C deposition.

Previous reports (Jensson et al., 1987; Lofberg et al., 1987; Thorsteinsson et al., 1988) have addressed aspects of cystatin C deposition in the central nervous system (CNS) of HCCAA patients and associated haemorrhages. In summary, these studies revealed that arterial cystatin C deposition was strongest in the leptomeninges, but also present in the cerebrum, cerebellum, basal ganglia and spinal cord. Overall, they agreed that deposition was present to a lesser extent in vessels of the white compared to grey matter. Haemorrhages

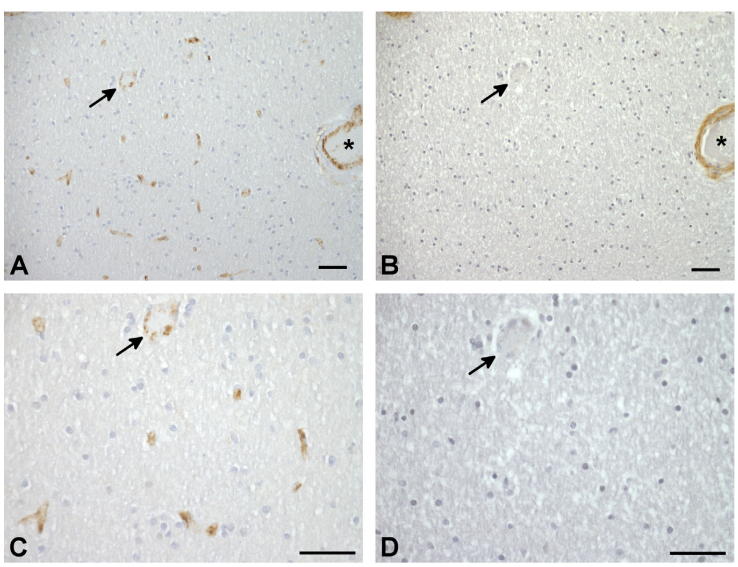

Fig. 1 – Capillaries were not, or minimally, affected in the HCCAA patients. (A) CD31 immunostain of the molecular layer in a cerebellar section from a patient showing CD31 immunoreactive capillaries (an example indicated by the arrow) and artery (asterisk). (B) Cystatin C immunostain from an adjacent section of that in (A) that shows a lack of cystatin C immunoreactivity in capillaries whereas the artery (asterisk) is cystatin C immunoreactive. Figures (C) (CD31 immunostain) and (D) (cystatin C immunostain) are higher magnification images of the same sections showing the same capillary as was indicated with the arrows in figures (A) and (B), as well as other capillaries in its surroundings. Scale bars: 50 μm on all figures.

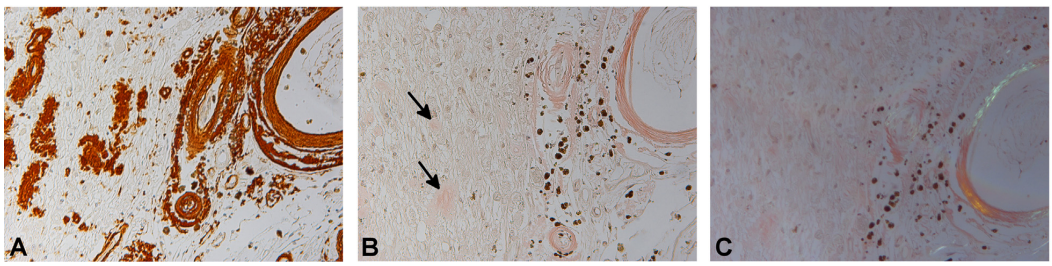

Fig. 2 – Congo red staining of thalamus. (A) Cystatin C immunostain of a region adjacent to the lateral ventricle in the thalamus that shows arterial cystatin C deposits as well as focal deposits and perivascular deposition. (B) Congo red staining of an adjacent section to that seen in (A) that shows Congo red staining of focal deposits (arrows). (C) The deposits in the artery showed green birefringence when viewed under polarised light, but the perivascular deposits and focal deposits did not.

were described in the cerebral cortex and basal ganglia, but also for some cases in the white matter. Thorsteinsson et al. (1988) specifically note perivascular cystatin C deposits in the hippocampus and basal ganglia.

Our results concur in general with previous studies regarding the topography of cystatin C distribution in HCCAA, but add important details, notably the novel observation of parenchymal focal cystatin C deposits which were observed in proximity to affected arteries in all brain areas examined as well as the observation of microinfarcts in 34.6% of the patients. We systematically evaluated capillary involvement and found that capillaries were either not, or minimally affected, suggesting that HCCAA can be classified as a type 2 CAA according to the classification suggested by Thal et al. (2002a). We addressed the severity of CAA due to cystatin C amyloid deposition in all patients examined in this study and found that, irrespective of age or brain area (grey or white matter), the severity of CAA in arteries and arterioles could be classified as stage 3 (Vonsattel et al., 1991). The neuroinflammatory response consisted of activated astrocytes and microglia/macrophages located around, and within, amyloid deposits in affected arteries as well as parenchymal deposits. Little or no neuroinflammatory reaction was detected in the parenchyma except around focal cystatin C deposits.

2. Results

2.1. *General vascular pathology*

Cystatin C deposition was systematically detected in almost all arteries, in all brain areas examined, but overall the most affected were smaller arteries and arterioles. Capillaries were either not, or minimally, affected (Fig. 1), as were veins. Throughout the brain cystatin C deposits were detected in all layers of the vessel wall of affected arteries/arterioles. Deposits within arterial walls showed birefringence when viewed under polarised light (Fig. 2C). The lumen ranged from relatively open in some arteries to completely occluded in smaller arteries/arterioles; an example of this can be seen in Fig. 3A and B. H&E staining revealed acellular thickening of the walls of small and medium-sized arteries and arterioles, and less often veins, by an amorphous, intensely eosinophilic, homogenous material. Affected vessels with a "double barrel" lumen were often observed with cystatin C deposition in both the outer and the inner walls of such "double barrels". These changes, associated with advanced amyloid angiopathy, were found mainly in leptomeningeal arteries. In some cases amyloid-laden vessels had undergone fibrinoid degeneration, or necrosis.

2.2. *Topographical distribution of cystatin C deposition*

The topographical distribution of cystatin C deposition, and the severity of CAA, was assessed in samples from 26 patients (Table 1). While samples from the cerebrum were available from all patients, the availability of sample material from the cerebellum, midbrain, and thalamus varied between patients (Table 1). Therefore, compared to cerebrum, the topographic assessment of cystatin C deposition in cerebellum, midbrain, and thalamus was only possible on a relatively small proportion of these 26 patients.

2.2.1. *Cerebrum*

Cystatin C immunoreactive amyloid was detected in leptomeningeal arteries in the cerebral sulci and in the leptomeningeal space as well as in arteries/arterioles in the grey and white matter. The cystatin C deposition was most pronounced in medium and small sized arteries and arterioles in the leptomeninges and in the cerebral cortex (Fig. 3A). Haemorrhages were observed in the grey matter of 24 out of 26 patients and occasionally in the white matter (data not shown). Perivascular cystatin C deposition was observed around arteries in the parenchyma. These deposits, although stained by Congo red, did not show birefringence under polarised light (Fig. 2A–C).

2.2.2. *Cerebellum*

Cystatin C immunostaining was detected in the leptomeningeal arteries/arterioles and in arteries in the molecular layer, granular layer, and white matter (Fig. 3B–D). The deposition was most severe in the leptomeningeal vessels and in the vessels of the molecular layer (Fig. 3B and C). Perivascular deposits were a frequent finding (Fig. 3B). Remnants of haemorrhages were observed in the molecular layer of 8 (out of 10) patients.

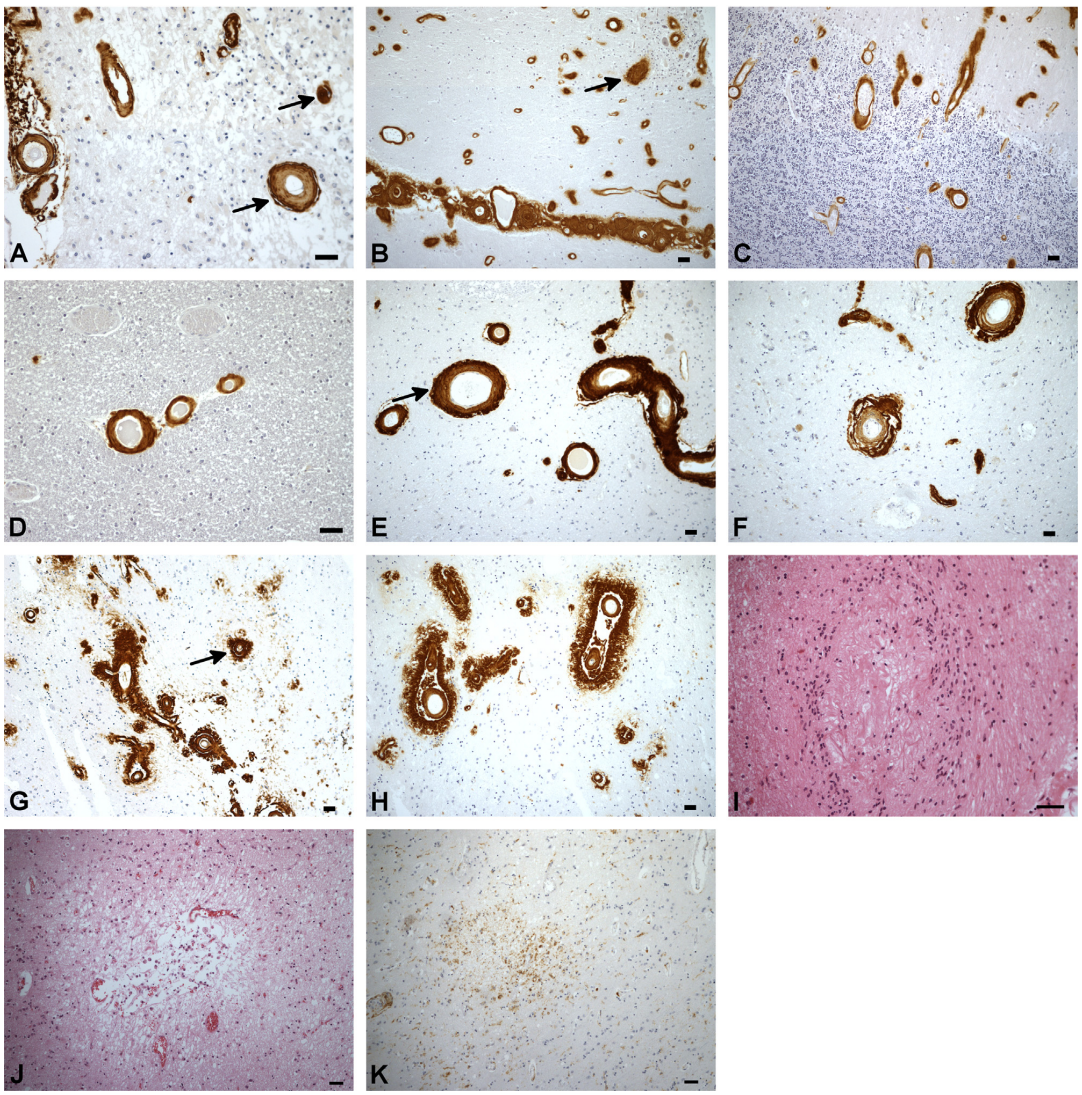

Fig. 3 – Cystatin C amyloid deposition in samples from the cerebrum, cerebellum, midbrain and thalamus in HCCAA. *Cerebrum*: **(A) Cystatin C immunoreactivity in arteries at the surface of the cerebral cortex in the sulcus and in leptomeninges.** *Cerebellum* **(B–D): (B) Cystatin C immunostain showing extensive cystatin C deposition in arteries of the leptomeninges, sulcus, and in the molecular layer and prominent perivascular amyloid deposits. (C) Cystatin C immunostaining of arteries in the granular layer, and in the white matter (D).** *Midbrain* **(E,F): (E) Severe amyloid deposition in arteries of the tectum. (F) Amyloid deposition in arteries in the superior colliculus.** *Thalamus* **(G,H): (G) Cystatin C immunostain of a region close to the ventricle showing arteries with prominent perivascular amyloid and focal deposits. (H) Cystatin C immunostain of a region adjacent to the lateral ventricle in the thalamus showing perivascular amyloid deposition.** *Microinfarcts* **(I–K): (I) H&E stain of a cerebellar section showing a microinfarct. (J) H&E stain of a section from the cerebrum showing a microinfarct. (K) CD68 immunostain of a section adjacent to that shown in (J) showing activated macrophages within the microinfarct. Scale bars: 50 μm on all figures.**

2.2.3. *Midbrain*

Vascular cystatin C amyloid deposits were found in all cases, most severe in the tectum and the colliculi of the superior cerebellar peduncle (Fig. 3E and F, respectively). Cystatin C immunoreactive arteries were also observed in the tegmentum, substantia nigra and cerebral peduncle. Perivascular deposits were frequently observed and many small arteries/arterioles in the regions mentioned had a completely occluded lumen. Remnants of haemorrhages were seen in all 6 patients.

Table 1 – An overview of the HCCAA patient and control post-mortem samples used in the study.

	Age	Gender	Leptomeninges	Cerebrum		Cerebellum	Midbrain	Thalamus
Patient 1	27	F	A, H	A, H	Q	n.a.	A, H	A, H
Patient 2	30	M	A, H	A, F, P, H, MI (7)	Q	A, F, P, H	A, F, P, H, MI (1)	A, F, P, H
Patient 3	57	F	A, H	A, H		A, MI (2)	n.a.	n.a.
Patient 4	25	F	A, H	A, F, P,H	Q	A, H	A, H	A, F, P, H
Patient 5	42	F	A	A, H, MI (4)	Q	A, H	n.a.	n.a.
Patient 6	29	M	A, H	A, F, P, H, MI (2)	Q	A, F, P, H	n.a.	A, F, P, H
Patient 7	30	F	A, H	A, H	Q	A, H	n.a.	n.a.
Patient 8	31	F	A, H	A, P, H, MI (3)	Q	A, F, P, H	A, H	n.a.
Patient 9	28	M	A	A, H	Q	A, H	n.a.	n.a.
Patient 10	32	F	A, H	A, H, MI (1)	Q	A	A, P, H, MI (1)	n.a.
Patient 11	40	M	A, H	A, P, H	Q	n.a.	n.a.	A, F, P, H
Patient 12	30	F	A, H	A, H, MI (1)		n.a.	n.a.	n.a.
Patient 13	41	F	A, H	A, H, MI (1)	Q	n.a.	A, H	n.a.
Patient 14	38	M	A	A	Q	n.a.	n.a.	n.a.
Patient 15	24	F	A	A, H		n.a.	n.a.	n.a.
Patient 16	36	M	A	A, H	Q	n.a.	n.a.	n.a.
Patient 17	23	M	A	A	Q	n.a.	n.a.	n.a.
Patient 18	33	M	A	A, H	Q	n.a.	n.a.	n.a.
Patient 19	29	F	A	A, P, H	Q	n.a.	n.a.	n.a.
Patient 20	49	M	A	A, H	Q	n.a.	n.a.	n.a.
Patient 21	22	M	A	A, H	Q	n.a.	n.a.	n.a.
Patient 22	79	M	A	A, H	Q	n.a.	n.a.	n.a.
Patient 23	52	F	A, H	A, F, P, H	Q	n.a.	n.a.	n.a.
Patient 24	33	M	A	A, H	Q	n.a.	n.a.	n.a.
Patient 25	61	M	A	A, H		n.a.	n.a.	n.a.
Patient 26	57	F	A, H	A, F, P, H, MI (3)		A, P, H, MI (1)	n.a.	n.a.
Control 1	52	M	X	X	Q	X	X	X
Control 2	30	M	X	X	Q	X	n.a.	X
Control 3	75	M	X	X	Q	n.a.	X	n.a.
Control 4	33	M	X	X	Q	X	X	X
Control 5	57	M	X	X	Q	n.a.	X	n.a.
Control 6	43	F	X	X	Q	X	n.a.	n.a.
Control 7	80	F	X	X	Q	X	n.a.	n.a.
Control 8	37	F	X	X	Q	n.a.	X	X
Control 9	45	F	X	X	Q	n.a.	n.a.	X

The table shows the gender (female (F) or male (M)) of the patients and controls included in the study and their age at death. The availability of samples from the brain areas indicated varied between individuals; n.a. indicates that tissue samples from a particular brain area were not available. The pattern of cystatin C deposition in samples is indicated for the brain areas examined as follows: deposition limited to arterial walls (A), perivascular deposition (P), and focal deposits (F). The presence of haemorrhages in the brain areas is indicated by H, the presence of microinfarcts is indicated by MI (with the number of microinfarcts in parenthesis), and Q indicates samples in which quantitative examination of IBA1, GFAP, and CD68 immunostaining was performed. For the control samples, X indicates that samples from the particular brain area were immunostained for cystatin C, CD68, GFAP, HLA-DR, CD31 and IBA1.

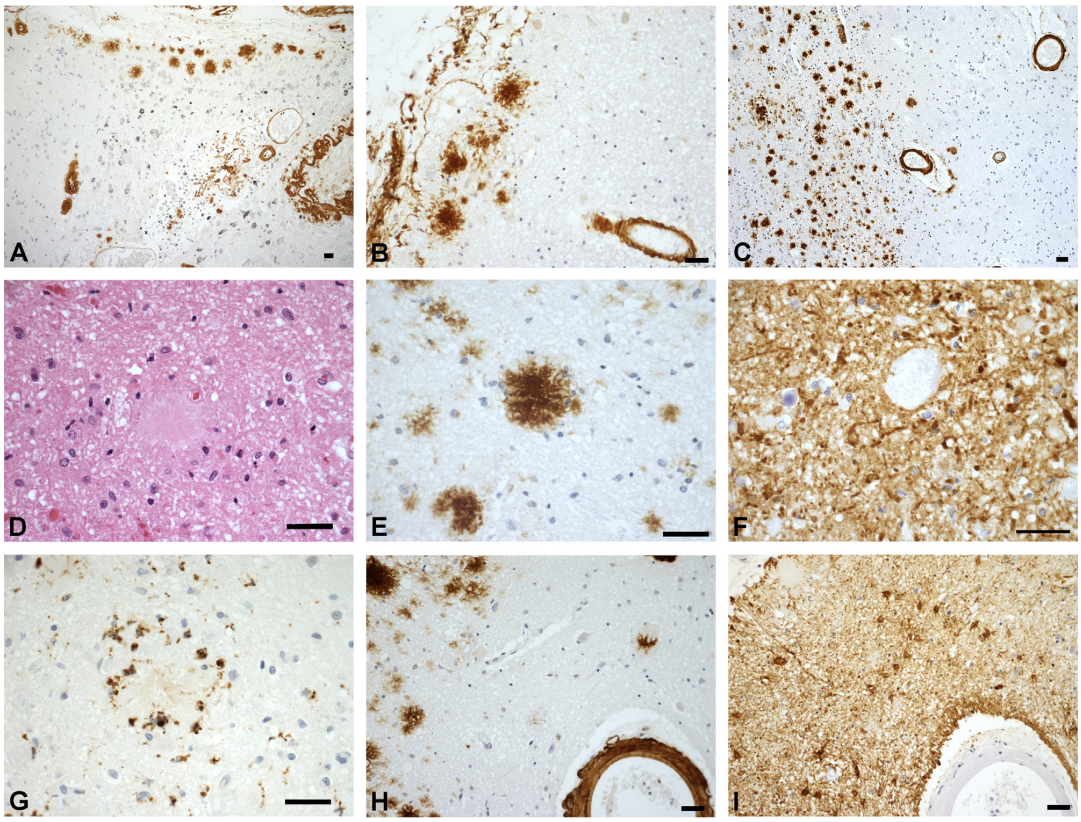

Fig. 4 – Cystatin C focal deposits in the cerebrum, cerebellum, thalamus, and midbrain. (A) Cystatin C focal deposits at the surface of a sulcus of the cerebrum; an artery with associated haemorrhage is located in the centre of the image. (B) Cystatin C focal deposits in the cerebellum proximal to a sulcus and affected arteries. (C) Cystatin C focal deposits in the thalamus proximal to the ventricle and affected arteries. (D) H&E stain of a region surrounding a focal deposit in the superior colliculus of the midbrain. Adjacent sample sections with the same deposit as shown in (D) were immunostained for cystatin C (E), GFAP (F), and CD68 (G) revealing a strong astrocytic response around the focal deposit as well as numerous macrophages around and within. (H) Cystatin C immunostaining of the tectum of the midbrain showing an affected artery and several focal deposits close to the artery (upper left corner). (I) An adjacent section of the same area as in (H) immunostained for GFAP demonstrating that in areas with affected arteries and associated focal deposits, the astrocytic response was more widespread than in regions where amyloid deposition was confined to the arterial walls, in which case the astrocytosis was limited to the close vicinity of the arteries. Scale bars: 50 μm on all figures.

2.2.4. *Thalamus*

In all five patients large haemorrhages were found and there were perivascular cystatin C deposits around most of the affected arteries (Fig. 3G and H). In addition, cystatin C deposition was observed in small and medium sized arteries in the choroid plexus, these deposits showed birefringence when stained with Congo red and viewed under polarised light.

2.2.5. *CAA severity*

Capillaries in the patients were either not, or minimally, affected (Fig. 1). Thal et al. (2002a) suggested a classification of CAA into CAA type 1 and type 2 dependant on capillary involvement, where capillaries are affected in type 1 but not type 2. The lack of capillary involvement in HCCAA would classify it as a CAA type 2. According to criteria defined by Vonsattel et al. (1991) the severity of CAA can be divided into three stages: mild, moderate and severe. By applying these criteria the CAA in the cerebrum, cerebellum, midbrain, and thalamus was graded as "severe" in all the patients. Examples of this are shown for cerebrum in Fig. 3A (examples indicated by arrows), cerebellum in Fig. 3B (example indicated by arrow), midbrain in Fig. 3E (example indicated by arrow), and thalamus in Fig. 3G (example indicated by arrow).

2.2.6. *Microinfarcts*

Microinfarcts were found in 9 of 26 patients (aged 29–57, median=32, two males and seven females, see Table 1 and Fig. 3I–K). The number of microinfarcts per section was variable between patients and ranged from 1 to 7 (Table 1). Microinfarcts were present in both grey and white matter and

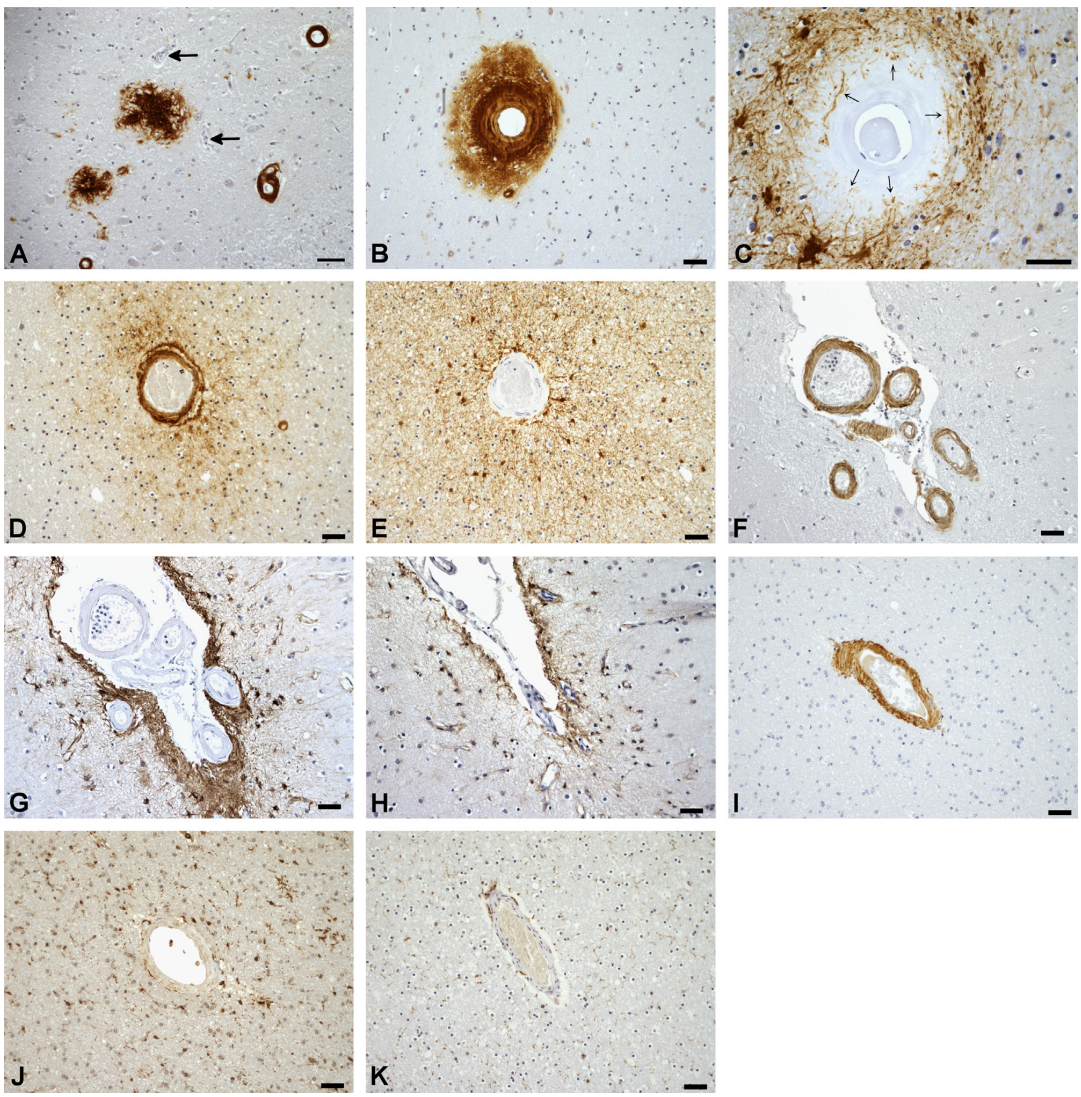

Fig. 5 – The association of reactive astrocytes and microglia with arterial cystatin C amyloid. (A) A section from the cerebrum immunostained for cystatin C that contains two focal deposits, and in close vicinity to them are two unaffected (cystatin C negative) capillaries (arrows). In addition the image contains two affected (cystatin C positive) arterioles. (B) A cortical artery in the grey matter of the cerebrum with cystatin C immunoreactvity throughout the entire vessel wall and deposition extending into the parenchyma. (C) An image of the same artery as in (B) that shows GFAP-positive hypertrophic astrocytes surrounding the artery and co-inciding with regions of parenchymal cystatin C deposition and astrocytic processes within the cystatin C deposition (arrows). (D) A cortical artery in the white matter of the cerebrum showing cystatin C immunoreactive deposition within the arterial wall and in the surrounding parenchyma. (E) The same artery as in (D) with reactive astrocytes around the artery and numerous GFAP-positive astrocytes in the surrounding parenchyma. (F) Leptomeningeal and cortical arteries with cystatin C immunoreactive amyloid. (G) An adjacent section to the one shown in (F), immunostained for GFAP, showing numerous GFAP-positive astrocytes located in the cerebral cortex adjacent to leptomeningeal arteries in a sulcus. (H) A limited number of GFAP-positive astrocytes detected in cerebral cortex adjacent to leptomeningeal arteries in a sulcus of control individual. (I) An artery in the white matter of the cerebrum in a patient with cystatin C-immunoreactive amyloid. (J) Immunostaining for IBA1 shows reactive microglia and "rounded" macrophage-like cells around the same artery as in (I). (K) CD68 reactive cells around the same artery as shown in (I) and (J). Scale bars: 50 μm on all figures.

were observed in the cerebrum of eight patients, the cerebellum of two patients and the midbrain of two patients (Table 1). The sizes of the microinfarcts in all cases ranged from 1 to 2 mm. Microinfarcts with and without cavities were found. Because we were using archived samples from autopsies we had a limited number of blocks per brain region per individual, which varied between patients (data not shown). In some sections, large ischemia-related infarcts as well as new and old haemorrhages made it difficult to evaluate the presence of microinfarcts. Therefore, we could not determine the presence of microinfarcts in such samples. The number of identified microinfarcts (Table 1) should be viewed in light of these limitations.

2.2.7. *Focal cystatin C deposits*

A novel observation was the detection of focal parenchymal cystatin C deposits. These deposits showed strong cystatin C immunoreactivity (Fig. 4A) and were visible by H&E staining and after Congo red staining, however, they did not show birefringence under polarised light (Fig. 2A–C) whereas cystatin C deposits in the walls of arteries located in the same areas did (Fig. 2C). The deposits were approximately 30–50 μm in diameter and could therefore be defined as "focal deposits" according to Duyckaerts et al. (2009). In contrast to "diffuse deposits", ranging from 50 μm to several hundred micrometres, focal deposits are visible after H&E staining (Duyckaerts et al., 2009).

Focal deposits were detected in the superficial layers of the cerebral cortex adjacent to the cerebral sulci and leptomeningeal space (Fig. 4A) in 5 of 26 patients (aged 25–57, median=30, three females and two males; see Table 1). They were also observed in the superficial molecular layer of the cerebellum (Fig. 4B) (three out of ten patients (aged 29–31, median=30, two males and one female; see Table 1)). In the thalamus, numerous focal deposits were observed (four of five patients, age 25–40, median=29.5, three males and one female; see Table 1) adjacent to the ventricular system (Fig. 4C). Finally, in the midbrain, focal deposits were observed in the tectum of one out of six patients (male, 30 years), most prominently in the superior colliculi (Fig. 4D and E). In all the brain regions mentioned above the focal deposits were most prominent in association with severely affected arteries especially in the superficial layers of the cerebral cortex, in the molecular layer of the cerebellum, in the paraventricular regions of the thalamus, and adjacent to the aqueduct in the midbrain.

2.3. *Neuroinflammatory response*

Reactive astrocytes were detected based on increased expression of glial fibrillary acidic protein (GFAP), hypertrophic processes and enlarged cell bodies (Sofroniew and Vinters, 2009). Activation of microglia was determined by cell morphology and immunostaining for ionised calcium-binding adaptor molecule 1 (IBA1), major histocompatibility complex class II-antigen (HLA-DR), and CD68.

2.3.1. *GFAP immunoreactivity*

In the control individuals, GFAP-positive astrocytes were detected in small numbers. These astrocytes were scattered in the grey and white matter and were weakly GFAP immunoreactive with fine cytoplasmic processes (Fig. 5H). In all HCCAA samples examined in this study, a build-up of GFAP-positive reactive astrocytes was observed in association with cystatin C deposition, both around arteries (Fig. 5B–G) and focal deposits (Fig. 4E–I). This applied to both white (Fig. 5D) and grey matter (Fig. 5B). The increase in GFAP immunoreactivity in the vicinity of patient arteries was significant ($P<0.0001$, Fig. 6A) compared to GFAP reactivity around arteries in the control samples as determined by quantitative analyses on cerebral samples from 21 patients and 9 controls (Table 1). Reactive astrocytes in the patients had characteristics of hypertrophic/gemistocytic astrocytes, i.e. thick processes and enlarged cell bodies (Fig. 5C and G). Overall, the degree of GFAP reactivity in the patients increased close to affected arteries and relative to the extent of cystatin C deposition, i.e. prominent deposition was associated with prominent astrocytosis. Astrocytes farther away from affected arteries were not hypertrophic (data not shown). As shown in Fig. 5C, reactive astrocytes encircled affected arteries forming a "glial scar" separating them from the surrounding tissue. GFAP immunoreactivity of astrocytes was strong in areas with perivascular deposition and focal deposits, and in some cases astrocyte processes were detected within the parenchymal deposits, an example of which can be seen when the GFAP immunoreactivity in Fig. 5C is compared to the cystatin C distribution of the same artery in Fig. 5B.

2.3.2. *IBA1 and HLA-DR immunoreactivity*

IBA1 immunoreactive microglia in the control samples were evenly distributed in the grey and white matter and displayed a ramified morphology with a relatively small cell body and fine processes (data not shown). In the HCCAA samples, IBA1 immunoreactive microglia were located around amyloid deposits of affected arteries (Fig. 5J and 7D), in the cerebral cortex adjacent to leptomeningeal blood vessels in the sulcus (Fig. 7E) and around focal deposits (data not shown). The intensity of IBA1 immunostaining around arteries in patient samples was significantly increased compared to controls ($P<0.0001$, Fig. 6B) as determined by analysis of arteries in cerebral samples from 21 patients and 9 controls (Table 1). The microglia proximal to affected arteries displayed features of activated microglia, i.e. a large cell body with thick, short processes (Fig. 5J and 7E). In contrast, microglia in parenchymal regions of patients, farther away from affected arteries, had morphological characteristics similar to those seen in the controls.

Cells in the media and adventitia of patient arteries were immunoreactive for HLA-DR (Fig. 7C), whereas there was no, or only sporadic, HLA-DR reactivity in arteries of controls (data not shown). Microglial cells in patients that were immunoreactive for IBA1 were also HLA-DR-positive as demonstrated by double staining for IBA1 and HLA-DR (Fig. 7D). These IBA1/HLA-DR positive cells had the morphological appearance of both activated microglial cells and macrophages (Fig. 7D–E).

2.3.3. *CD68 immunoreactivity*

CD68 positive cells in the patients were clustered around and within amyloid-laden arteries as shown on adjacent sections

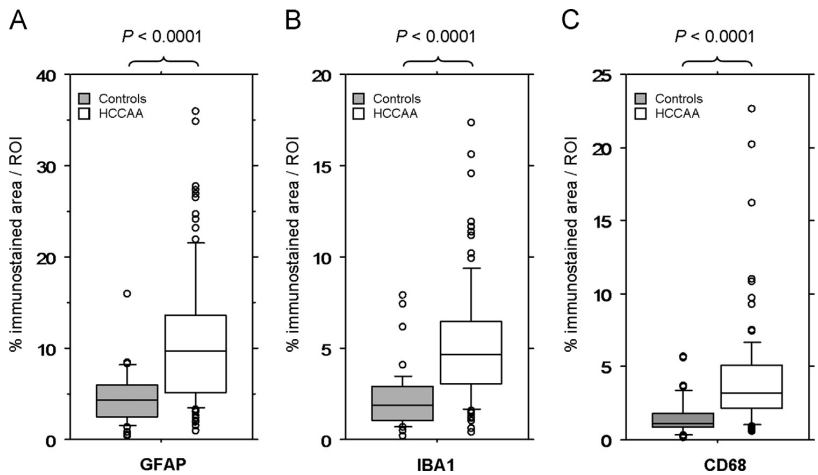

Fig. 6 – Results from quantitative analyses of GFAP, IBA1 and CD68 immunostaining around affected arteries in the cerebrum. Box and whisker plots that show the results from quantitative analyses of GFAP, IBA1 and CD68 immunostaining in patient and control samples. The whiskers show the 10th percentile and the 90th percentile. Values that fall above the 90th percentile and below the 10th percentile are presented as open circles. (A) The plot shows the % of GFAP immunostaining (per ROI, as defined in the experimental procedures) around cerebral arteries of 9 controls (median (50th percentile)=4.3, n=45 (measurements)) and 21 HCCAA patients (median=9.7, n=105 (measurements)). The % GFAP staining in the patients was significantly higher than in the controls (P<0.0001, Mann–Whitney U-test). (B) The plot shows the % IBA1 immunostaining per ROI around cerebral arteries of 9 controls (median=1.9, n=45 (measurements)) and 21 HCCAA patients (median=4.7, n=105 (measurements)). The % IBA1 staining in the patients was significantly higher than in the controls (P<0.0001, Mann–Whitney U-test). (C) The plot shows the % CD68 immunostaining per ROI around cerebral arteries of 9 controls (median=1.2, n=45 (measurements)) and 21 HCCAA patients (median=3.2, n=105 (measurements)). The % CD68 staining in the patients was significantly higher than in the controls (P<0.0001, Mann–Whitney U-test).

(Fig. 7A and B). CD68 positive cells were also observed around focal deposits (Fig. 4E and G). The increase in CD68 immunoreactivity around arteries observed in patients compared to controls was significant (P<0.0001, Fig. 6C) as determined by analysis of arteries in cerebral samples from 21 patients and 9 controls (Table 1). A higher degree of CD68 reactivity was observed around arteries with severe CAA or parenchymal deposits. Numerous CD68 positive macrophages were detected in infarcts after haemorrhages and around leptomeningeal arteries (data not shown). In contrast to the clustered distribution around arteries in HCCAA, CD68 reactive cells were scattered in the parenchyma of control samples (data not shown).

3. Discussion

The distribution of cystatin C deposition in HCCAA has been addressed, to some extent, in the literature (Jensson et al., 1987; Lofberg et al., 1987; Thorsteinsson et al., 1988). However, we decided to perform a detailed analysis of the topography of cystatin C deposition, and associated haemorrhages, on the samples available (Table 1), with regard to: (i) its association to neuroinflammation and (ii) the relative severity of CAA in different brain regions.

3.1. *Topography of arterial cystatin C deposition*

We detected cystatin C deposition in leptomeningeal arteries as well as in arteries of the grey and white matter in the cerebrum, cerebellum, thalamus, and midbrain. Capillaries were not, or minimally affected which is in agreement with the results of Blondal et al. (1989). The detection of CAA (cystatin C amyloid, ACys) in the thalamus and midbrain of HCCAA patients in this study is a novel observation, whereas CAA in the basal ganglia, leptomeninges, cerebrum and cerebellum has previously been described (Jensson et al., 1987; Lofberg et al., 1987). The distribution of CAA in HCCAA differs from that described for vascular Aβ in HCHWA-D where it is mainly seen in meningocortical vessels of the cerebral hemispheres and only rarely in vessels of the cerebellum, hippocampus, basal ganglia and brain stem, but in contrast to HCCAA, almost never in vessels of the white matter (Maat-Schieman et al., 1996). The distribution of CAA in HCCAA also differs from that of vascular Aβ in sporadic CAA where it is mainly found in the leptomeningeal and cortical vessels of the cerebral lobes and cerebellum and is uncommon in the basal ganglia, thalamus, brainstem and white matter (Yamada and Naiki, 2012).

As described by Thal et al. (2003, 2008) the progression of CAA (Aβ) throughout the brain can be divided into three stages based on distribution. In stage 1 CAA is detected in

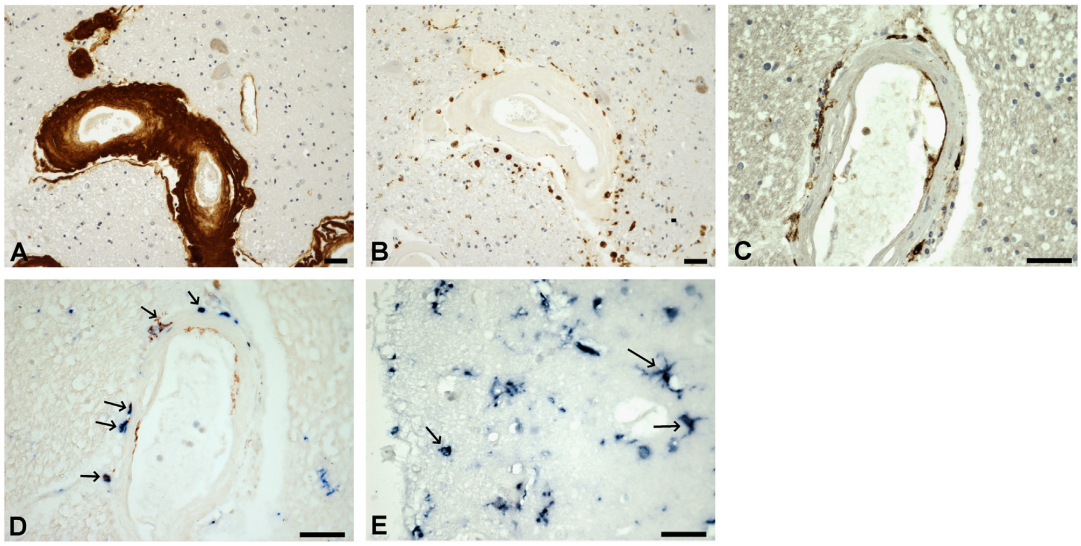

Fig. 7 – The association of activated microglia with arterial cystatin C amyloid. (A) Cystatin C immunoreactivity in arteries and arterioles of a patient in the white matter of the cerebrum. The lumen of arterioles (top left) were completely occluded. (B) Numerous CD68 immunoreactive macrophages in association with the cystatin C amyloid in the arteries shown in (A). (C) Immunostaining for HLA-DR that shows reactive microglia around a patient artery in the cerebral white matter and (D) double immunostaining of the same artery for IBA1 (blue) and HLA-DR (red) showing that the activated IBA1 positive microglia are also HLA-DR positive. (E) IBA1 positive microglia in the cerebrum of a patient located close to leptomeningeal vessels in a sulcus with large cell bodies and thick and short processes. Scale bar: 50 μm on all figures.

leptomeningeal and neocortical vessels, in stage 2 in allocortical and midbrain vessels, and in stage 3 it is present in the basal ganglia, thalamus and in the lower brainstem, too. In this study, CAA (ACys) was present in all thalamic samples available (5 patients). Four of these patients were younger than 30 years of age (Table 1). Stage 3 CAA in such young individuals underlines the rapid disease progression in HCCAA compared to the other CAA types.

Applying the severity scale by Vonsattel et al. (1991) defining the CAA related changes within the arteries themselves (e.g. degree of amyloid deposition and smooth muscle cell loss) the CAA (ACys) in all HCCAA cases in this study would be classified as "severe". Cystatin C immunoreactivity was invariably present in all layers of the walls of medium and small sized arteries and arterioles, irrespective of the area under examination (leptomeninges, cerebrum, cerebellum, thalamus, or midbrain), accompanied by severe smooth muscle cell loss.

3.2. *Location of haemorrhages*

Haemorrhages were found in all areas of the brain examined, variable between patients (Table 1). Haemorrhages in the cerebellum and thalamus were not specifically mentioned in previous studies on HCCAA (Jensson et al., 1987; Lofberg et al., 1987; Thorsteinsson et al., 1988). This distribution of haemorrhages in HCCAA is more widespread than described in Aβ-related HCHWA-D and sporadic CAA. In HCHWA-D haemorrhages are predominantly found in the cerebral cortex, the subcortical white matter, and may also be found in the leptomeninges (Wattendorff et al., 1995). In sporadic CAA (Aβ), haemorrhages are found in the cerebral lobes but usually not found in the basal ganglia, thalamus and pons, because these areas are usually only affected in severe cases (Yamada and Naiki, 2012).

With respect to this more widespread nature of haemorrhages in HCCAA, it is interesting to note that wild-type cystatin C (non-amyloid) in some cases co-localises with Aβ in vascular (and parenchymal) amyloid deposits (Levy et al., 2001). This co-localisation in Aβ-CAA has been reported to increase the likelihood of fatal haemorrhages in both sporadic Aβ-CAA and HCHWA-D cases (Itoh et al., 1993; Maat-Schieman et al., 1997; Maruyama et al., 1990; Vinters et al., 1990). As suggested by Winkler et al. (2001), this indicates that the identity of the depositing proteins in the vessel wall is an important determinant of haemorrhage likelihood. Relevant to this, patients with Familial British Dementia (FBD) or Familial Danish Dementia (FDD) which show vascular deposits of Bri- or Dan-amyloid (ABri or ADan), respectively, do not necessarily suffer severe haemorrhages (Vidal et al., 1999, 2000). Therefore, it may be speculated that the more widespread occurrence of haemorrhages seen in HCCAA might to some extent be due to the nature of cystatin C itself, in addition to the severity of its deposition.

3.3. *Microinfarcts*

Microinfarcts in HCCAA have not been described before. We found microinfarcts in 9 of 26 patients in the cerebrum, cerebellum and midbrain, variable between patients (Table 1).

Microinfarcts have been associated with CAA in the literature (Olichney et al., 1997; Soontornniyomkij et al., 2010), especially severe CAA (Soontornniyomkij et al., 2010). There are, however, some conflicting reports regarding this association. Ellis et al. (1996) did not find a significant correlation between CAA and microinfarcts, but rather a correlation between CAA, haemorrhages and ischemia-related infarcts. Studies by Thal et al. (2002a) and Kovari et al. (2013) both concluded that microinfarcts in CAA could not be attributed to CAA alone but also to other associated mechanisms. Soontornniyomkij et al. (2010) have suggested that these conflicting results could be due to differences in criteria used to grade the severity of CAA.

As discussed, the CAA in all 26 patients included in this study could be classified as severe. The percentage of patients with confirmed microinfarcts was 34.6%, which could be an underestimate due to complicating factors in some of the samples which made it difficult to evaluate the presence of microinfarcts, e.g. large ischemia-related infarcts and new and old haemorrhages. Furthermore, because we were using archived samples from autopsies we had a limited number of blocks per brain region per individual, which varied between patients. Due to this, it is difficult to state unequivocally from this data whether there is a direct association between microinfarcts and severe CAA in HCCAA. However, it should be noted that microinfarcts have been classified as associated with age-related complications, independent of CAA, such as hypertension, atherosclerosis, and microembolisms (Kovari et al., 2013). The data from the study described here shows microinfarcts in relatively young individuals (median = 32 years), thus they can hardly be classified as age-related, suggesting a link between the severe CAA in these patients and the microinfarcts.

3.4. *Focal parenchymal cystatin C deposits*

A novel observation in this study was the presence of parenchymal focal cystatin C deposits in all regions examined, most prominently in the thalamus (Fig. 4C). This observation was striking, given the relatively young age of the patients. The deposits were always in the close vicinity of affected arteries (Fig. 4A). While the cystatin C deposits in vessel walls showed birefringence under polarised light after Congo red staining, neither perivascular nor parenchymal deposits showed such birefringence, suggesting that they may not contain cystatin C as completely formed amyloid fibrils and have therefore not reached the stage of being "cored" plaques. The distribution of parenchymal deposits in the brain of Alzheimer's patients is used to grade the clinical stage of the disease into five phases of increasing clinical severity (Thal et al., 2002b). According to this grading, the most advanced stages, i.e. phases 4 and 5, are characterised by deposits in the brainstem and cerebellum, respectively. In this study focal deposits were observed in 4 of 5 available samples (age range 25–40, Table 1) from the thalamus and 3 of 9 available samples (age range 29–31, Table 1) from the cerebellum. Applying these criteria to the clinical progression in those HCCAA patients, the progression would be classified as phases 4 and 5. However, the deposits were always closely associated with affected arteries suggesting that their distribution correlates with the severity of CAA (Thal et al., 2003, 2008) already discussed. Irrespective of which classification is used, the advanced stage of cystatin C deposition in these young patients accentuates the speed of the disease progression in HCCAA.

3.5. *The neuroinflammatory response to cystatin C deposition*

Studies on other amyloid disorders that can have a CAA component, e.g. AD, have mostly focused on CNS reactions around the prominent parenchymal amyloid deposits (Eikelenboom et al., 2006; Itagaki et al., 1989; Loeffler et al., 2008; Wyss-Coray and Rogers, 2012). Inflammatory processes occur early during the course of AD (Eikelenboom et al., 2006) and reactive astrocytes, microglia, complement proteins, and cytokines have been shown to cluster around and within amyloid plaques and near neurofibrillary tangles (Itagaki et al., 1989; Loeffler et al., 2008). In general, reactive astrocytes play a part in damage control after CNS injury by surrounding the lesion, proliferating, and becoming hypertrophic, resulting in the formation of a glial scar (Sofroniew, 2009; Sofroniew and Vinters, 2009). This response is aimed to seal off the damaged area and thus preserve less affected tissue and the blood–brain barrier (Sofroniew, 2009).

We observed consistent astrocytosis around arteries in HCCAA, with and without perivascular deposition, in all regions examined. This pathology differs to some extent from that seen in AD-CAA (Aβ) and HCHWA-D (Aβ). In AD-CAA gliosis is not consistently observed around arteries in which Aβ is limited to the arterial wall, but is rather observed around arteries surrounded by perivascular amyloid (Mandybur, 1989). In HCHWA-D gliosis has mainly been described around cerebrocortical arteries (Maat-Schieman et al., 1996, 2004). The consistency and extent of reactive astrocytes observed in the relatively young HCCAA patients underlines the aggressive nature of the vascular damage in this disease compared to the other forms of CAA (Aβ), which affect older individuals. This could indicate that the astrocytes in HCCAA are reacting to both the cystatin C deposition and disruptions of the blood–brain barrier. The latter is in line with our previous observation of endothelial attenuation in arteries of HCCAA (Snorradottir et al., 2013).

CD68 and IBA1-positive cells were clustered around amyloid-laden arteries and within focal deposits in the HCCAA patients. As reviewed by Eikelenboom et al. (2008) this is similar to the microglial response detected around affected arteries and capillaries in HCHWA-D and so called 'vascular AD' with microcapillary angiopathy, but differs from AD where activated microglia are limited to the amyloid plaques, i.e. absent around amyloid-laden vessels. In vitro studies suggest that microglia from AD patients can phagocytose amyloid, although their ability to degrade amyloid seems to be impaired (Fiala et al., 2005). There are reports on Aβ peptides being internalised by astrocytes and astrocytic hypertrophic processes degrading Aβ-containing plaques and thus preventing the deposition of extracellular Aβ in AD (Wyss-Coray and Rogers, 2012). Together with our results, this suggests that the microglia and astrocytes in HCCAA respond to cystatin C amyloid in a manner similar to that observed in the immune response to Aβ in AD.

3.6. Conclusions

Glial scar formation involves the deposition of ECM proteins at the site of injury, such as collagen IV and laminin, that are secreted by fibroblasts at the site of damage (Kawano et al., 2012). Proteoglycans are also associated with such fibrotic changes (Bartus et al., 2012).

We have previously reported that there is an excessive deposition of ECM proteins, notably collagen IV, laminin, and the proteoglycan aggrecan in HCCAA vessels (Snorradottir et al., 2013). Here we report the presence of reactive astrocytes, activated IBA1/HLA-DR positive microglia and CD68 positive macrophages in association with affected arteries in HCCAA. Thus, the arterial pathology seen in HCCAA has the distinguishing features of a glial scar. The attenuation of endothelia in amyloid laden arteries (Snorradottir et al., 2013), along with the nature of the glial response described here, suggests that the glial scar is a response to blood–brain barrier disruption, as well as to the amyloid deposition itself, in an attempt to restore the integrity of the barrier and limit the extent of damage.

Our results revealed that cystatin C deposition in HCCAA is always spatially associated with arteries, i.e. parenchymal focal deposits were never seen in areas with no arteries. In this respect it is relevant that cystatin C deposition in HCCAA patients is not limited to the central nervous system. It has been observed in several peripheral tissues (Benedikz et al., 1990; Olafsson et al., 1996). This could be due to the fact that cystatin C is widely expressed throughout the body (Abrahamson et al., 1990). Taken together with the fact that cystatin C deposition in the CNS is either limited to arteries, or regions proximal to arteries, this supports an origin of cystatin C amyloid from the cell types within the arterial wall itself, e.g. adventitial fibroblasts or smooth muscle cells, as previously shown by Wang et al. (1997). The spreading of cystatin C into the parenchyma in the form of perivascular deposits and focal deposits could be due to "overload" within the arterial walls as a result of impaired removal by perivascular drainage, thus supporting the scenario suggested by Weller et al. (1998) that amyloid build-up in CAA (Aβ) is due to failure in perivascular drainage of amyloid forming proteins via the arterial walls. As we have previously reported (Snorradottir et al., 2013) there is a significant alteration in the basement membrane of HCCAA arteries, accompanied by accumulation of extracellular matrix proteins that could both influence arterial cystatin C build up by trapping amyloid, as well as reducing arterial elasticity which is necessary for efficient perivascular drainage (Kalaria et al., 1996). This would thus result in a similar scenario as has been determined in normal ageing i.e. decreased efficiency in perivascular drainage due to basement membrane thickening which in turn enhances age-related Aβ deposition in CAA (Kalaria et al., 1996; Weller et al., 1998).

4. Experimental procedure

4.1. Samples

Formalin fixed and paraffin-embedded sections (5 μm) from brain autopsy samples were obtained from the Department of Pathology, Landspitali National University Hospital, Reykjavik, Iceland. Permits for use of patient and control samples in this study were obtained from the National Bioethics Committee and the Data Protection Authorities in Iceland. HCCAA is a very rare disease, even in terms of the small Icelandic population (325,671 on January 1st 2014 (Statistics Iceland)). We used archived material from autopsies performed over a period of 48 years. The tissue samples used (Table 1) were from the leptomeninges, cerebrum, cerebellum, midbrain, and thalamus. The availability of samples from these areas varied between individual patients examined (Table 1). The topography of cystatin C deposition was evaluated in samples from the cerebrum, cerebellum, midbrain and thalamus of these 26 patients. Cerebellar samples were available from 10 patients (aged 25–57, median=30.5; 3 males and 7 females), midbrain samples from 6 patients (aged 27–41, median=30.5; 1 male and 5 females) and thalamus samples from 5 patients (aged 25–40, median=29; 3 males and 2 females). The neuroinflammatory response was evaluated in cerebral samples from 21 patients (9 females and 12 males, median age=32). The control samples (Table 1) used throughout the study were from 9 individuals (4 females and 5 males, median age=45) with no signs of amyloid angiopathy and from the same brain areas as the HCCAA brain samples.

4.2. Immunostaining

The procedures for immunostaining with the PAP (DAKO) and Vectastain ABC Elite kit (Vector laboratories) were as previously described (Snorradottir et al., 2013). The details of the antibodies that were used for immunostaining are provided in Table 2. Double staining with antibodies against IBA1 and HLA-DR was performed with the Multivision Polymer Detection System (Lab-Vision) according to the manufacturer's protocol. Haematoxylin and eosin (H&E) staining, Perls' Prussian blue staining, and Congo red staining were done using standard methods.

4.3. Quantification of CD68, GFAP, and IBA1 immunostaining around arteries

GFAP, CD68 and IBA1 immunostaining in the patient and control samples was quantified by semi-automated image analysis in the ImageJ software (http://rsbweb.nih.gov/,%20v1.47). Brightfield images of each cortical section were captured on a Nikon Eclipse 50i microscope, equipped with a Nikon DS-Fil digital camera and a Nikon Digital Sight DS-U2 camera controller, at a resolution of 2560 × 1920 pixels using a Nikon x10/0.3NA objective. RGB colour images of the sections were imported to ImageJ. Five arteries of various sizes from cerebral grey and white matter were randomly chosen in each cortical section. Each artery was measured from its outer boundaries, both vertically and horizontally. An oval region of interest (ROI) surrounding the artery was defined by adding 150 μm in every direction to the vertical/horizontal measurements. Further processing was performed as previously described (Snorradottir et al., 2013); it should be noted that for these analyses the a* channel was selected for analyses, because it yielded a higher contrast between the signal and differential staining or section background than the other two CIELAB channels. For statistical analyses the difference between patients and controls (5 arteries per each patient (n=21) and control (n=9)) was assessed using the Mann–Whitney U test in the Statview v5.0.1 software.

Table 2 – Antibodies used in the study.

Target protein	Company, catalogue nr.	Species	Pre-treatment	Method	Dilution and incubation
CD31	DAKO, M0823	Mouse monoclonal	EnVision™ FLEX[a]	PAP	1:10 for 30 min at RT[b]
CD68	DAKO, M0876	Mouse monoclonal	Citrate buffer, pH 6.0	PAP	1:200 overnight at 4 °C
Cystatin C	DAKO, A0451	Rabbit polyclonal	None	PAP	1:500 for 60 min at RT[b]
GFAP	DAKO, Z0334	Rabbit polyclonal	None	PAP	1:250 for 60 min at RT[b]
HLA-DR	DAKO, M0746	Mouse monoclonal	Citrate buffer, pH 6.0	Vectastain kit	1:25 overnight at 4 °C
IBA1	Wako, 19741	Rabbit polyclonal	Citrate buffer, pH 6.0	Vectastain kit	1:1000 for 60 min at RT[b]

The table shows what primary antibodies were used for immunostaining in the study, as well as the staining kits and experimental conditions used for each antibody.
[a] EnVision™ FLEX, High pH, DAKO, K8000.
[b] RT: room temperature.

4.4. *Evaluation of microinfarcts*

The evaluation of microinfarcts was based on a method described by Soontornniyomkij et al. (2010). Briefly, H&E stained sections were screened for microinfarcts (≤ 5 mm) by light microscopy with a $10\times$ lens and their presence confirmed with a $20\times$ lens. When a microinfarct was found its presence was further confirmed in an adjacent CD68 immunostained section. The number of microinfarcts per patient sample were counted (Table 1).

Acknowledgments

This work was supported by grants from the Icelandic Centre for Research (RANNÍS), the University of Iceland Research Fund, the Memorial fund of Hafdis Kjartansdottir, the Memorial fund of Helga Jonsdottir and Sigurlidi Kristjansson, and the Heilavernd fund. We would like to thank S. Arnadottir and M. Jonsdottir for technical assistance and our collaborators at the Department of Pathology, Landspitali National University Hospital, Iceland.

REFERENCES

Abrahamson, M., Olafsson, I., Palsdottir, A., Ulvsback, M., Lundwall, A., Jensson, O., Grubb, A., 1990. Structure and expression of the human cystatin C gene. Biochem. J. 268, 287–294.

Bartus, K., James, N.D., Bosch, K.D., Bradbury, E.J., 2012. Chondroitin sulphate proteoglycans: key modulators of spinal cord and brain plasticity. Exp. Neurol. 235, 5–17.

Benedikz, E., Blondal, H., Gudmundsson, G., 1990. Skin deposits in hereditary cystatin C amyloidosis. Virchows Arch. A Pathol. Anat. Histopathol. 417, 325–331.

Biffi, A., Greenberg, S.M., 2011. Cerebral amyloid angiopathy: a systematic review. J. Clin. Neurol. 7, 1–9.

Blondal, H., Guomundsson, G., Benedikz, E., Johannesson, G., 1989. Dementia in hereditary cystatin C amyloidosis. Prog. Clin. Biol. Res. 317, 157–164.

Duyckaerts, C., Delatour, B., Potier, M.C., 2009. Classification and basic pathology of Alzheimer disease. Acta Neuropathol. 118, 5–36.

Eikelenboom, P., Veerhuis, R., Scheper, W., Rozemuller, A.J., van Gool, W.A., Hoozemans, J.J., 2006. The significance of neuroinflammation in understanding Alzheimer's disease. J. Neural Transm. 113, 1685–1695.

Eikelenboom, P., Veerhuis, R., Familian, A., Hoozemans, J.J., van Gool, W.A., Rozemuller, A.J., 2008. Neuroinflammation in plaque and vascular beta-amyloid disorders: clinical and therapeutic implications. Neurodegener. Dis. 5, 190–193.

Ellis, R.J., Olichney, J.M., Thal, L.J., Mirra, S.S., Morris, J.C., Beekly, D., Heyman, A., 1996. Cerebral amyloid angiopathy in the brains of patients with Alzheimer's disease: the CERAD experience, Part XV. Neurology 46, 1592–1596.

Fiala, M., Lin, J., Ringman, J., Kermani-Arab, V., Tsao, G., Patel, A., Lossinsky, A.S., Graves, M.C., Gustavson, A., Sayre, J., Sofroni, E., Suarez, T., Chiappelli, F., Bernard, G., 2005. Ineffective phagocytosis of amyloid-beta by macrophages of Alzheimer's disease patients. J. Alzheimers Dis. 7, 221-232; discussion 255–262.

Ghiso, J., Jensson, O., Frangione, B., 1986. Amyloid fibrils in hereditary cerebral hemorrhage with amyloidosis of Icelandic type is a variant of gamma-trace basic protein (cystatin C). Proc. Natl. Acad. Sci. USA 83, 2974–2978.

Gilbert, J.J., Vinters, H.V., 1983. Cerebral amyloid angiopathy: incidence and complications in the aging brain. I. Cerebral hemorrhage. Stroke 14, 915–923.

Graffagnino, C., Herbstreith, M.H., Schmechel, D.E., Levy, E., Roses, A.D., Alberts, M.J., 1995. Cystatin C mutation in an elderly man with sporadic amyloid angiopathy and intracerebral hemorrhage. Stroke 26, 2190–2193.

Gudmundsson, G., Hallgrimsson, J., Jonasson, T.A., Bjarnason, O., 1972. Hereditary cerebral haemorrhage with amyloidosis. Brain 95, 387–404.

Itagaki, S., McGeer, P.L., Akiyama, H., Zhu, S., Selkoe, D., 1989. Relationship of microglia and astrocytes to amyloid deposits of Alzheimer disease. J. Neuroimmunol. 24, 173–182.

Itoh, Y., Yamada, M., Hayakawa, M., Otomo, E., Miyatake, T., 1993. Cerebral amyloid angiopathy: a significant cause of cerebellar as well as lobar cerebral hemorrhage in the elderly. J. Neurol. Sci. 116, 135–141.

Jensson, O., Gudmundsson, G., Arnason, A., Blondal, H., Petursdottir, I., Thorsteinsson, L., Grubb, A., Lofberg, H., Cohen, D., Frangione, B., 1987. Hereditary cystatin C (gamma-trace) amyloid angiopathy of the CNS causing cerebral hemorrhage. Acta Neurol. Scand. 76, 102–114.

Kalaria, R.N., Premkumar, D.R., Pax, A.B., Cohen, D.L., Lieberburg, I., 1996. Production and increased detection of amyloid beta protein and amyloidogenic fragments in brain microvessels, meningeal vessels and choroid plexus in Alzheimer's disease. Brain Res. Mol. Brain Res. 35, 58–68.

Kawano, H., Kimura-Kuroda, J., Komuta, Y., Yoshioka, N., Li, H.P., Kawamura, K., Li, Y., Raisman, G., 2012. Role of the lesion scar in the response to damage and repair of the central nervous system. Cell Tissue Res. 349, 169–180.

Kovari, E., Herrmann, F.R., Hof, P.R., Bouras, C., 2013. The relationship between cerebral amyloid angiopathy and

cortical microinfarcts in brain ageing and Alzheimer's disease. Neuropathol. Appl. Neurobiol. 39, 498–509.
Levy, E., Sastre, M., Kumar, A., Gallo, G., Piccardo, P., Ghetti, B., Tagliavini, F., 2001. Codeposition of cystatin C with amyloid-beta protein in the brain of Alzheimer disease patients. J. Neuropathol. Exp. Neurol. 60, 94–104.
Loeffler, D.A., Camp, D.M., Bennett, D.A., 2008. Plaque complement activation and cognitive loss in Alzheimer's disease. J. Neuroinflammation. 5, 9.
Lofberg, H., Grubb, A.O., Nilsson, E.K., Jensson, O., Gudmundsson, G., Blondal, H., Arnason, A., Thorsteinsson, L., 1987. Immunohistochemical characterization of the amyloid deposits and quantitation of pertinent cerebrospinal fluid proteins in hereditary cerebral hemorrhage with amyloidosis. Stroke 18, 431–440.
Maat-Schieman, M., Roos, R., van Duinen, S., 2005. Hereditary cerebral hemorrhage with amyloidosis-Dutch type. Neuropathology 25, 288–297.
Maat-Schieman, M.L., van Duinen, S.G., Bornebroek, M., Haan, J., Roos, R.A., 1996. Hereditary cerebral hemorrhage with amyloidosis-Dutch type (HCHWA-D): II – a review of histopathological aspects. Brain Pathol. 6, 115–120.
Maat-Schieman, M.L., van Duinen, S.G., Rozemuller, A.J., Haan, J., Roos, R.A., 1997. Association of vascular amyloid beta and cells of the mononuclear phagocyte system in hereditary cerebral hemorrhage with amyloidosis (Dutch) and Alzheimer disease. J. Neuropathol. Exp. Neurol. 56, 273–284.
Maat-Schieman, M.L., Yamaguchi, H., Hegeman-Kleinn, I.M., Welling-Graafland, C., Natte, R., Roos, R.A., van Duinen, S.G., 2004. Glial reactions and the clearance of amyloid beta protein in the brains of patients with hereditary cerebral hemorrhage with amyloidosis-Dutch type. Acta Neuropathol. 107, 389–398.
Mandybur, T.I., 1989. Cerebral amyloid angiopathy and astrocytic gliosis in Alzheimer's disease. Acta Neuropathol. 78, 329–331.
Maruyama, K., Ikeda, S., Ishihara, T., Allsop, D., Yanagisawa, N., 1990. Immunohistochemical characterization of cerebrovascular amyloid in 46 autopsied cases using antibodies to beta protein and cystatin C. Stroke 21, 397–403.
Olafsson, I., Thorsteinsson, L., Jensson, O., 1996. The molecular pathology of hereditary cystatin C amyloid angiopathy causing brain hemorrhage. Brain Pathol. 6, 121–126.
Olichney, J.M., Ellis, R.J., Katzman, R., Sabbagh, M.N., Hansen, L., 1997. Types of cerebrovascular lesions associated with severe cerebral amyloid angiopathy in Alzheimer's disease. Ann. N. Y. Acad. Sci. 826, 493–497.
Palsdottir, A., Abrahamson, M., Thorsteinsson, L., Arnason, A., Olafsson, I., Grubb, A., Jensson, O., 1988. Mutation in cystatin C gene causes hereditary brain haemorrhage. Lancet 2, 603–604.
Palsdottir, A., Snorradottir, A.O., Thorsteinsson, L., 2006. Hereditary cystatin C amyloid angiopathy: genetic, clinical, and pathological aspects. Brain Pathol. 16, 55–59.
Palsdottir, A., Helgason, A., Palsson, S., Bjornsson, H.T., Bragason, B.T., Gretarsdottir, S., Thorsteinsdottir, U., Olafsson, E., Stefansson, K., 2008. A drastic reduction in the life span of cystatin C L68Q carriers due to life-style changes during the last two centuries. PLoS Genet. 4, e1000099.
Snorradottir, A.O., Isaksson, H.J., Kaeser, S.A., Skodras, A.A., Olafsson, E., Palsdottir, A., Bragason, B.T., 2013. Deposition of collagen IV and aggrecan in leptomeningeal arteries of hereditary brain haemorrhage with amyloidosis. Brain Res. 1535, 106–114.
Sofroniew, M.V., 2009. Molecular dissection of reactive astrogliosis and glial scar formation. Trends Neurosci. 32, 638–647.
Sofroniew, M.V., Vinters, H.V., 2009. Astrocytes: biology and pathology. Acta Neuropathol. 119, 7–35.
Soontornniyomkij, V., Lynch, M.D., Mermash, S., Pomakian, J., Badkoobehi, H., Clare, R., Vinters, H.V., 2010. Cerebral microinfarcts associated with severe cerebral beta-amyloid angiopathy. Brain Pathol. 20, 459–467.
Thal, D.R., Ghebremedhin, E., Rub, U., Yamaguchi, H., Del Tredici, K., Braak, H., 2002a. Two types of sporadic cerebral amyloid angiopathy. J. Neuropathol. Exp. Neurol. 61, 282–293.
Thal, D.R., Rub, U., Orantes, M., Braak, H., 2002b. Phases of A beta-deposition in the human brain and its relevance for the development of AD. Neurology 58, 1791–1800.
Thal, D.R., Ghebremedhin, E., Orantes, M., Wiestler, O.D., 2003. Vascular pathology in Alzheimer disease: correlation of cerebral amyloid angiopathy and arteriosclerosis/lipohyalinosis with cognitive decline. J. Neuropathol. Exp. Neurol. 62, 1287–1301.
Thal, D.R., Griffin, W.S., de Vos, R.A., Ghebremedhin, E., 2008. Cerebral amyloid angiopathy and its relationship to Alzheimer's disease. Acta Neuropathol. 115, 599–609.
Thorsteinsson, L., Blondal, H., Jensson, O., Gudmundsson, G., 1988. Distribution of cystatin C amyloid deposits in the icelandic patients with hereditary cytstatin C amyloid angiopathy. In: Isobe, T., Araki, S., Uchino, F., Kito, S., Tsubura, E. (Eds.), Amyloid and amyloidosis. Plenum Publishing Corp, New York, pp. 585–590.
Vidal, R., Frangione, B., Rostagno, A., Mead, S., Revesz, T., Plant, G., Ghiso, J., 1999. A stop-codon mutation in the BRI gene associated with familial British dementia. Nature 399, 776–781.
Vidal, R., Revesz, T., Rostagno, A., Kim, E., Holton, J.L., Bek, T., Bojsen-Moller, M., Braendgaard, H., Plant, G., Ghiso, J., Frangione, B., 2000. A decamer duplication in the 3' region of the BRI gene originates an amyloid peptide that is associated with dementia in a Danish kindred. Proc. Natl. Acad. Sci. USA 97, 4920–4925.
Vinters, H.V., Gilbert, J.J., 1983. Cerebral amyloid angiopathy: incidence and complications in the aging brain. II. The distribution of amyloid vascular changes. Stroke 14, 924–928.
Vinters, H.V., Nishimura, G.S., Secor, D.L., Pardridge, W.M., 1990. Immunoreactive A4 and gamma-trace peptide colocalization in amyloidotic arteriolar lesions in brains of patients with Alzheimer's disease. Am. J. Pathol. 137, 233–240.
Vonsattel, J.P., Myers, R.H., Hedley-Whyte, E.T., Ropper, A.H., Bird, E.D., Richardson Jr., E.P., 1991. Cerebral amyloid angiopathy without and with cerebral hemorrhages: a comparative histological study. Ann. Neurol. 30, 637–649.
Wang, Z.Z., Jensson, O., Thorsteinsson, L., Vinters, H.V., 1997. Microvascular degeneration in hereditary cystatin C amyloid angiopathy of the brain. APMIS 105, 41–47.
Wattendorff, A.R., Bots, G.T., Went, L.N., Endtz, L.J., 1982. Familial cerebral amyloid angiopathy presenting as recurrent cerebral haemorrhage. J. Neurol. Sci. 55, 121–135.
Wattendorff, A.R., Frangione, B., Luyendijk, W., Bots, G.T., 1995. Hereditary cerebral haemorrhage with amyloidosis, Dutch type (HCHWA-D): clinicopathological studies. J. Neurol. Neurosurg. Psychiatry 58, 699–705.
Weller, R.O., Massey, A., Newman, T.A., Hutchings, M., Kuo, Y.M., Roher, A.E., 1998. Cerebral amyloid angiopathy: amyloid beta accumulates in putative interstitial fluid drainage pathways in Alzheimer's disease. Am. J. Pathol. 153, 725–733.
Winkler, D.T., Bondolfi, L., Herzig, M.C., Jann, L., Calhoun, M.E., Wiederhold, K.H., Tolnay, M., Staufenbiel, M., Jucker, M., 2001. Spontaneous hemorrhagic stroke in a mouse model of cerebral amyloid angiopathy. J. Neurosci. 21, 1619–1627.
Wyss-Coray, T., Rogers, J., 2012. Inflammation in Alzheimer disease – a brief review of the basic science and clinical literature. Cold Spring Harb. Perspect. Med. 2, a006346.
Yamada, M., Itoh, Y., Shintaku, M., Kawamura, J., Jensson, O., Thorsteinsson, L., Suematsu, N., Matsushita, M., Otomo, E., 1996. Immune reactions associated with cerebral amyloid angiopathy. Stroke 27, 1155–1162.
Yamada, M., Naiki, H., 2012. Cerebral amyloid angiopathy. Prog. Mol. Biol. Transl. Sci. 107, 41–78.

Paper III

Laboratory Investigation (2017), 1–12

Pathological changes in basement membranes and dermal connective tissue of skin from patients with hereditary cystatin C amyloid angiopathy

Asbjorg Osk Snorradottir[1,2], Helgi J Isaksson[2], Saevar Ingthorsson[3,4], Elias Olafsson[5,6], Astridur Palsdottir[1] and Birkir Thor Bragason[1]

Hereditary cystatin C amyloid angiopathy (HCCAA) is a genetic disease caused by a mutation in the cystatin C gene. Cystatin C is abundant in cerebrospinal fluid and the most prominent pathology in HCCAA is cerebral amyloid angiopathy due to mutant cystatin C amyloid deposition with associated cerebral hemorrhages, typically in young adult carriers. Analyses of post-mortem brain samples shows that pathological changes are limited to arteries and regions adjacent to arteries. The severity of pathological changes at post-mortem has precluded the elucidation of the evolution of histological changes. Mutant cystatin C deposition in carriers is systemic and has, for example, been described in the skin, suggesting similar pathological mechanisms both in the brain and outside of the central nervous system. The aim of this study was to use skin biopsies from asymptomatic and symptomatic carriers to study intermediate events in HCCAA pathogenesis. We found that cystatin C deposition in minimally affected samples was limited to the basement membrane (BM) between the dermis and epidermis. When the deposits were more advanced, they extended to other BM regions in the skin. Our results showed that the immunoreactivity of the BM protein COLIV was increased to a similar extent in all carrier biopsies and cystatin C deposits were in close association with COLIV. The density of fibroblasts in the upper dermis of carrier skin was increased, whereas the distribution of other cell types examined did not differ compared with control biopsies. COLIV and cystatin C immunoreactivity in carrier biopsies was closely associated with the fibroblasts. The results of this study, in conjunction with our previous results regarding pathological BM changes in leptomeningeal arteries of patients, suggest that BM changes are early and important events in HCCAA pathogenesis that could facilitate cystatin C deposition and aggregation.

Laboratory Investigation advance online publication, 9 January 2017; doi:10.1038/labinvest.2016.133

Hereditary cystatin C amyloid angiopathy[1] (HCCAA; Online Mendelian Inheritance in Man entry 105150; also referred to as hereditary cerebral hemorrhage with amyloidosis-Icelandic type (HCHWA-I)[2,3]) is a very rare autosomal dominant genetic disease caused by a single base substitution mutation in the gene of the secreted cysteine protease inhibitor cystatin C, *CST3*.[4–6] The disease is classified as a cerebral amyloid angiopathy (CAA). The disease-causing mutation has only been found in Iceland (population ~ 332 750 as of 1 January 2016 (Statistics Iceland)) with one exception.[7] It results in the exchange of leucine for glutamine at amino acid 68 of the protein and will hereafter be referred to as L68Q-*CST3*. Mutant cystatin C forms amyloid deposits in the walls of cerebral arteries resulting in fatal cerebral hemorrhages in young adults.[8–10]

The arterial pathology underlying cerebral hemorrhages in HCCAA is observed in brain arteries and arterioles both in the white and gray matter and is characterized by extensive changes in the composition and structure of the arterial walls.[9,10] In addition to deposition of cystatin C amyloid, these changes include severe smooth muscle cell loss, accumulation of extracellular matrix proteins, eg, the basement membrane proteins collagen IV (COLIV) and laminin, attenuation of the endothelial layer and associated neuroinflammation in proximity to affected arteries.[9,10] These changes result in rupture of arteries/arterioles causing cerebral hemorrhages of

[1]Institute for Experimental Pathology at Keldur, University of Iceland, Reykjavik, Iceland; [2]Department of Pathology, Landspitali University Hospital, Reykjavik, Iceland; [3]Stem Cell Research Unit, Biomedical Center, University of Iceland, Reykjavik, Iceland; [4]Department of Laboratory Haematology, Landspitali University Hospital, Reykjavik, Iceland; [5]Faculty of Medicine, University of Iceland, Reykjavik, Iceland and [6]Department of Neurology, Landspitali University Hospital, Reykjavik, Iceland
Correspondence: AO Snorradottir, Department of Pathology, Landspitali University Hospital, Baronsstigur, Reykjavik 101, Iceland.
E-mail: aos3@hi.is

Received 27 June 2016; revised 3 November 2016; accepted 6 November 2016; published online 9 January 2017

various degrees and microinfarcts, often presenting as partial paralysis, dementia, and personality changes. The cause of death is usually due to cerebral hemorrhage.

Our previous results[10] have shown that the extent of the CAA pathology observed in post-mortem brain samples from patients is invariably 'severe' throughout the brain, as per the criteria defined by Vonsattel *et al*.[11] The lack of moderate and intermediate pathological changes in such post-mortem samples has made it difficult to decipher the sequence of events leading to the end-stage pathology. Unfortunately, there is no animal model of the disease. Transgenic mice have been produced that express the mutant allele under the control of the neuron-specific Thy-1 promoter[12] as well as the human *CST3* promoter[13] but neither model developed HCCAA pathology.

HCCAA is a systemic disorder in that cystatin C is not only deposited within the central nervous system (CNS) of patients but also deposited in peripheral tissues such as lymph nodes, submandibular salivary glands, seminal vesicles, spleen, and skin, suggesting that similar pathological mechanisms are at play in the periphery as in the CNS.[8,14–16]

Our previous results[10] show that the pathological changes in post-mortem HCCAA brain samples are always spatially associated with arteries, consisting of the damage within the wall itself, the neuroinflammatory reaction to this damage, and in some cases perivascular amyloid and focal deposits in the parenchyma around arteries. We and others[10,17] have suggested that the cerebral cystatin C amyloid in HCCAA might originate from cells in the arterial wall itself. However, the extensive vascular damage in cerebral post-mortem samples makes it difficult to conclude about the cell types involved from such tissue samples.

Benedikz *et al*[16] described skin deposition of cystatin C in L68Q-*CST3* carriers. The aim of the study described here was to extend on this knowledge and perform a detailed immunohistochemical comparison of skin biopsies from carriers with those from healthy controls to determine whether carrier skin biopsies could provide information about the progression of pathological changes in HCCAA with an emphasis on identifying the cell type responsible for cystatin C tissue deposits.

Table 1 An overview of the individuals from which skin biopsies were obtained for the study

	Age	*Gender*	*Disease status*
Carrier	27	M	S
Carrier	48	M	S
Carrier	51	F	S
Carrier	53	M	S
Carrier	33	M	S
Carrier	27	F	S
Carrier	22	M	S
Carrier	22	F	S
Carrier	61	M	A
Carrier	67	M	A
Carrier	45	F	A
Carrier	29	F	A
Carrier	23	F	A
Carrier	35	F	A
Control	31	F	
Control	30	M	
Control	57	F	
Control	42	M	
Control	68	F	
Control	46	F	
Control	39	F	
Control	64	F	
Control	65	M	
Control	30	F	
Control	28	M	

Abbreviations: F, female; M, male.
Symptomatic (S) carriers were defined as those who had suffered one or more cerebral hemorrhages leading to hospitalization at the time of biopsy. Asymptomatic (A) carriers had not been hospitalized due to hemorrhages before biopsy. Age refers to the age of the sample donor at the time of sampling.

MATERIALS AND METHODS

Tissue Samples

The samples used in this study were acquired by informed consent. The acquisition and use of the samples was according to permits (04-046-S2 and 15-060-S1) from the National Bioethics Committee in Iceland. All samples were processed at the Department of Pathology, Landspitali National University Hospital, Reykjavik, Iceland. Punch skin biopsies (4 mm, central back, one per individual) were obtained from 14 HCCAA L68Q-*CST3* carriers (7 males and 7 females, aged 22–67 years, median = 34 years; Table 1) and 11 healthy controls (4 males and 7 females, aged 28–68 years, median = 42 years; Table 1). Of these 14 carriers, 8 were symptomatic and the remaining 6 asymptomatic (Table 1). The category symptomatic was defined as cerebral hemorrhage leading to documented hospitalization before the time of biopsy. Asymptomatic carriers had not been hospitalized due to cerebral hemorrhage before biopsy. All tissue samples were formalin-fixed and paraffin-embedded. They were cut into 1.5 μm sections for hematoxylin and eosin (H&E) staining and 5 μm serial sections for immunohistochemistry, immunofluorescence confocal microscopy, and Congo red staining. H&E staining was done using standard methods.

Immunohistochemistry

Sections were de-paraffinized and rehydrated in xylene and ethanol. They were then immunostained using the EnVision

Table 2 Antibodies used in the study

Target protein	*Company*	*Species*	*Pretreatment*	*Antibody dil.*
Collagen IV	Sigma, C1926	Mouse monocl. monocl.	Proteinase K[a]	1:500
Cystatin C	Sigma, HPA013143, (HPA013143)	Rabbit polycl.	None	1:100
E-cadherin	BD, BD610921	Mouse monocl.	TE buffer, pH 9.0	1:100
pSMAD2/3	Santa Cruz, sc-11769	Rabbit polycl.	TE buffer, pH 9.0	1:200
p63	Dako, M7317	Mouse monocl.	TE buffer, pH 9.0	1:50
Smooth muscle actin	Abcam, ab7817	Mouse monocl.	TE buffer, pH 9.0	1:100
Vimentin	Dako, M7020	Mouse monocl.	TE buffer, pH 9.0	1:500

Abbreviations: dil., dilution; monocl., monoclonal; polycl., polyclonal.
The table shows details of the primary antibodies used for immunohistochemistry and immunofluorescence experiments.
[a]Protease XVII, Sigma, P8038, 1 μg/ml.

Detection System Peroxidase/DAB, Rabbit/Mouse kit (Dako, K4065). Pretreatment of samples for epitope retrieval was required for some of the antibodies used (Table 2). Incubations with primary antibodies were performed at room temperature for 30 min. Antibody dilutions (Table 2) were determined in preliminary experiments. After incubation with a primary antibody, sections were incubated with EnVision FLEX/HRP. Sections were washed between steps with Tris-buffered NaCl solution with Tween 20, pH 7.6 (Dako, S3306). All sections were incubated with 3,3′-diaminobenzidine solution (Dako, K4065) for 10 min. Sections were counterstained with haematoxylin for 5 min followed by washing with tap water for 10 min. Finally, sections were dehydrated with 100% ethanol and xylol followed by coverslipping with mounting medium (Pertex, Histolab). Images were acquired with a Nikon Eclipse 50i microscope equipped with a Nikon DS-Fil digital camera and a Nikon Digital Sight DS-U2 camera controller. Image panels were constructed using the GNU Image Manipulation Program (GIMP 2.8.10).

Immunofluorescence Microscopy

Sections were de-paraffinized and rehydrated in xylene and ethanol. Pretreatment of samples for epitope retrieval was required (Table 2). Sample sections were blocked with 5% goat serum and stained using two or three primary antibodies in conjunction. Samples were incubated with primary antibodies overnight at 4 °C except for combinations including the COLIV antibody that were incubated for 1 h at room temperature. The primary antibody combinations were as follows: (a) anti-cystatin C and anti-COLIV; (b) anti-cystatin C and anti-vimentin; (c) anti-cystatin C and anti-α smooth muscle actin; (d) anti-cystatin C and anti-E-cadherin; (e) anti-cystatin C and anti-p63; (f) anti-cystatin C, anti-COLIV, and anti-vimentin; and (g) anti-vimentin and anti-pSMAD2-/3. The details of the antibodies used are provided in Table 2. Following incubation with primary antibodies, the sections were further incubated (1 h at room temperature), as required, with DAPI (1:2000, Sigma-Aldrich, D9542) and one or more of the following secondary antibodies: 1:1000 Alexa Fluor 647 goat anti-rabbit IgG (Life Technologies, cat#A11247), 1:1000 Alexa Fluor 488 goat anti-mouse IgG (Life Technologies, cat#A11008), 1:1000 Alexa Fluor 488 goat anti-mouse IgG1 (Life Technologies, cat#A21121), 1:1000 Alexa Fluor 488 goat anti-mouse IgG2a (Life Technologies, cat#A21131), or 1:1000 Alexa Fluor 546 goat anti-mouse IgG2a (Life Technologies, cat#A21133). The sections were then washed with buffer and water, air-dried, and coverslipped with Fluoromount^{TM} (Sigma-Aldrich, F4680) and sealed. Between all the above-mentioned steps in the sample processing, sections were washed with ImmunoFluorescence IMF buffer pH 7.5 (0.1% TX-100, 0.15 M NaCl, 5 mM EDTA, and 20 mM HEPES, pH 7.5). Immunofluorescence was visualized and captured using an Olympus FV1200 confocal laser scanning microscope. Image panels were constructed using the GNU Image Manipulation Program (GIMP 2.8.10).

Quantification of Cystatin C and COLIV Immunostaining in Skin Biopsies

Cystatin C and COLIV immunostaining in the patient and control biopsies was quantified by semi-automated image analysis using the ImageJ software (http://rsbweb.nih.gov/,v1.47) and a method previously described.[9,10] Bright-field images of a section from all individuals were captured on a Nikon Eclipse 50i microscope equipped with a Nikon DS-Fil digital camera and a Nikon Digital Sight DS-U2 camera controller at a resolution of 2560×1920 pixels using a Nikon $\times 4/0.3$NA objective. RGB color images of the sections were imported to ImageJ. On each image, a rectangular 1300×1300 pixels region of interest (ROI) was defined. The ROI was positioned so that one edge was placed at the periphery of the epidermis ensuring that the ROI extended over the epidermis and well into the dermis. Subsequent processing yielding the % area coverage of cystatin C or COLIV immunoreactivity within each ROI was performed as previously described.[9,10] Statistical analyses on quantitative data were performed with

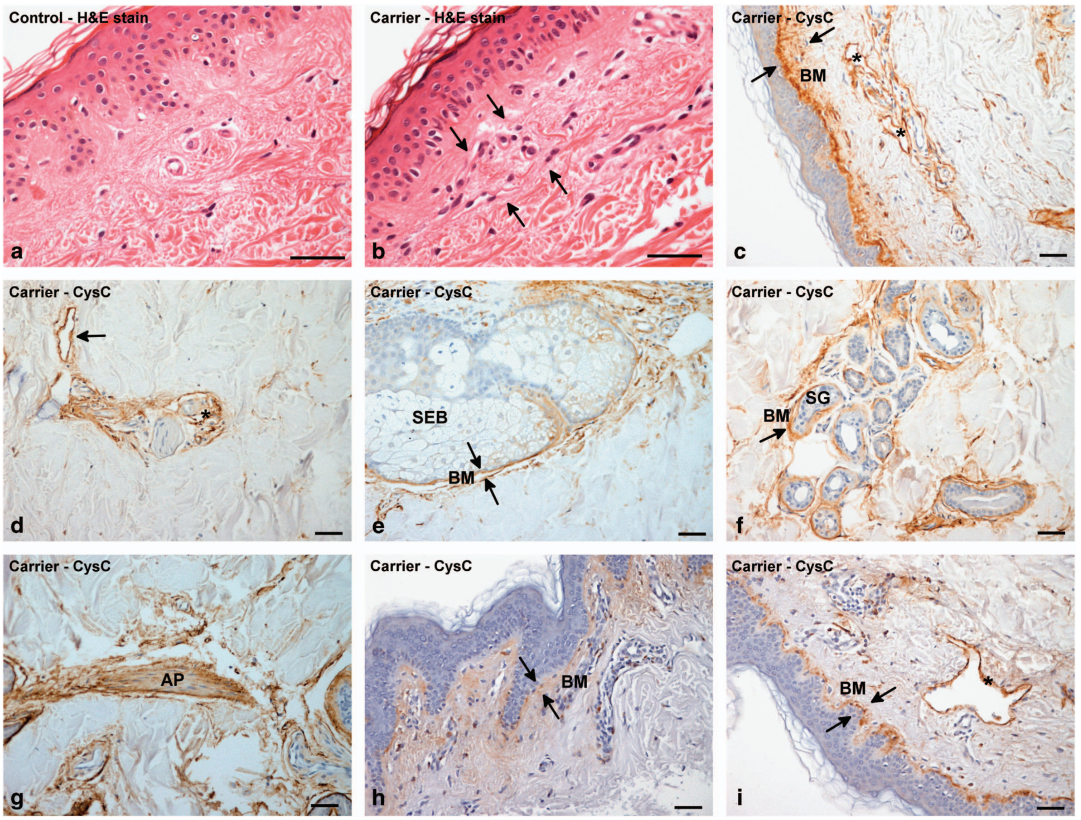

Figure 1 Increased density of cells in the upper dermis of L68Q-*CST3* carrier biopsies and the distribution of cystatin C immunoreactivity in biopsies from symptomatic and asymptomatic carriers. (**a**, **b**) Hematoxylin and eosin (H&E) staining of a control biopsy (**a**) that shows normal epidermis and upper dermis in contrast to a carrier biopsy (**b**) showing an increased number of cells in the upper dermis (arrows). Examples of cystatin C immunoreactivity in symptomatic carriers: (**c**) strong cystatin C immunoreactivity in the basement membrane (BM, arrows) between dermis and epidermis (asterisks indicate vessels in the upper dermis with cystatin C immunoreactive BMs), (**d**) cystatin C immunoreactivity in the BM of a vein (arrow) and arteries (asterisk) in the hypodermis, (**e**) in the BM (arrows) surrounding a sebaceous gland (SEB) in the dermis, (**f**) in the BM (arrow) around sweat glands (SG) in the hypodermis, and (**g**) associated with an arrector pili (AP) muscle. Examples of cystatin C immunoreactvity in asymptomatic carriers: (**h**) relatively weak and diffuse cystatin C immunoreactivity in the BM between the dermis and epidermis (arrows), and (**i**) moderate cystatin C deposition in the BM between the dermis and epidermis (arrows) and in the BM of a vessel (asterisk) in the dermis. Scale bars: 50 μm in all figures.

GraphPad Instat. The box plot was prepared in StatView v5.0.1.

RESULTS

Skin Structure in Carriers and Controls

One skin biopsy per individual (Table 1) was taken from the central back. Examination of H&E-stained sections did not reveal any major deviations from normal skin tissue structure (epidermis/dermis) in the samples from the carriers compared with controls except that there was an increased cell density in the upper dermis of carrier skin, right below the epidermis (Figures 1a and b). H&E staining revealed mild inflammation in biopsies from two carriers. Focusing on arteries, which are the most affected structures in brain tissue of HCCAA patients,[9,10] H&E staining of carrier skin biopsies did not reveal pathological changes in dermal arteries/arterioles akin to the acellular, homogenous, arterial walls observed in post-mortem brain samples from HCCAA patients.

Cystatin C Deposition in Carrier Biopsies was Associated with Basement Membranes

Cystatin C immunoreactive deposits were observed in skin biopsies from all the carriers, examples are shown in Figures 1c–i, whereas biopsies from controls were all negative with the cystatin C antibody dilution used for the immunohistochemistry (data not shown). Congo red staining of the carrier skin biopsies did not show birefringence under

polarized light (data not shown), suggesting that the cystatin C deposits did not contain fully formed amyloid.

The extent of cystatin C distribution in the skin biopsies differed between symptomatic and asymptomatic carriers in that it was more widespread in the former. In symptomatic carriers, cystatin C immunoreactivity was observed in the basement membrane between the epidermis and dermis (Figure 1c) extending down into the dermis and up into the epidermis (Figure 1c). It was present in basement membranes of dermal arteries, arterioles and veins (Figures 1c and d), sebaceous glands (Figure 1e), hair follicles, fat/sweat glands (Figure 1f), and arrector pili muscles (Figure 1g).

In contrast to cerebral arteries, in which cystatin C immunoreactivity extends through all layers of the arterial wall and the arteries are often occluded,[9,10] cystatin C immunoreactivity in dermal vessels was mainly observed in their basement membrane (arteries) but in some cases throughout the entire wall of veins (Figures 1c and d), which are minimally affected in the brain; occluded vessels were never observed.

In three of the six asymptomatic carriers, cystatin C immunoreactivity was exclusively observed in the basement membrane between the epidermis and dermis (example shown in Figure 1h) with no immunoreactivity around the skin structures mentioned above with respect to the symptomatic carriers. However, in the remaining three asymptomatic carriers, immunoreactivity was observed around these structures but to a lesser extent than in the symptomatic carriers (Figure 1i).

A quantitative comparison of cystatin C immunoreactivity between asymptomatic and symptomatic carriers revealed significantly higher levels of immunoreactivity in the latter group ($P<0.0001$, unpaired *t*-test, Figure 2, left panel). There was no significant correlation between the age of carriers and cystatin C immunoreactivity ($P=0.99$, Pearson $r=-0.003$).

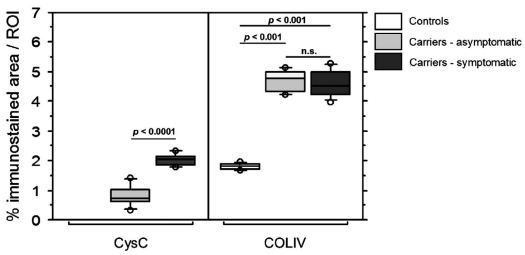

Figure 2 A box and whisker plot that shows the results from quantitative analyses of cystatin C and COLIV in carrier and control biopsies. The whiskers show the 10th percentile and the 90th percentile. Values that fall above the 90th percentile and below the 10th percentile are presented as open circles. Left panel: the plot shows the % cystatin C immunoreactivity per region of interest (ROI) in skin biopsies of six asymptomatic carriers (light gray box, median (50th percentile) = 0.75) and eight symptomatic carriers (dark gray box, median = 2.04). The % cystatin C staining per ROI in the carrier biopsies was significantly higher than that in the controls ($P<0.0001$, unpaired *t*-test). Note: there was no cystatin C immunoreactivity in the control biopsies ($n=11$) thus no box is shown for the controls. Right panel: the plot shows the % COLIV immunoreactivity per ROI in biopsies of 11 controls (empty box, median = 1.84), 6 asymptomatic carriers (light gray box, median = 4.77), and 8 symptomatic carriers (dark gray box, median = 4.52). The % COLIV immunoreactivity per ROI of the asymptomatic and symptomatic carriers was significantly higher than that of the controls ($P<0.001$ and $P<0.001$, respectively (ANOVA with Tukey's post test)). The % COLIV immunoreactivity per ROI was not significantly (NS) different between asymptomatic and symptomatic carriers ($P>0.05$ (ANOVA with Tukey's post test)). A full color version of this figure is available at the *Laboratory Investigation* journal online.

COLIV Immunoreactivity was Increased in Carrier Biopsies

The distribution of COLIV immunoreactivity in the biopsies was similar to that of cystatin C immunoreactivity in the symptomatic carriers, ie, it was present in dermal arteries, arterioles, and veins, in the basement membrane between the epidermis and dermis and around hair follicles, fat/sweat glands, sebaceous glands, and arrector pili muscles (Figures 3a–e).

Quantitative analyses showed that COLIV immunoreactivity was significantly elevated in both asymptomatic and symptomatic carriers compared with controls ($P<0.001$ and $P<0.001$, respectively, ANOVA with Tukey's post test (Figure 2, right panel)). There was, however, no significant difference in COLIV immunoreactivity between the asymptomatic and symptomatic carriers ($P>0.05$, ANOVA with Tukey's post test (Figure 2, right panel)). Within the carriers, there was no significant correlation between the amount of cystatin C and COLIV deposition ($P=0.72$, Pearson $r=-0.104$), suggesting that COLIV immunoreactivity did not increase with cystatin C deposition, ie, disease progression.

In the biopsies from the carriers, the elevated COLIV immunoreactivity was especially evident in the basement membrane between the epidermis and dermis (Figure 3b). Whereas the distribution of COLIV immunoreactivity in this region of the control biopsies consisted of a thin, relatively well defined, line (Figure 3d), the COLIV immunoreactivity in this area of the carrier biopsies was more extensive and diffuse, ie, it extended to some extent into the epidermis and more extensively down into the dermis, surrounding nuclei in the upper dermis (Figure 3b), indicating changes in basement membrane structure between the epidermis and dermis in the carrier biopsies.

Analysis by confocal immunofluorescence microscopy confirmed the close spatial association between cystatin C and COLIV deposition in the carrier biopsies implied by the standard immunohistochemistry data. This was especially evident in vessel walls and the upper dermis, and was sometimes to the degree of overlap of fluorescent markers (co-localization; Figures 3e–g). Even when the location of the two proteins was not completely co-localized in vessels, cystatin C was in close proximity slightly peripheral to COLIV (Figure 3g).

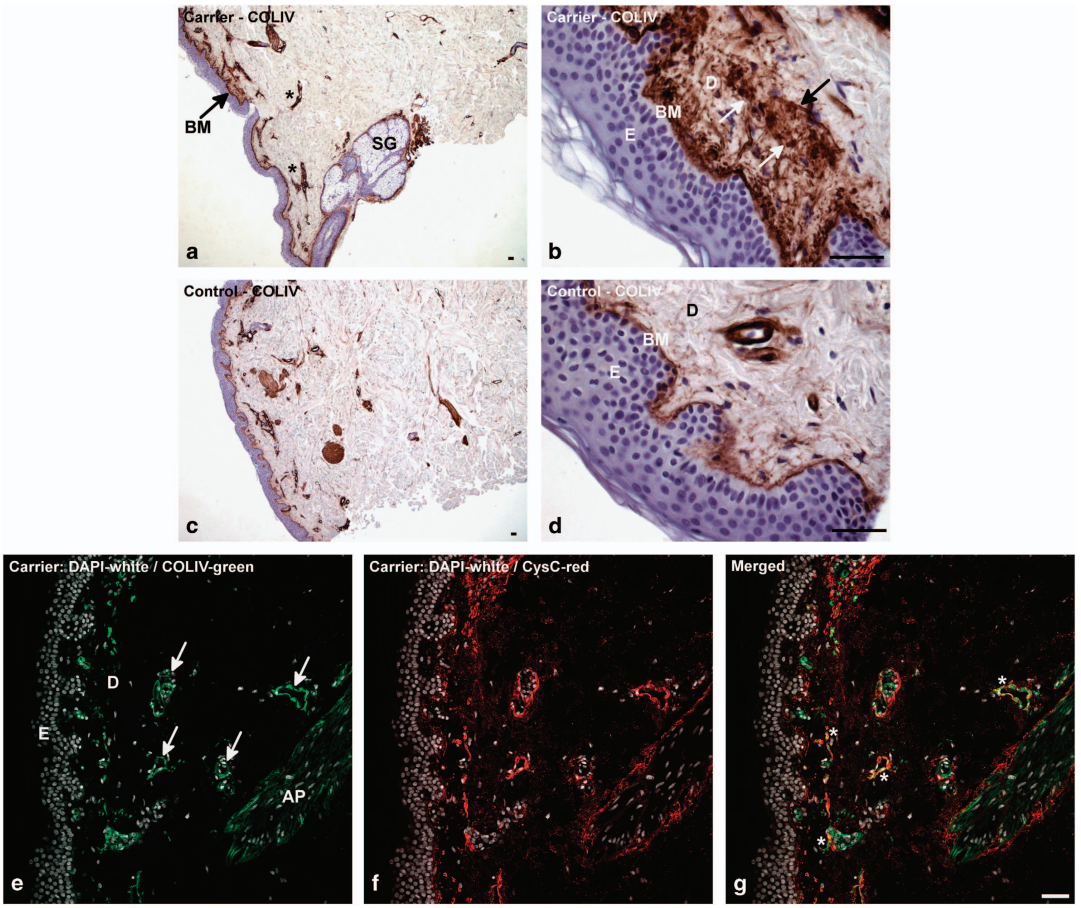

Figure 3 The distribution of COLIV immunoreactivity in skin biopsies from L68Q-*CST3* carriers and controls. (**a**) COLIV immunoreactivity in the skin of a carrier. This low-magnification image shows the overall distribution of COLIV immunoreactivity in the basement membrane (BM, arrow) between the epidermis and dermis as well as in the BM of vessels (examples shown with asterisks) and sebaceous glands (SG). (**b**) An image taken of the same sample as in **a** at a higher magnification showing extensive COLIV immunoreactivity in the BM between the dermis (D) and epidermis (E) as well as an increased density of COLIV immunoreactive cells (white arrows) in the upper dermis and thread-like collagen immunoreactive structures (black arrow). (**c**) A low-magnification image of COLIV immunoreactivity in the skin of a control. The image shows COLIV immunoreactivity in the same areas as in the carrier (**a**) but to a lesser extent. (**d**) An image taken of the same sample as in **c** (same magnification as in **b**) that shows a thin and well-defined BM between the dermis (D) and epidermis (E) in comparison with that of the carrier in **b**. This image also shows fewer cell nuclei in the upper dermis of the control, compared with the carrier sample shown in **b**. (**e**–**g**) Immunofluorescence staining of a carrier biopsy: (**e**) COLIV immunoreactivity in cells of the upper dermis (D), BM of vessels (arrows), and arrector pili (AP) muscle, (**f**) cystatin C immunoreactivity in the upper dermis and in the BMs of the same vessels and the arrector pili muscle indicated in **e**. The merged image (**g**) shows spatial overlap (co-localization) of the green fluorescent label of COLIV and the red fluorescent label of cystatin C giving a yellow color (examples indicated by asterisks). Scale bars: 50 μm in all figures.

Cystatin C and COLIV Deposition in Carrier Biopsies was Associated with Fibroblasts

The distribution of cell types in the biopsies, in relation to the cystatin C and COLIV deposition, was examined using immunohistochemistry and confocal immunofluorescence analyses with antibodies to cell-type markers, ie, antibodies to vimentin, which is a known fibroblast marker, α-smooth muscle actin (αSMA), which is a smooth muscle cell marker, the epithelial cell adhesion molecule E-cadherin, and p63 whose expression is restricted to epithelial cells of stratified epithelia in normal skin.

As mentioned, there was an increase in cell density in the upper dermis of the carrier biopsies. These cells were immunoreactive for vimentin (Figures 4a–d), but not for

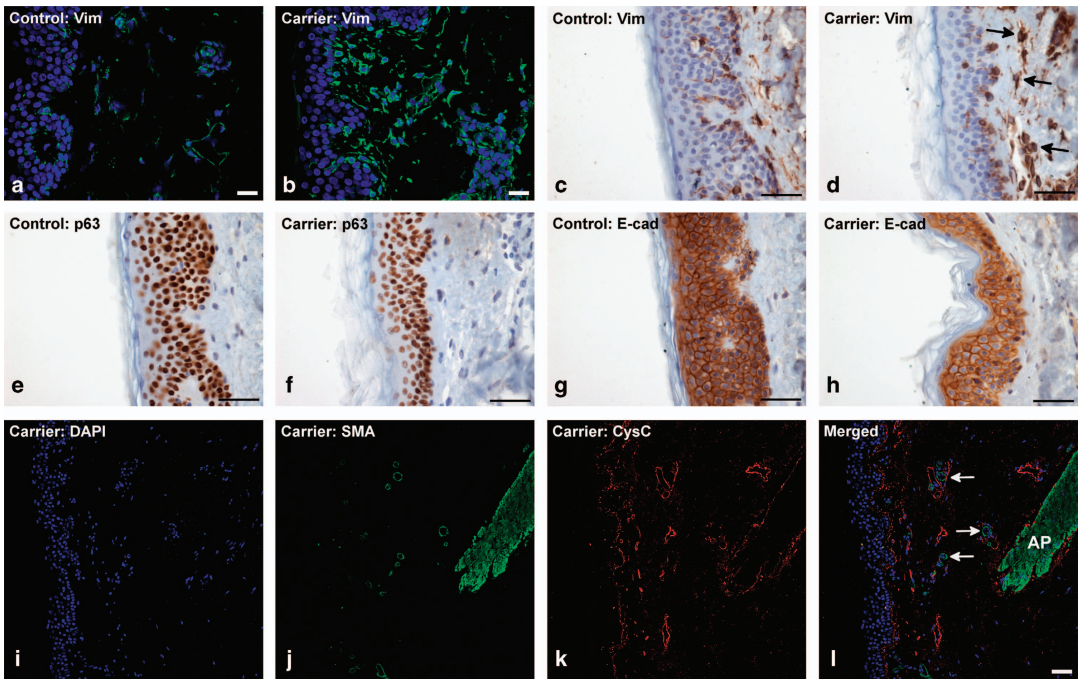

Figure 4 Increased density of vimentin-positive cells in the upper dermis of L68Q-*CST3* carriers biopsies. (**a**) Vimentin (green fluorescence) immunofluorescence staining (blue fluorescence: DAPI) in the upper dermis of a control biopsy. (**b**) An image of a similar area (as in **a**) in a carrier biopsy highlighting the increased number of vimentin-positive cells. (**c**) Vimentin immunoreactivity in the epidermis and upper dermis of a control biopsy. (**d**) Vimentin immunoreactivity in the epidermis and upper dermis of a carrier showing a different morphology (arrows) of the vimentin-positive cells compared with controls. (**e**) p63 immunoreactivity in the epidermis and upper dermis of a control biopsy. (**f**) p63 immunoreactivity in the same area in a carrier biopsy. (**g**) E-cadherin immunoreactivity in the epidermis and upper dermis of a control biopsy. (**h**) E-cadherin immunoreactivity in the same area of a carrier biopsy. (**i–l**) Immunofluorescence staining of a carrier biopsy showing that αSMA immunoreactivity was limited to vessels (**l**, arrows) and arrector pili (**l**, AP) muscle in the dermis and did not co-localize with cystatin C. Scale bars: 50 μm in all figures.

p63, E-cadherin, or αSMA (Figures 4e–l), indicating that they were fibroblasts. E-cadherin and p63 immunoreactivity in carrier and control biopsies was restricted to the epidermis, and αSMA immunoreactivity in the carrier biopsies was limited to the smooth muscle cells of dermal arteries/arterioles and arrector pili muscle cells (Figure 4l) as in the controls (data not shown). Vimentin-positive cells in the upper dermis were also COLIV positive, as was the case around vessels (Figures 5a–c), accentuating the identity of these cells as fibroblasts.

Morphologically, the fibroblasts in the upper dermis were characterized by an enlarged cell body and the vimentin immunostaining highlighted thicker processes extending from the cell bodies (Figure 4d) compared with vimentin-positive cells in the same area of the controls (Figure 4c). In addition to the upper dermis, cells with a fibroblast marker phenotype were, in general, observed in all cystatin C and COLIV-positive areas of the carrier biopsies and in some instances cystatin C immunoreactivity seemed to be intracellular in such cells (Figures 5a–c).

pSMAD2/3 Immunoreactivity in Carrier Biopsies

The involvement of TGFβ signaling in the stimulation of extracellular matrix protein production is well documented,[18] and TGFβ signaling has been associated with fibrotic connective tissue disorders of the skin.[19] Relevant to the increased density of fibroblasts and COLIV deposition in the carrier biopsies, TGFβ has been linked to enhanced proliferation of adult skin fibroblasts.[20]

Phosphorylation of SMAD2/3 is a well documented downstream event in the TGFβ signaling pathway.[18] We examined pSMAD2/3 immunoreactivity in the carrier and control biopsies to see whether we could detect evidence of elevated TGFβ signaling in the carrier biopsies. Our results showed that nuclei of the extended fibroblast population in the carrier biopsies were immunoreactive for pSMAD2/3 (Figures 6a–f). Similar immunoreactivity was, however, also observed in the sparser fibroblast population in the same area of the control skin biopsies (Figures 6g–i). Thus, although there was a difference in the extent of nuclear pSMAD2/3 immunoreactivity between the carrier and control biopsies, this was

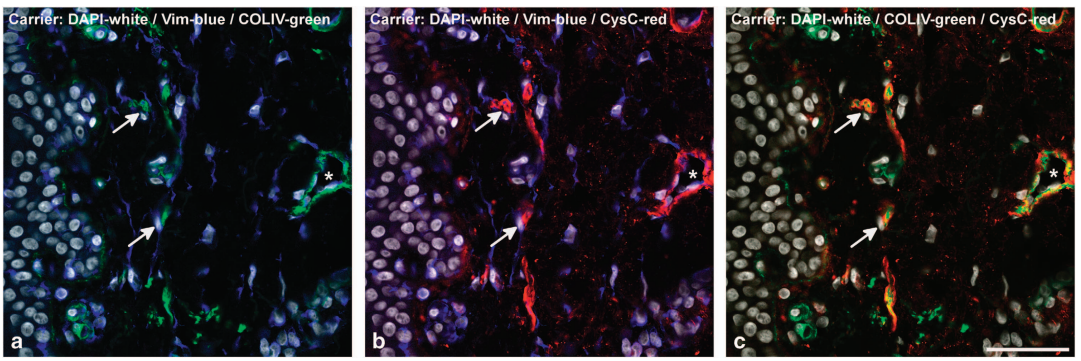

Figure 5 Co-localization of cystatin C, COLIV, and vimentin in skin biopsies of L68Q-*CST3* carriers. (**a–c**) Immunofluorescence staining showing a close association between vimentin, COLIV, and cystatin C immunoreactivity. The arrows and asterisk indicate examples of cells and a vein (respectively) with a spatial overlap of all three fluorescent labels. Scale bars: 50 μm in all figures.

mainly due to the denser fibroblast population in the upper dermis of the carrier biopsies compared with the controls.

DISCUSSION

Cystatin C Deposition in Carrier Biopsies

Because of its strong cerebral presentation HCCAA is rightly classified as a CAA disorder. However, our results (Palsdottir *et al*[8] and data not shown) and those of others[15,16,21] show that, although the most advanced pathological changes are found in the CNS, the pathology in HCCAA is not confined to the CNS, but is systemic and characterized by the presence of cystatin C deposits and Congo red birefringent amyloid in peripheral tissues of patients as well as in the brain. This suggests that the cell types involved in the pathogenesis of HCCAA are not limited to the CNS.

The study described here was performed on a peripheral tissue, skin, which was chosen because cystatin C deposits have been described previously by others in the skin of HCCAA patients and carriers,[16] due to ease of access and the relatively non-invasive nature of sampling, and also because cell types, similar to those that are present in walls of cerebral arteries and we have suggested[10] could be responsible for the production of the cystatin C that forms amyloid, are also present in skin, suggesting that this tissue type could provide data relevant to the understanding of HCCAA pathogenesis.

The location of cystatin C deposits in the skin of L68Q-*CST3* carriers examined in this study concurred with that described previously by Benedikz *et al*.[16] Those authors commented that cystatin C deposition seemed to be more extensive in individuals that had a longer history of the disease. The results of our quantitative analysis reported here confirmed this and showed a statistically significant difference in the quantity of cystatin C deposition dependent on disease status, ie, symptomatic carriers had significantly higher levels of cystatin C immunoreactivity than asymptomatic carriers, indicating that the extent of cystatin C deposition in the skin of carriers to some extent mirrors the progression of the disease in the CNS that can be variable.

Cystatin C deposits in the carrier skin biopsies examined in this study did not show green birefringence after Congo red staining, suggesting that the deposits did not consist of fully formed amyloid that is invariably observed in cerebral arteries of HCCAA patients. This is similar to the results described by Benedikz *et al*;[16] however, they observed amyloid-like threads by electron microscopy analyses in some of the skin biopsies they examined from HCCAA patients.

Congo red birefringent cystatin C amyloid has been described in post-mortem samples from peripheral tissues of patients other than skin, ie, in vessels of lymph nodes, spleen, adrenal cortex, and submandibular salivary glands[8,15,21] as well as in the interlobular connective tissue of submandibular salivary glands. These observations show that cystatin C deposits progress to amyloid form in the periphery as well as in the CNS, and that cystatin C amyloid in patients is not necessarily confined to vessel walls. Due to the lack of Congo red birefringence in the skin biopsies examined in this study, we concluded that the pathological situation in the carrier biopsies could be described as mild to intermediate and might therefore provide data relevant to early/intermediate events in HCCAA pathogenesis.

There was no correlation between age and cystatin C deposition within the carrier cohort that contained samples from individuals from 22 to 67 years old (Table 1). Our genealogy database shows that the average lifespan of carriers born since 1900 is 31 years (median = 29 years).[22] The upper 10th percentile is ≥ 49 years and the lower 10th percentile ≤ 20 years. We have arbitrarily defined late-onset carriers as those whose lifespan falls in the top 10th percentile and early-onset carriers as those that present with symptoms ≤ 35 years of age. The carrier cohort involved in this study contained samples from both late- and early-onset carriers. Results from our previous work[10] have led us to conclude that despite the

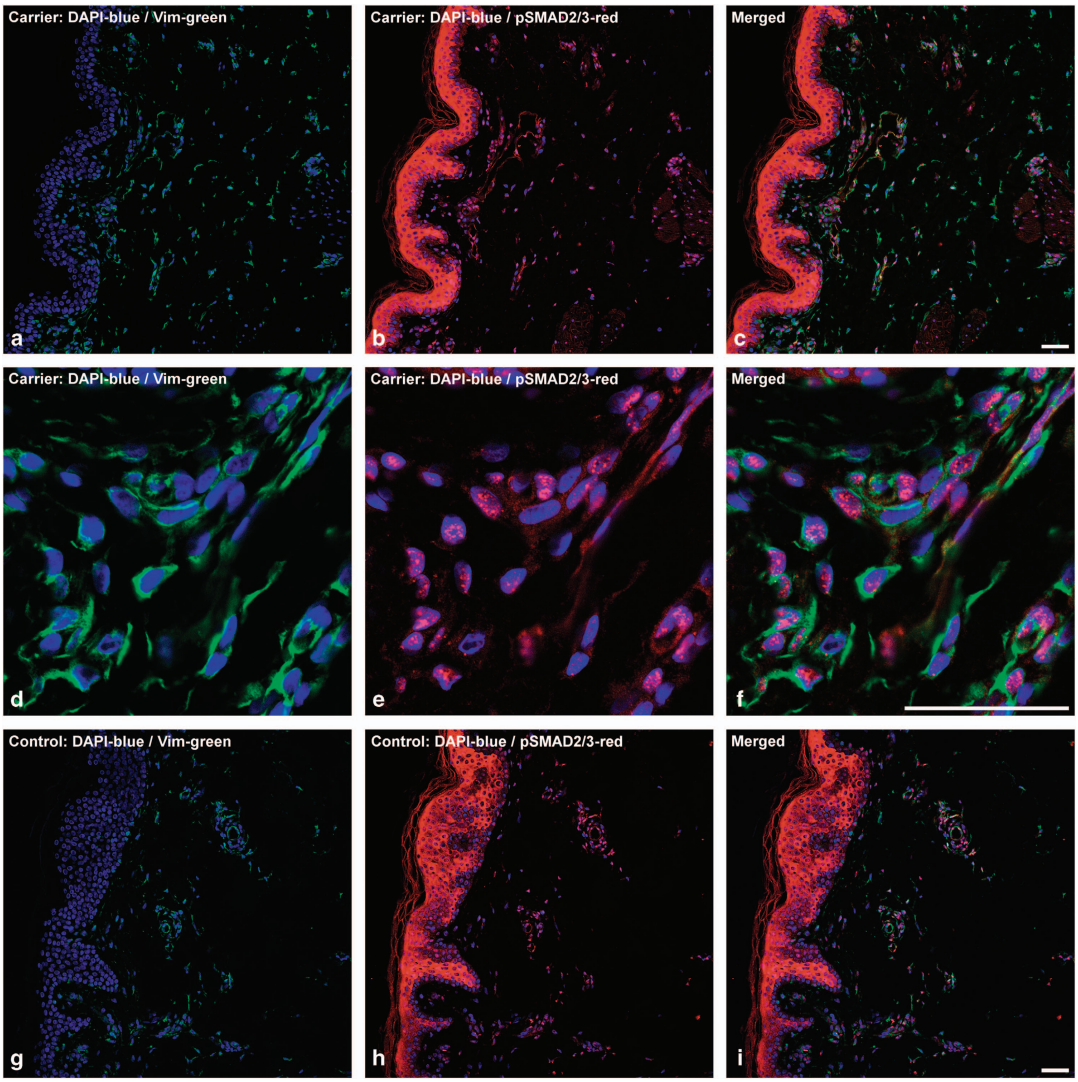

Figure 6 Fibroblasts with nuclear pSMAD2/3 immunoreactivity in skin biopsies of L68Q-*CST3* carriers and controls. Immunofluorescence staining (blue: DAPI, green: vimentin, and red: pSMAD2/3) of a carrier (**a**–**f**) and control biopsy (**g**–**i**) showed that vimentin-positive fibroblasts in both carriers and controls displayed pSMAD2/3 immunoreactivity in the nucleus. The difference in pSMAD2/3 immunoreactivity between the carrier and control biopsies was due to the increased density of fibroblasts in the carriers (**a**) compared with controls (**g**). (**d**–**f**) Images taken of a carrier biopsy at higher magnification showing nuclear pSMAD2/3 immunoreactivity in vimentin-positive fibroblasts. Scale bars: 50 μm in all figures.

delayed onset of symptoms, late-onset carriers succumb to the same end-stage pathology as those with an early onset. Therefore, rather than negating the effects of the mutation, there seem to be some factors, internal or external, that can retard the pathological process. Thus, we would not necessarily have expected a correlation between age and cystatin C deposition in the carrier skin biopsies examined in the present study.

Cystatin C Deposition and the Basement Membrane

Examination of the skin biopsies from the carriers showed that cystatin C immunoreactivity in three asymptomatic carriers was exclusively observed in the basement membrane region between the dermis and epidermis, suggesting that initial deposition occurs in that area. In correlation with disease progression, cystatin C immunoreactivity in the carrier biopsies became more intense and widespread,

extending down into the upper dermis surrounding structures within the dermis, ie, arteries, veins, glands, and arrector pili muscle, and also extending to some extent up into the epidermis. The deposition, in both symptomatic and asymptomatic carriers, was closely linked to the distribution of the basement membrane collagen COLIV that in turn was closely linked to the expanded population of dermal fibroblasts, whereas there was a lack of a systematic association of cystatin C or COLIV with the markers p63, E-cadherin, or αSMA.

We have previously described extensive basement membrane abnormalities in cerebral arteries/arterioles of HCCAA patients, characterized by deposition of COLIV as well as other extracellular matrix proteins.[9] The results from that study raised the question whether the deposition was primary, instigating amyloid deposition, or a reactive response to amyloid deposition and/or vascular damage. However, the severity of the pathology in the post-mortem brain samples made it impossible to conclude about the matter.

Our results showed that in contrast to the cystatin C immunoreactivity that differed between asymptomatic and symptomatic carriers, there was what could be termed a 'fixed' elevation of COLIV immunoreactivity in the carrier biopsies tightly associated with cystatin C deposition and fibroblasts. That is, cystatin C immunoreactivity increased with disease progression, ie, asymptomatic *vs* symptomatic, but not COLIV immunoreactivity.

The structure of the basement membrane between the epidermis and dermis is formed by several proteins, such as COLIV, that are contributed by the keratinocytes of the epidermis and dermal fibroblasts.[23] Some of the proteins are exclusively expressed by either cell type; COLIV is contributed by both.[23] Our results did not reveal differences in the structure of the epidermis in carrier biopsies compared with controls, but an increase in the density of dermal fibroblasts, which would suggest that the elevation of COLIV immunoreactivity in this region of the carrier biopsies, was associated with the increased density of dermal fibroblasts.

Extracellular matrix proteins, such as COLIV, have been detected in amyloid deposits in Alzheimer's disease (AD) and the CAA disorder Hereditary Cerebral Hemorrhage with Amyloidosis—Dutch type (HCHWA-D), and studies have suggested that they are actively involved in the pathogenesis of these diseases.[24–28] A recent study by Lepelletier *et al*[29] found that changes in ECM components, ie, COLIV, perlecan and fibronectin, occur in early stages of subclinical AD and that subsequent to the subclinical stage, COLIV expression did not increase further as the disease progressed. Furthermore, they observed correlation between Aβ and COLIV staining. Our results suggests a similar scenario in HCCAA to that described by Lepelletier *et al*[29] for COLIV and Aβ in AD, ie, COLIV deposition in HCCAA could be an early event in the pathogenesis of the disease, caused by an increased density of dermal fibroblasts, that forms a scaffold facilitating the deposition and aggregation of cystatin C and subsequent amyloid formation, but does not itself increase as the disease progresses.

Our conclusions based on the results presented here, and our previously reported results,[9] are that rather than there being a specific cell type responsible for production of the cystatin C that forms amyloid, a key step in the pathogenesis of HCCAA are basement membrane changes that form a scaffold that promotes deposition and aggregation of cystatin C, which is ubiquitously expressed throughout the body.[30] In the skin, these basement membrane changes are associated with an increased density of dermal fibroblasts.

Dermal Arteries and Veins in Carrier Biopsies

Cystatin C amyloid deposition in brain arteries is invariably accompanied by severe smooth muscle cell loss,[9,17] and Wang *et al*[17] suggested that they could be an origin of vascular amyloid in HCCAA. Our results showed that the distribution of αSMA immunoreactivity did not differ between carrier and control biopsies and they did not indicate a causal relationship between smooth muscle cells and cystatin C deposition.

It has been reported that solubilized cystatin C amyloid is toxic to cerebrovascular smooth muscle cells.[31] Smooth muscle cells in arteries/arterioles are surrounded by basement membrane; therefore, the smooth muscle cell death observed in cerebral arteries and arterioles in HCCAA might be due to the combination of this toxicity and the affinity of cystatin C for basement membrane.

Interestingly, cystatin C deposition in the skin biopsies was systematically observed in the walls of veins/venules. Such deposition is rarely observed within the CNS where veins and venules are minimally, or not, affected.[10] However, immunoreactivity in venous sinuses of the spleen of HCCAA patients has been described.[8] The reason for this difference between the CNS and the periphery could be the tight association of cystatin C deposition with the basement membrane collagen COLIV and the fact that veins/venules in the periphery differ from those in the CNS in that the latter have very little basement membrane (reviewed by Hawkes *et al*[32]).

Similarities with Other Skin Disorders

There are some similarities between the pathological profile of the L68Q-*CST3* biopsies and that described in the literature for connective tissue disorders of the skin, eg, systemic sclerosis, keloids, and hypertrophic scars. Specifically, these disorders are also characterized by excess collagen production and an increased density of dermal fibroblasts (reviewed by Canady *et al*[19]). However, there are no reports of macroscopic clinical changes in the skin of HCCAA carriers and whereas the other skin disorders are characterized by disturbances in immune parameters and/or inflammation, we did not observe inflammation in the carrier biopsies (except mild inflammation in two cases) and the biopsy sites on the carriers could not be associated with any previous wounds.

A recent study on keloids described epithelial-to-mesenchymal transition (EMT) changes in the disorder.[33] EMT of the skin is associated with E-cadherin downregulation in skin epidermal cells (epithelia) with concomitant upregulation of, eg, vimentin and p63 in the same cells.[34–36] As already mentioned, analyses of the distribution of E-cadherin and p63 immunoreactivity in L68Q-*CST3* carrier biopsies did not reveal deviations from that observed in the controls. Cells that were immunoreactive for these markers were mainly located in the epidermis and we did not systematically observe an increased induction of mesenchymal characteristics in these cells, ie, vimentin immunoreactivity. Thus, we did not see unequivocal evidence of EMT in the epidermis of the HCCAA carrier samples.

Myofibroblasts are an activated fibroblast type that can be derived by EMT from several cell types, e.g., fibroblasts, and are characterized by upregulated αSMA expression and enhanced ECM production.[37] They are generally observed in normal wound healing and in association with classic fibrosis such as fibrotic connective tissue disorders of the skin[38,39] and various other tissues.[37] The morphology of the fibroblasts in the upper dermis of carrier biopsies, ie, their enhanced vimentin immunoreactivity as well as the increased density of these cells and their association with COLIV deposition, raised the question whether they were myofibroblasts. Their lack of αSMA immunoreactivity, however, suggested that they did not fall into this category but does not rule out the possibility that they were proto-myofibroblasts.[37]

Cystatin C and TGFβ

Cystatin C has been reported to antagonize TGFβ signaling by binding to the TGFβ type II receptor (TGFβRII) preventing its interaction with TGFβ and affecting signaling downstream of the receptor.[40,41] Therefore, changes in extracellular cystatin C levels could potentially affect signaling through TGFβRII. Studies on the processing of mutant and wild-type human cystatin C in primary cells and cell lines have reported intracellular retention, and accumulation, of the mutant protein[42–44] and extracellular instability due to proteolysis.[45] Cumulatively, this would be expected to result in lower amounts of extracellular cystatin C in tissue heterozygous for the L68Q-*CST3* mutation compared with wild type, as is indeed the case in cerebrospinal fluid (CSF) of carriers that have less than half the normal value of cystatin C in their CSF.[46]

TGF-β initiates its pro-fibrotic action on fibroblasts by binding to TGFβRII whose interaction with TGFβRI results in the phosphorylation of the latter and subsequent activation of SMAD2/3 by phosphorylation. Phosphorylated SMAD2/3 then forms a complex with SMAD4 that shuttles to the nucleus and stimulates the transcription of several genes, eg, those of collagen.[20,47,48]

We examined the distribution of pSMAD2/3 in the skin biopsies from the carriers and controls. The results showed that the denser population of fibroblasts in the carrier skin biopsies displayed nuclear immunoreactivity for pSMAD2/3. As expected, due to the normal ongoing nature of cell signaling processes, similar immunoreactivity was also observed in the sparser fibroblast population of the control biopsies.

The results from the pSMAD2/3 immunostaining and the deposition of COLIV and the increased density of fibroblasts in the carrier biopsies observed in this study, coupled with lower extracellular levels of cystatin C suggested above and the association of cystatin C with TGFβRII, suggest that similar to fibrotic disorders of the skin,[19] it is possible that TGFβ could be a factor in the proliferation of dermal fibroblasts in the skin of carriers, and the expansion of COLIV deposition, as a direct consequence of expression of the mutant *CST3* allele. This aspect requires further study. However, when compared with other skin diseases with a similar fibrotic phenotype, it would seem that the pathological changes in HCCAA occur at a much slower rate than in, eg, trauma-induced disorders such as keloids.

CONCLUSIONS

The results of the present study suggest that basement membrane changes facilitate cystatin C deposition in the skin of L68Q-*CST3* carriers. We have previously described advanced basement membrane abnormalities in leptomeningeal arteries of HCCAA patients,[9] notably, COLIV and laminin deposition, in association with cystatin C amyloid. Taken together, the results reported here and those of the previous study suggest that basement membrane changes are early and important events in HCCAA pathogenesis.

Cystatin C is ubiquitously expressed throughout the body and it is one of the most abundant proteins in normal CSF.[49] Basement membrane changes, notably, COLIV deposition, could be pivotal in the pathogenesis of the disease by affecting arterial function in the CNS and, therefore, perivascular drainage of cystatin C resulting in arterial accumulation of cystatin C and eventually amyloid formation. This scenario would be similar to that of sporadic CAA, which is associated with reduced perivascular drainage of Aβ due to age-related arteriosclerosis.[50]

ACKNOWLEDGMENTS

Our studies on HCCAA have been supported by the Icelandic Centre for Research (RANNÍS), the University of Iceland Research Fund, the Memorial fund of Hafdis Kjartansdottir, the Memorial fund of Helga Jonsdottir and Sigurlidi Kristjansson, and the Heilavernd fund. We thank Angelos A. Skodras for technical advice and our collaborators at the Department of Pathology, Landspitali National University Hospital, Iceland, for their assistance with sample processing.

DISCLOSURE/CONFLICT OF INTEREST

The authors declare no conflict of interest.

1. Jensson O, Gudmundsson G, Arnason A, *et al.* Hereditary cystatin C (gamma-trace) amyloid angiopathy of the CNS causing cerebral hemorrhage. Acta Neurol Scand 1987;76:102–114.
2. Gudmundsson G, Hallgrimsson J, Jonasson TA, *et al.* Hereditary cerebral haemorrhage with amyloidosis. Brain 1972;95:387–404.

3. Cohen DH, Feiner H, Jensson O, *et al.* Amyloid fibril in hereditary cerebral hemorrhage with amyloidosis (HCHWA) is related to the gastroentero-pancreatic neuroendocrine protein, gamma trace. J Exp Med 1983;158:623–628.
4. Ghiso J, Jensson O, Frangione B. Amyloid fibrils in hereditary cerebral hemorrhage with amyloidosis of Icelandic type is a variant of gamma-trace basic protein (cystatin C). Proc Natl Acad Sci USA 1986;83:2974–2978.
5. Levy E, Lopez-Otin C, Ghiso J, *et al.* Stroke in Icelandic patients with hereditary amyloid angiopathy is related to a mutation in the cystatin C gene, an inhibitor of cysteine proteases. J Exp Med 1989;169: 1771–1778.
6. Palsdottir A, Abrahamson M, Thorsteinsson L, *et al.* Mutation in cystatin C gene causes hereditary brain haemorrhage. Lancet 1988;2:603–604.
7. Graffagnino C, Herbstreith MH, Schmechel DE, *et al.* Cystatin C mutation in an elderly man with sporadic amyloid angiopathy and intracerebral hemorrhage. Stroke 1995;26:2190–2193.
8. Palsdottir A, Snorradottir AO, Thorsteinsson L. Hereditary cystatin C amyloid angiopathy: genetic, clinical, and pathological aspects. Brain Pathol 2006;16:55–59.
9. Snorradottir AO, Isaksson HJ, Kaeser SA, *et al.* Deposition of collagen IV and aggrecan in leptomeningeal arteries of hereditary brain haemorrhage with amyloidosis. Brain Res 2013;1535:106–114.
10. Osk Snorradottir A, Isaksson HJ, Kaeser SA, *et al.* Parenchymal cystatin C focal deposits and glial scar formation around brain arteries in hereditary cystatin C amyloid angiopathy. Brain Res 2015;1622: 149–162.
11. Vonsattel JP, Myers RH, Hedley-Whyte ET, *et al.* Cerebral amyloid angiopathy without and with cerebral hemorrhages: a comparative histological study. Ann Neurol 1991;30:637–649.
12. Kaeser SA, Herzig MC, Coomaraswamy J, *et al.* Cystatin C modulates cerebral beta-amyloidosis. Nat Genet 2007;39:1437–1439.
13. Mi W, Pawlik M, Sastre M, *et al.* Cystatin C inhibits amyloid-beta deposition in Alzheimer's disease mouse models. Nat Genet 2007;39: 1440–1442.
14. Lofberg H, Grubb AO, Nilsson EK, *et al.* Immunohistochemical characterization of the amyloid deposits and quantitation of pertinent cerebrospinal fluid proteins in hereditary cerebral hemorrhage with amyloidosis. Stroke 1987;18:431–440.
15. Thorsteinsson L, Blondal H, Jensson O, *et al.* Distribution of cystatin C amyloid deposits in icelandic patients with hereditary cystatin C amyloid angiopathy. In: Isobe T, Shukuro A, Fumiya U, *et al.* (eds). Amyloid and Amyloidosis. Plenum Publishing Corporation: New York, 1988, pp 585–590.
16. Benedikz E, Blondal H, Gudmundsson G. Skin deposits in hereditary cystatin C amyloidosis. Virchows Arch A Pathol Anat Histopathol 1990;417:325–331.
17. Wang ZZ, Jensson O, Thorsteinsson L, *et al.* Microvascular degeneration in hereditary cystatin C amyloid angiopathy of the brain. Apmis 1997;105:41–47.
18. Massague J. TGFbeta signalling in context. Nat Rev Mol Cell Biol 2012;13:616–630.
19. Canady J, Karrer S, Fleck M, *et al.* Fibrosing connective tissue disorders of the skin: molecular similarities and distinctions. J Dermatol Sci 2013;70:151–158.
20. Armatas AA, Pratsinis H, Mavrogonatou E, *et al.* The differential proliferative response of fetal and adult human skin fibroblasts to TGF-beta is retained when cultured in the presence of fibronectin or collagen. Biochim Biophys Acta 2014;1840:2635–2642.
21. Löfberg H, Grubb AO, Nilsson EK, *et al.* Immunohistochemical characterization of the amyloid deposits and quantitation of pertinent cerebrospinal fluid proteins in hereditary cerebral hemorrhage with amyloidosis. Stroke 1987;18:431–440.
22. Palsdottir A, Helgason A, Palsson S, *et al.* A drastic reduction in the life span of cystatin C L68Q carriers due to life-style changes during the last two centuries. PLoS Genet 2008;4:e1000099.
23. Marinkovich MP, Keene DR, Rimberg CS, *et al.* Cellular origin of the dermal-epidermal basement membrane. Dev Dyn 1993;197:255–267.
24. Perlmutter LS. Microvascular pathology and vascular basement membrane components in Alzheimer's disease. Mol Neurobiol 1994;9: 33–40.
25. Kalaria RN, Pax AB. Increased collagen content of cerebral microvessels in Alzheimer's disease. Brain Res 1995;705:349–352.
26. van Duinen SG, Maat-Schieman ML, Bruijn JA, *et al.* Cortical tissue of patients with hereditary cerebral hemorrhage with amyloidosis (Dutch) contains various extracellular matrix deposits. Lab Invest 1995;73: 183–189.
27. van Horssen J, Otte-Holler I, David G, *et al.* Heparan sulfate proteoglycan expression in cerebrovascular amyloid beta deposits in Alzheimer's disease and hereditary cerebral hemorrhage with amyloidosis (Dutch) brains. Acta Neuropathol 2001;102:604–614.
28. Zarow C, Barron E, Chui HC, *et al.* Vascular basement membrane pathology and Alzheimer's disease. Ann NY Acad Sci 1997;826:147–160.
29. Lepelletier FX, Mann DM, Robinson AC *et al.* Early changes in extracellular matrix in Alzheimer's disease. Neuropathol Appl Neurobiol; e-pub ahead of print 6 November 2016; doi: 10.1111/nan.12295.
30. Abrahamson M, Olafsson I, Palsdottir A, *et al.* Structure and expression of the human cystatin C gene. Biochem J 1990;268:287–294.
31. Vilhjalmsson DT, Blondal H, Thormodsson FR. Solubilized cystatin C amyloid is cytotoxic to cultured human cerebrovascular smooth muscle cells. Exp Mol Pathol 2007;83:357–360.
32. Hawkes CA, Jayakody N, Johnston DA, *et al.* Failure of perivascular drainage of beta-amyloid in cerebral amyloid angiopathy. Brain Pathol 2014;24:396–403.
33. Yan L, Cao R, Wang L, *et al.* Epithelial-mesenchymal transition in keloid tissues and TGF-beta1-induced hair follicle outer root sheath keratinocytes. Wound Repair Regen 2015;23:601–610.
34. Kalluri R, Weinberg RA. The basics of epithelial-mesenchymal transition. J Clin Invest 2009;119:1420–1428.
35. Jonsdottir HR, Arason AJ, Palsson R, *et al.* Basal cells of the human airways acquire mesenchymal traits in idiopathic pulmonary fibrosis and in culture. Lab Invest 2015;95:1418–1428.
36. Nakamura M, Tokura Y. Epithelial-mesenchymal transition in the skin. J Dermatol Sci 2011;61:7–13.
37. Hinz B. Myofibroblasts. Exp Eye Res 2016;142:56–70.
38. Andrews JP, Marttala J, Macarak E, *et al.* Keloids: the paradigm of skin fibrosis—Pathomechanisms and treatment. Matrix Biol 2016;51:37–46.
39. Kissin EY, Merkel PA, Lafyatis R. Myofibroblasts and hyalinized collagen as markers of skin disease in systemic sclerosis. Arthritis Rheum 2006;54:3655–3660.
40. Sokol JP, Schiemann WP. Cystatin C antagonizes transforming growth factor beta signaling in normal and cancer cells. Mol Cancer Res 2004;2:183–195.
41. Sokol JP, Neil JR, Schiemann BJ, *et al.* The use of cystatin C to inhibit epithelial-mesenchymal transition and morphological transformation stimulated by transforming growth factor-beta. Breast Cancer Res 2005;7:R844–R853.
42. Thorsteinsson L, Georgsson G, Asgeirsson B, *et al.* On the role of monocytes/macrophages in the pathogenesis of central nervous system lesions in hereditary cystatin C amyloid angiopathy. J Neurol Sci 1992;108:121–128.
43. Benedikz E, Merz GS, Schwenk V, *et al.* Cellular processing of the amyloidogenic cystatin C variant of hereditary cerebral hemorrhage with amyloidosis, Icelandic type. Amyloid 1999;6:172–182.
44. Bjarnadottir M, Wulff BS, Sameni M, *et al.* Intracellular accumulation of the amyloidogenic L68Q variant of human cystatin C in NIH/3T3 cells. Mol Pathol 1998;51:317–326.
45. Wei L, Berman Y, Castano EM, *et al.* Instability of the amyloidogenic cystatin C variant of hereditary cerebral hemorrhage with amyloidosis, Icelandic type. J Biol Chem 1998;273:11806–11814.
46. Grubb A, Jensson O, Gudmundsson G, *et al.* Abnormal metabolism of gamma-trace alkaline microprotein. The basic defect in hereditary cerebral hemorrhage with amyloidosis. N Engl J Med 1984;311: 1547–1549.
47. Macias MJ, Martin-Malpartida P, Massague J. Structural determinants of Smad function in TGF-beta signaling. Trends Biochem Sci 2015;40: 296–308.
48. Fisher GJ, Shao Y, He T, *et al.* Reduction of fibroblast size/mechanical force down-regulates TGF-beta type II receptor: implications for human skin aging. Aging cell 2016;15:67–76.
49. Irani DN. *Cerebrospinal Fluid in Clinical Practice*. Elsevier Health Sciences. Saunders Elsevier: Philadelphia, PA (ISBN: 978-1-4160-2908-3), 2009.
50. Weller RO, Boche D, Nicoll JA. Microvasculature changes and cerebral amyloid angiopathy in Alzheimer's disease and their potential impact on therapy. Acta Neuropathol 2009;118:87–102.